

**EXPERIMENTAL INVESTIGATION ON THE STRUCTURAL PERFORMANCE  
OF TWO-STOREY CROSS-LAMINATED TIMBER SHEAR WALLS**

by

**Sedigheh Gheisari**

BSc Degree in Civil Engineering, Hormozgan University, 2001  
MSc in Structural Engineering, University of Shiraz, 2008

THESIS SUBMITTED IN PARTIAL FULFILLMENT OF  
THE REQUIREMENTS FOR THE DEGREE OF  
ENTER DEGREE NAME  
IN  
ENGINEERING

UNIVERSITY OF NORTHERN BRITISH COLUMBIA

March 2024

© Sedigheh Gheisari, 2024

## Abstract

Rapid urbanization has led to an increasing demand for sustainable living and working spaces. In response, renewable materials like wood, especially in the form of Cross-laminated timber (CLT), have gained traction due to their sustainability, cost-efficiency, and versatility. However, there remains an insufficiency of experimental tests on multi-storey CLT structures, and the limited studies conducted so far have predominantly used conventional light frame connections.

This thesis is centered on evaluating the performance of two-storey CLT shear walls with self-tapping screw (STS) connections, addressing a significant research gap. The research involves experimental tests conducted on two-storey CLT shear walls, with a focus on the effect of the shear connections between floors and tension strap connections as well as the effects of acoustic insulation layers and the presence of perpendicular CLT shear walls on the structural performance.

Load-displacement curves showed linear behavior up to the intended lateral displacement, with STS-connected CLT shear walls meeting NBCC drift criteria of 2% height of the structure. Rocking was the primary factor influencing lateral displacement, with tension straps playing an important role. Strengthening shear brackets and adding dead load increased load-carrying capacity by almost 25%. Screw installation angle at tension straps had minimal impact. Also, test results showed that the addition of an acoustic layer had a slight adverse effect, while perpendicular shear walls boosted load-carrying capacities by 15%. In addition, Sliding contributed about 10% to lateral deformations. Panel distortion was minimal, affirming rigid body behavior, and CLT panels acted as rigid diaphragms. This study findings provide valuable insights into the behavior of CLT shear walls, highlighting the importance of appropriate tension strap connections and detailing.

# Table of Contents

Abstract.....	i
Table of Contents .....	ii
List of Figures.....	v
List of Tables .....	xii
Acknowledgements .....	xiii
1 Introduction .....	1
1.1 Environmental impact of construction industry.....	1
1.2 Cross-laminated timber lateral load resisting systems.....	1
1.3 Objective.....	2
1.4 Thesis overview .....	3
1.5 Scope and limitations.....	3
2 Literature review.....	4
2.1 Cross-laminated timber shear walls.....	4
2.1.1 Cross-laminated timber .....	4
2.1.2 CLT shear walls.....	5
2.2 Previous studies on CLT shear walls .....	6
2.2.1 Panel-to-panel connections.....	6
2.2.2 Angle brackets and hold-downs .....	8
2.2.3 CLT shear walls.....	9
2.2.4 UNBC tests on CLT shear walls.....	10
2.2.5 Full-scale CLT building tests .....	13
2.3 Design of CLT shear walls .....	15
2.3.1 Analytical models.....	15
2.3.2 Design provisions in Canada .....	16
2.3.3 Design provisions in the United States.....	17
2.3.4 Design provisions in Europe.....	18
2.3.5 Recent proposal for capacity-based design of CLT shear walls.....	19
2.4 Summary of literature review .....	20

3	Two-storey CLT shear wall tests.....	22
3.1	Objective.....	22
3.2	Description of two-storey structures.....	22
3.3	Materials.....	24
3.3.1	CLT panels.....	24
3.3.2	Spline joints.....	24
3.3.3	Hold downs.....	25
3.3.4	Tension straps.....	25
3.3.5	Shear brackets.....	27
3.3.6	Acoustic separation layers.....	28
3.4	Test series overview.....	29
3.5	Methods.....	34
3.5.1	Assembly.....	34
3.5.2	Instrumentation.....	35
3.5.3	Loading.....	38
3.6	Test results.....	39
3.6.1	Results test #H1a.....	39
3.6.2	Results test #H1b.....	45
3.6.3	Results test #H1c.....	52
3.6.4	Results test #H2a.....	59
3.6.5	Results test #H2b.....	67
3.6.6	Results test #H3a.....	75
3.6.7	Results test #H3b.....	83
3.6.8	Results test #H4a.....	91
3.6.9	Results test #H4b.....	99
3.7	Failure modes.....	108
4	Analyses and Discussions.....	113
4.1	Horizontal storey displacements at target displacements.....	113
4.2	Inter-storey drifts.....	120
4.3	Load-carrying Capacities at target displacements.....	124
4.4	Shear wall uplifts at hold-downs & tension straps.....	128
4.5	Shear wall uplift at inner corners.....	133

4.6	The impact of SB on panel sliding.....	138
4.7	Panel-to-panel slip .....	142
4.8	Panel distortion .....	144
4.9	Kinematic behavior of CLT shear walls .....	145
4.10	Comparison of 1 <sup>st</sup> storey drifts to previous single-storey results.....	150
5.	Conclusions .....	153
5.1	Summary of findings .....	153
5.2	Outlook.....	154
	References .....	156
	Appendix 1: Failure modes after testing.....	164
A.1.1.	Structure #1.....	164
A.1.2.	Structure #2.....	166
A.1.3.	Structure #3.....	169
A.1.4.	Structure #4.....	173
	Appendix 2. Detailed results .....	177
A.2.1.	Load-carrying resistance at target displacement .....	177
A.2.2.	Storey displacements at target displacements .....	178
A.2.3.	Shear wall uplifts at hold-downs and tension straps.....	180
A.2.4.	Shear wall uplifts at inner corners .....	182
A.2.5.	Shear wall sliding .....	184
A.2.6	Panel-to-panel slip .....	186
A.2.7	Panel distortion .....	187

## List of Figures

Figure 2.1. CLT panel configuration [3] .....	4
Figure 2.2. CLT construction: a) platform-type b) balloon-type [10] .....	5
Figure 2.3. CLT shear wall: a) single panel and b) coupled panel [19] .....	6
Figure 2.4. Panel-to-panel connections a) spline; b) half-lap, and c) butt joint [20].....	7
Figure 2.5 HD and SB connected to a concrete floor [29] .....	8
Figure 2.6. Test setup (coupled two-panel shear wall) [37] .....	11
Figure 2.7 CLT structure tests: a) SOFIE project [38]; (b) FPInnovations [39] .....	14
Figure 3.1. Two-storey CLT structure	22
Figure 3.2. Two-storey CLT structure a) plan, b) front view, c) side view.....	23
Figure 3.3. Spline joint in CLT shear walls a) sketch, b) photo, c) ASSY ECO screw .	24
Figure 3.4. HD: a) side view, b) photo c) ASSY Kombi LT STS [3] .....	25
Figure 3.5. Tension strap: a) sketch; b) photo type 1, c) photo type 2; d) photo type 3, e) ASSY Kombi LT STS used in tension strap, f) 45° washer [3] .....	26
Figure 3.6. Custom SB: a) side view; b) photo; c) type 1, attached by STSs on both sides; d) type 2, attached by bolts and STSs.....	28
Figure 3.7. Acoustic separation layer Xylofon type 50 SHORE: a) photo; b) sketch[61] .....	28
Figure 3.8. Structure #1c: a) full view, b) TS with perp. screws.....	29
Figure 3.9. Structure #2: a) test H2a with perp. screws; b) test H2b with 45° inclined screws .....	30
Figure 3.10. Structure #3a: a) full view, b) tension strap with perp. and 45° inclined screws; c) SB with bolts and STSs .....	31
Figure 3.11. Structure #3b: a) full view, b) tension strap with perp. and 45° inclined screws; c) SB with STS on both legs.....	31
Figure 3.12. Structure #4a: a) full view, b) test H4a with acoustic layer.....	32

Figure 3.13. Structure #4b: a) full view; b) test H4b perpendicular shear walls.....	32
Figure 3.14. Assembly of structure: a) steel base fixture, b) installation of walls on base, c) installing 1 <sup>st</sup> level floor panel and weights, d) adding pre-assembled 2 <sup>nd</sup> storey .....	34
Figure 3.15. The location of sensors: a) south face b) north face.....	36
Figure 3.16. Sensors: a) 1 <sup>st</sup> storey displacement free end, b) 2 <sup>nd</sup> storey displacement free end, c) 1 <sup>st</sup> storey sliding, d) 2 <sup>nd</sup> storey sliding, e) HD uplift, f) 1 <sup>st</sup> storey inner corner uplift, g) tension strap uplift, h) 2 <sup>nd</sup> storey inner corner uplift, i) 1 <sup>st</sup> storey panel-panel slip, j) 2 <sup>nd</sup> storey panel-panel slip, (k) panel distortion, (l) 2 <sup>nd</sup> floor sliding .....	37
Figure 3.17. Load application (a) protocol, (b) schematic, c) photo of fixture .....	38
Figure 3.18. H1a (a) total storey displacements, (b) individual storey displacements...	40
Figure 3.19. H1a uplift at: (a) hold downs (b) tension straps.....	41
Figure 3.20. H1a inner corner uplifts at: (a) 1 <sup>st</sup> storey, (b) 2 <sup>nd</sup> storey .....	42
Figure 3.21. H1a sliding of shear wall at: (a) base level, (b) 1 <sup>st</sup> floor .....	44
Figure 3.22. H1a Panel-to-panel slip for: (a) 1 <sup>st</sup> storey, (b) 2 <sup>nd</sup> storey .....	45
Figure 3.23. H1b (a) total storey displacements, (b) individual storey displacements...	46
Figure 3.24. H1b uplift at: (a) hold downs (b) tension straps.....	48
Figure 3.25. H1b inner corner uplifts at: (a) 1 <sup>st</sup> storey, (b) 2 <sup>nd</sup> storey .....	49
Figure 3.26. H1b sliding of shear wall at: (a) base level, (b) 1 <sup>st</sup> level.....	50
Figure 3.27. H1b Panel-to-panel slip for: (a) 1 <sup>st</sup> storey, (b) 2 <sup>nd</sup> storey.....	51
Figure 3.28, H1c (a) total storey displacements, (b) individual storey displacements...	53
Figure 3.29. H1c uplifts at (a) the HDs, (b) tension straps.....	54
Figure 3.30. H1c inner corner uplifts at (a) 1 <sup>st</sup> storey, (b) 2 <sup>nd</sup> storey .....	55
Figure 3.31. H1c panel sliding at: a) base level, b) 1 <sup>st</sup> level left, c) 1 <sup>st</sup> level right .....	57
Figure 3.32. H1c Panel-to-panel slip for: (a) 1 <sup>st</sup> storey, (b) 2 <sup>nd</sup> storey .....	59

Figure 3.33. H2a (a) total storey displacements, (b) individual storey displacements...	60
Figure 3.34. H2a uplifts at (a) the HDs, (b) tension straps.....	62
Figure 3.35. H2a inner corner uplifts at (a) 1 <sup>st</sup> storey, (b) 2 <sup>nd</sup> storey .....	63
Figure 3.36. H2a panel sliding at a) base level, b) 1 <sup>st</sup> level left, c) 1 <sup>st</sup> level right .....	65
Figure 3.37. H2a panel displacements in test, a) 1 <sup>st</sup> storey, b) 2 <sup>nd</sup> storey.....	66
Figure 3.38. H2b (a) total storey displacements, (b) individual storey displacements...	68
Figure 3.39. H2b uplifts at (a) the HDs, (b) tension straps.....	69
Figure 3.40. H2b inner corner uplifts at (a) 1 <sup>st</sup> storey, (b) 2 <sup>nd</sup> storey .....	70
Figure 3.41. H2b panel sliding at a) base level, b) 1 <sup>st</sup> level left side, c) 1 <sup>st</sup> level right side .....	72
Figure 3.42. H2b panel sliding at 2 <sup>nd</sup> floor.....	73
Figure 3.43. H2b panel displacements in test, a) 1 <sup>st</sup> storey, b) 2 <sup>nd</sup> storey .....	74
Figure 3.44. H3a (a) total storey displacements, (b) individual storey displacements...	76
Figure 3.45. H3a uplifts at (a) the HDs, (b) tension straps.....	77
Figure 3.46. H3a inner corner uplifts at (a) 1 <sup>st</sup> storey, (b) 2 <sup>nd</sup> storey.....	78
Figure 3.47. H3a panel sliding at: (a) base level, (b) 1 <sup>st</sup> floor left, (c) 1 <sup>st</sup> floor right .....	80
Figure 3.48: H3a panel sliding at 2 <sup>nd</sup> floor .....	81
Figure 3.49. H3a Panel-to-panel slip for: (a) 1 <sup>st</sup> storey, (b) 2 <sup>nd</sup> storey .....	82
Figure 3.50. H3b (a) total storey displacements, (b) individual storey displacements...	84
Figure 3.51. H3b uplifts at (a) the HDs, (b) tension straps.....	85
Figure 3.52. H3b inner corner uplifts at (a) 1 <sup>st</sup> storey, (b) 2 <sup>nd</sup> storey .....	87
Figure 3.53. H3b panel sliding at: a) base level, b) 1 <sup>st</sup> level floor left side, c) 1 <sup>st</sup> level right side.....	88
Figure 3.54. H3b panel sliding at 2 <sup>nd</sup> level floor .....	89
Figure 3.55. H3b panel displacements at: a) 1 <sup>st</sup> storey, b) 2 <sup>nd</sup> storey .....	90

Figure 3.56. H4a (a) total storey displacements, (b) individual storey displacements...	92
Figure 3.57. H4a uplifts at (a) the HDs, (b) tension straps.....	93
Figure 3.58. H4a inner corner uplifts at (a) 1 <sup>st</sup> storey, (b) 2 <sup>nd</sup> storey .....	94
Figure 3.59. H4a panel sliding at a) base level, b) 1 <sup>st</sup> level left, c) 1 <sup>st</sup> level right .....	96
Figure 3.60. H4a panel sliding at 2 <sup>nd</sup> level floor .....	97
Figure 3.61. H4a panel displacements in test, a) 1 <sup>st</sup> storey, b) 2 <sup>nd</sup> storey.....	98
Figure 3.62. H4a panel distortion .....	99
Figure 3.63. H4b (a) total storey displacements, (b) individual storey displacements.	100
Figure 3.64. H4b uplifts at (a) the HDs, (b) tension straps.....	102
Figure 3.65. H4b inner corner uplifts at (a) 1 <sup>st</sup> storey, (b) 2 <sup>nd</sup> storey .....	103
Figure 3.66. H4b panel sliding at a) base level, b) 1 <sup>st</sup> level floor, c) 2 <sup>nd</sup> level floor ....	105
Figure 3.67. H4b panel sliding at 2 <sup>nd</sup> level floor .....	106
Figure 3.68. H4b panel displacements in test, a) 1 <sup>st</sup> storey, b) 2 <sup>nd</sup> storey .....	107
Figure 3.69. Relative displacement of the wall segments during CW rocking .....	108
Figure 3.70. Spline joint after test: a) plywood, b) screws, c) CLT panel under spline	109
Figure 3.71. Tension strap after test: a) screws, b) CLT panel under tension strap, c) floor panel bending.....	110
Figure 3.72. SB after test: a, b) deformed SB, c) deformed screws, d) embedment in the CLT panel under SB .....	111
Figure 3.73. Brittle local failure in the corner of CLT panel after test: a) H3a, b) H4a	112
Figure 3.74. HD after testing.....	112
Figure 4.1. Individual floor displacements at the test: (a) H1a monotonic pulling, (b) H1b monotonic pushing, (c) H1c cyclic	114
Figure 4.2. Lateral displacements for the tests conducted on structure #H1b and #H1c at positive cycles, (a) 1 <sup>st</sup> floor, (b) 2 <sup>nd</sup> floor [mm].....	115

Figure 4.3. Lateral displacements for the tests conducted on structure #Hb and #H1c at negative cycles, (a)1 <sup>st</sup> floor, (b) 2 <sup>nd</sup> floor [mm].....	116
Figure 4.4. 1 <sup>st</sup> storey displacements @ +/- 100% target displacement.....	117
Figure 4.5. 1 <sup>st</sup> storey displacements @ +/- 130% target displacement.....	117
Figure 4.6. 2 <sup>nd</sup> storey displacements @ +/- 100% target displacements .....	118
Figure 4.7. 2 <sup>nd</sup> storey displacements @ +/- 130% target displacements .....	118
Figure 4.8. 1 <sup>st</sup> and 2 <sup>nd</sup> floor contribution percentages to +100% target displacement .	120
Figure 4.9. 1 <sup>st</sup> and 2 <sup>nd</sup> floor contribution percentages to +130% target displacement .	121
Figure 4.10. 1 <sup>st</sup> and 2 <sup>nd</sup> floor drift ratios @ +100% target displacement .....	122
Figure 4.11. 1 <sup>st</sup> and 2 <sup>nd</sup> floor drift ratios @ +130% target displacement .....	122
Figure 4.12. 1 <sup>st</sup> and 2 <sup>nd</sup> storey displacements @ (a) 3% drift, (b)4% drift.....	123
Figure 4.13. Load-carrying capacity @ 40%, 70% and 100% target displacements for the monotonic and cyclic tests conducted on the structure #H1 .....	125
Figure 4.14. Load-carrying capacity @ -40%, -70% and -100% target displacements for the monotonic and cyclic tests conducted on the structure #H1.....	126
Figure 4.15. Load-carrying capacity @ +100% and +130% target displacement.....	128
Figure 4.16. Load-carrying capacity @ -100% and -130% target displacement.....	128
Figure 4.17. Uplifts at HDs at target displacements [mm].....	129
Figure 4.18. Uplifts at left-side tension straps at target displacements [mm] .....	130
Figure 4.19. Uplifts at left-side HDs and tension straps @ 100% target displacement	131
Figure 4.20. Uplifts at left-side HDs and tension straps @ 130% target displacement	131
Figure 4.21. Uplifts at right-side HDs and tension straps @ -100% target displacement .....	132
Figure 4.22. Uplifts at right-side HDs and tension straps @ -130% target displacement .....	132

Figure 4.23. Uplift at 1 <sup>st</sup> storey right-side inner corner @100% and 130% target displacement [mm] .....	133
Figure 4.24. Uplift at left-side HD and right-side inner corner @ 130% target displacement .....	134
Figure 4.25. Uplift at 1 <sup>st</sup> storey right-side inner corner at positive target displacements .....	135
Figure 4.26. Uplift at 1 <sup>st</sup> storey left-side inner corner at negative target displacements .....	135
Figure 4.27. individual rotations of CP shear wall panels after test: (a) #H2a; (b) #H3a .....	136
Figure 4.28. Lifting the left corner upward due to the uplift in the right corner. ....	136
Figure 4.29. Uplift at 2 <sup>nd</sup> storey left-side inner corners @ target displacements .....	137
Figure 4.30. Uplift at 2 <sup>nd</sup> storey right-side inner corners @ target displacements.....	137
Figure 4.30. Shear wall sliding at left-side base level at +100% & +130% target displacements .....	138
Figure 4.31. Shear wall sliding at 1 <sup>st</sup> floor @ +100% target displacement.....	139
Figure 4.32. Shear wall sliding at 1 <sup>st</sup> floor @ +130% target displacement.....	139
Figure 4.34. Shear wall sliding at left-side 2 <sup>nd</sup> floor @ +100% & +130%target displacement .....	141
Figure 4.35. 1 <sup>st</sup> floor contribution percentage to the total lateral displacement .....	141
Figure 4.36. Base and 2 <sup>nd</sup> level sliding contribution to the total lateral displacement [%] .....	142
Figure 4.37. Panel-to-panel slip in the 1 <sup>st</sup> and 2 <sup>nd</sup> level @ +/-100% target displacements .....	143
Figure 4.38. Panel-to-panel slip in the 1 <sup>st</sup> and 2 <sup>nd</sup> level @ +/-130% target displacements .....	143

Figure 4.39. Panel-to-panel slips and inner corner uplifts of the 2 <sup>nd</sup> floor @ 130% target displacement .....	144
Figure 4.40. Panel distortion @ -100% and -130% target displacement [mm].....	145
Figure 4.41. Lateral deformation components for a two-storey CLT building .....	146
Figure 4.42. Comparison Sliding and rocking contribution percentages to the total lateral displacements in all structures.....	148

## List of Tables

Table 2.1. Result summary of the previous single-storey CLT shear wall tests .....	12
Table 3.1. Test parameters	33
Table 4.1. Contribution percentage of components to the total lateral displacements	149
Table 4.2. Comparison between single-storey shear walls [37] and current study .....	151

## **Acknowledgements**

I would like to express my deepest gratitude to Professor Thomas Tannert for his great support, feedback, guidance, and knowledge he shared with me. I could not have undertaken this journey without his supervision.

I am also immensely thankful for the invaluable feedback provided by Dr. Zhou and Dr. Pan, whose expertise and insightful comments significantly enriched my research. Their constructive input greatly contributed to the depth and quality of my work, and I am truly grateful for the opportunity to benefit from their mentorship throughout this academic endeavor. The project was funded by the government of British Columbia through a Forest Innovation Investment (FII) grant (22/23-UNBC-CLT-W23-049) and the BC Leadership Chair in Hybrid Wood Structures Engineering.

The support received from: Kalesnikoff Lumber Co. Ltd. And MTC Solutions Inc (in-kind contribution in form of CLT panels and self-tapping screws supplied at discounted prices); Aspect Structural Engineers, Fast+Epp, TIMBER Engineering Inc. and FPInnovations (in from of supporting the FII application), as well as the UNBC technicians Michael Billups, James Andal and Ryan Stern, and students Juan Jaimes (Sebastian) Pico and Andres Restrepo Ramirez is greatly appreciated.

I dedicate this work to my parents, who have always loved me unconditionally and whose great examples have taught me to work hard for the goals that I aspire to achieve.

# **1 Introduction**

## **1.1 Environmental impact of construction industry**

The urban population reached 4.45 billion in 2021, and it is estimated that by 2030 around 60% of the world live in urban zones, creating a large need for suitable housing and working space. To fulfill this demand, common concrete construction practices would create a massive carbon footprint [1] [2]. These environmental issues highlight the importance of using renewable and sustainable building materials, such as wood, to reduce carbon footprint [3] [4]. The amount of carbon stored in timber exceeds the carbon produced from harvesting to installation; therefore, wood buildings are considered a sustainable option [5] [6]. Compared to steel or concrete buildings, wood buildings have lower environmental impact in embodied energy, air and water pollution, global warming, solid waste, and weighted resource consumption [7]. As a result of lower on-site labor costs and prefabrication of elements, wood structures can be cost-effective compared to concrete and steel [8].

## **1.2 Cross-laminated timber lateral load resisting systems**

In the last two decades, tall mass timber buildings have gained popularity due to an increased emphasis on the use of sustainable resources. The widespread usage of cross-laminated timber (CLT) in multi-storey buildings is due to its light weight, biaxial strength, fire resistance, the ability to create various forms, and dimensional stability [9] [10]. As the allowable height of timber structures in building codes increased, so did the demand on the Lateral Load Resisting System (LLRS). The Canadian Standard for Engineering Design in Wood (CSA-O86) [11] provides generic design guidance for platform-framed CLT shear walls, it does not (yet) include analytical models that can

effectively predict their strength and stiffness. Moreover, most previous research on CLT shear walls was based on single-storey walls, whereas the few studies on multi-storey shear walls were carried out using conventional shear brackets (SB) and hold-downs (HD) from light-frame construction. In consequence, there is a need for more studies on multi-storey CLT shear walls, also using high-performance connections, such as self-tapping screws (STS) instead of conventional connections. Tension straps are connections utilized to vertically link different stories within multi-storey timber structures, while insulation layers are employed to minimize vibrations and hinder sound transfer between these stories. Many experimental studies have concentrated on HDs that prevent uplift on the first storey. However, there remains an inadequate investigation into tension straps and their precise influence on second storey uplift and the overall behavior of these structures. The impact of incorporating an acoustic layer on the structural performance has not been thoroughly studied.

### **1.3 Objective**

The main objective of this research is to evaluate experimentally the strength and stiffness of two-storey CLT shear walls. The specific objectives are to investigate the effects of:

- different shear connections between floors;
- different tension strap connections between floors;
- presence acoustic insulation layer; and
- presence perpendicular CLT shear walls.

## **1.4 Thesis overview**

The state of the art on CLT shear walls is presented in Chapter 2. The experimental tests conducted at UNBC are documented in Chapter 3, and subsequently analyzed and discussed in Chapter 4. Chapter 5 summarizes the findings and proposes future work.

## **1.5 Scope and limitations**

This research focuses on the lateral displacements and lateral load-carrying capacity of two-storey coupled-panel CLT shear walls as LLRS. The impact of compression zones, frictional effects, the biaxial behavior of fasteners, and the presence of openings are not considered. Fire design, acoustics, other building physics considerations, cost analyses, and constructability are out of the scope of this research.

## 2 Literature review

### 2.1 Cross-laminated timber shear walls

#### 2.1.1 Cross-laminated timber

Engineered mass-timber products have been developed to address the challenges of traditional lumber products, such as limited size, low fire resistance, and low dimensional stability [8]. In the 1990s, CLT was introduced in Austria and Germany. As shown in Figure 2.1, CLT commonly consists of an odd number of layers (lamellas) orthogonally glued and pressed together [12]. The panel dimensions can be produced up to 19.5 m in length, 3 m in width, and 400 mm in thickness [7]. In addition to advantageous thermal, acoustic, and fire-resistant characteristics, CLT structures can be quickly erected, leading to a rapid construction process [13] [8]. Moreover, CLT provides high level of prefabrication during the manufacturing process [14]. Owing to its high in-and out-of-plane strength, stiffness, and in-plane dimensional stability, CLT has found its place in construction of roofs, floors, and shear walls [15]. The amount of plastic deformation a material can tolerate before reaching failure is called ductility. CLT shear walls, however, behave as rigid bodies and do not exhibit any ductility: therefore, in CLT buildings, connections are responsible for providing ductility [16].

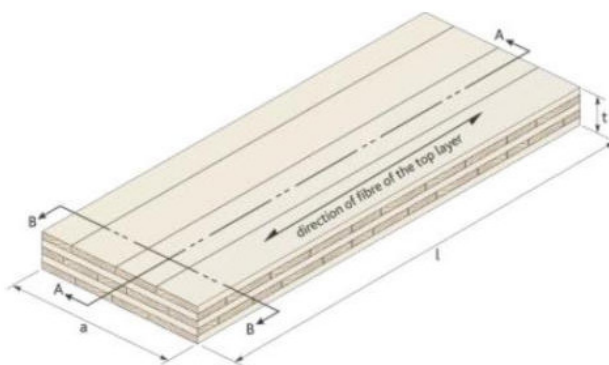


Figure 2.1. CLT panel configuration [3]

### 2.1.2 CLT shear walls

A structure is subjected to gravity loads from the weight of the structure components, snow, and occupancy loads, as well as lateral loads caused by wind and earthquakes. A structure requires a LLRS to withstand these lateral loads. The design consideration for lateral loads in structures becomes increasingly crucial as the height of the building increases.

The magnitude of earthquake load is proportional to the weight of structures; since wood buildings are lighter than other types of structures, they are influenced by lower seismic loads, and consequently lower loads are transferred to the foundations [17]. Various LLRS, such as moment-resisting frames, braced moment frames, light frame shear walls, CLT shear walls, and hybrid systems, may be employed [18]. Among these LLRS, CLT shear walls have received significant attention in research and design standards development.

There are two CLT building construction methods [3]: i) balloon-type buildings, where CLT walls span over multiple stories; and ii) platform-type buildings, where the floor of each level is the base for the next, see Figure 2.2.



Figure 2.2. CLT construction: a) platform-type b) balloon-type [10]

CLT shear walls exhibit near rigid body behavior under in-plane loads, and most deformation happens in connections that led to lateral load energy dissipation; as a result, connection deformation determines the CLT shear wall stiffness. Earthquake energy Dissipative connections should be designed with ductility, while non-dissipative connections should preserve their elastic properties.

According to the number of attached panels in each shear wall, they are categorized as single wall (SW) and coupled CLT shear walls (CP), see Figure 2.3. To enhance the lateral stiffness and promote a monolithic behavior (referred to as SW behavior), relatively rigid vertical joints with high yield strength are employed. However, in cases where greater wall ductility is desired, vertical joints are designed to yield and effectively dissipate energy, exhibiting what is known as coupled panel behavior (CP behavior).

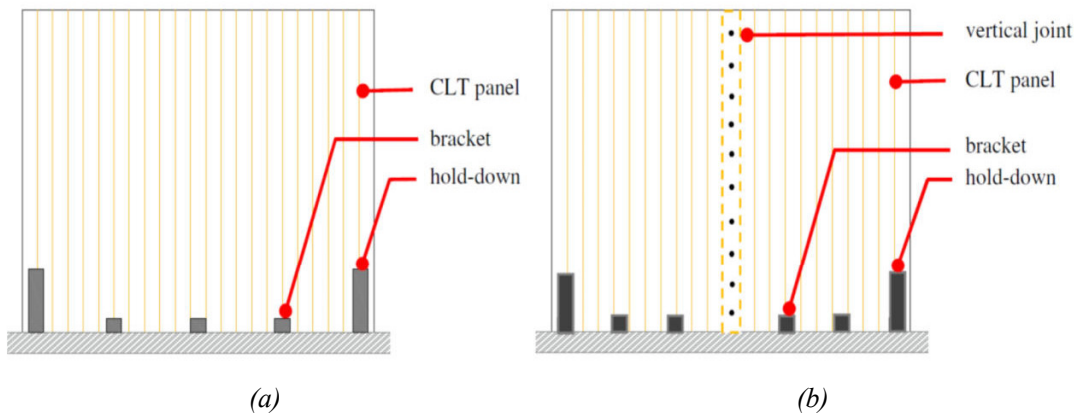


Figure 2.3. CLT shear wall: a) single panel and b) coupled panel [19]

## 2.2 Previous studies on CLT shear walls

### 2.2.1 Panel-to-panel connections

Designing a ductile structure enables the system to go into the inelastic zone and resist seismic loads more efficiently. Since the panels do not provide any ductility, the connections are responsible for providing ductility in CLT shear walls [16]. Wall-to-wall

or floor-to-floor connection, wall-to-foundation connection, and wall-to-floor connection are the three types of connections in CLT shear walls. Half-lap joint, spline joint, and butt joints are typical panel-to-panel connection; see Figure 2.4. Splines made of plywood or LVL can be put into the CLT panels on one or both sides or placed on their surface in conjunction with nails or screws. Commonly, STS or nails are the preferred fastener when CLT panels are coupled.

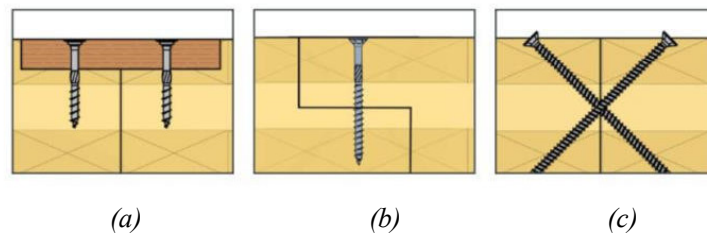


Figure 2.4. Panel-to-panel connections a) spline; b) half-lap, and c) butt joint [20]

Brown et al. [21] tested two CLT layups with 8 mm and 12 mm STSs and compared STSs installed inclined to STSs installed perpendicular to the CLT surface. The result showed that the most ductility was observed in a ratio of 90° STS to two inclined STS. Hossain et al. [22] conducted quasi-static and reversed cyclic tests on CLT connections made of STS connections with double inclinations of fasteners to examine the shear resistance of this innovative connection. Although very high stiffness and capacity of the connection were observed. Hossain et al. [23] performed reversed cyclic and quasi-static monotonic tests on half-lap joints with a combination of STSs in shear and withdrawal and showed that this innovative layup combined high stiffness of STS loaded in withdrawal and high ductility of STSs loaded in shear. Loss et al. [24] studied CLT panel assemblies connected with butt joints with crossed STSs that had a different angle of insertion. The connections were tested under quasi-static monotonic and reversed-cyclic loading, and it was observed that inclination angle significantly affects the performance.

## 2.2.2 Angle brackets and hold-downs

SB and HD are used to link CLT shear walls to the foundation, the concrete podium, or the CLT slab below, using metal fasteners [19], as shown in Figure 2.5. At the corners of CLT shear walls, L-shaped steel anchors have been employed as HD to resist uplifting. Nails are used to fasten the vertical legs to the walls, while anchorage bolts secure the horizontal leg to the foundation. SB are used to attach walls and floors; their primary function, according to Pozza et al. [25], is to handle shear forces, even if some SB can support both horizontal and vertical loads [13]. Shen et al. [26] conducted experimental tests and numerical studies on seven types of bracket connections regarding the tension and shear forces. They compared five analysis methods for the determination of yield points of CLT connections and concluded that based on the bilinear approach Yasumura & Kawai method improved results compared to ASTM E2126 [27] and EN12512 [28].

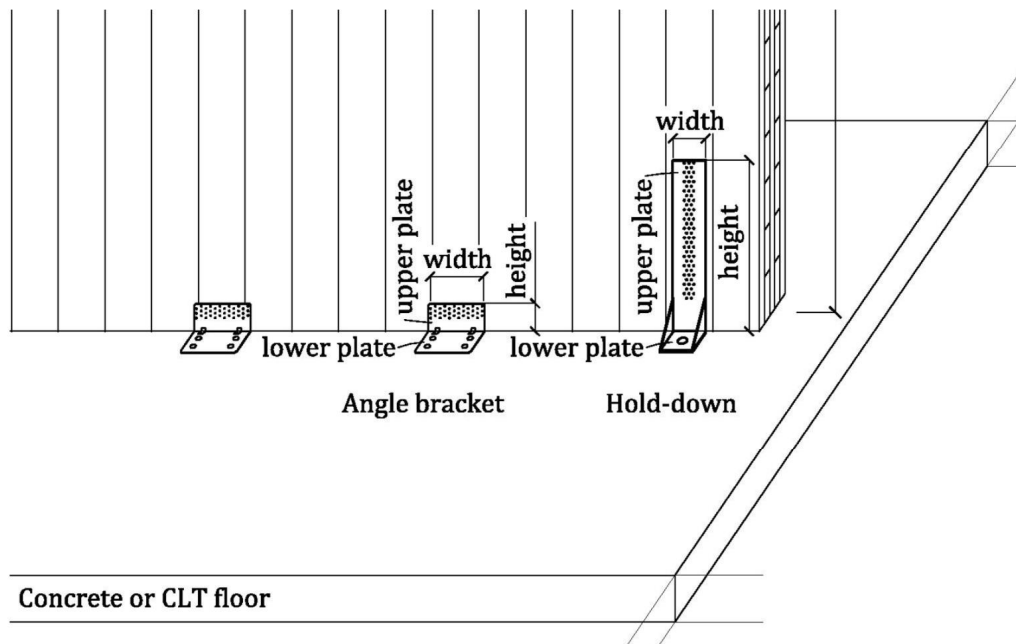


Figure 2.5 HD and SB connected to a concrete floor [29]

### 2.2.3 CLT shear walls

Popovski et al. [30] conducted monotonic and quasi-static tests on single and coupled CLT shear walls with different aspect ratios and connection types. Results showed that CLT shear walls with nails or screws and bracket connection exhibit adequate seismic performance and the existence of step joints in longer CLT shear walls enhances the ductility and reduces the wall stiffness. Popovski and Karacabeyli [31] studied CLT shear walls to determine their ductility. The finding showed that increasing the vertical load increased the wall rigidity; in addition, seismic performance and ductility of shear walls can be improved by using nails in discrete HD. It is not recommended to use diagonally positioned long screws for connecting CLT walls to the floor in seismic-prone areas due to the limited ductility of walls. An effective solution is to utilize step joints in longer walls, not only to reduce wall stiffness and thereby decrease seismic input loads but also to enhance the wall's deformation capabilities. Gavric et al. [32] tested the different anchoring systems and different types of panel-to-panel joints in coupled CLT shear walls. They observed negligible deformation in CLT, while most of the deformation occurred in connections; in addition, a parametric study regarding various aspect ratios and the number of segmentations showed a significant increase in ductility despite the decrease in stiffness and strength. Gavric et al. [33] conducted cyclic tests on CLT walls to investigate their energy dissipation. Lower elastic stiffness and strength capacity were observed in coupled wall behavior compared to single wall behavior. On the other hand, coupled wall behavior provided more displacement capacity and ductility. Sliding and rocking were the main contributing factors to wall displacement. Test results demonstrated that the presence of a vertical load on the top of the wall and HD at the edges of shear walls could control the displacement. Also, SB must remain elastic while HD participate in energy dissipation.

Amini et al. [34] conducted cyclic and shake table tests on high-aspect-ratio CLT shear walls, and a numerical model was suggested and validated using the test results. This study revealed that these shear walls might be used in the retrofit of soft storey structures. van de Lindt et al. [35] performed several quasi-static cyclic tests on some CLT shear walls with different aspect ratios in the United States. The Response Modification Factor (R factor) is a parameter used in seismic design to account for the energy dissipation and ductility of a structure during an earthquake. It represents the factor by which seismic forces are reduced when calculating the design forces for structural elements. Higher R values are associated with more ductile structures that can absorb and dissipate energy. They suggested an R factor of 3 for CLT shear walls with aspect ratios between 2:1 to 4:1. Amini et al. [36] used the FEMA P-695 procedure to identify the seismic design parameters of CLT shear walls, including response modification and overstrength factors, as well as the deflection amplification factor. The experimental result showed that connections behave nonlinearly, and the increase of gravity load on CLT shear walls leads to an increase in the stiffness and strength of the walls. Also, the aspect ratio of 4:1 resulted in less stiffness compared to the 2:1 aspect ratio, because the kinematic motion was mostly rocking instead of a combination of sliding and rocking.

#### **2.2.4 UNBC tests on CLT shear walls**

The behavior of CLT shear walls with STS connections was investigated at the UNBC Wood Innovation and Research Laboratory in Prince George [37], as illustrated in Figure 2.6. A total of 26 one-storey shear walls were tested under monotonic push-over and reverse cyclic loading. Shear walls consisted of 5-ply grade VJ-1 panels with two aspect ratios (2:1 and 3:1) and different configurations (single-panel couple-panel and triple-panel) were tested. D-Fir plywood splines were used for panel-to-panel connection, attached with partially threaded  $\varnothing 8 \times 100$  mm STSs. Two HD were used in all

configurations, these were attached to the outer edge of the shear wall. One shear bracket (SB) was installed in the middle of each panel. D-Fir plywood splines, 3000 mm x 140 mm x 25 mm, were flush mounted in rabbets. The number of screws that attached the spline to the panel in the different layouts were 11, 13, 16 or 19 per panel edge side. All HD and SB were connected with ASSY Kombi LT fully threaded STSs  $\varnothing 12 \times 120$  mm. Throughout all tests, a dead load of 10 kN/m was applied to the shear walls; the monotonic pushover tests were carried out at a loading rate of 15 mm/min until the wall resistance fell below 80% of the applied maximum force  $F_{\max}$ . Following the condensed CUREE loading history [27], the reversed cyclic tests had a target displacement of 65% of the displacement attained in the monotonic tests when the load fell to 80%  $F_{\max}$ .



*Figure 2.6. Test setup (coupled two-panel shear wall) [37]*

For the reversed cyclic testing, the maximum forces from both positive and negative phases ( $F_{\max+}$  and  $F_{\max-}$ ) were recorded. The measurements at the top right corner of the shear walls were made to determine the displacements,  $d_{F_{\max+}}$ , and  $d_{F_{\max-}}$ , corresponding to these forces. To identify the yield point (displacement  $d_y$  and strength  $F_y$ ), ultimate point (displacement  $d_u$  and strength  $F_u$ ), stiffness ( $K_c$ ), and ductility ( $\mu$ ), the equivalent energy elastic plastic (EEEP) process was utilized.

*Table 2.1. Result summary of the previous single-storey CLT shear wall tests*

Wall	Load	#STS in HD	# STS in spline	Label	$F_{\max}$ [kN]	$d_{F_{\max}}$ [mm]
Single 3 m x 1.5 m	Mon	15	-	SP1-2:1-15-M	126.2	106.5
		11	-	SP2-2:1-11-M	102.6	79.6
	Cyc	15	-	SP3-2:1-15-C	119.8	91.1
		11	-	SP4-2:1-11-C	125.0	112.1
Coupled 3 m x 1.5m	Mon	15	19	CP1-2:1-15-19-M	212.6	125.6
		13	19	CP2-2:1-13-19-M	177.8	119.8
		11	19	CP3-2:1-11-19-M	162.7	89.0
		9	19	CP4-2:1-9-19-M	168.4	99.3
		9	16	CP5-2:1-9-16-M	172.1	116.6
		9	13	CP6-2:1-9-13-M	136.6	86.0
	Cyc	11	19	CP7-2:1-11-19-C	142.4	75
		11	19	CP8-2:1-11-19-C	174.4	70
		9	16	CP9-2:1-9-16-C	149.6	70
		9	16	CP10-2:1-9-16-C	161.1	70
Coupled 3 m x 1 m	Mon	11	19	CP11-3:1-11-19-M	124.9	140.0
		9	16	CP12-3:1-9-16-M	104.3	137.0
	Cyc	11	19	CP13-3:1-11-19-C	109.7	104.1
		11	19	CP14-3:1-11-19-C	102.8	80.1
		9	16	CP15-3:1-9-16-C	89.8	80
		9	16	CP16-3:1-9-16-C	93.6	104.1
Triple 3 m x 1 m	Mon	11	19	TP1-3:1-11-19-M	155.2	95.9
		9	16	TP2-3:1-9-16-M	148.6	138.6
	Cyc	11	19	TP3-3:1-11-19-C	147.5	80.1
		11	19	TP4-3:1-11-19-C	150.6	104.1
		9	16	TP5-3:1-9-16-C	124.4	80.1
		9	16	TP5-3:1-9-16-C	138	104.1

The strength and stiffness of the connections increased linearly with the number of screws. In comparison, the design values of STSs derived from connection tests under cyclic loading were roughly three times higher than those calculated according to CSA O86. This highlights a significant level of over-design in energy-dissipating connections, indicating that they may not fulfill their intended purpose when designed according to CSA O86.

Furthermore, the strength and associated displacement of the shear walls showed a consistent decline as the number of screws in the HD configuration decreased. This linear decline in strength was also evident in the spline joints connections. The aspect ratio of the coupled shear walls played a crucial role; specifically, when the aspect ratio was 2:1, load-carrying capacity and stiffness were increased by 40% and 80% respectively while, a 30% reduction in deformation capacity in these configurations with a 2:1 aspect ratio was observed.

### **2.2.5 Full-scale CLT building tests**

Ceccotti et al. conducted the most extensive research, named SOFIE, on CLT buildings regarding their seismic behavior, fire, and durability. Three full-scale structures (one-storey, three-storey, and seven-storey), as illustrated in Figure 2.7a, were subjected to earthquakes using a 3D shake table. The findings showed that CLT panels behave as rigid bodies while connections dissipate energy. Moreover, the pattern, type, and number of the connectors significantly affected the behavior of CLT shear walls. [38]

At FPInnovations, Popovski and Gavric [39] performed monotonic and cyclic tests on a two-storey CLT structure to study the behavior of the structure, see Figure 2.7b. The finding showed that the type and number of fasteners and panel aspect ratio affect the displacement behavior of shear walls. The primary goal of the test was to study the 3-D

structural behavior of the CLT structure under lateral loads. The tested structures showed satisfactory behavior in accordance with the design objectives. The failure mechanism was similar in all tests, despite changing the number of screws in perpendicular panel-to-panel connections, different numbers of HD, and the direction of loading. Sliding, and rocking of the first storey panels resulted in shear failure of the nails in the brackets that finally caused structure failure. After reaching the maximum force, no global instabilities were observed, though. In addition, torsion was found not to have significant viable effects on the structures' stability, integrity, and lateral resistance. Almost no slip between the floor panels was witnessed as a result of the floor diaphragm's rigid behavior. Corner vertical connections exhibited completely rigid behavior, and a significant contribution to the stiffness and the strength of the structure was observed due to presence of transverse walls. Also, the existence of the window in the wall panel did not affect the rigidity of the walls, while the presence of the doors and windows led to in-plane flexibility.

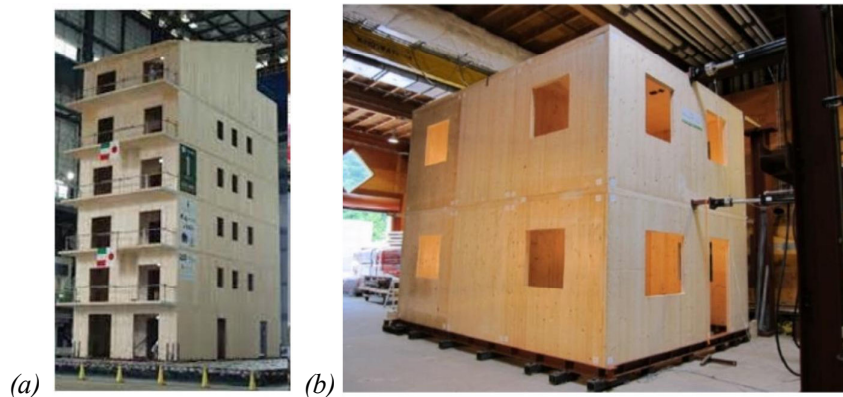


*Figure 2.7 CLT structure tests: a) SOFIE project [38]; (b) FPInnovations [39]*

Van de Lindt et al. [40] performed shake-table tests on a full-scale two-storey building with CLT shear walls. The R-factor for this structure was equal to 4, and the design was done in accordance with the lateral force procedure specification of ASCE7-16 [41]. Different panel aspect ratios, different walls, and the effect of transverse walls were

studied. The result revealed that all tests had passed the safety level required by the code, and the presence of the transverse wall did not eliminate the rocking of the shear walls and resulted in better performance of the structural system. The study demonstrated the feasibility of combining a CLT rocking-wall system with a heavy-timber gravity system to obtain an improved seismic performance during earthquakes.

Limited knowledge stems from shaking table tests on full-scale CLT buildings, mostly exhibiting a maximum inter-story drift below 4%. To bridge this gap, Momose and Isoda performed a study on a two-story shake table experiment with a maximum drift of 8.77%, utilizing author-developed analysis software to replicate seismic behavior at large deformations. The proposed analytical method consistently matched experimental results for both overall and detailed behaviors of CLT buildings. [42]

Isoda et al. examined common wide-panel walls with openings for windows and doors in full model CLT buildings, finding that corner cracks at these openings are the primary failure mechanism under lateral loads. Investigating crack initiation and propagation, bending tests on L- and T-shape specimens and three-point bending and shear tests on beam sections revealed three types of brittle failure: bending failure of the beam or column, and rolling shear failure.[43]

## **2.3 Design of CLT shear walls**

### **2.3.1 Analytical models**

CLT shear walls are designed by determining their stiffness and load-bearing capacity, using equilibrium equations that consider the geometry of walls, external load, and connection properties. Lukacs et al. [44] compared various approaches to determine the stiffness and capacity of CLT shear walls. Most of them provide the analytical procedure based on the static equilibrium equation. The CLT panels are assumed to be rigid bodies,

and the deformation of the system is dependent on the characteristics of the connections. Also, sliding and uplift are carried by SB and HD; therefore, they are considered in all procedures. Shahnewaz et al. [45] suggested an analytical formulation for a single-panel CLT shear wall by considering the bi-lateral behavior of shear connections in CLT shear walls. Shahnewaz et al. [46] investigated the lateral resistance of CLT shear walls in platform-type CLT buildings. They offered formulas in accordance with the type of kinematic motion (rocking or a combination of rocking and sliding) for single and coupled walls to identify the in-plane resistance of CLT shear walls. Both single and coupled panels used different configurations of HD and SB.

Nolet et al. [47] presented an analytical method to predict the non-linear behavior of multi-panel CLT shear walls and showed that the panel aspect ratio and connection properties are the most influential factors. Casagrande et al. [48], using the minimum total potential energy principle, predicted the mechanical behavior of one-storey multi-panel CLT shear walls. The results gained from the kinematic model show that when stiff HD are applied, each panel has its center of rotation, while applying the flexible HD leads to increasing uplift in the multi-panel shear wall.

### **2.3.2 Design provisions in Canada**

Building structural design in Canada must adhere to the objective-based National Building Code of Canada [1]. A design specification that would cover CLT produced in accordance with the ANSI/APA PRG 320 standard [49] had been reserved for CSA O86 Clause 8 in 2014 [50]. Two years later, CSA-O86 [51] was updated with design guidelines for CLT elements and connections and Clause 11.9 "Design of CLT shear walls and diaphragms". These requirements were limited to platform-type constructions with a maximum height of 20 m in high seismic zones and no more than 30 m in low seismic

zones. For the CLT panels to develop their desired kinematic motion, the energy dissipative connections must be designed in such a way that: i) yield mode governs, ii) at least moderate ductility at the connection level is achieved, and iii) adequate deformation capacity is offered. The aspect ratio of all CLT shear wall segments that are regarded to be a part of the LLRS was limited to 2:1 to 4:1 and sliding should be avoided. Prior to CSA O86 2019 [52], discrete HD could be considered as a dissipative connection, but it is now required that they be designed as a non-dissipative connection.

Using capacity design techniques, a structure can be built to sustain earthquake loads while ensuring that certain ductile components undergo inelastic deformations while brittle components are capacity protected. The vertical joints between walls, shear connections between shear walls and the foundation, and shear connections between shear walls and the floors below should be the only dissipative elements. All non-dissipative connections and CLT panels are intended to continue to be elastic under the force and displacement requirements created when energy-dissipative connections reach the 95<sup>th</sup> percentile of their ultimate resistance or target displacement. However, for multi-panel CLT walls, where the overall behavior may be a result of connection behavior, CSA O86 does not yet provide any specific methods for predicting LLRS resistance.

### **2.3.3 Design provisions in the United States**

The ANSI/APA PRG320 (ANSI 2017) [49] standard promoted the inclusion of a CLT chapter in the 2015 edition of the National Design Specification for Wood Construction (NDS) [53] and the adoption of CLT in the 2015 International Building Code [54]. The NDS requirements are used to establish the design shear strength of CLT shear walls and diaphragms.

In contrast to conventional wood-frame shear wall and diaphragm systems, the calculated shear strength for CLT shear walls and diaphragms relies directly on fundamental engineering mechanics principles. This determination incorporates the guidelines of the National Design Specification for Wood Construction for both connection design and CLT panel design. When estimating deflection, it is essential to consider all potential sources, such as panel bending, panel and/or connector shear, and fastener deformation. These deflection estimates are either based on fundamental engineering mechanics principles or derived from relevant testing.

The 2021 IBC [55] contains clauses that permit the use of mass-produced wood products or non-combustible materials under Types IV-A, IV-B, and IV-C. These types have greater fire resistance ratings and non-combustible protection levels than the preceding heavy timber construction type (now known as Type IV-HT). The code defined guidelines for the construction of mass timber structures up to 18 stories tall with Type IV-A occupancy for commercial and residential purposes. A comprehensive set of performance-based code modifications for mass timber buildings are included in the IBC. Although LLRS are included in the code, there are considerable limitations. In the IBC and ASCE 7-16 [41], wood frame plywood shear walls were essentially the only permitted timber lateral system. Additionally, the 2021 NDS [53] Special Design Provisions for Wind and Seismic (SDPWS) address CLT lateral systems and the 2022 version of ASCE 7 [56] includes seismic design provisions for CLT shear walls.

#### **2.3.4 Design provisions in Europe**

Even though CLT was developed in Europe more than 20 years ago, there are no design regulations for CLT structures other than the product regulation. The future Eurocode 8 [57] will include CLT [58] [59], with two behavior factor  $q$  values for medium and high

ductility, CLT structures will be classified as dissipative structures therefore, CLT is poised to be increasingly recognized and embraced as a viable option for lateral load-resisting frames, gaining widespread popularity in structural applications. Constructions made of monolithic CLT wall elements will be separated from those made of "segmented" CLT walls, which are composed of multiple panels connected by mechanical fasteners like STS. It's important to note that the number of stories will not be restricted. According to the capacity-based methodology, the following components need to be constructed with overstrength: (i) CLT panels; (ii) joints between floor panels; (iii) joints between floors and walls below; and (iv) joints between perpendicular walls. The HD inserted at wall ends and at wall openings, as well as the shear joints between walls and the floor underneath them and between walls and the foundation, are all intended to dissipate energy. Additionally, the vertical connections between subsequent wall panels within segmented shear walls should be taken into consideration as dissipative [58].

### **2.3.5 Recent proposal for capacity-based design of CLT shear walls**

The current O86 guidance for CLT does not provide specific guidance on the hierarchy of connection types. A methodology for a yielding hierarchy between dissipative and non-dissipative connections was presented by Casagrande et al. [60]. The proposal provides specific design recommendations for each type of connection. Three ductility classes serve as the foundation for the proposed capacity-based design methodology. Three different over-strength factors are also defined:  $\alpha_{nd}$ , which protects non-dissipative components when dissipative connections yield,  $\alpha_d$ , which ensures a sequence of yielding among dissipative connections, and  $\alpha_s$ , which protects shear connections and restricts sliding. Level 1 of the ductility class is assigned to CLT structures made up of either single or multi panel shear walls that are intended to respond elastically and do not

require the dissipative components, or all elements that are designed not to yield. HD are considered to be the main dissipative elements in Level 2 that are single panel or multiple panels shear walls and show SW rocking behavior primarily. However, vertical joints may be assumed to act as either a dissipative or non-dissipative component in the case of multi-panel shear walls. When connections mostly dissipate energy by fastener yielding and the kinematic behavior of the wall is CP rocking, the ductility class reaches Level 3. The criterion that HD yields after the vertical joints have already yielded guarantees that CP, rather than SW, rocking behavior is attained. Either Level 2 or 3 demand the over-design of components with restricted ductility [60].

## **2.4 Summary of literature review**

As CLT is becoming more common; Multi-storey CLT structures in either platform- or balloon-type applications, have become a practical reality, even in seismically active areas, thanks to their lightweight and the dissipative response of CLT shear walls connections. CLT panels, as rigid bodies, cannot dissipate energy during earthquakes, requiring a further understanding of their connections that contribute to the energy dissipation and analytical approaches to predict their behavior.

The seismic performance of CLT buildings has been a focus of numerous studies for the past 20 years. The kinematic motion of various configurations of CLT shear walls, including single-panel and couple-panel, is another research topic that has been recently under the spotlight. Vertical joints have been observed as the primary energy dissipation mechanism for CLT shear walls; multi-panel shear walls exhibited higher ductility and energy dissipation ability. Greater aspect ratio panels have substantially more deformation capacity but much less rigidity.

The review also notes that most of the studies on CLT shear walls have focused on single-storey structures with conventional connections and one of the missing areas is multi-storey CLT buildings. Primarily the SOFIE and FPInnovations projects investigated multi-storey CLT buildings; but they have used conventional CLT connections. To address this gap and gain a deeper understanding of the behavior of multi-storey CLT buildings, experimental tests were conducted on the STS connections in two-storey CLT structures. These tests included tension straps that vertically connect the stories and shear brackets on the second storey that connect the 2<sup>nd</sup> storey walls to the 1<sup>st</sup> floor. Additionally, the study examined the impact of applying an acoustic layer that is used in some CLT structures, focusing on its effects on lateral displacement and load-carrying capacity, along with considering the influence of perpendicular shear walls.

### 3 Two-storey CLT shear wall tests

#### 3.1 Objective

The objective of the experimental investigations was to evaluate the seismic performance of platform-type two-storey CLT shear walls. The specific objectives were to investigate the effects of:

- 1) Different tension strap connections between floors;
- 2) Different shear connections between floors;
- 3) Presence acoustic insulation layers; and
- 4) Presence of perpendicular CLT shear walls.

#### 3.2 Description of two-storey structures

The structures were 1.5 m x 2.0 m in plan and 5.3 m tall. The shear walls were 2.5 m tall, and the first and second storey slab thicknesses were 0.139 m. A representative photo is shown in Figure 3.1, the plan and elevations of the structure are shown in Figure 3.2.



Figure 3.1. Two-storey CLT structure

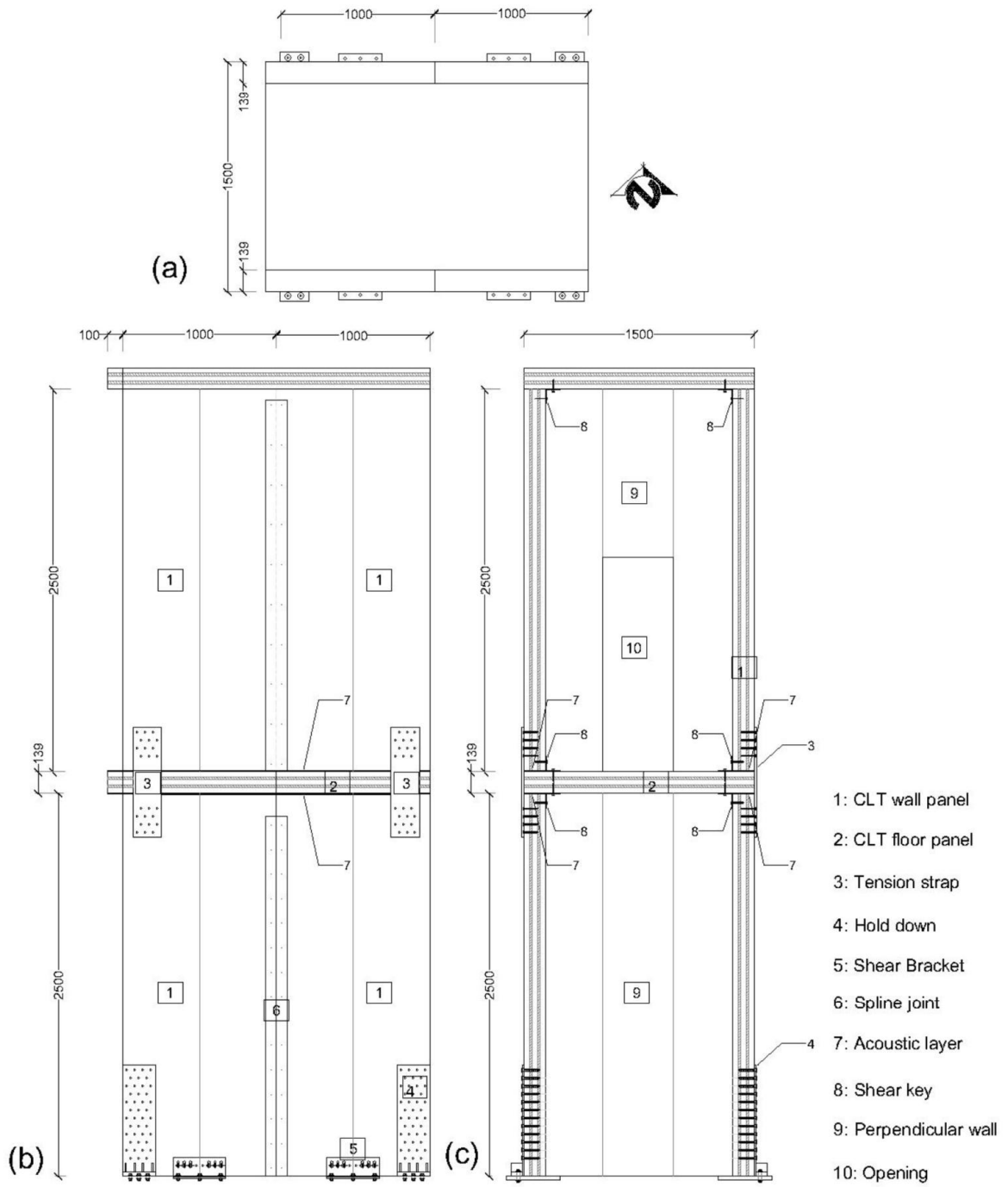


Figure 3.2. Two-storey CLT structure a) plan, b) front view, c) side view

### 3.3 Materials

#### 3.3.1 CLT panels

The CLT panels were strength grade V2.2, 5-ply, 139 mm thick (35+17+35+17+35), 2.5 m tall and 1.0 m wide for an aspect ratio of 2.5:1. The average moisture content and apparent density of the CLT were measured as 10.6% and 475 kg/m<sup>3</sup>, respectively.

#### 3.3.2 Spline joints

The panel-to-panel vertical connections were surface mounted 25 mm × 140 mm × 2500 mm D-Fir plywood splines attached to the panel with partially threaded  $\varnothing 8 \times 100$  mm STSs as shown in Figure 3.3 [20]; the edge distance of the screws and the spacing between the screws were 30 mm and 150 mm, respectively. The splines were attached to the panels with 16 and 11 STSs in the first and 2<sup>nd</sup> floor, respectively, per panel edge side (total per spline 22 and 32, respectively).

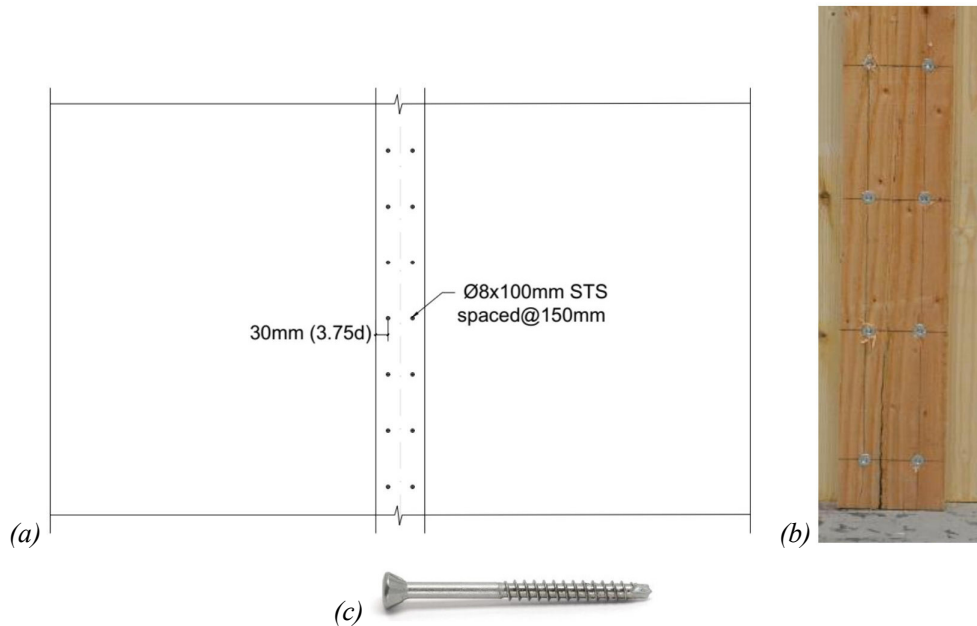


Figure 3.3. Spline joint in CLT shear walls a) sketch, b) photo, c) ASSY ECO screw

### 3.3.3 Hold downs

HD were made of custom steel plates of grade 44W/300W. The HD were 212 mm wide, 719 mm high, with a 70 mm long base plate, thickness equal to 12.7 mm (vertical part) and 25 mm (base plate). 42  $\varnothing$  13 mm holes were prepared in the vertical part for installing STSs while 21 fully-threaded STSs  $\varnothing$  12  $\times$  120 mm [20] were installed; the base plate had 3  $\varnothing$  19 mm holes for installing bolts to the foundation, see Figure 3.4.

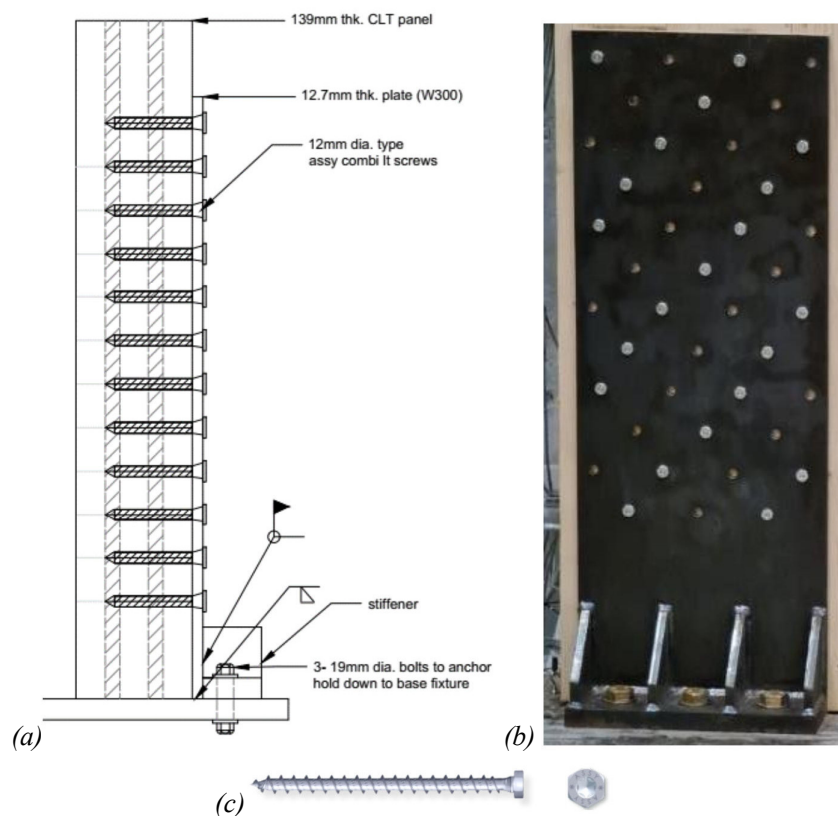


Figure 3.4. HD: a) side view, b) photo c) ASSY Kombi LT STS [3]

### 3.3.4 Tension straps

Tension straps vertically connected the shear walls over the two stories; these were made of custom steel plates of grade 44W/300W. The tension straps were 186 mm wide, 713 mm or 929 mm high, thickness equal to 4.8 mm.

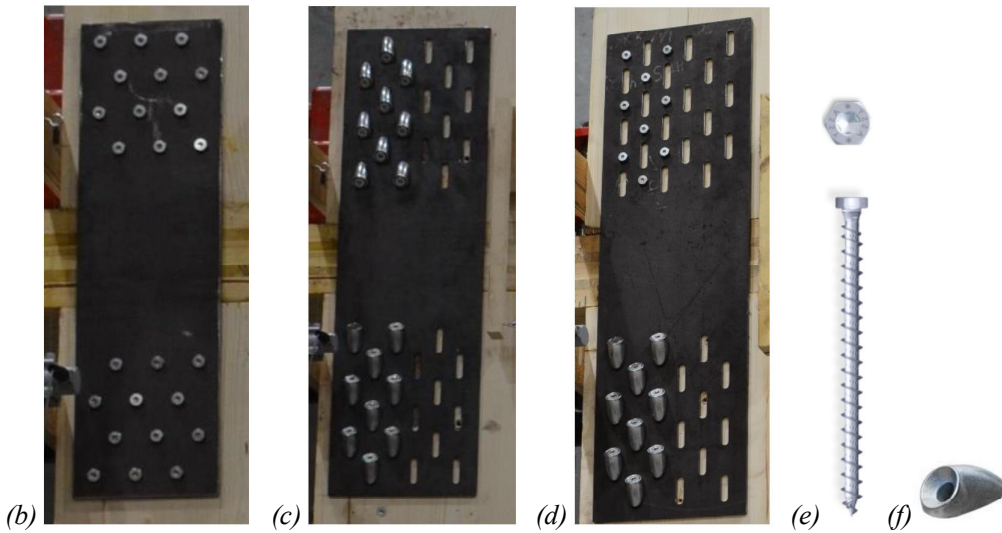
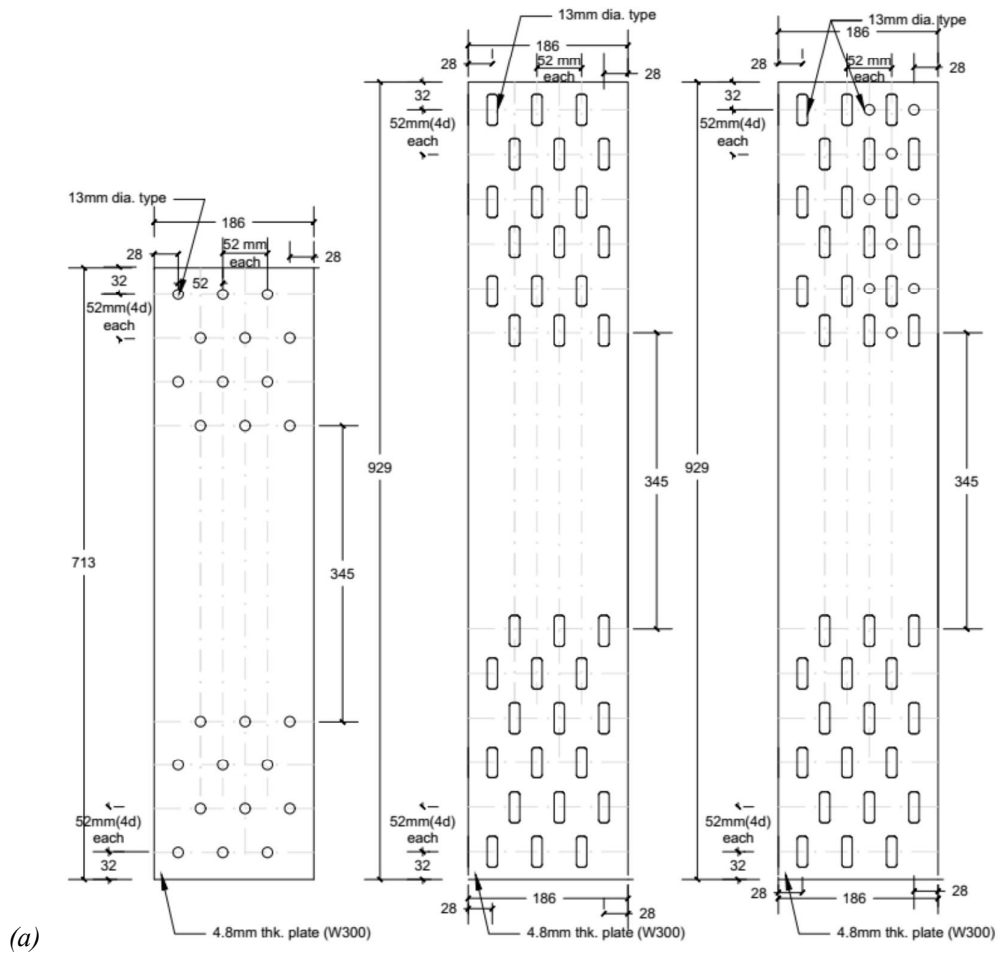


Figure 3.5. Tension strap: a) sketch; b) photo type 1, c) photo type 2; d) photo type 3, e) ASSY Kombi LT STS used in tension strap, f) 45° washer [3]

According to the literature in CLT connections the most ductility was observed in STS inclination angle of  $90^\circ$  compared to inclined STS with  $45^\circ$ . [22] In order to observe the effect of ductility two inclination angles of  $45^\circ$  and  $90^\circ$  for fasteners in tension strap were tested. One type for installing all screws at  $90^\circ$  angle had a total of 24  $\varnothing 13$  mm holes; in these 8, 9 or 12  $\varnothing 12$  mm  $\times$  120 mm fully-threaded ASSY Kombi LT STSs [20] were installed at each end (Figure 3.5 a, b). The second type for installing all screws at  $45^\circ$  had a total of 36  $\varnothing 13$  mm slots where 9  $\varnothing 12 \times 160$  mm ASSY VG STSs [20] were installed at each combined with  $45^\circ$  washers (Figure 3.5c). A third type consisted of a combination of both inclination angles, where a total of 36  $\varnothing 13$  mm slots and 9  $\varnothing 13$  mm holes were prepared and 9  $\varnothing 12 \times 160$  mm ASSY VG STSs [3] with the angle of  $45^\circ$  were installed in the bottom of tension strap while 9  $\varnothing 12 \times 120$  mm ASSY Kombi LT STSs with  $90^\circ$  angle were on the top of tension strap (Figure 3.5d).

### **3.3.5 Shear brackets**

SB were made of custom steel plates of grade 44W/300W. The SB was 340 mm wide with a length of the vertical and horizontal plate equal to 127 mm and 89 mm, respectively, and a constant thickness of 6.35 mm.

It had 8 vertical slots, 11 mm wide for installing the STSs to eliminate any uplift resistance so that only shear is resisted. ASSY Kombi LT screw  $\varnothing 12 \times 120$  mm was used as fastener for SB, see Figure 3.6 a and b. Two types of connectors were used in the SB, either 3 STSs were used in each sides of the SB as shown in Figure 3.6 c and d; or the SB was attached by 4, 6 or 8 STSs on the vertical leg while, while 3 bolts were installed on the horizontal leg (Figure 3.6d).

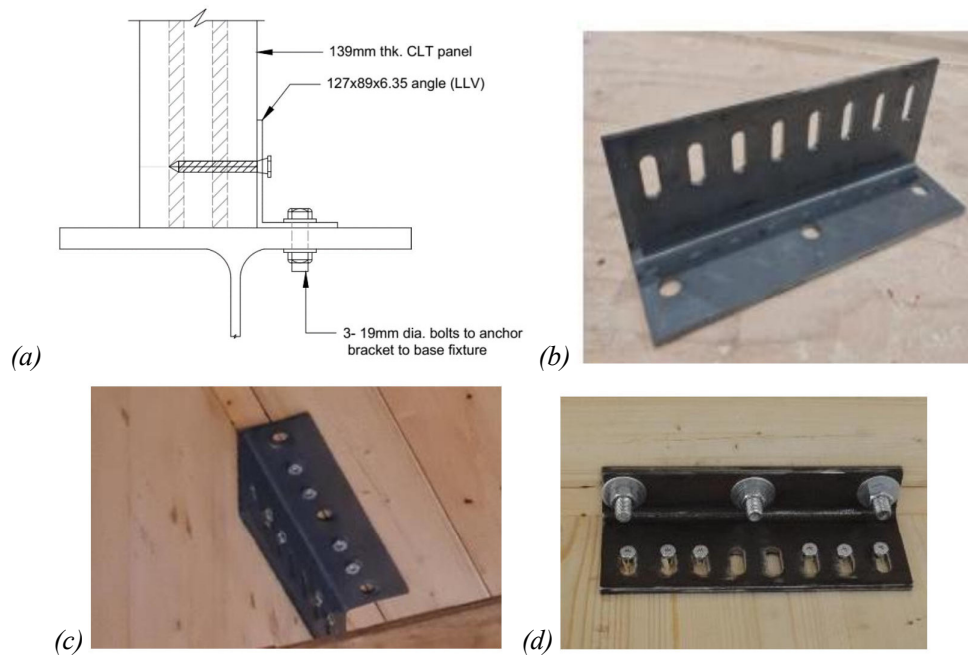


Figure 3.6. Custom SB: a) side view; b) photo; c) type 1, attached by STSs on both sides; d) type 2, attached by bolts and STSs

### 3.3.6 Acoustic separation layers

The material that was used as an acoustic separation layer was Xylofon [61]. It is a high-performance resilient profile that is designed to reduce flanking sound transmission in platform CLT building. Made of a polyurethane compound, it is available in from 35 to 90 shore (hardness measurement scale used for the Xylofon material) depending on the bearing load. In this study 50 shore was selected. The width of the layer is 140 mm with the thickness of 6 mm, see Figure 3.7.

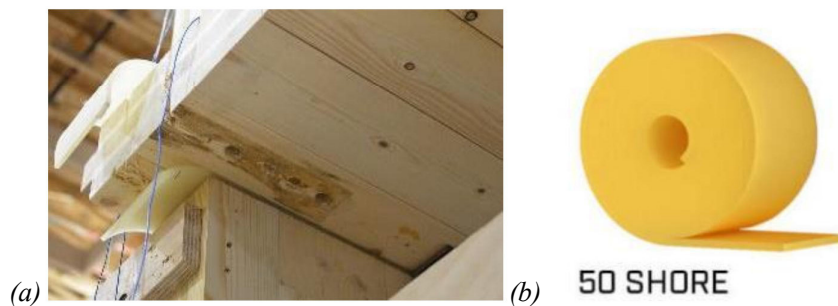


Figure 3.7. Acoustic separation layer Xylofon type 50 SHORE: a) photo; b) sketch[61]

### 3.4 Test series overview

Testing was conducted four structures, with Structure #1 subjected to three tests, while the other structures (structure #2, #3 and #4) underwent two tests each. In total, nine tests were performed on the four structures. The four structures had the same connections for spline joints, SB, and HD; the different parameters, as summarized in Table 3.1, were as follows:

**In structure #1** three tests were conducted on this structure: **#H1a** and **#H1b** were subjected to monotonic loading and **#H1c** reversed cyclic loading. the top SBs of the first level floor had 3 bolts + 6 STSs, while bottom and top SBs of the 2<sup>nd</sup> level floor had 3 bolts + 4 STSs. Notably, in the structures **#H1a** and **#H1b** there were no SBs on the top of the 2<sup>nd</sup> level, and the floor panel was attached to the underlying shear walls using STSs applied perpendicular to the roof panel. Tension straps were attached with 8 STSs installed at 90° (Figure 3.8b). No additional dead load was applied.

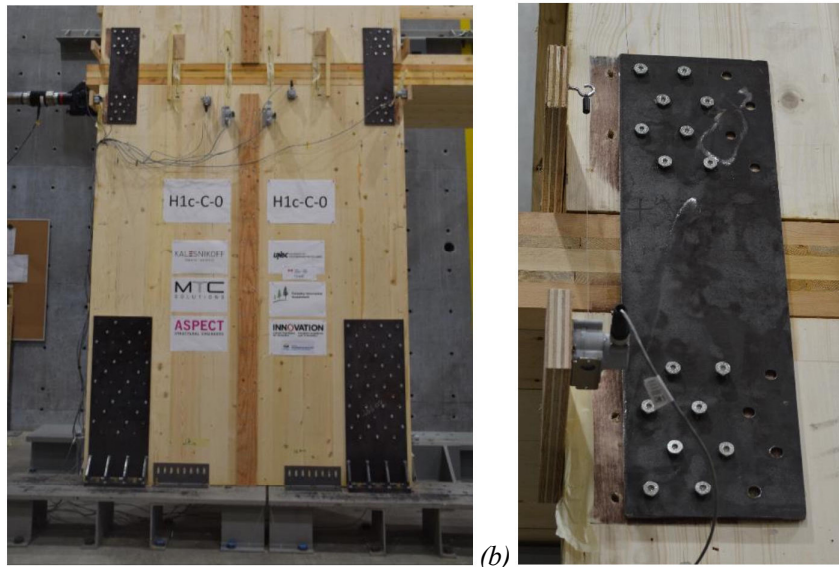
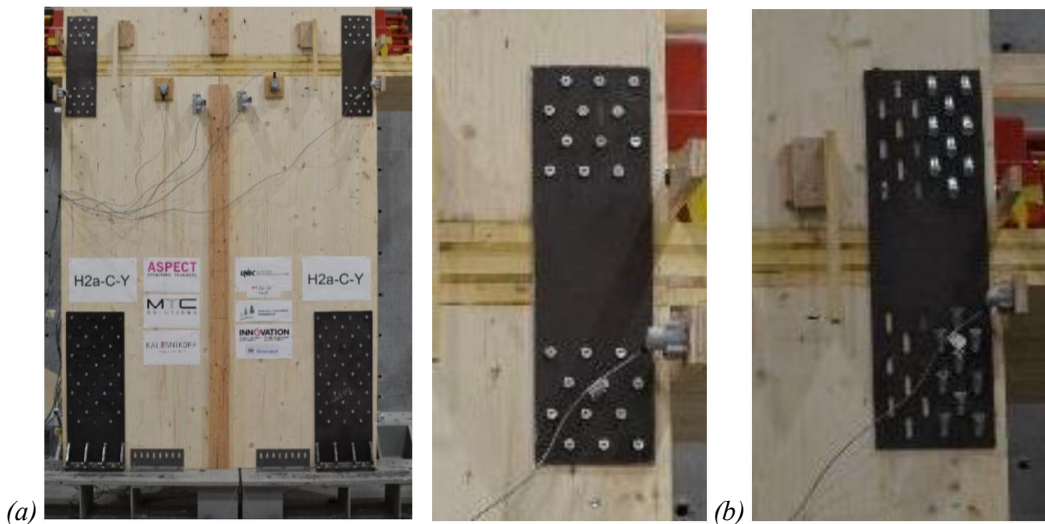


Figure 3.8. Structure #1c: a) full view, b) TS with perp. screws

**In structure #2**, the top SB of the first storey had 3 bolts + 6 STSs, the bottom SB of the 2<sup>nd</sup> storey had 3 bolts + 4 STSs, while the 2<sup>nd</sup> level floor SB had 3 bolts + 8 STSs. A dead load of 2 tons was applied to each floor, and both tests were conducted under reversed cyclic loading tests. Two tension strap STS installation angles were compared: **#H2a** 12  $\phi$  12 mm x 120 mm STSs were installed at 90° (Figure 3.9a); and **#H2b** 9  $\phi$  12 mm x 160 mm STSs were installed at 45° as shown in Figure 3.9b.



*Figure 3.9. Structure #2: a) test H2a with perp. screws; b) test H2b with 45° inclined screws*

**In structure #3**, the tension straps were connected by 9  $\phi$  12 mm x 160 mm STSs installed at 45° on the lower level, while it had 9  $\phi$  12 mm x 120 mm STS installed at 90° on the upper shear wall, as shown in Figure 3.10b. The bottom SB of the 2<sup>nd</sup> storey had 3 bolts + 6 STSs; the 2<sup>nd</sup> level floor SB had 3 bolts + 8 STSs. A dead load of 2 tons was applied to each floor, and both tests were conducted under reversed cyclic loading tests. The effect of different shear connections between floors was investigated: **#H3a** had 3 bolts + 6 STSs in the top SB of the first storey as shown in Figure 3.10c; and **#H3b** had 6 STSs on each side of the SB, see Figure 3.11c.

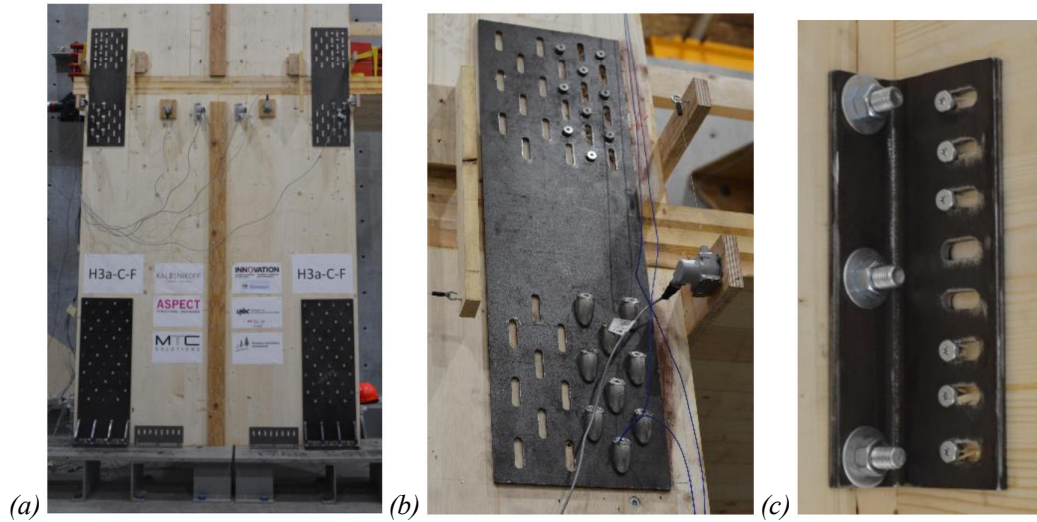


Figure 3.10. Structure #3a: a) full view, b) tension strap with perp. and 45° inclined screws; c) SB with bolts and STSs

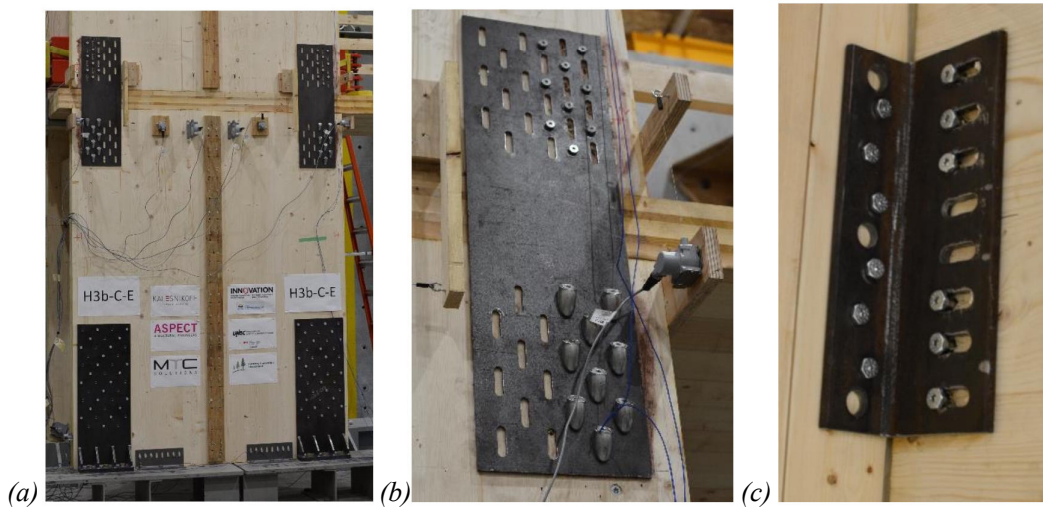


Figure 3.11. Structure #3b: a) full view, b) tension strap with perp. and 45° inclined screws; c) SB with STS on both legs

The tests conducted in the current study were a continuation of the single-storey shear wall tests at UNBC; therefore, the number of screws in connections was selected in such a way that the results could be compared with each other. The number of screws in HDs and spline joints in the 1<sup>st</sup> storey were identical in two test series, while the number of

screws in the 2<sup>nd</sup> floor was less than 1<sup>st</sup> floor due to less storey shear. These values are presented in the Table 3.1.

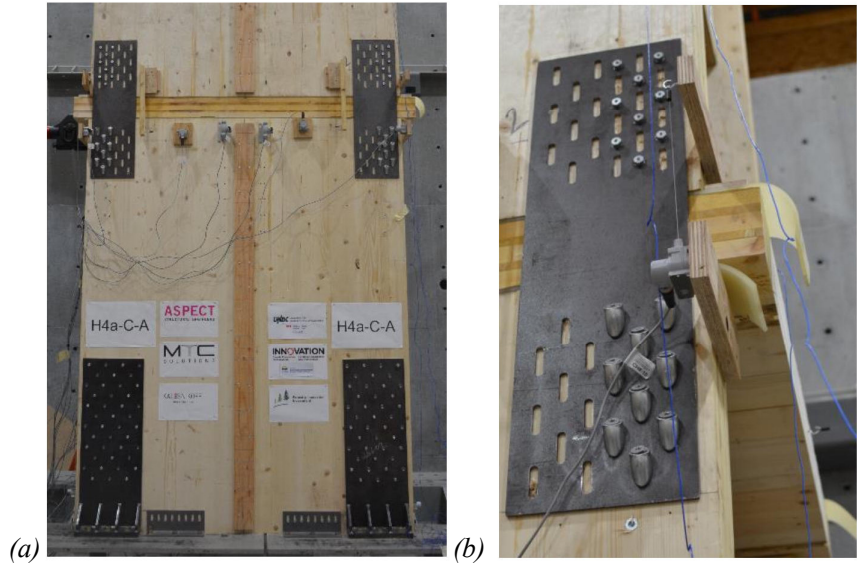


Figure 3.12. Structure #4a: a) full view, b) test H4a with acoustic layer

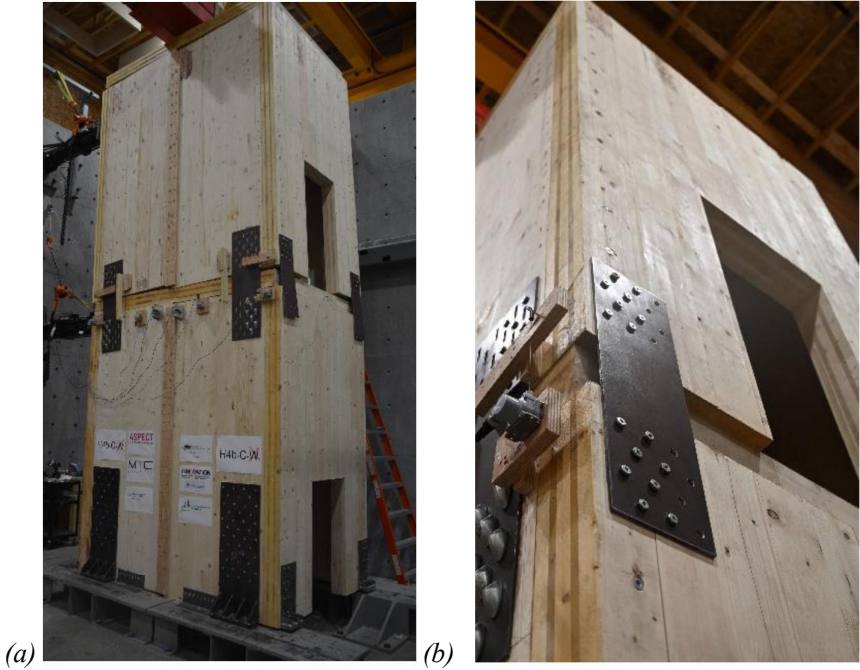


Figure 3.13. Structure #4b: a) full view; b) test H4b perpendicular shear walls

Table 3.1. Test parameters

Test	Load	1 <sup>st</sup> level bottom SB	1 <sup>st</sup> level top SB	2 <sup>nd</sup> level bottom SB	Tension strap bottom	Tension strap top	Dead load	End wall	Ac. mat
H1a-M-0	Mon	3 Bolts + 6 s	3 Bolts + 4 STSs	None <sup>1</sup>	8x STSs 1 2 x 1 2 0	8x STSs 12x120 @9 0 °			
H1b-M-0	Mon	3 Bolts + 6 STSs	3 Bolts + 4 STSs	None <sup>1</sup>	8x STSs 1 2 x 1 2 0	8x STSs 12x120 @9 0 °			
H1c-C-0	Rev. Cycl	3 Bolts + 6 STSs	3 Bolts + 4 STSs	3 Bolts + 4 STSs	8x STSs 12x120@90 °	8x STSs 12x120 @9 0 °			
H2a-C-Y	Rev. Cycl	3 Bolts + 6 STSs	3 Bolts + 4 STSs	3 Bolts + 8 STSs	12x STSs 1 2 x 1 2 0	12x STSs 12x120 @9 0 °	2+2 tons		
H2b-C-P	Rev. Cycl	3 Bolts + 6 STSs	3 Bolts + 4 STSs	3 Bolts + 8 STSs	9x STSs 1 2 x 1 6 0	9x STSs 10x160 @4 5 °	2+2 tons		
H3a-C-F	Rev. Cycl	3 Bolts + 6 STSs	3 Bolts + 6 STSs	3 Bolts + 8 STSs	9x STSs 1 2 x 1 6 0	9x STSs 12x120 @9 0 °	2+2 tons		
H3b-C-E	Rev. Cycl	6 STSs + 6 STSs	3 Bolts + 6 STSs	3 Bolts + 8 STSs	9x STSs 1 2 x 1 6 0	9x STSs 12x120 @9 0 °	2+2 tons		
H4a-C-A	Rev. Cycl	6 STSs + 6 STSs	3 Bolts + 6 STSs	3 Bolts + 8 STSs	9x STSs 1 2 x 1 6 0	9x STSs 12x120 @9 0 °	2+2 tons		X
H4b-C-W	Rev. Cycl	6 STSs + 6 STSs	3 Bolts + 6 STSs	3 Bolts + 8 STSs	9x STSs 1 2 x 1 6 0	9x STSs 12x120 @9 0 °	2+2 tons	X	
H4c-C-N	Rev. Cycl	6 STSs + 6 STSs	3 Bolts + 6 STSs	3 Bolts + 8 STSs	9x STSs 1 2 x 1 6 0	9x STSs 12x120 @9 0 °	2+2 tons		

Note 1) Tests #H1a and #H1a did not have SBs at the 2<sup>nd</sup> level floor and shear was transferred through STSs between roof panel and underneath shear walls.

## 3.5 Methods

### 3.5.1 Assembly

The structures were constructed on a steel base fixture that was bolted down to a reaction floor (Figure 3.14a) by using a crane CLT walls were lifted and put on the base fixture (Figure 3.14b). The CLT panels were connected to the base fixture using SB and HD.



*Figure 3.14. Assembly of structure: a) steel base fixture, b) installation of walls on base, c) installing 1<sup>st</sup> level floor panel and weights, d) adding pre-assembled 2<sup>nd</sup> storey*

The structures were built in a platform style that means first storey ceiling panels were the base for the 2<sup>nd</sup> storey walls. To simulate the dead loads, additional masses of 2 ton on each floor slab were applied on the floor, (Figure 3.14c) and finally the pre-assembled

2<sup>nd</sup> storey consisted of walls and 2<sup>nd</sup> level floor panel rests on the top of the first storey panel as shown in Figure 3.14d. In the first structure tests no additional weight was applied while weights of 2 tons on each floor slab were applied in the other tests.

### 3.5.2 Instrumentation

There was a total of 32 sensors installed to measure:

- Load and stroke from the actuators;
- Horizontal displacement of the 1<sup>st</sup> and 2<sup>nd</sup> storey slabs (#1, and #2);
- Sliding against steel base fixture in the base level (#12, and #28);
- Sliding over intermediate diaphragm (#16, #19, #21, and #22);
- Sliding at top of structure “ 2<sup>nd</sup> level ” (#5, and #31);
- Uplift of shear walls at HD (#11, #16, #27, and #32);
- Uplift of tension straps (#5, #21, #10, and #26);
- Uplift of inner corners of the 1<sup>st</sup> storey panels (#13, #14, #29, and #30);
- Uplift of inner corners of the 2<sup>nd</sup> storey panels (#7, #8, #23, and #24);
- Relative slip between wall panels (#4, #20 for 1<sup>st</sup> storey, #3, #19 for 2<sup>nd</sup> storey);
- Distortion of the CLT panels (#17, and #18);

Three types of measurement instruments were used in the tests: two types of string pots, and one type of a Linear Variable Differential Transducer (LVDT). Half of the sensors were installed on the North side and half of them on the South side shear walls. The sensor locations are illustrated in Figure 3.15 and selected sensors are shown in Figure 3.16.

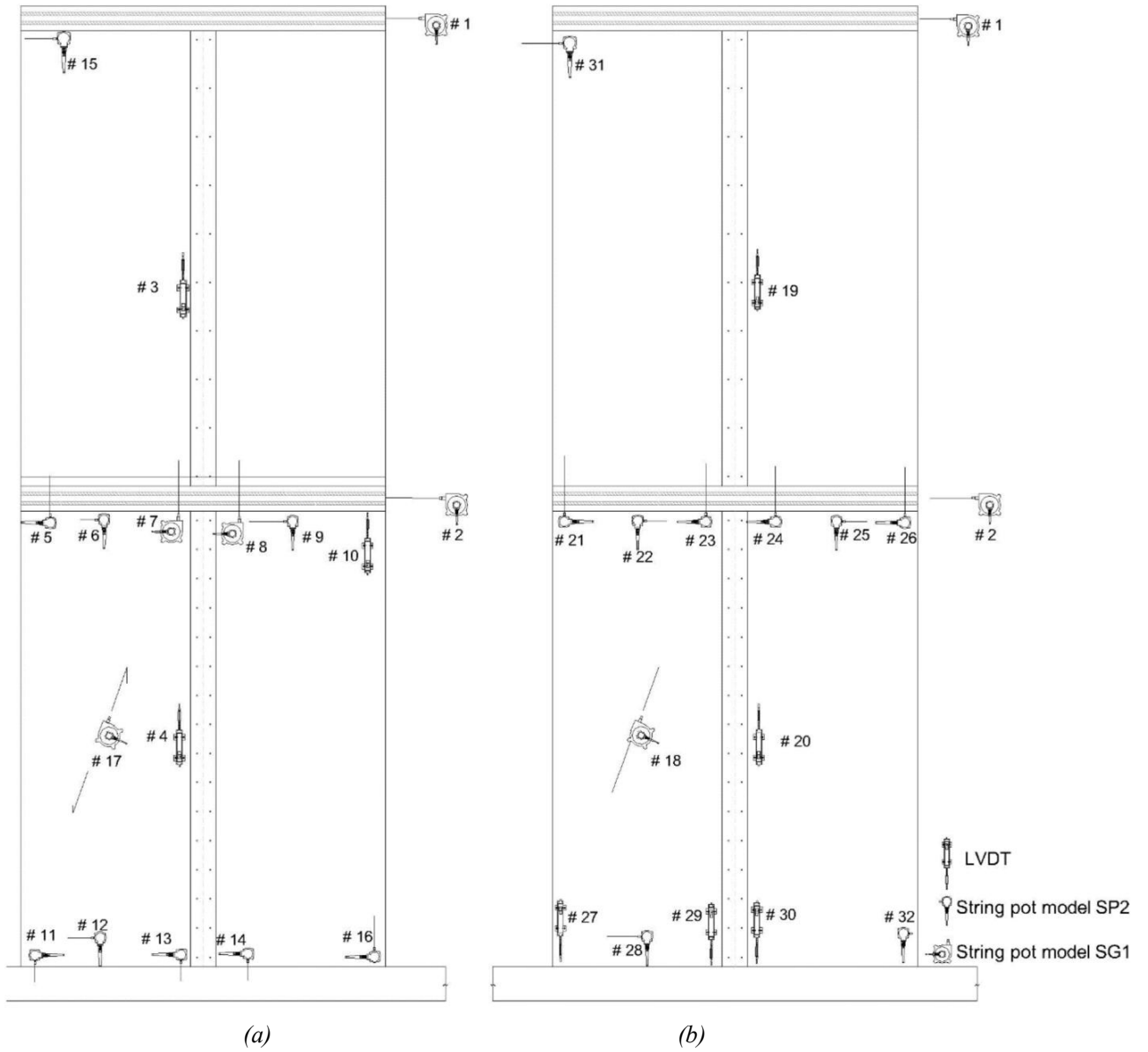


Figure 3.15. The location of sensors: a) south face b) north face

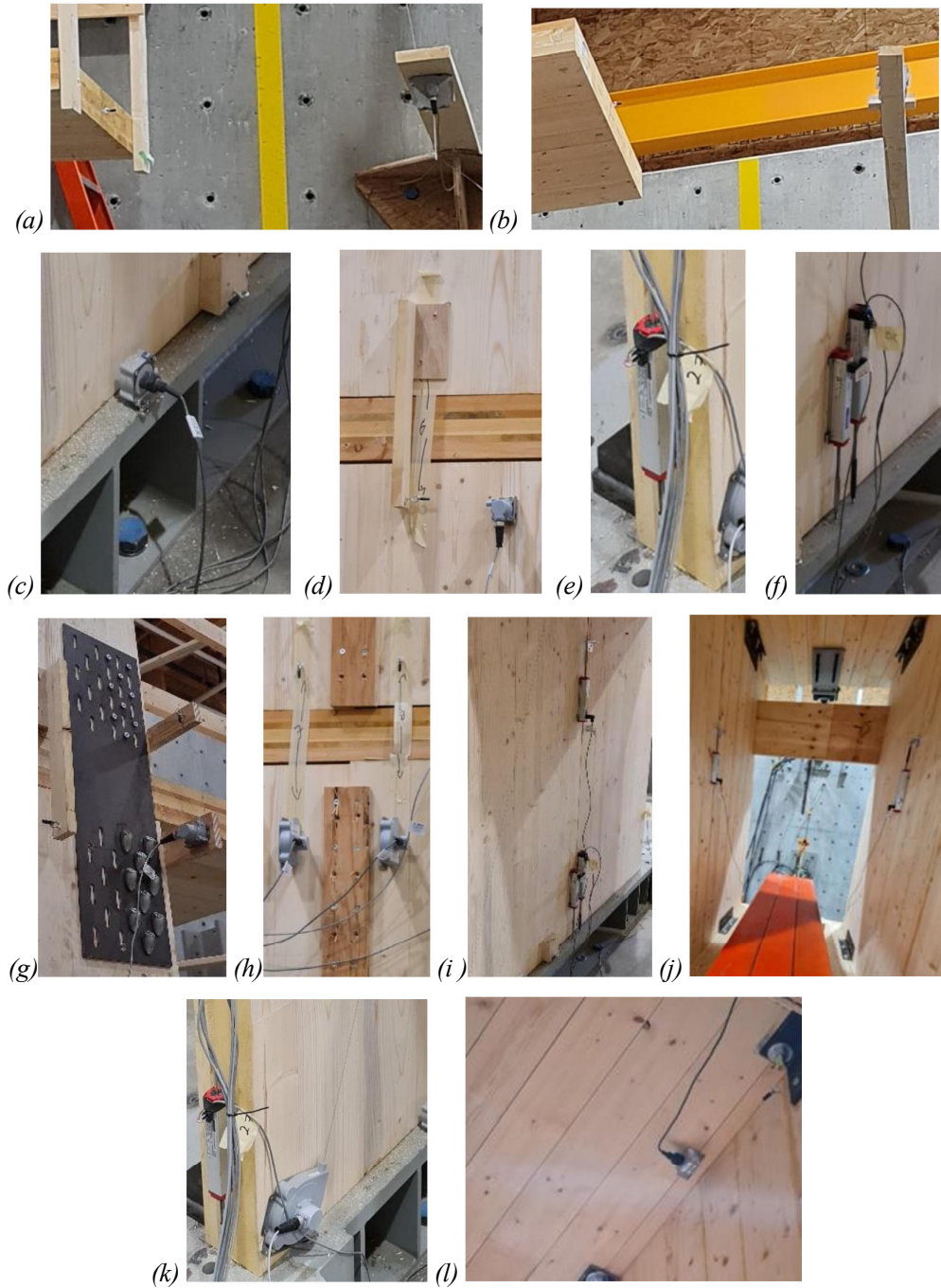


Figure 3.16. Sensors: a) 1<sup>st</sup> storey displacement free end, b) 2<sup>nd</sup> storey displacement free end, c) 1<sup>st</sup> storey sliding, d) 2<sup>nd</sup> storey sliding, e) HD uplift, f) 1<sup>st</sup> storey inner corner uplift, g) tension strap uplift, h) 2<sup>nd</sup> storey inner corner uplift, i) 1<sup>st</sup> storey panel-panel slip, j) 2<sup>nd</sup> storey panel-panel slip, (k) panel distortion, (l) 2<sup>nd</sup> floor sliding

### 3.5.3 Loading

Two monotonic tests, one pulling and one pushing, were conducted because the symmetrical configuration enabled the execution of two tests with minimal connection repairs required in between, in addition, the second test was done to assess if there is any asymmetrical response between pull and push loads. The monotonic pushover tests were conducted at a rate of loading of 15 mm/min until reaching the target displacement of 3% (150 mm) inter storey drift (ISD). The reversed cyclic tests followed the Consortium of Universities for Research in Earthquake Engineering (CUREE) loading history [62] as illustrated in Figure 3.17a, with a 100% target displacement of 150 mm, and continued with further cycles of 130%, and 160% of target displacement.

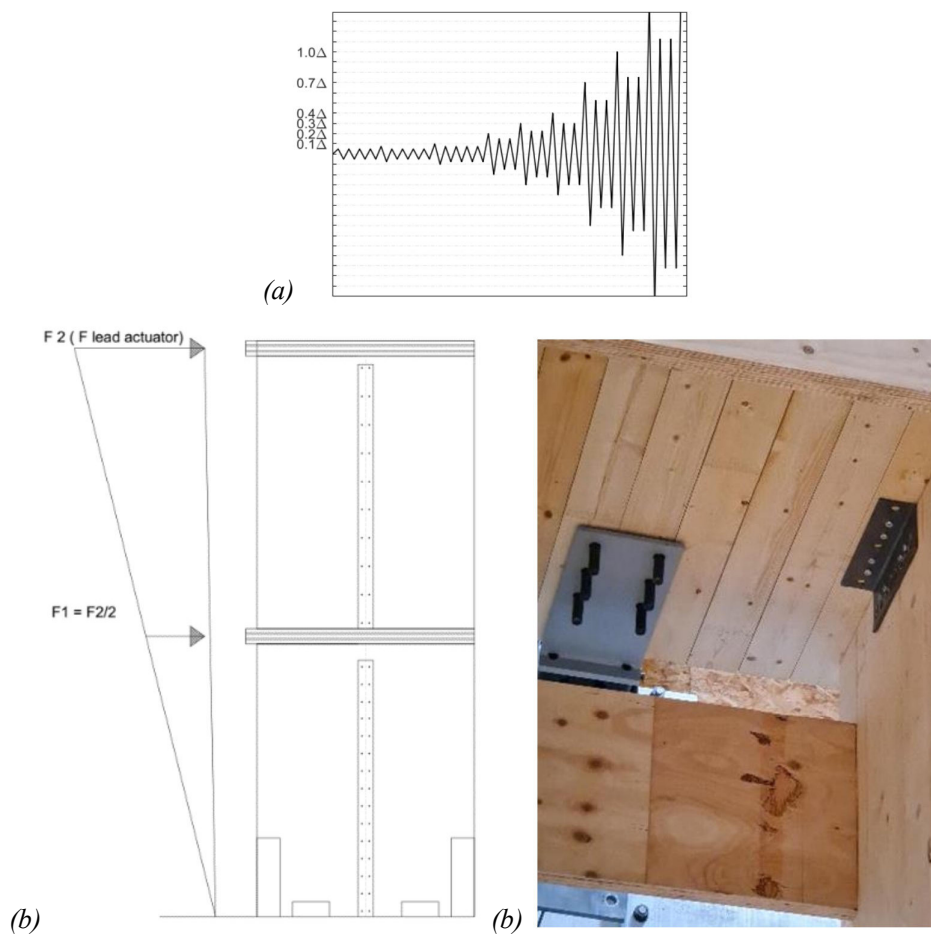


Figure 3.17. Load application (a) protocol, (b) schematic, (c) photo of fixture

### **3.6 Test results**

In this sequence of tests, two monotonic tests and seven reverse cyclic tests were conducted. The targeted displacement for these tests was maintained at 150 mm, equivalent to a 3% drift of the structures. Consequently, in the monotonic tests, the structures were pushed to 150 mm, due to financial constraints, the monotonic tests were not intended to be pushed to failure or damage, while in the reverse cyclic tests, various cycles involved both positive (40%, 70%, 100%, 130%, and 160%) and negative (-40%, -70%, -100%, -130%, and -160%) target displacements. The subsequent section presents the test results for different structures.

#### **3.6.1 Results test #H1a**

##### **Horizontal storey displacements**

The horizontal storey displacements are depicted in Figure 3.18. In this test, the structure was subjected to a displacement of -157 mm (pulling forces) before the test was stopped. The load-displacement graph displayed a nearly linear relationship up to a 20 mm displacement, characterized by a steeper slope. Beyond this point, the slope decreased, indicating a failure in the structure connections and the graph continued to rise until reaching the -100% target displacement, with the total load  $F_{@-100\%}$  reaching 283 kN. Given that the objective was not to induce a total structural failure of the structure, the displacement was not extended beyond this limit. Importantly, it is worth noting that the capacity of the structure did not exhibit any discernible decrease.

At -100% target displacement, the lateral displacements of the 1<sup>st</sup> and 2<sup>nd</sup> stories were both 75 mm, and the graphs for these displacements were almost identical. Since there were no intention for general failure of the structure, it was not pulled more than this, it did not show any capacity decrease though.

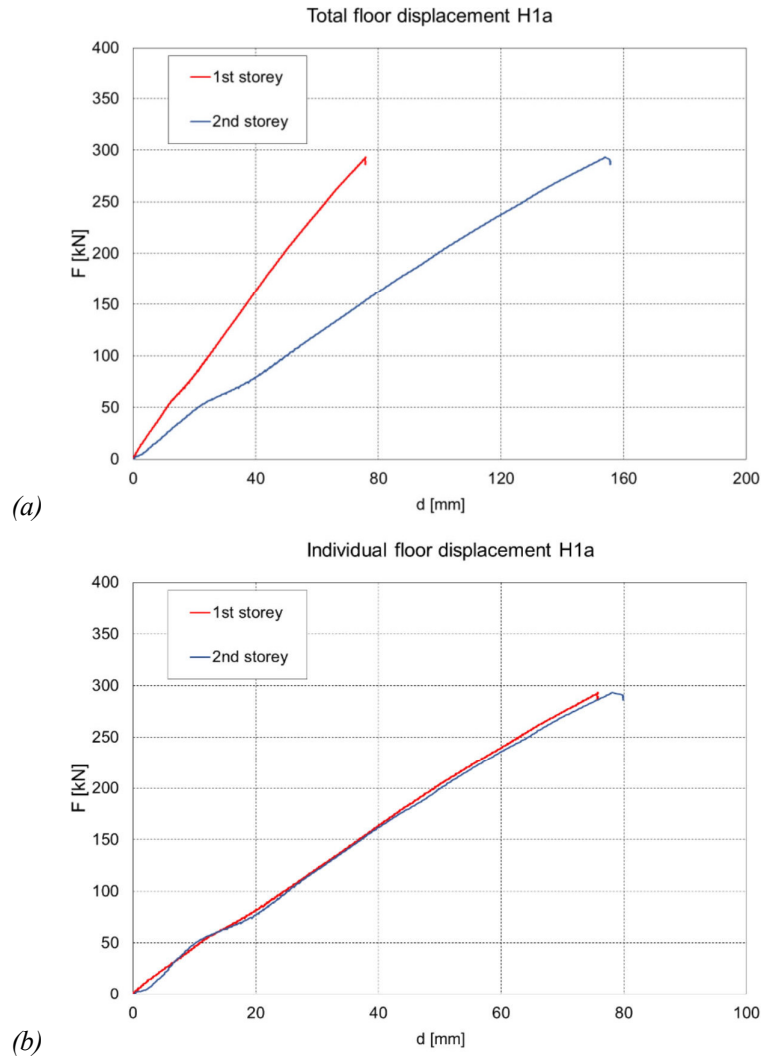


Figure 3.18. H1a (a) total storey displacements, (b) individual storey displacements

### Hold down and tension strap uplift

The vertical uplift experienced in the four HD and tension straps (two on the front and back shear walls each) are illustrated in Figure 3.19. The graph of the load-displacement curves was bi-linear. This structure was subjected to a pulling force, causing the right-side HD to undergo tension as shown in Figure 3.19a. The load increased steadily until reaching 60 kN, resulting in a 1.2 mm uplift in the HD. However, after this point, there was a significant decrease in stiffness, followed by a gradual increase with a softer slope. The load continued to rise, reaching a  $F_{@-100\%}$  of 283 kN, accompanied by a 17 mm uplift.

On the left side, the HD acted predominantly in compression. The load increased to approximately 40 kN, causing a -1.2 mm uplift. Subsequently, the slope became steeper, indicating an increase in stiffness. The load continued to rise to its maximum level, accompanied by a -3.3 mm uplift (compression).

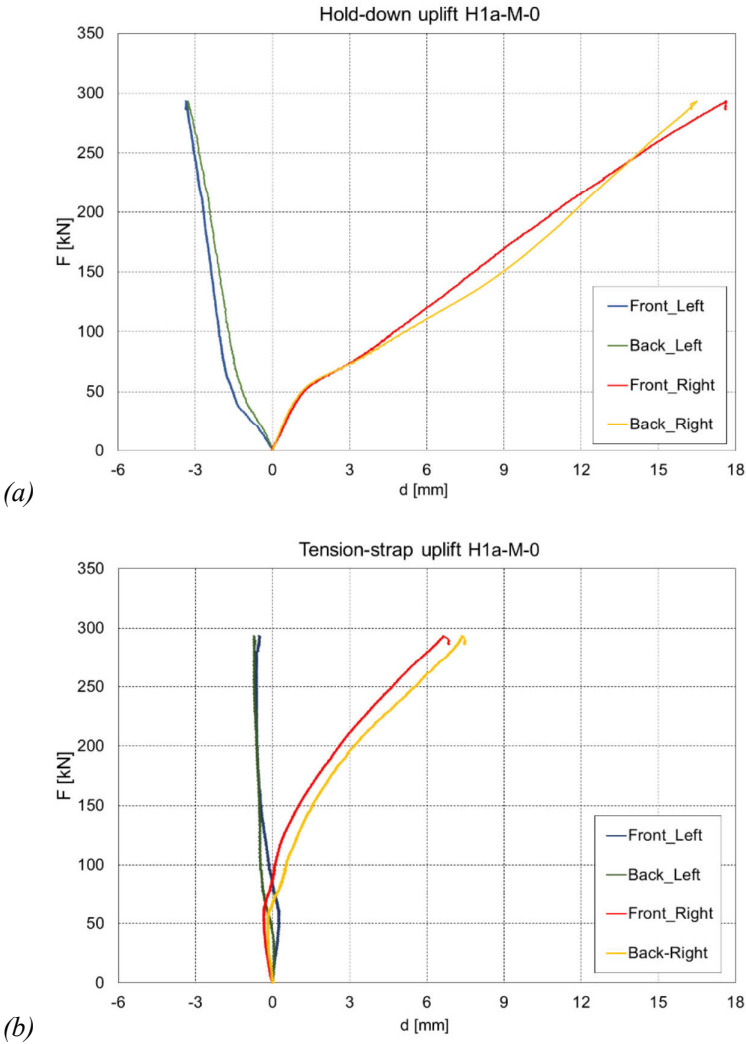


Figure 3.19. H1a uplift at: (a) hold downs (b) tension straps

The graph depicting the uplift of the tension straps exhibits a bilinear pattern for each HD, as shown in Figure 3.19b. The force steadily increased with minimal uplift until reaching 60 kN. Beyond this point, on the right side of the shear wall, there was a notable

decrease in stiffness, indicating the initiation of structural failure. Subsequently, there was a gradual increase with a gentler slope, ultimately resulting in an uplift of 7 mm at the -100% target displacement. Conversely, the tension straps on the left side of the shear wall were subject to slight compression forces, resulting in negative uplifts of -0.7 mm at the +100% target displacement.

**First and second storey inner corner uplifts**

The vertical uplift experienced in the four inner corners of the coupled shear walls are illustrated in Figure 3.20.

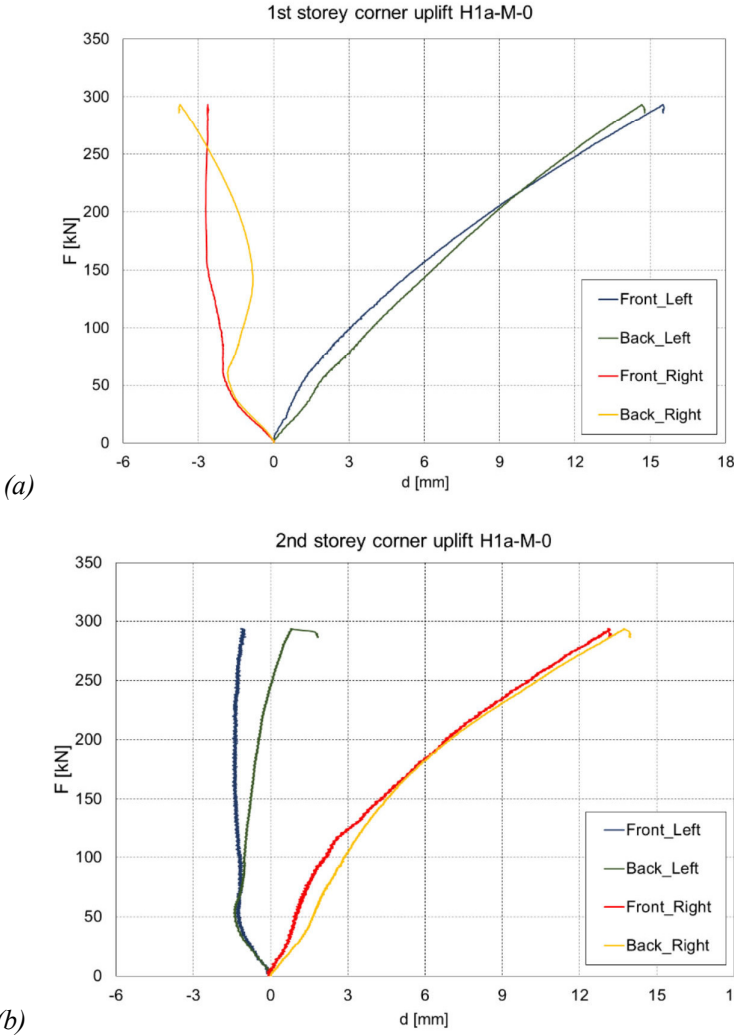


Figure 3.20. H1a inner corner uplifts at: (a) 1<sup>st</sup> storey, (b) 2<sup>nd</sup> storey

The curve of the load-displacement was quasi-linear when the total load reached 60 kN and then with a softer slope culminated in  $F_{@-100\%}$  of 283 kN at -100% target displacement. The corresponding left side inner corner uplifts in the 1<sup>st</sup> storey shear wall (Figure 3.20a) were 14.5 mm and 15.5 mm mirroring the HD uplifts of the 1<sup>st</sup> storey. The negative uplifts correspond to compression in the panel corners. At the -100% target displacement, the uplifts on the right side of the shear wall were close to -3 mm.

The inner corner uplifts in the 2<sup>nd</sup> storey shear wall, depicted in Figure 3.20b, varied from -1 to 1 mm at the -100% target displacements in left-side panel corners and 13 mm and 14 mm in right corners. The displacements in the corners of the 1<sup>st</sup> and 2<sup>nd</sup> stories exhibit an interesting relationship where they are essentially mirror images of each other. When the corners on the 1<sup>st</sup> storey were subjected to compression, the corresponding corners on the 2<sup>nd</sup> storey underwent uplift, and conversely, when the 1<sup>st</sup> storey corners experienced uplift, the corresponding 2<sup>nd</sup> storey corners were subjected to compression.

### **Panel sliding**

The sliding values at the base and 1<sup>st</sup> level floor are shown in Figure 3.21. There was only a small amount of sliding at the base level, with the highest values being -0.8 mm and 0.8 mm for the front and 1.3mm and 3.3 mm for back side panels, respectively, when the displacement was increased to -100% target displacement, see Figure 3.21a. The sliding at the 1<sup>st</sup> level floor, as shown in Figure 3.21b, exhibited values ranging from 14.5 mm to 15.1 mm in front and from 17.5 mm to 19.3 mm in back SB at the +100% target displacement. These sliding values contributed approximately 10% to the overall lateral displacement.

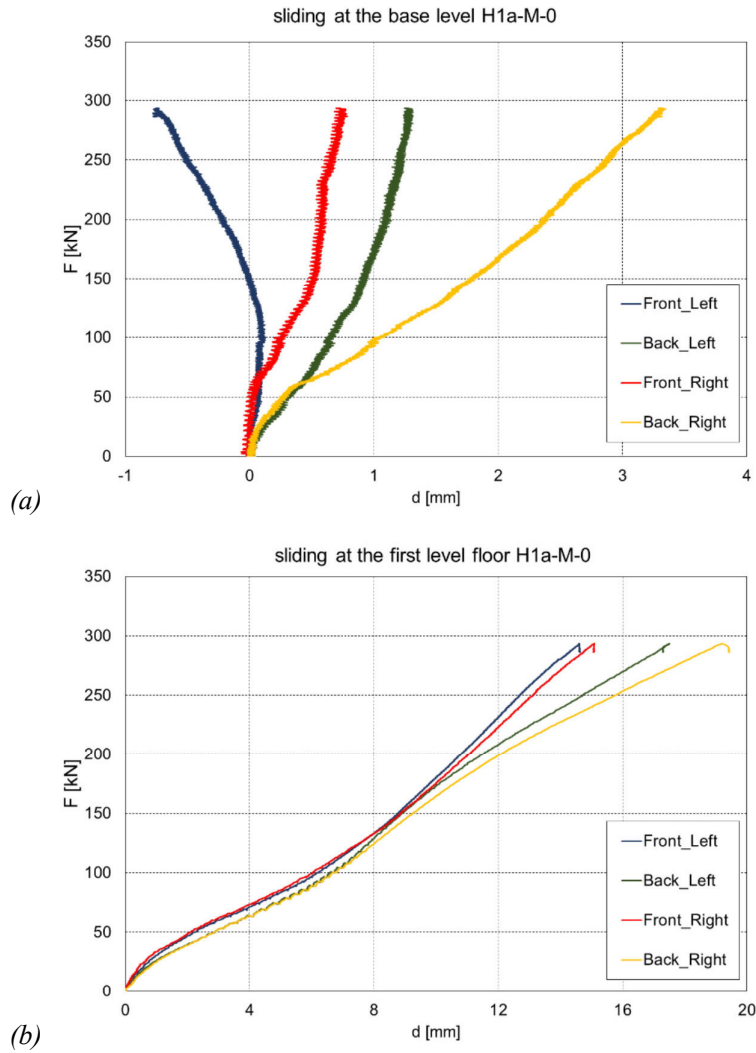


Figure 3.21. H1a sliding of shear wall at: (a) base level, (b) 1<sup>st</sup> floor

### Panel to-panel slip

Herein Panel-to-panel slip are presented in Figure 3.22. The 1<sup>st</sup> storey load-displacement curve was quasi-linear up to the -100% target displacement with the total load  $F_{@-100\%}$  of 283 kN. The corresponding panel slips, as shown in Figure 3.22a, was approximately 21 mm, with minimal variation between the back and front panels.

The recorded panel slips in the 2<sup>nd</sup> storey shear wall, as shown in Figure 3.22b, exhibited an upward trend in the front panels. This trend continued until reaching 60 kN, at which point a notable reduction in stiffness was observed. Subsequently, the force increased,

reaching the -100% target displacement. At the -100% target displacement, the panel slips in the front panels measured 6.3 mm. Due to an instrumentation error, complete data for the back panel was not recorded; consequently, the graph is truncated at 93 kN.

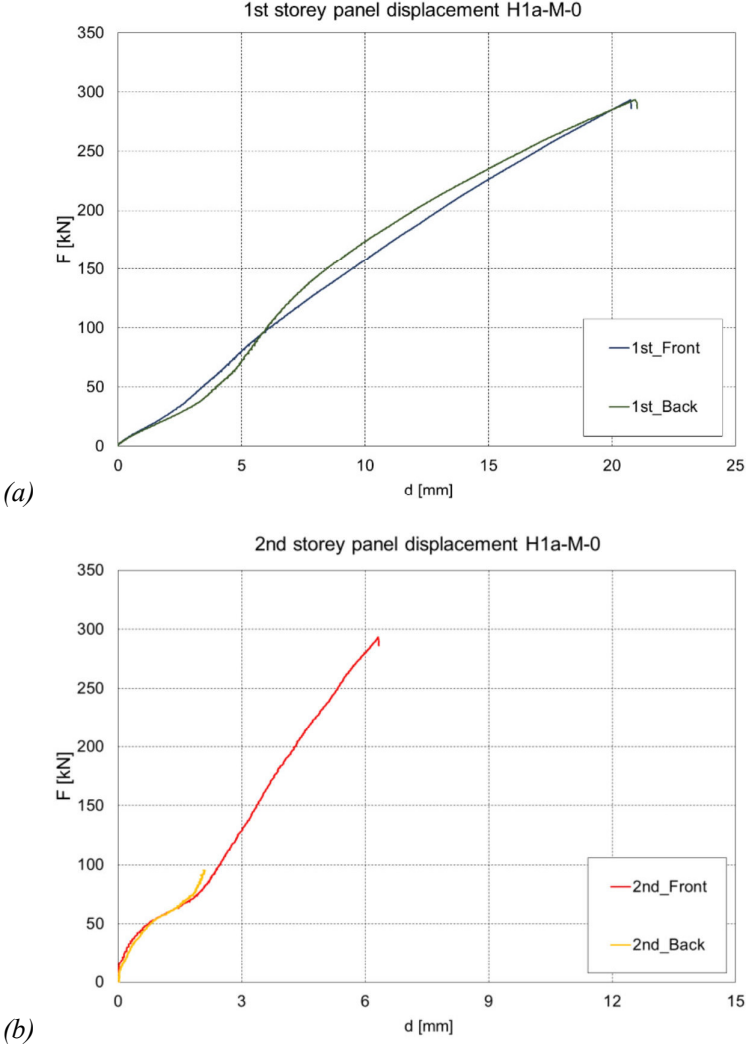


Figure 3.22. H1a Panel-to-panel slip for: (a) 1<sup>st</sup> storey, (b) 2<sup>nd</sup> storey

**3.6.2 Results test #H1b**

**Horizontal storey displacements**

In this test, the structure underwent a displacement of 158 mm before the test was halted. It is worth noting that the primary distinction between the H1a and H1b tests lies in the

type of load they experienced. The horizontal storey displacements are shown in Figure 3.23. H1a was subjected to a monotonic pulling, whereas H1b was subjected to lateral pushing.

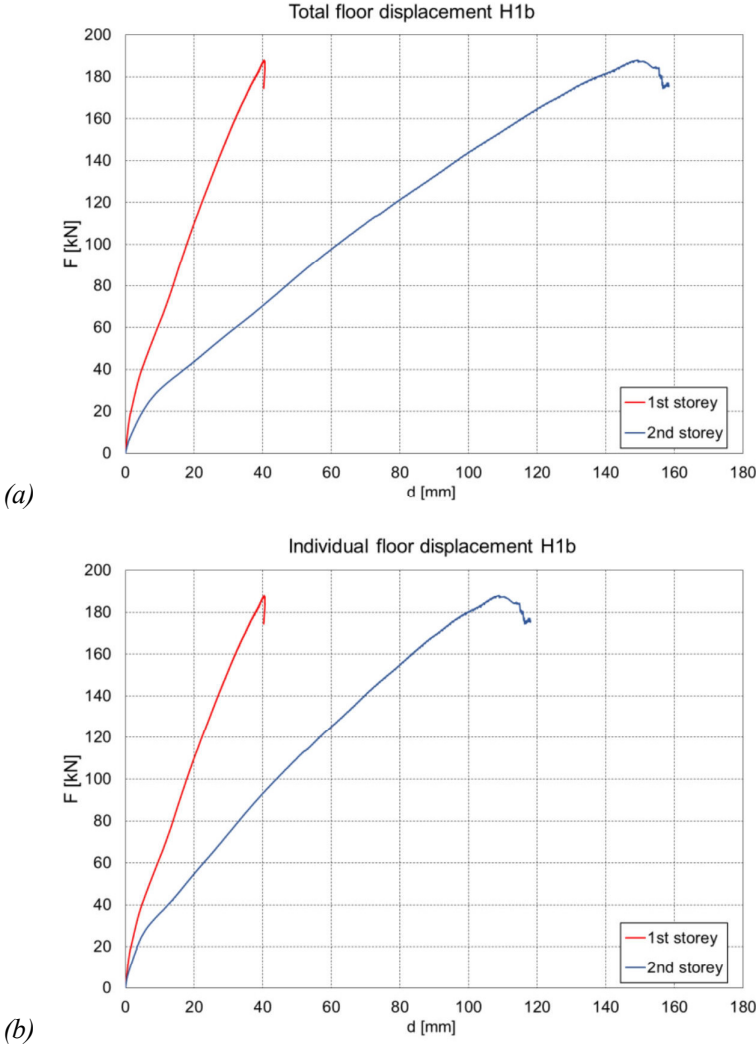


Figure 3.23. H1b (a) total storey displacements, (b) individual storey displacements

The load-displacement graph displayed a nearly linear relationship up to a 4.5 mm displacement with 25 kN force, characterized by a steep slope. Beyond this point, the slope decreased, indicating a failure in the structure connections and stiffness reduction. Despite this, the graph continued to ascend until it reached the 100% target displacement,

with the total load  $F_{@+100\%}$  peaking at 187 kN. Given that the intent was not to induce a complete structural failure of the structure, the displacement was not extended beyond this threshold. At +100% target displacement, the lateral displacements of the 1<sup>st</sup> and 2<sup>nd</sup> stories were 40 mm and 110 mm respectively, therefore, the 2<sup>nd</sup> storey drift was almost 275% of the 1<sup>st</sup> storey drift.

### **Hold down and tension strap uplift**

The vertical uplift experienced in the four HD and tension straps are illustrated in Figure 3.24. The graphs of the load-displacement curves were bi-linear. This structure was subjected to a pushing force, causing the left-side HD to undergo tension (see Figure 3.24a). The load increased steadily until reaching 40 kN, resulting in almost zero uplift in left-side HD. However, after this point, there was a significant decrease in stiffness, followed by a gradual increase with a softer slope. The load continued to rise, reaching a  $F_{@+100\%}$  of 187 kN, accompanied by a 10 mm uplift.

On the right side, the HD acted predominantly in compression. The load increased to approximately 60 kN, causing a -3 mm uplift. Subsequently, the slope became steeper, indicating an increase in stiffness. The load continued to rise to its maximum level, accompanied by a -4 mm uplift.

The graph illustrating the uplift of the tension straps displays a bilinear pattern for each strap, as shown in Figure 3.24b. The force steadily increased with minimal uplift until it reached 30 kN. However, beyond this point, a significant decrease in stiffness became apparent on the left side of the shear wall, indicating the initial stages of tension strap screw failure. Subsequently, there was a gradual resurgence with a gentler slope, resulting in an uplift of 10 mm and 14 mm on the front and back tension straps, respectively, at the +100% target displacement. Conversely, the tension straps on the right side of the shear

wall experienced compression forces, leading to negative uplifts of -3 mm and -4.5 mm on the back and front tension straps, respectively, at the +100% target displacement.

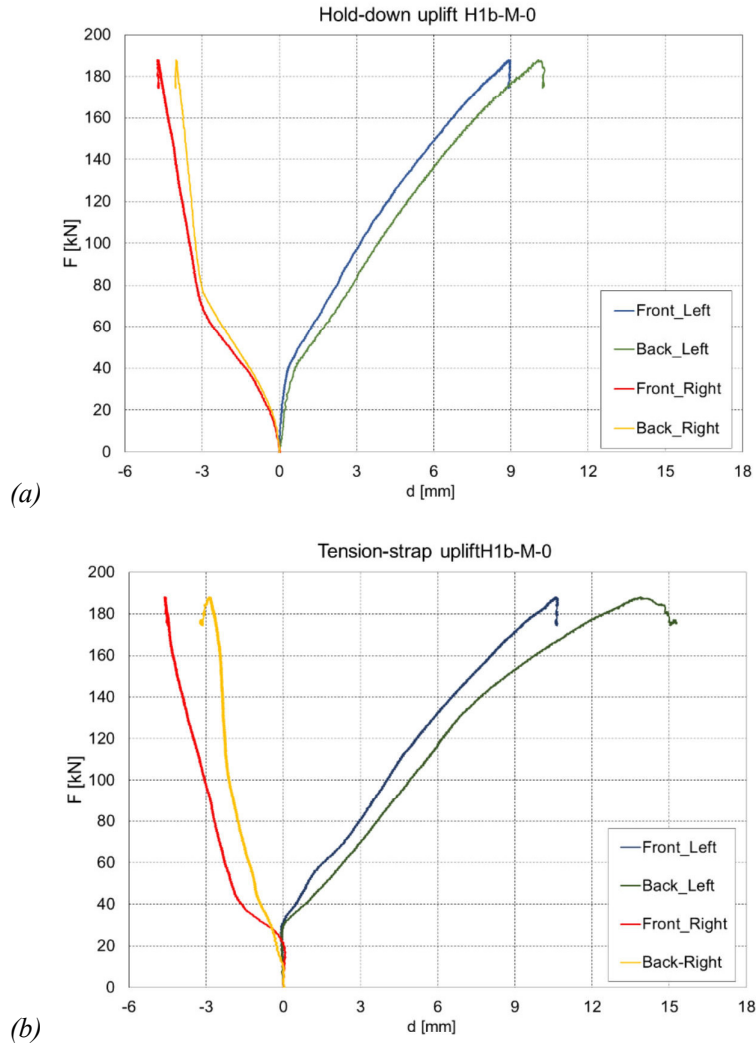


Figure 3.24. H1b uplift at: (a) hold downs (b) tension straps

### First and second storey inner corner uplifts

The vertical uplift experienced in the four inner corners of the coupled shear walls are illustrated in Figure 3.25. The curve of the load-displacement shows zero uplift till the point that total load reached to 30 kN and then almost linearly increased to  $F_{@+100\%}$  of 187 kN at +100% target displacement.

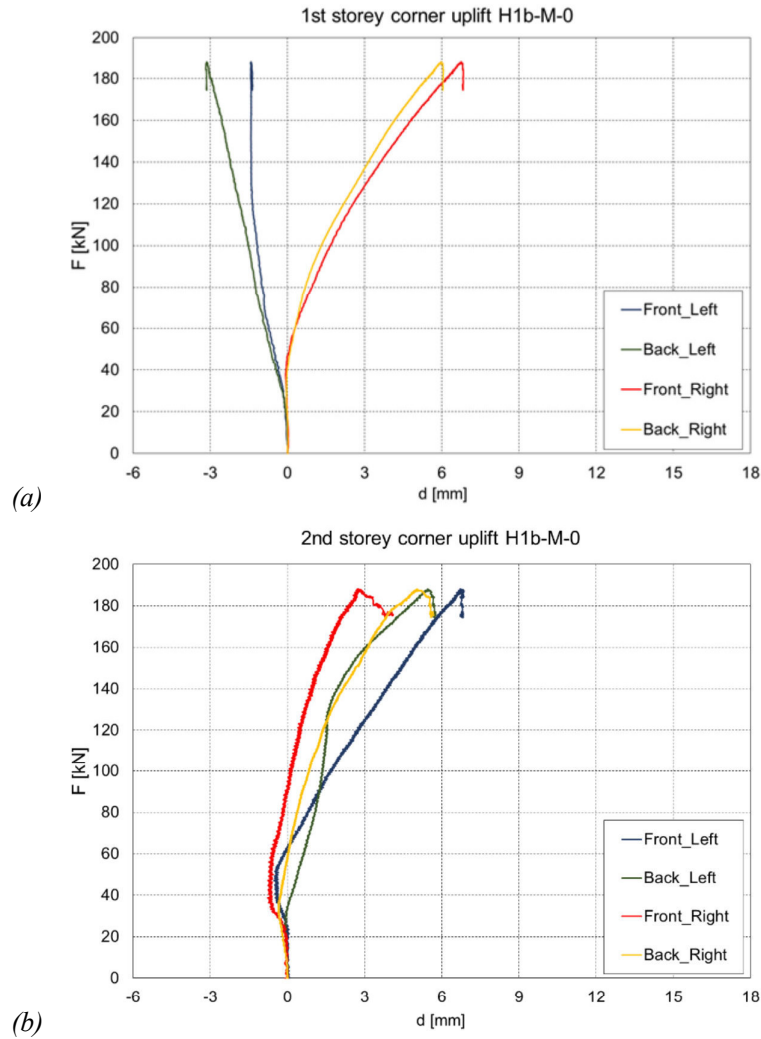


Figure 3.25. H1b inner corner uplifts at: (a) 1<sup>st</sup> storey, (b) 2<sup>nd</sup> storey

The corresponding right side inner corner uplifts in the 1<sup>st</sup> storey shear wall (Figure 3.25a) were 6 mm and 6.7 mm mirroring the HD uplifts of the 1<sup>st</sup> storey. The negative uplifts correspond to compression in the panel corners. At the +100% target displacement, the uplifts on the left side of the shear wall were -1.4 mm to -3 mm on front and back panels. The inner corner uplifts in the 2<sup>nd</sup> storey shear walls, depicted in Figure 3.25b, varied from 3 mm to 6.5 mm at the +100% target displacements. Notably, there were no instances of compression observed in the panel corners.

## Panel sliding

The sliding values at the base and 1<sup>st</sup> level floor are shown in Figure 3.26.

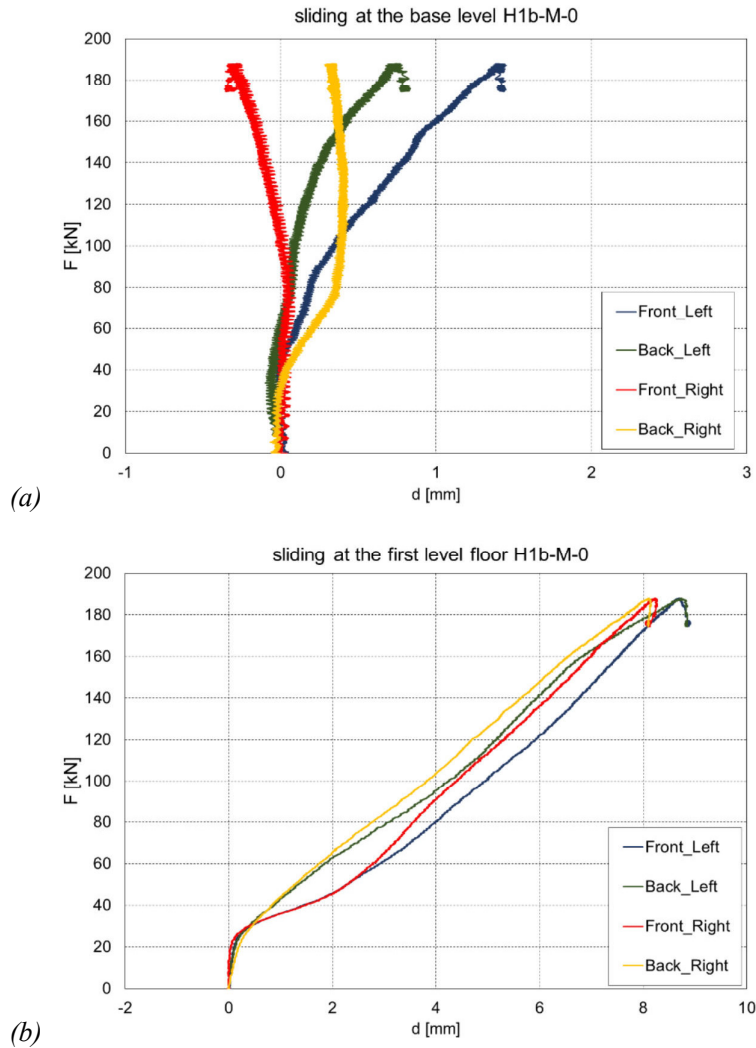


Figure 3.26. H1b sliding of shear wall at: (a) base level, (b) 1<sup>st</sup> level

There was only a small amount of sliding at the base level, with the highest values being 0.3 mm and 1.3 mm for the right and back side panels, respectively, when the displacement was increased to -100% target displacement, see Figure 3.26a. The sliding at the 1<sup>st</sup> level floor, as shown in Figure 3.26b, exhibited values ranging from 8 mm to 9

mm in right and back SB at the +100% target displacement. These sliding values contributed approximately 7% to the overall lateral displacement.

### Panel-to-panel slip

The Panel-to-panel slips are presented in Figure 3.27.

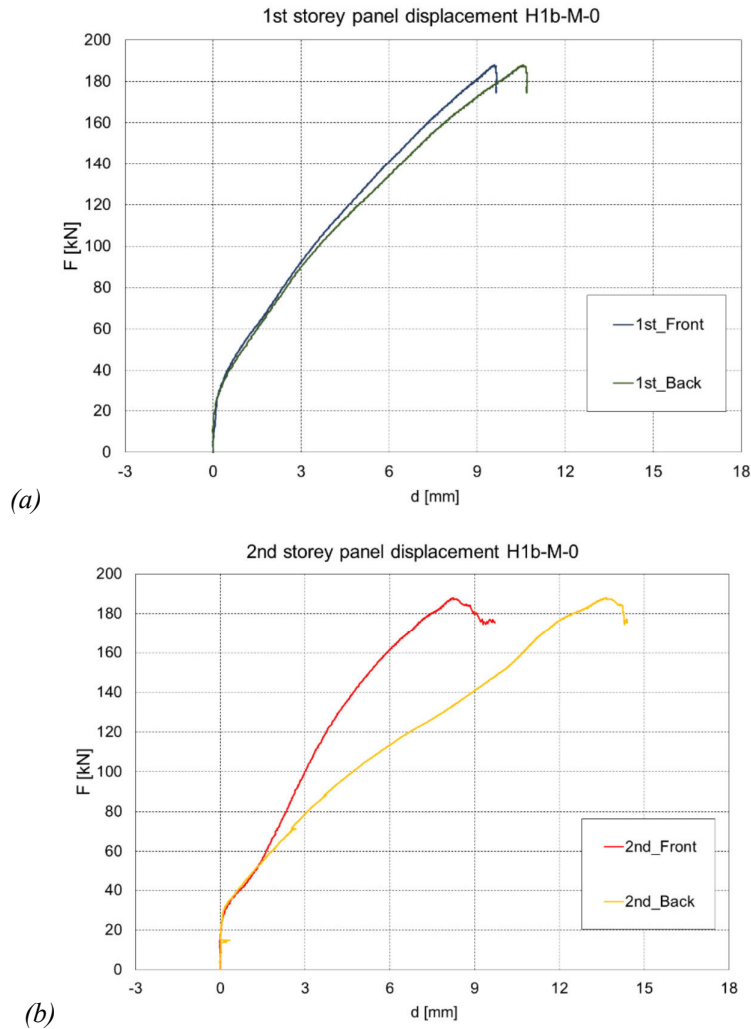


Figure 3.27. H1b Panel-to-panel slip for: (a) 1<sup>st</sup> storey, (b) 2<sup>nd</sup> storey

The 1<sup>st</sup> storey load-displacement curve was quasi-linear up to the +100% target displacement with the total load  $F_{@+100\%}$  of 187 kN. The corresponding panel slips, as

shown in Figure 3.27a, was approximately 10.2 mm, with minimal variation between the back and front panels.

The panel slips recorded in the 2<sup>nd</sup> storey shear wall, as depicted in Figure 3.27b, remained stable with no noticeable slip until they reached 30 kN. Afterward, a linear upward trend in the back panels emerged. This trend persisted until it reached a total load  $F_{@+100\%}$  of 187 kN. However, the behavior of the front panel differed from this linear trend. Instead, an increase in stiffness was observed at 50 kN, and this continued until it reached 8.3 mm of slip at the +100% target displacement.

### **3.6.3 Results test #H1c**

#### **Horizontal storey displacements**

The horizontal storey displacements are illustrated in Figure 3.28. The envelope of the load-displacement curve was quasi-linear to 100% of the target displacement (equal to 150 mm) with the total load  $F_{@+100\%}$  reaching 205 kN. During the subsequent displacement cycle (195 mm), the total load increased to 249 kN.

The positive and negative envelopes were similar, with the negative force  $F_{@-100\%}$  reaching approximately -143 kN and  $F_{@-130\%} = -250$  kN. The lateral displacements (1<sup>st</sup> storey drift) of the first floor were 55 mm and -42 mm for the positive and negative 100% target displacement respectively. The 2<sup>nd</sup> storey drifts were 95 mm and -109 mm and therefore roughly 220% of the 1<sup>st</sup> floor drifts.

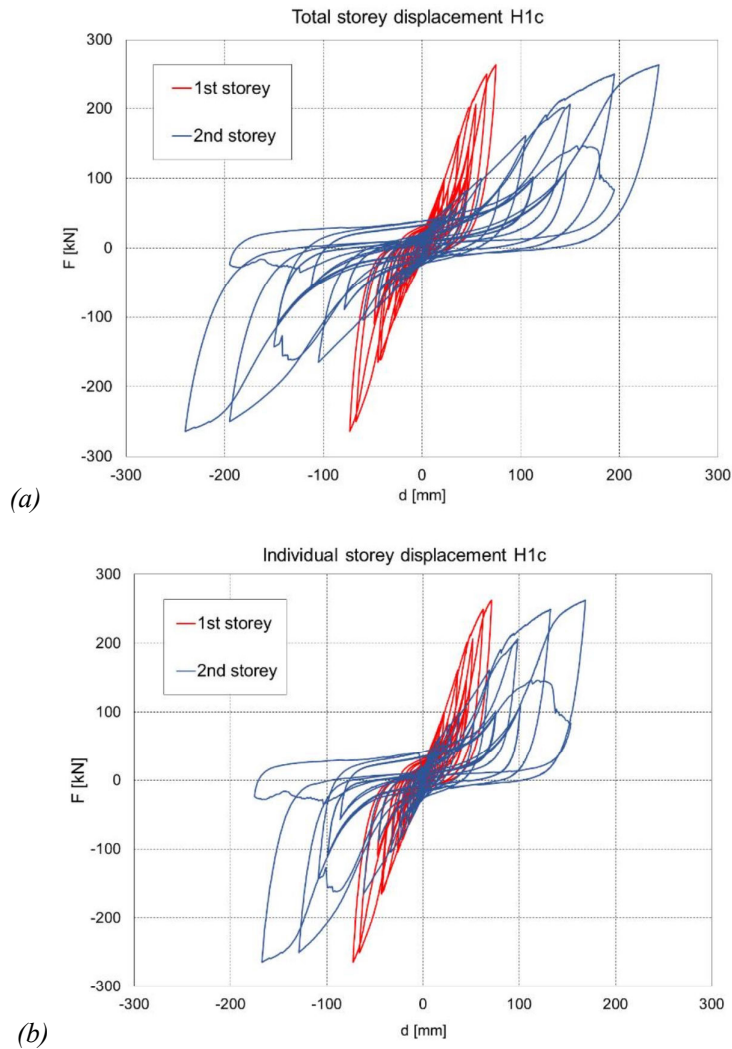


Figure 3.28, H1c (a) total storey displacements, (b) individual storey displacements

### Hold down and tension strap uplift

The uplift forces resulted from lateral loads are resisted by HD that connect the first storey to the base fixture and tension straps that connect first storey to the second storey. The vertical uplift experienced in the four HD and tension straps (two on the front and back shear walls each) are illustrated in Figure 3.29. The envelopes of the load-displacement curves were all quasi-linear up to the +130% target displacement when the total load  $F_{@+130\%}$  reached 249 kN. The corresponding HD uplifts (Figure 3.29a) on the left side of the shear wall were 14.5 mm and 14 mm. At the -130% target displacement, the uplifts

on the right side of the shear wall were 15.2 mm and 15.5 mm. The negative HD uplifts correspond to compression in the panel corners. The maximum compressions at the +/- 130% target displacements ranged from 4.4 mm to 6.4 mm.

The tension strap uplifts (Figure 3.29b) on the left side of the shear wall were 25 mm and 22.2 mm at the +/-130% target displacement indicating onset of failure which in the next cycle, reached 36.7 mm and 30.5 mm during the +160% target displacement. The tension strap uplifts on the right side of the shear wall were 20.3 and 21.9 mm indicating onset of failure which in the next cycle with uplifts exceeding 30 mm.

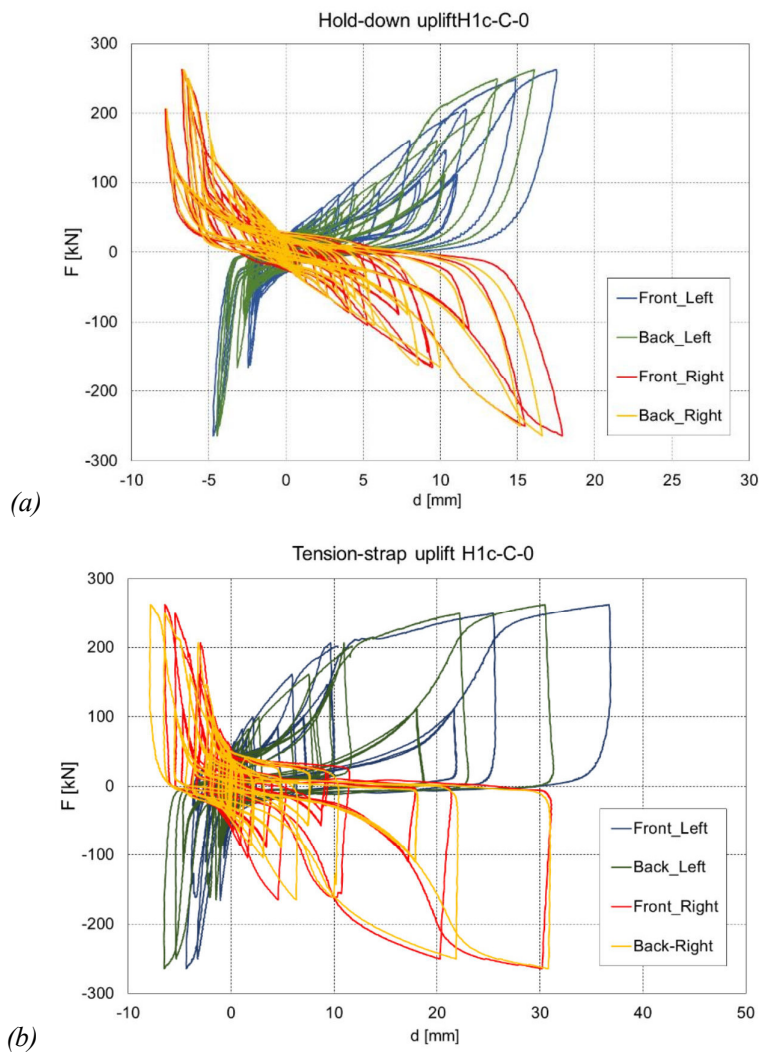


Figure 3.29. H1c uplifts at (a) the HDs, (b) tension straps

### First and second storey inner corner uplifts

The vertical uplift experienced in the four inner corners of the coupled shear walls are illustrated in Figure 3.30. The envelopes of the load-displacement curves were all quasi-linear up to the +100% target displacement when the total load  $F_{@+100\%}$  reached 205 kN.

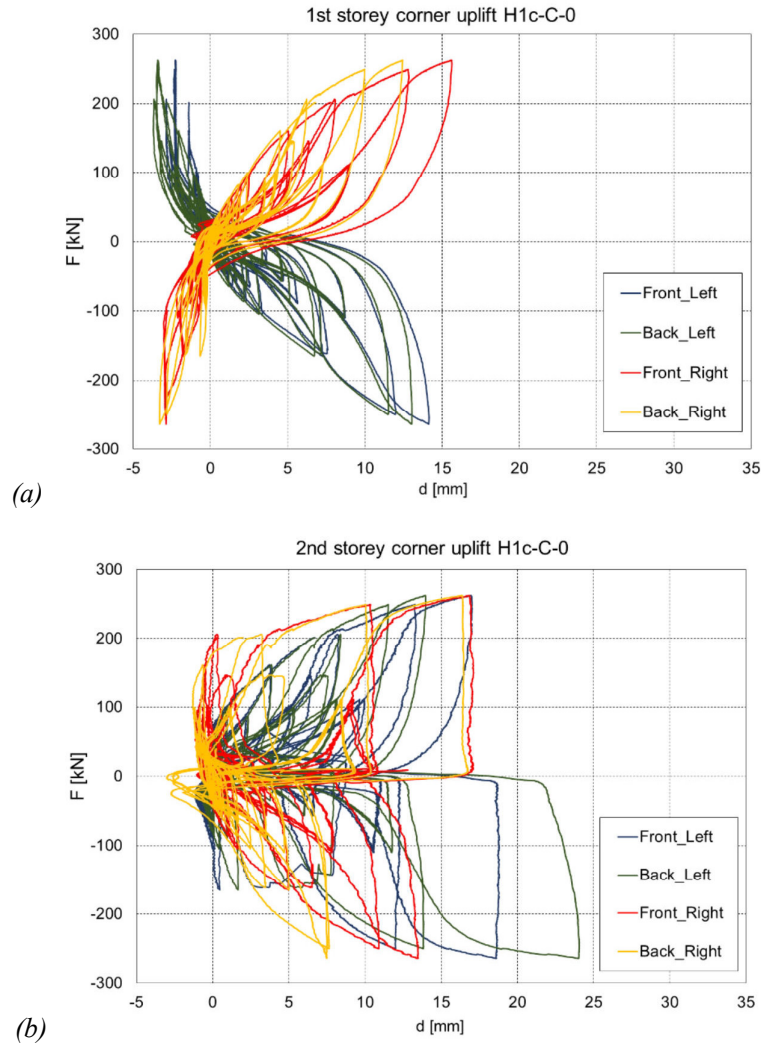


Figure 3.30. H1c inner corner uplifts at (a) 1<sup>st</sup> storey, (b) 2<sup>nd</sup> storey

The corresponding right side inner corner uplifts in the 1<sup>st</sup> storey shear wall (Figure 3.30a) were 7.9 mm and 6.4 mm. At the -100% target displacement, the uplifts on the left side of the shear wall ranged from 7.1 mm to 7.4 mm, closely mirroring the HD uplifts of the

1<sup>st</sup> storey. Differences between positive and negative target displacements were minimal. The negative uplifts correspond to compression in the panel corners; these were close to 2.7 mm on the right panels and 1.7 mm on the left panels.

The inner corner uplifts in the 2<sup>nd</sup> storey shear wall, depicted in Figure 3.30b, varied from 0.3 mm to 8.3 mm at the +/-100% target displacements. These uplift values increased in the subsequent cycle, ranging between 7.6 mm and 13.8 mm. Notably, there was almost no compression observed in the three inner corners since they were consistently slightly lifted by the opposite side panel during uplift, but the back right corner experienced a compression of -2 mm, indicating a slight downward displacement in that specific corner.

### **Panel sliding**

Shear wall panel sliding is resisted by SB; the sliding values at each level are shown in Figure 3.31. It must be noted that the sliding at the 1<sup>st</sup> level floor is the total relative displacement between the shear walls of the 1<sup>st</sup> and 2<sup>nd</sup> stories; given the sensor installation, the recorded values also include the cumulative overturning effect of the 2<sup>nd</sup> storey. Further analyses, beyond the scope of this thesis are required to evaluate the actual sliding behavior as a function of the acting lateral load at this level.

The displacement caused by sliding at the base level (depicted in Figure 3.31a) observed at the +100% target displacement, were 2.0 mm for the front side panel and 1.9 mm for the back side panel. Based on these observations, it can be concluded that although sliding was not entirely prevented, its overall contribution at the base level was less than 5% of the storey drift. The sliding at the 1<sup>st</sup> level floor, as shown in Figure 3.31b, exhibited values ranging from 9.9 mm to 12 mm at the +100% target displacement, and from 11 mm to 14.5 mm at the -100% target displacement. These sliding values contributed approximately 10% to the overall lateral displacement.

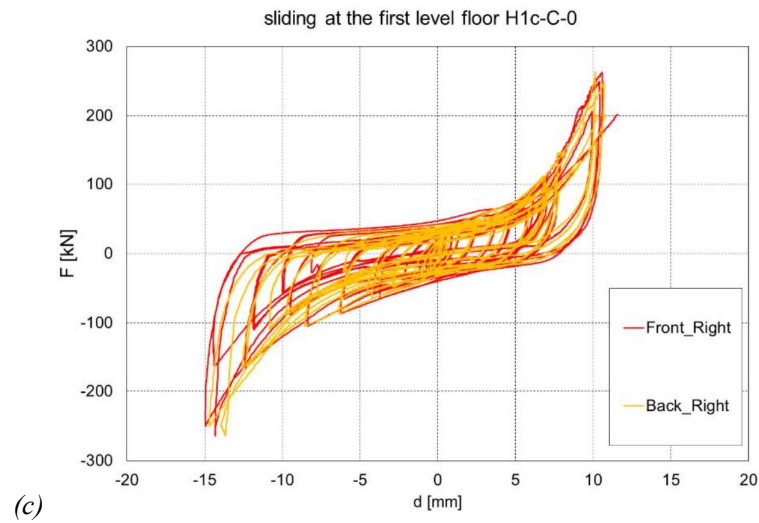
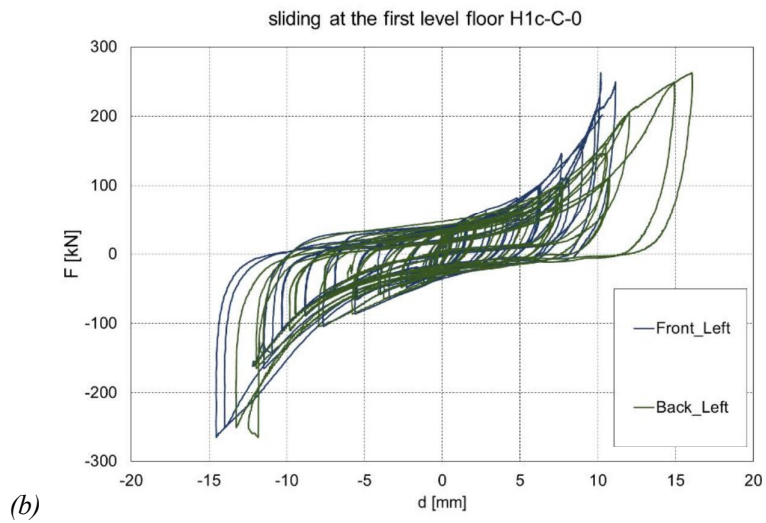
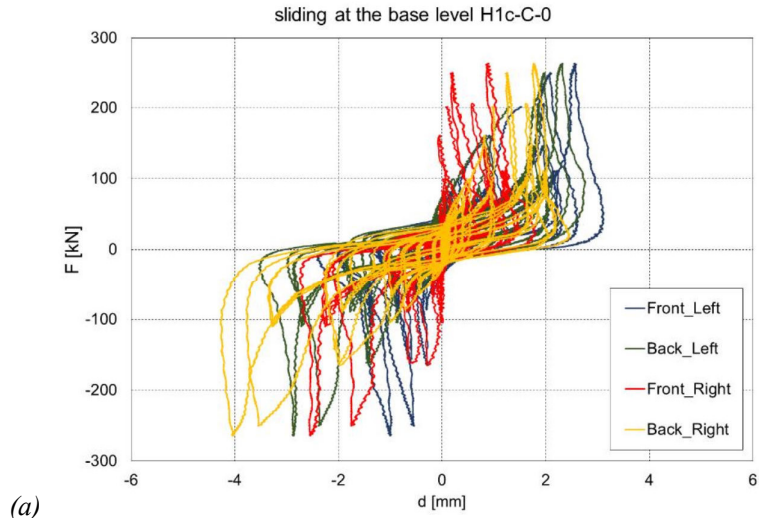
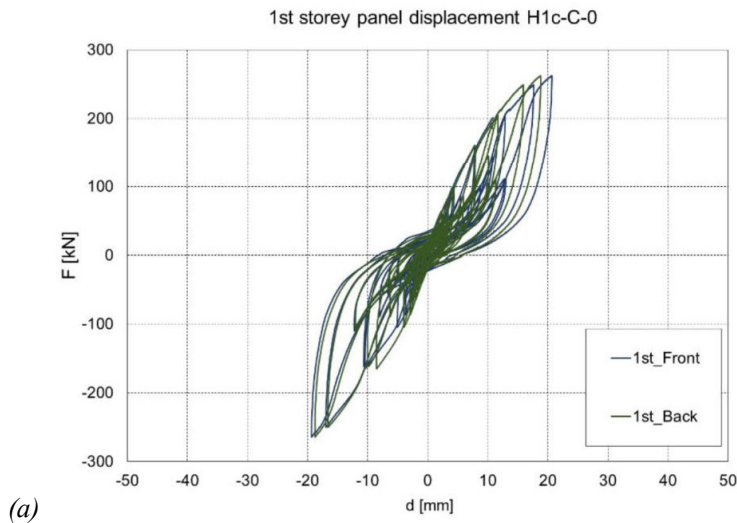


Figure 3.31. H1c panel sliding at: a) base level, b) 1<sup>st</sup> level left, c) 1<sup>st</sup> level right

### Panel-to-panel slip

In coupled panel shear wall kinematics, the individual panels are expected to displace relative to each other, herein referred to as Panel-to-panel slip, as presented in Figure 3.32. This displacement in the spline joints acts as one major energy dissipation mechanism. The envelopes of the 1<sup>st</sup> storey load-displacement curves were all quasi-linear up to the +100% target displacement. The corresponding panel slips, as shown in Figure 3.32a, were approximately 12.3 mm, with minimal variation between the back and front panels or positive and negative cycles. The panel slips observed in the 2<sup>nd</sup> storey shear wall, as depicted in Figure 3.32b, formed a linear envelope up to the 100% target displacement, with the total load  $F_{@+100\%}$  reaching 205 kN. At the +100% target displacement, the panel slips were measured as 6.4 mm (front) and 9.5 mm (back). Conversely, at the -100% target displacement, the panel slips increased to 15.5 mm (front) and 17.5 mm (back).



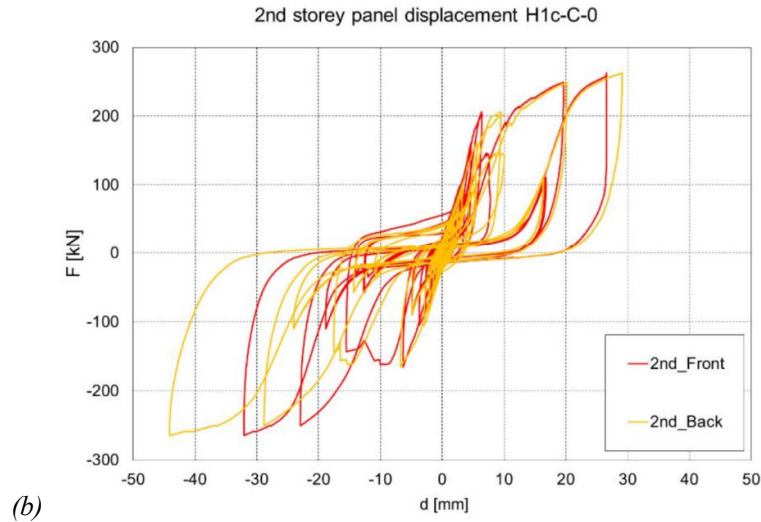


Figure 3.32. H1c Panel-to-panel slip for: (a) 1<sup>st</sup> storey, (b) 2<sup>nd</sup> storey

### 3.6.4 Results test #H2a

#### Horizontal storey displacements

The horizontal storey displacements are illustrated in Figure 3.33. The load-displacement curve displayed a quasi-linear pattern up to 130% of the target displacement (equivalent to 195 mm), with the total load  $F_{@+130\%}$  reaching 316 kN. However, in the subsequent displacement cycle (top actuator displacement 240 mm), the total load only reached 336 kN, and certain components of the load resisting system experienced failure.

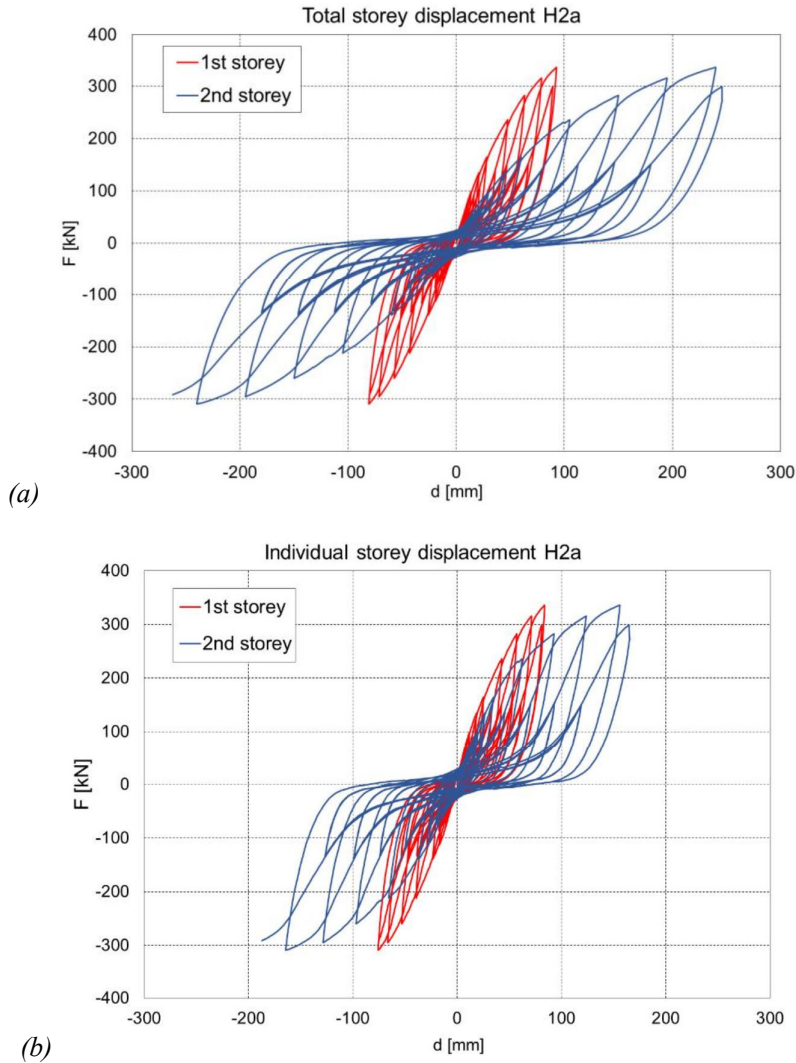


Figure 3.33. H2a (a) total storey displacements, (b) individual storey displacements

Both the positive and negative envelopes exhibited similar characteristics, with the maximum negative force at -130% of the target displacement  $F_{@-130\%}$  reaching approximately -295 kN. The lateral displacements of the first floor were 79 mm for the positive 130% target displacement and -71 mm for the negative 130% target displacement. Comparatively, the 2<sup>nd</sup> storey drifts were larger, measuring 116 mm and -124 mm, respectively, which is approximately 60% greater than the 1<sup>st</sup> storey drifts.

### **Hold down and tension strap uplift**

The load-displacement curves exhibited quasi-linear envelopes until the +130% target displacement, where the total load ( $F_{@+130\%}$ ) reached 316 kN. Figure 3.34 illustrates that the corresponding uplifts in the HD on the left side of the shear wall were 20 mm. Conversely, at the -130% target displacement, the uplifts on the right side of the shear wall measured 21 mm. When the uplifts in the HD are negative, the panel corners undergo compression. At the 130% target displacement, the maximum compression observed at these corners ranged from 3 mm to 4.8 mm.

The tension strap uplifts (Figure 3.34b) on the left side of the shear wall were 13.7 mm at the +130% target displacement, while they reached 17.8 mm during the +160% target displacement. The tension strap uplifts on the right side of the shear wall were 13.7 and 18.2 mm at the -130% target displacement that increased to 18.9 mm and 25.6 mm in the next cycle. At 160% target displacements, the maximum compression at tension straps ranged from 2.3 mm to 5 mm.

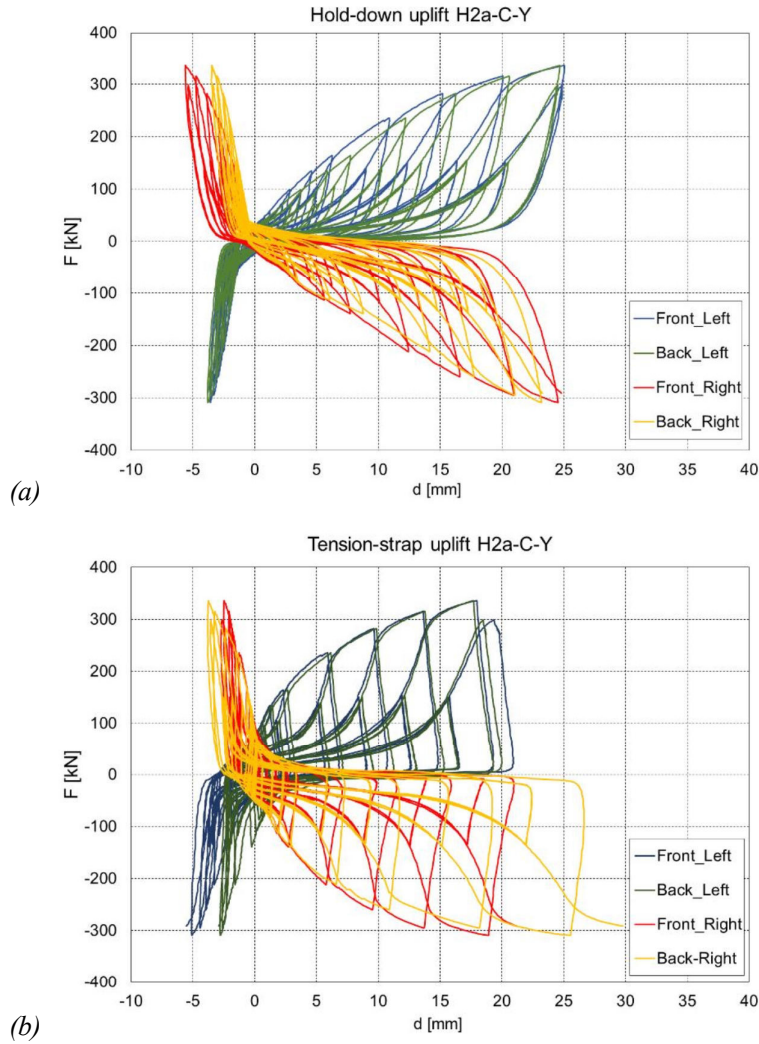


Figure 3.34. H2a uplifts at (a) the HDs, (b) tension straps

### First and second storey inner corner uplifts

Figure 3.35 shows the vertical uplift at the four inner corners of the coupled shear walls. The load-displacement curves' envelopes were mostly quasi-linear until the load  $F_{@+130\%}$  reached 316 kN at the +130% target displacement. In the 1<sup>st</sup> storey shear wall (Figure 3.35a), the corresponding uplifts at the inner corners were 16 mm and 18.6 mm on the right side of the shear wall. At the -130% target displacement, the uplifts on the left side of the shear wall varied from 15.3 mm, which closely resembled the HD uplifts of the 1<sup>st</sup> storey. The differences between the positive and negative uplifts were minimal.

The negative uplifts are linked to the compression at the corners of the panel. The front panels and the back right panel had almost no compression, while the back left panel had 2.2 mm of compression. In the 2<sup>nd</sup> storey shear wall (as shown in Figure 3.35b), the inner corners were lifted by 11.3 mm to 17.4 mm when the target displacement was +/-130%. During the following cycle, these values increased to between 15.4 mm and 24.3 mm. There was no compression observed in the inner corners, as they were always slightly lifted by the panel on the opposite side.

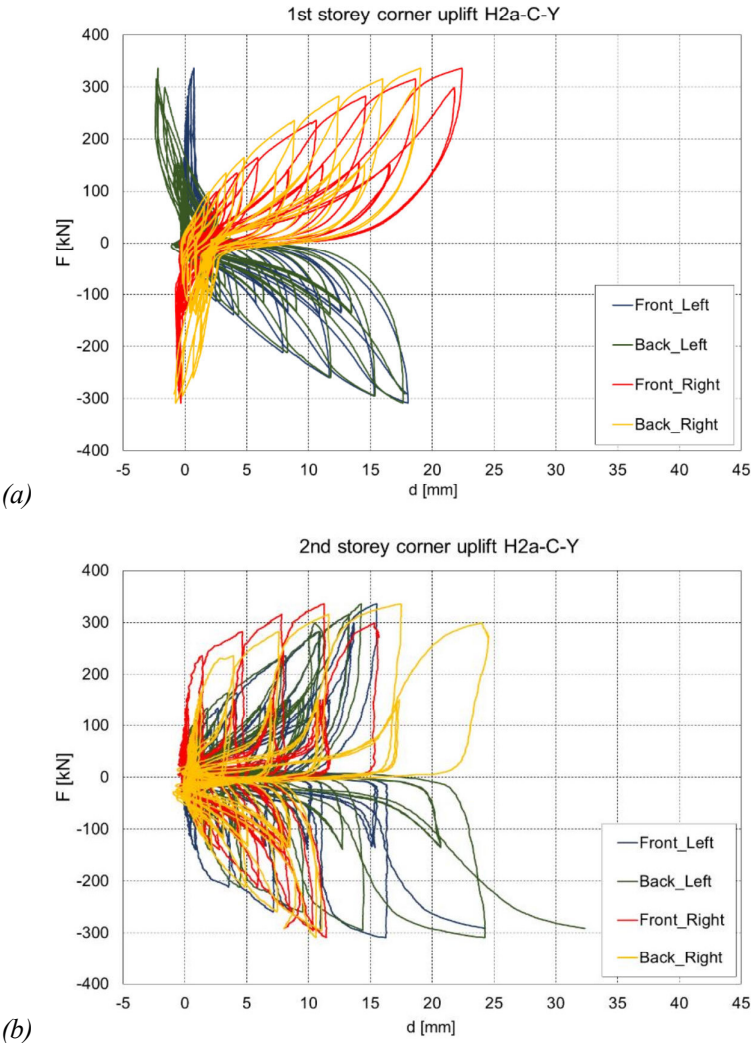


Figure 3.35. H2a inner corner uplifts at (a) 1<sup>st</sup> storey, (b) 2<sup>nd</sup> storey

### **Panel sliding**

The sliding values at the base and 1<sup>st</sup> level floor are shown in Figure 3.36. There was only a small amount of sliding at the base level, with the highest values being 2.3 mm and 2.8 mm for the front and back side panels, respectively, when the displacement was increased to +130% target displacement, see Figure 3.36a.

At the 1<sup>st</sup> level floor, the sliding values were higher, ranging from 8.3 mm to 12.7 mm when the displacement was reached to +130% target displacement and from 5.2 mm to 10.3 mm when the displacement was reached to -130% target displacement, as shown in Figure 3.36b. These values contribute around 10% of the total lateral displacement of the two-storey shear wall and should not be ignored in design. Despite this, there was no reduction in strength, and the stiffness even seemed to be increasing. Additionally, there was no damage observed in the actual SB.

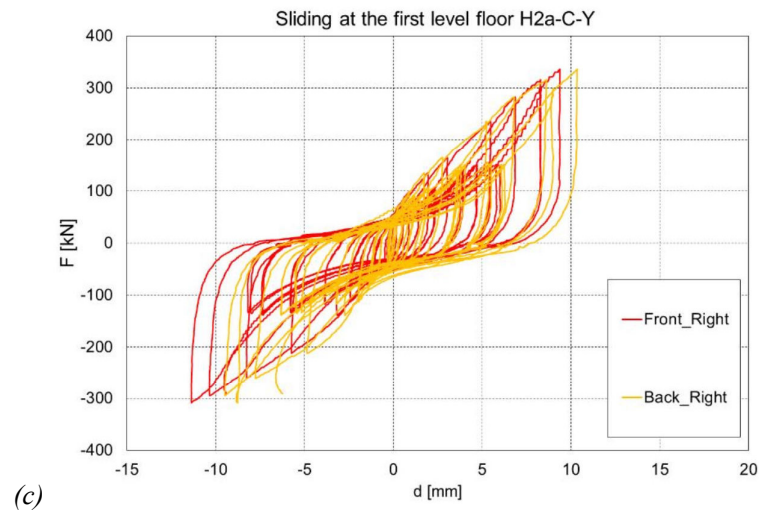
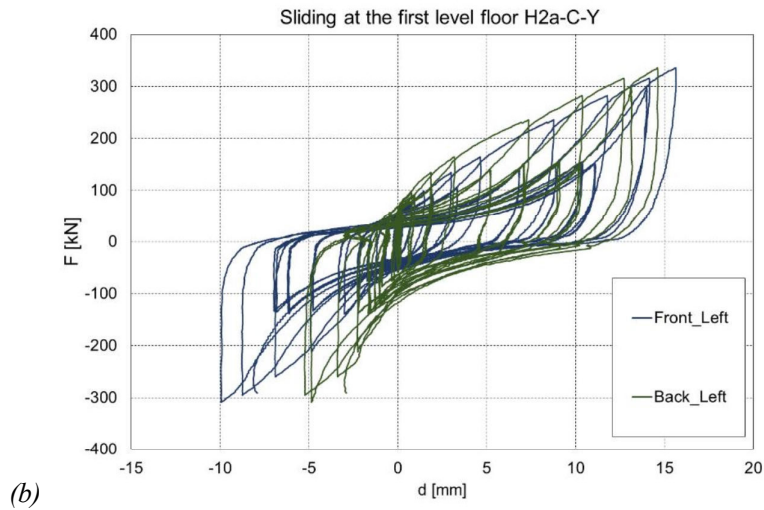
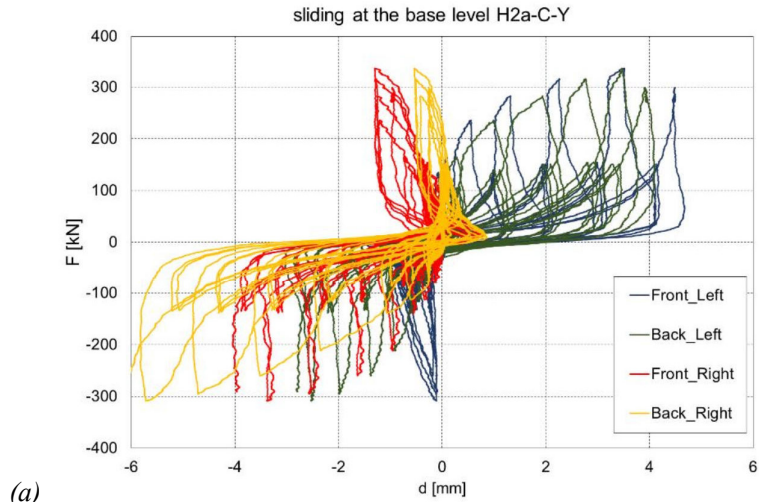


Figure 3.36. H2a panel sliding at a) base level, b) 1<sup>st</sup> level left, c) 1<sup>st</sup> level right

### Panel-to-panel slip

The Panel-to-panel slip is presented in Figure 3.37. The load-displacement curves exhibited nearly linear behavior up to a displacement of +130%, at which point the total load  $F_{@+130\%}$  reached 316 kN. Concurrently, the corresponding panel slips, as shown in Figure 3.37a, were approximately 22 mm and did not significantly differ between the front and back panels or between positive and negative cycles.

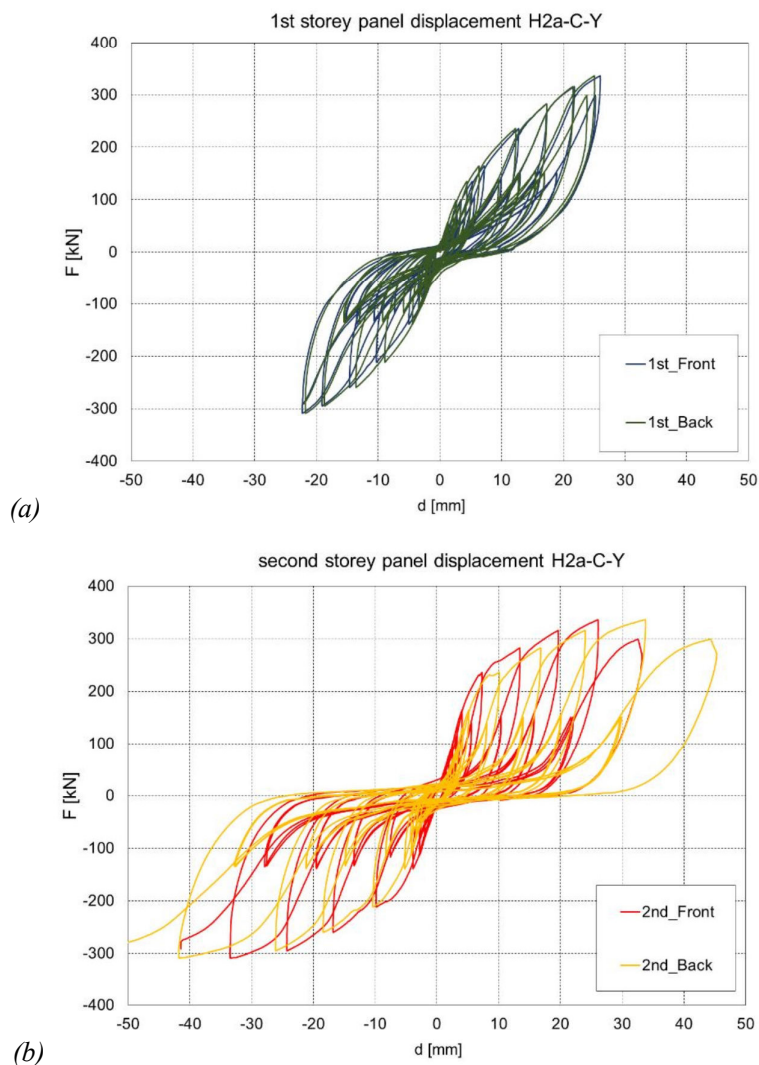


Figure 3.37. H2a panel displacements in test, a) 1<sup>st</sup> storey, b) 2<sup>nd</sup> storey

Figure 3.37b depicts that the panel slips in 2<sup>nd</sup> storey shear wall create a linear envelope until the +130% target displacement. At this displacement level, sliding measured approximately 19.7 mm at the front and 24 mm at the back, and 24.3 mm at the front and 26.1 mm at the back when at the -130% target displacement. Throughout the testing, there was no observed compression.

### **3.6.5 Results test #H2b**

#### **Horizontal storey displacements**

The horizontal storey displacements are illustrated in Figure 3.38. The envelope of the load-displacement curve was quasi-linear to 130% of the target displacement (equal to 195 mm in cycle 38) with the total load  $F_{@+130\%}$  reaching 311 kN. During the subsequent displacement cycle (top actuator displacement 240 mm), the total load only reached 296 kN, and parts of the load resisting system failed.

The positive and negative envelopes were very similar, with the maximum negative force at -130% of the target displacement  $F_{@-130\%}$  reaching approximately 300 kN. The lateral displacements (1<sup>st</sup> storey drift) of the first floor were 75 mm and -70 mm for the positive and negative 130% target displacement respectively. The 2<sup>nd</sup> storey drifts were 120 mm and 125 mm and therefore roughly 70% larger.

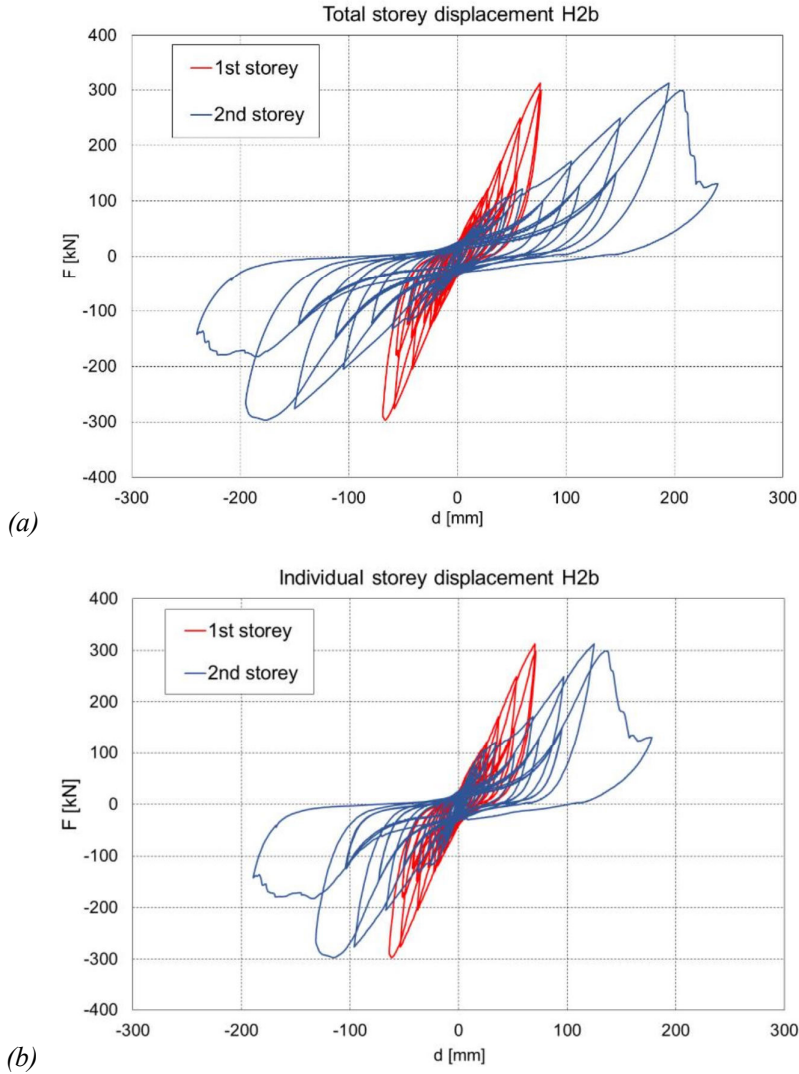


Figure 3.38. H2b (a) total storey displacements, (b) individual storey displacements

### Hold down and tension strap uplift

The vertical uplift experienced in the four HD and tension straps (two on the front shear back shear walls each) are illustrated in Figure 3.39. The envelopes of the load-displacement curves were all quasi-linear up to the +130% target displacement when the total load  $F_{@+130\%}$  reached 311 kN. The corresponding HD uplifts (Figure 3.39a) on the left side of the shear wall were 18 mm and 18.5 mm. At the -130% target displacement, the uplifts on the right side of the shear wall were 21 mm and 15 mm. The negative HD

uplifts correspond to compression in the panel corners. The maximum compressions at the 130% target displacements ranged from 2 mm to 4 mm. The tension strap uplifts (Figure 3.39b) on the left side of the shear wall were 2.6 mm and 4.7 mm at the +130% target displacement, while they reached 6.3 mm and 3.2 mm during the +160% target displacement. The tension strap uplifts on the right side of the shear wall were 10.4 and 23.5 mm indicating onset of failure which in the next cycle with uplifts exceeding 47 mm.

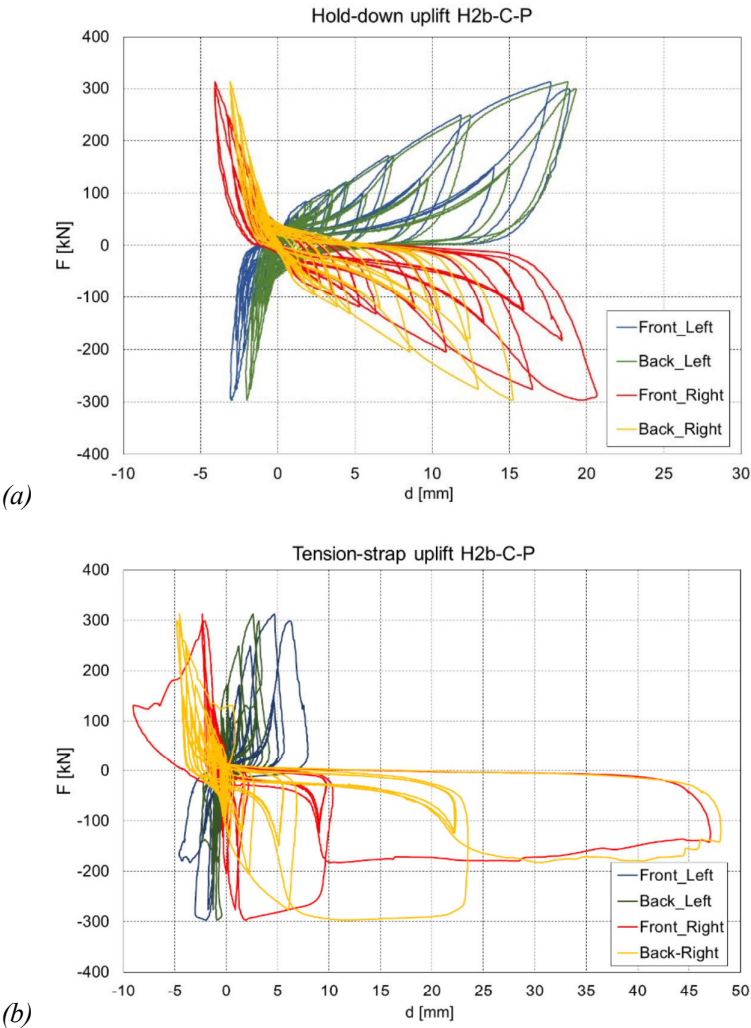


Figure 3.39. H2b uplifts at (a) the HDs, (b) tension straps

### First and second storey inner corner uplifts

The vertical uplift experienced in the four inner corners of the coupled shear walls are illustrated in Figure 3.40. The envelopes of the load-displacement curves were all quasi-linear up to the +130% target displacement when the total load  $F_{@+130\%}$  reached 311 kN.

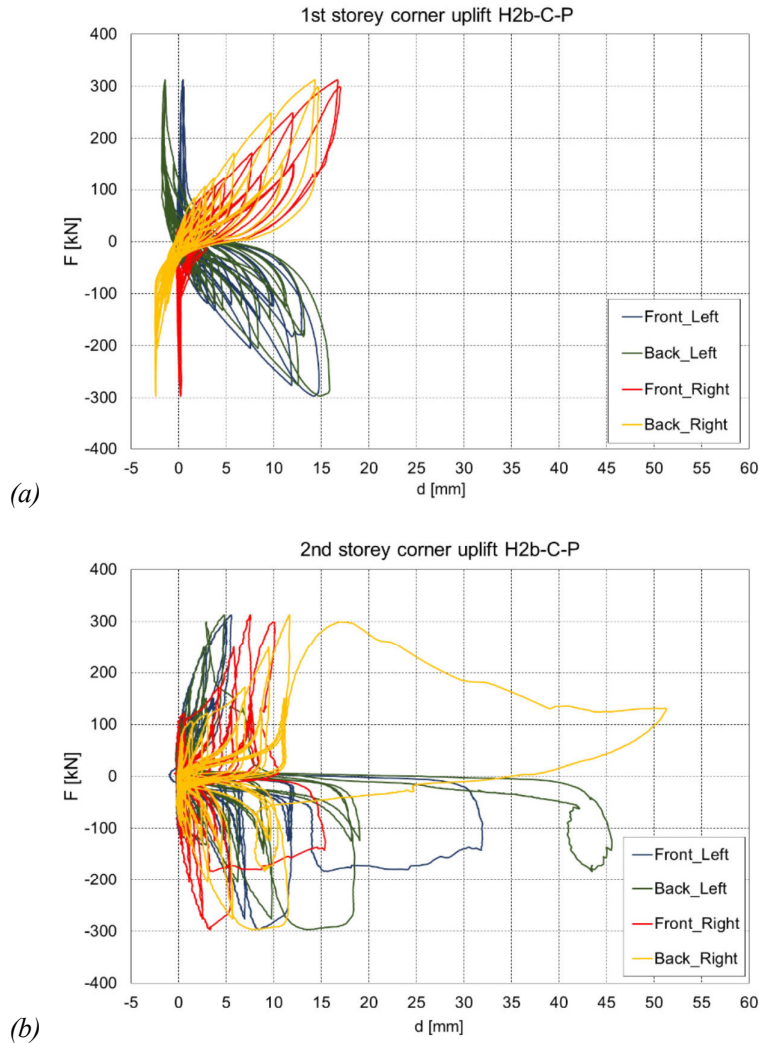


Figure 3.40. H2b inner corner uplifts at (a) 1<sup>st</sup> storey, (b) 2<sup>nd</sup> storey

The corresponding inner corner uplifts in the 1<sup>st</sup> storey shear wall (Figure 3.40a) were 16.7mm and 14.3 mm. At the -130% target displacement, the uplifts on the left side of the shear wall ranged from 14.8 mm to 15.8 mm, closely mirroring the HD uplifts of the

1<sup>st</sup> storey. Differences between positive and negative target displacements were minimal. The negative uplifts correspond to compression in the panel corners; these were close to zero on the front panels and between 2 mm and 4mm on the back panels.

The inner corner uplifts in the 2<sup>nd</sup> storey shear wall (Figure 3.40b) ranged from 3 mm to 18 mm at the +/-130% target displacements and increased to values of up to 23 mm during the subsequent cycle when the structure exceeded its capacity. No compression was observed as the inner corners were always slightly lifted by the opposite side panel.

### **Panel sliding**

The sliding values at each level (base level, 1<sup>st</sup> level floor, and 2<sup>nd</sup> level floor) are shown in Figure 3.42. The sliding at the base level (Figure 3.42a) was very small, with maximum values at the +130% target displacement of 1.1 mm and 1.6 mm for the front and back side panels, respectively. The sliding at the 2<sup>nd</sup> level floor (Figure 3.42c) was even smaller with actually negative values at the +130% target displacement and 2 mm and 4 mm at the -130% target displacement. From these observations, it can be concluded, that while sliding was not completely prevented, the overall contributions of sliding at the base level and the 2<sup>nd</sup> level floor when measured directly between shear wall panel and floor were less than 5% of the storey displacement.

The sliding at the 1<sup>st</sup> level floor (Figure 3.42b) reached values from 14 mm to 20 mm at the +130% target displacement and from 9 mm and 16 mm at the -130% target displacement. These values therefore contribute roughly 10% of the overall lateral displacement of the 2-storey shear wall and cannot be neglected in design. However, no strength degradation was observed, rather, the stiffness seems to be increasing, and no damage in the actual SB was observed.

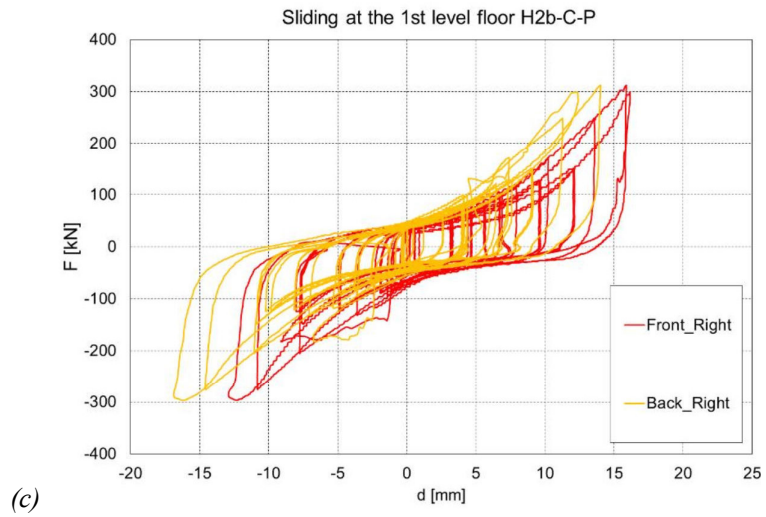
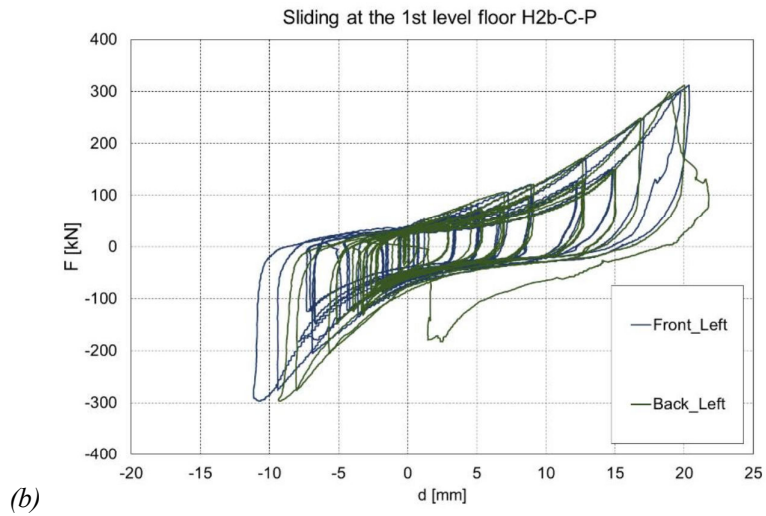
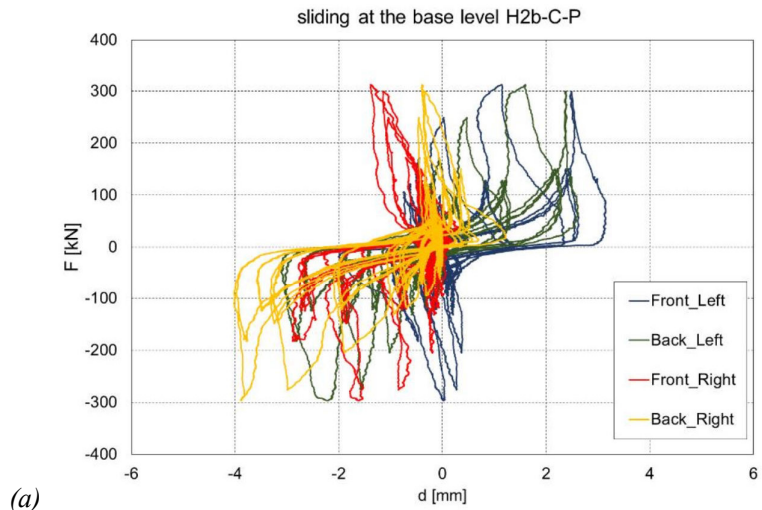


Figure 3.41. H2b panel sliding at a) base level, b) 1<sup>st</sup> level left side, c) 1<sup>st</sup> level right side

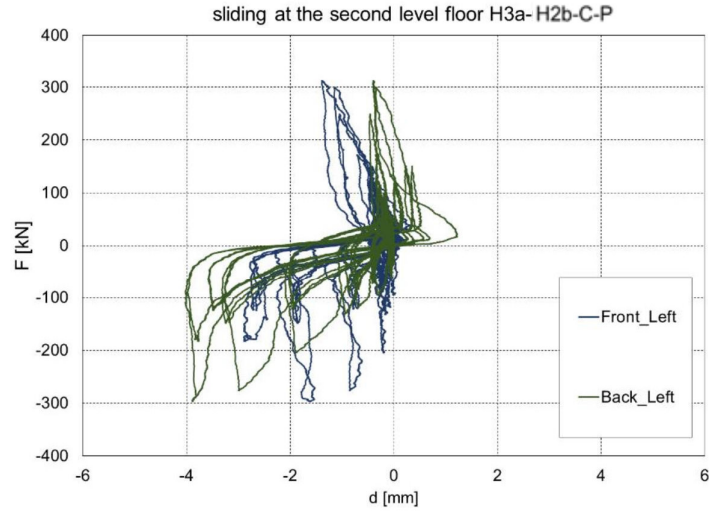


Figure 3.42. H2b panel sliding at 2<sup>nd</sup> floor

### Panel-to-panel slip

The Panel-to-panel slips are presented in Figure 3.43. The envelopes of the 1<sup>st</sup> storey load-displacement curves were all quasi-linear up to the +130% target displacement when the total load  $F_{@+130\%}$  reached 311 kN. The corresponding panel slips (Figure 3.43a) were approximate 20 mm, with almost no difference between back and front panels or positive and negative cycles.

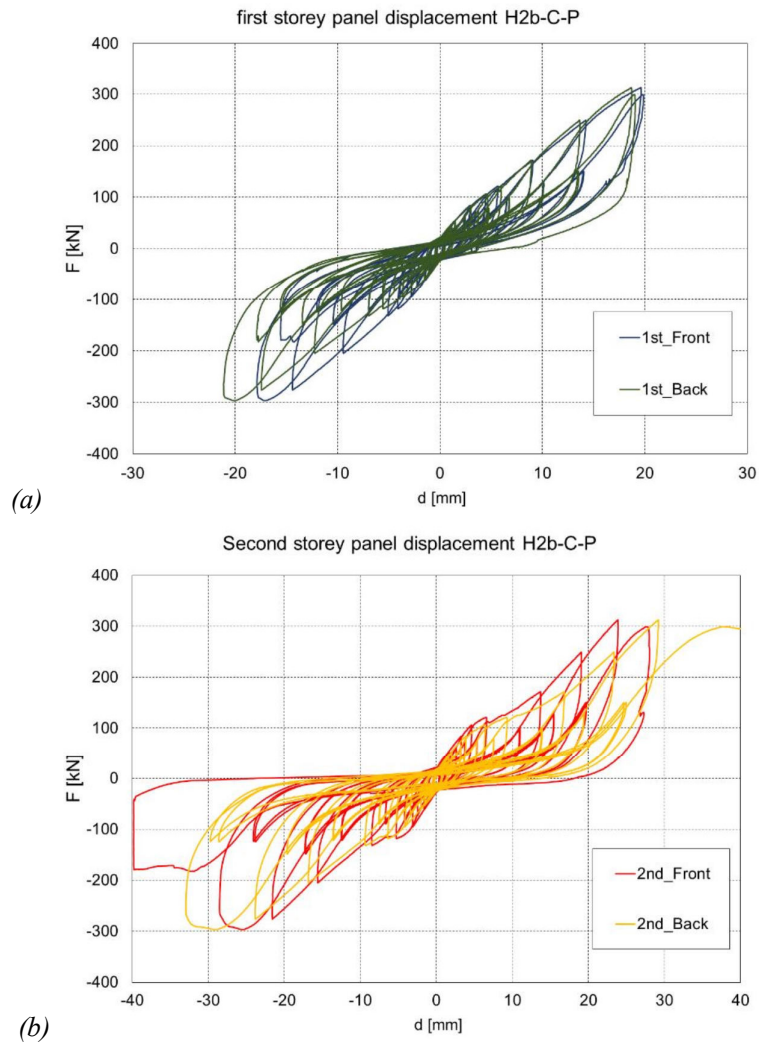


Figure 3.43. H2b panel displacements in test, a) 1<sup>st</sup> storey, b) 2<sup>nd</sup> storey

The panel slips in the 2<sup>nd</sup> storey shear wall (Figure 3.43b) did not create a linear envelope but exhibited a small but noticeable drop in stiffness when the total load reached approximately 120 kN. At the +130% target displacement were 24 mm (front) and 29 mm (back) and 22 mm (front) and 24 mm (back) at -130% target displacement. The spline connection in the back panel failed during the subsequent cycle when pushed to the 160% target displacement. No compression was observed as the inner corners.

### 3.6.6 Results test #H3a

#### Horizontal storey displacements

The horizontal storey displacements are illustrated in Figure 3.44. The load-displacement curve's envelope demonstrated a quasi-linear relationship up to +100% of the target displacement (equivalent to 150 mm in cycle 31), with the total load  $F_{@+100\%}$  reaching 299 kN. However, the positive and negative envelopes exhibited discrepancies. The maximum negative force at -130% of the target displacement, denoted as  $F_{@-130\%}$ , reached approximately -284 kN. Notably, due to detachment of the 2<sup>nd</sup> floor, the graph did not extend to -160% of the target displacement.

The lateral displacements, specifically the 1<sup>st</sup> storey drift, measured 72 mm and -66 mm for the +100% and -100% of the target displacement, respectively. Similarly, the 2<sup>nd</sup> storey drifts were 78 mm and -84 mm for the +100% and -100% of the target displacement, respectively, demonstrating an increase of roughly 25% compared to the 1<sup>st</sup> floor.

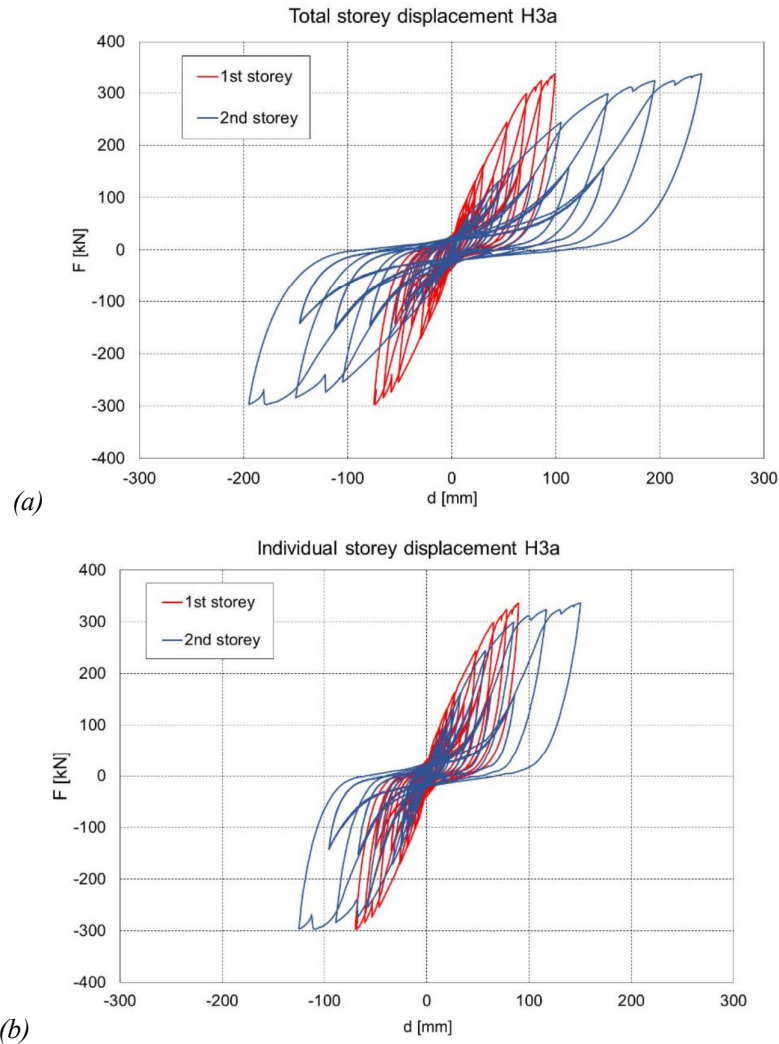


Figure 3.44. H3a (a) total storey displacements, (b) individual storey displacements

### Hold down and tension strap uplift

It was observed that all the load-displacement curves' envelopes were quasi-linear until the target displacement of +100%. At this point, the total load of  $F_{@+100\%}$  was found to be 336 kN, with corresponding HD uplifts of 16.6 mm on the left side of the shear wall for both HD, as shown in Figure 3.45a. On the right side of the shear wall, at the -100% target displacement, uplifts of 15.2 mm and 13.7 mm were recorded. The maximum compression values at the +100% and -100% target displacement ranged from 3.8 mm to 2 mm.

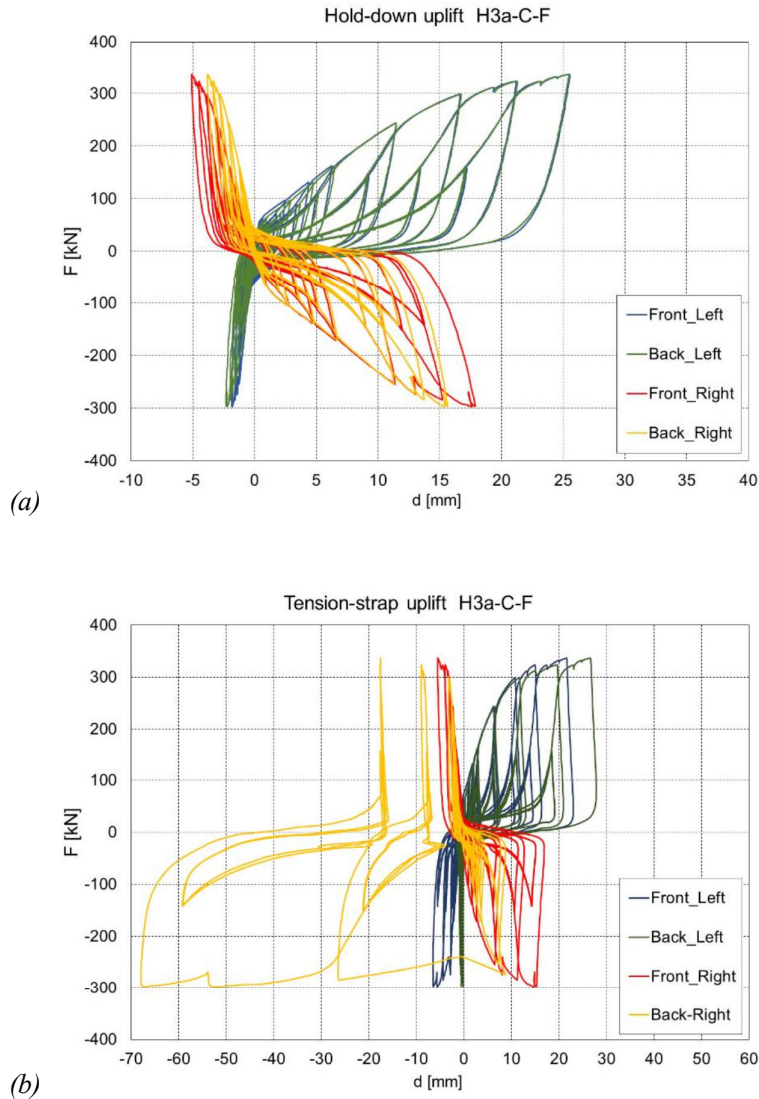


Figure 3.45. H3a uplifts at (a) the HDs, (b) tension straps

During the +100% target displacement, the tension strap uplifts on the left side of the shear wall measured 10.8 mm and 11.7 mm. As the target displacement increased to +130%, these uplifts further rose to 15 mm and 19.6 mm. On the front right side of the shear wall, the tension strap uplift was initially 11.2 mm at the -100% target displacement. It then increased to 15.3 mm at mm at a target displacement of -130%, while on the back right side, it was 26.3 mm indicating a set of failure that was followed by an increase of -68 mm at a target displacement of -130%. In the compression zone, three points tolerated

compressions ranging from -0.4 mm to -4.4 mm at +/-100% target displacement. However, the back right corner experienced a compression of -18 mm, at the last cycle.

### First and second storey inner corner uplifts

Figure 3.46 demonstrates the vertical uplift observed in the four internal corners of the joined shear walls. The load-displacement curves' envelopes were almost linear until the target displacement of +100%, where the total load of  $F_{@+100\%}$  was 299 kN.

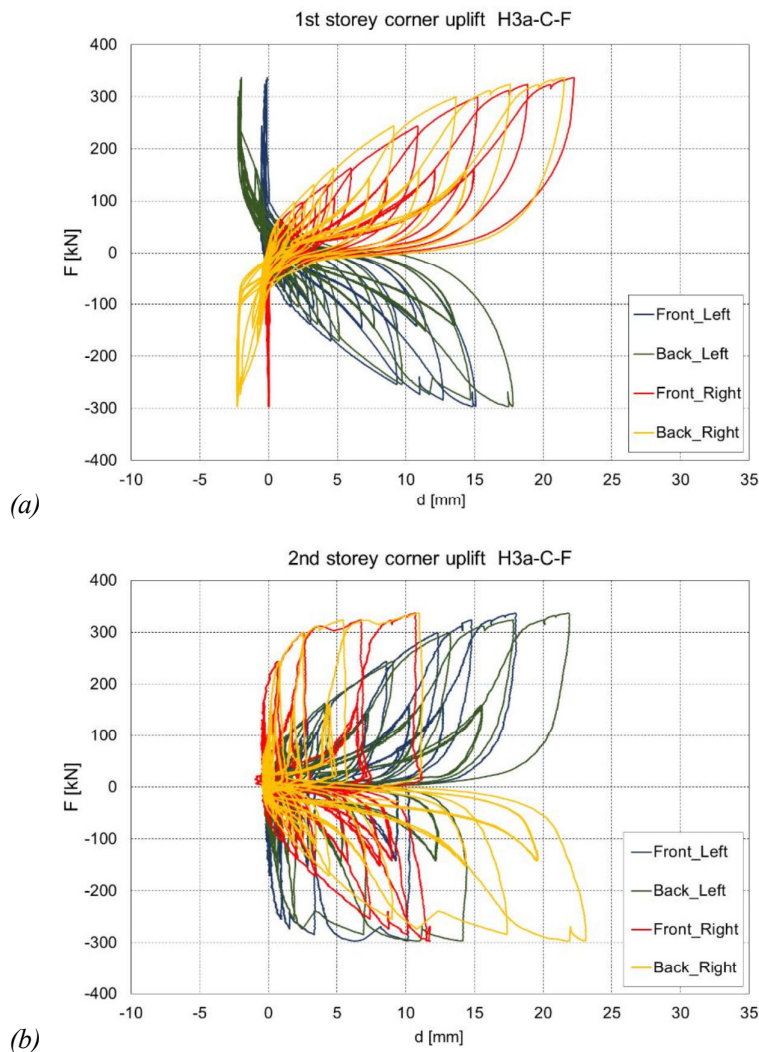


Figure 3.46. H3a inner corner uplifts at (a) 1<sup>st</sup> storey, (b) 2<sup>nd</sup> storey

In the first-storey shear wall, the corresponding inner corner uplifts were 13.6 mm and 15.2 mm on the right side of the shear wall, see Figure 3.46a. On the left side of the shear wall, at the -100% target displacement, uplifts ranged from 12.7 mm to 14.7 mm. The uplift differences between positive and negative target displacements were minimal. The negative uplifts indicate compression in the panel corners. The front panels had almost zero compression, while the back panels had compression of 2.2 mm. In the 2<sup>nd</sup> storey shear wall (Figure 3.46b), the inner corner uplifts varied between 2.5 mm and 17.3 mm during the +/-100% target displacements. These uplifts increased to value 4.8 mm and 23.1 mm in the +/-130% target displacement. The inner corners were never compressed.

### **Panel sliding**

The sliding observed at the base level (Figure 3.48a) was very small, with maximum values at the +130% target displacement measuring 1.9 mm and 2.3 mm for the front and back side panels, respectively. At the 2<sup>nd</sup> level floor (Figure 3.48c), the sliding measured 11.8 mm and 3.9 mm for the front and back side panels, respectively, at the +130% target displacement. These values increased to 16.25 mm and 13.7 mm at the +160% target displacement, indicating a failure in the screws of the SB. The slide was less than 1 mm at the -130% target displacement.

At the 1<sup>st</sup> level floor, sliding values illustrated in Figure 3.48b were higher, ranging from 15.3 mm to 17.7 mm when the displacement was increased to +130% of the target displacement, and from 12.9 mm to 19.6 mm when the displacement was reached to -130% of the target displacement. These values account for approximately 10% of the total lateral displacement of the 2-storey shear wall, and they are significant for design considerations. However, there was no reduction in strength, and the stiffness even appeared to be increasing. Moreover, no damage was observed in the SB themselves.

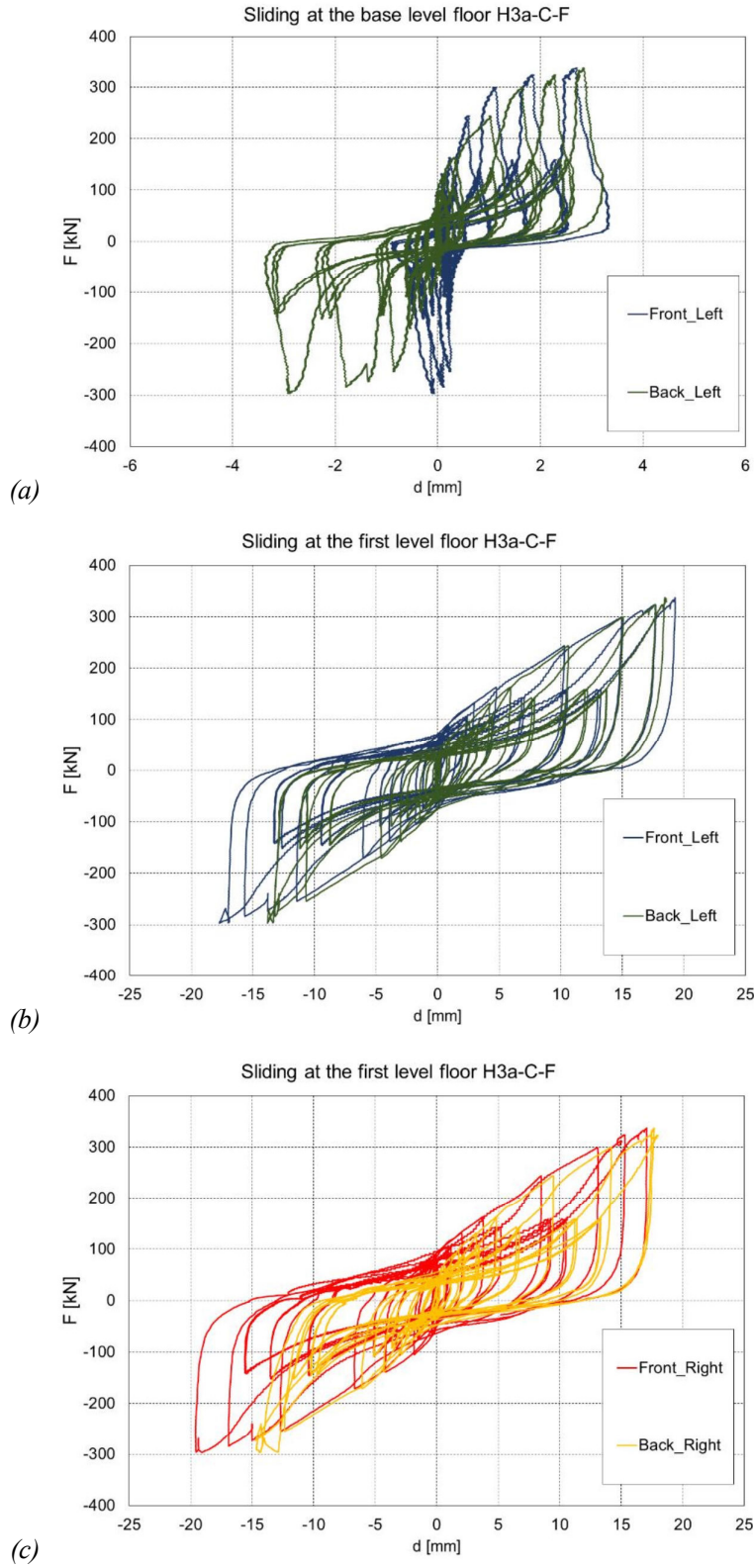


Figure 3.47. H3a panel sliding at: (a) base level, (b) 1<sup>st</sup> floor left, (c) 1<sup>st</sup> floor right

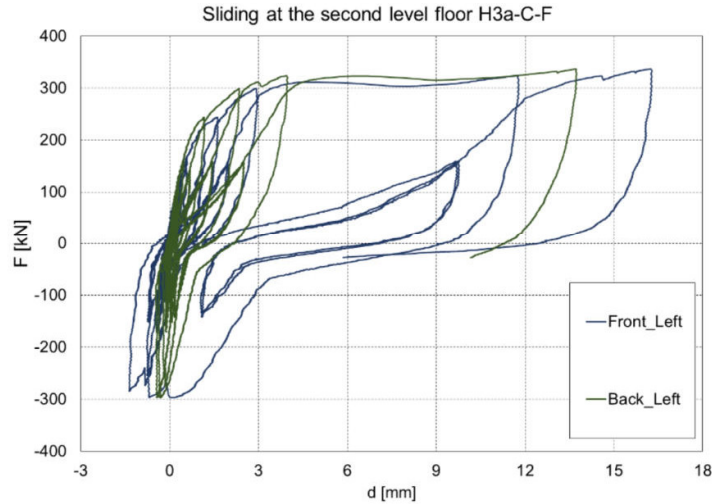


Figure 3.48: H3a panel sliding at 2<sup>nd</sup> floor

### Panel-to-panel slip

The Panel-to-panel slips are presented in Figure 3.49. The load-displacement curves demonstrated mostly linear behavior up to a displacement of +100% target displacement. At this point, the total load, indicated as  $F_{@+100\%}$ , reached 299 kN.

Simultaneously, the 1<sup>st</sup> storey panel slips corresponding to this displacement, as depicted in Figure 3.49a, were approximately 18 mm in positive and 17 mm in negative cycles.

Figure 3.49b demonstrates that the panel slips in the 2<sup>nd</sup> floor shear wall produce a linear envelope up to +70% target displacement. At this displacement, the front panel slid 6mm, and at the -70% target displacement, the back panel slid 6.1 mm. The maximum slip at +/160% target displacement was 22mm.

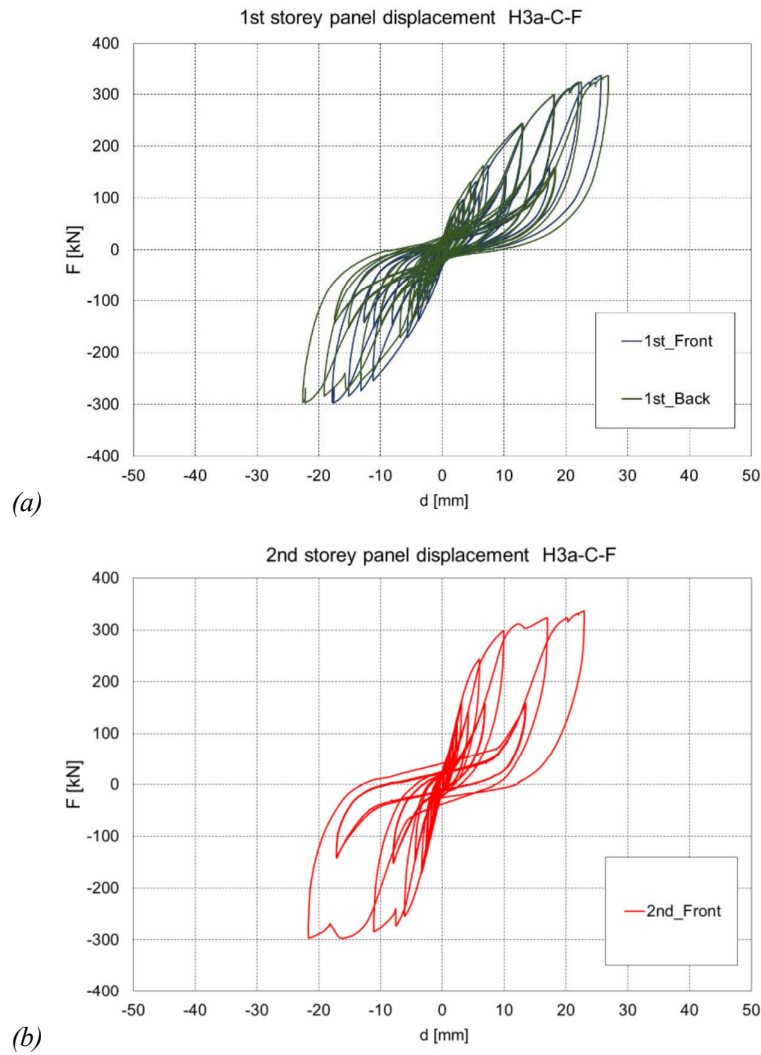


Figure 3.49. H3a Panel-to-panel slip for: (a) 1<sup>st</sup> storey, (b) 2<sup>nd</sup> storey

### Panel distortion

The distortion of two 1<sup>st</sup> storey panel was measured. Both panels mostly distorted during their respective compression cycles with the maximum values reaching 1.5 mm and 3.5 mm, while the distortion during their tension cycles was less than 1 mm.

### 3.6.7 Results test #H3b

#### Horizontal storey displacements

The horizontal storey displacements are illustrated in Figure 3.50. The load-displacement curve exhibited a nearly linear pattern up to 130% of the target displacement, equivalent to 195 mm, with a maximum total load of 313 kN. However, in the subsequent displacement cycle (with a top actuator displacement of 240 mm), the total load only reached 321 kN, and certain parts of the load-resisting system experienced failure. The positive and negative envelopes of the curve were quite similar, with the maximum negative force occurring at -160% of the target displacement  $F_{@-160\%}$ , reaching approximately 336 kN, followed by a slight decrease in the next cycle to 332 kN. The lateral displacements of the first floor were approximately 94 mm and -88 mm for the +/- 130% target displacements, respectively. In contrast, the 2<sup>nd</sup> storey drifts were around 101 mm and -107 mm, making them roughly 15% larger than the 1<sup>st</sup> storey displacements.

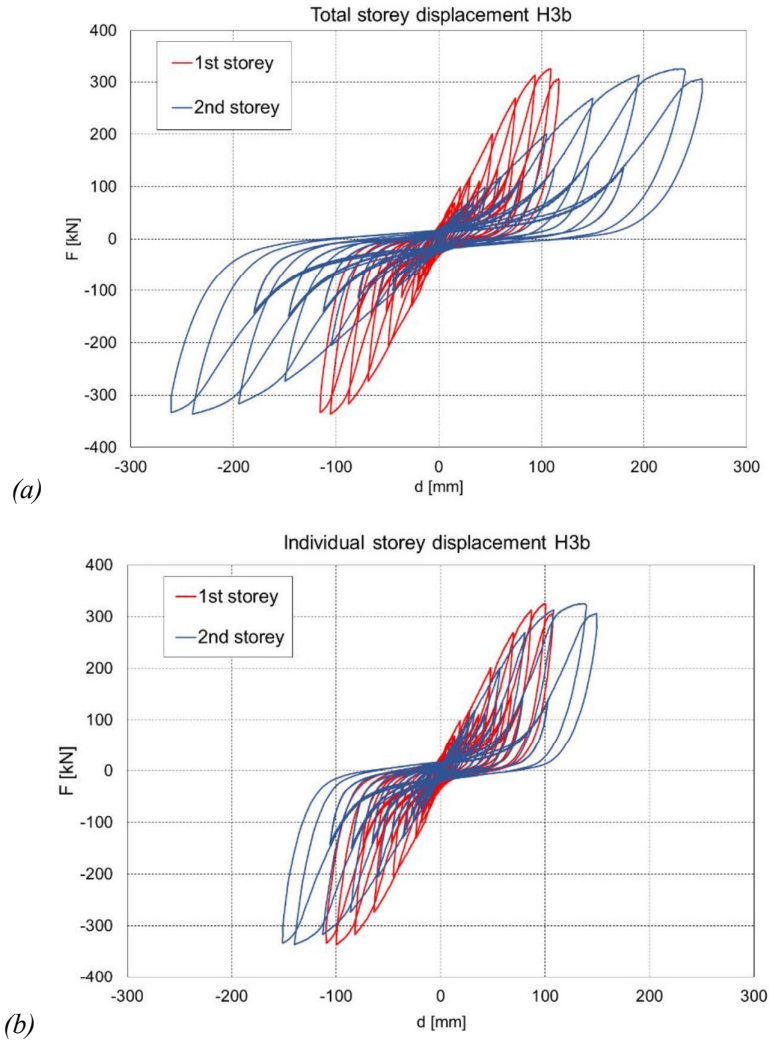


Figure 3.50. H3b (a) total storey displacements, (b) individual storey displacements

### Hold down and tension strap uplift

The vertical uplift experienced in the four HD and tension straps (two on the front shear back shear walls each) are illustrated in Figure 3.51. The load-displacement curves exhibited quasi-linear behavior up to the +130% target displacement, with the total load  $F_{@+130\%}$  reaching 313 kN.

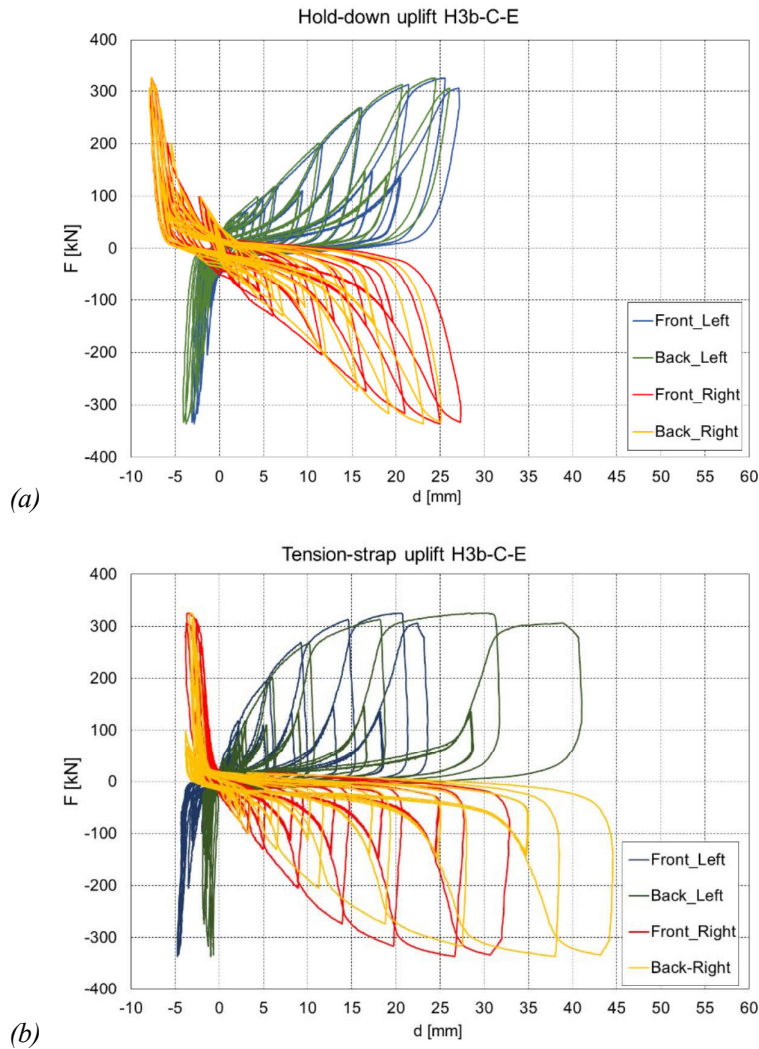


Figure 3.51. H3b uplifts at (a) the HDs, (b) tension straps

On the left side of the shear wall, the corresponding uplifts (Figure 3.51a) were measured at 21.2 mm and 21.3 mm. Conversely, at the -130% target displacement, the uplifts on the right side of the shear wall were recorded at 21 mm and 19.2 mm. The negative uplifts indicate compression occurring in the panel corners. The maximum compressions observed at the +/-130% target displacements ranged from 2.5 mm to 7.3 mm.

The uplifts of the tension straps (Figure 3.51b) on the left side of the shear wall measured 14.6 mm and 18.2 mm at the +130% target displacement and increased to 20.8 mm and 31.2 mm at the +160% target displacement. On the right side of the shear wall, the tension

strap uplifts were 19.7 mm and 27 mm at the -130% target displacement, which further increased to 26.7 mm and 38 mm in the subsequent cycle. The negative uplifts for the tension straps ranged from 1 mm to 5 mm.

### **First and second storey inner corner uplifts**

Figure 3.52 illustrates the vertical uplift experienced in the four inner corners of the coupled shear walls. The load-displacement curves displayed quasi-linear behavior up to the +130% target displacement, with the total load reaching 313 kN at  $F_{@+130\%}$ . In the 1<sup>st</sup> storey shear wall on the right side (Figure 3.52a), the corresponding uplifts in the inner corners measured 15.1 mm and 17.7 mm. At the -130% target displacement, the uplifts on the left side of the shear wall ranged from 17.1 mm to 17.7 mm. The differences between positive and negative target displacements were minimal. The negative uplifts in the panel corners indicated compression, measuring around 1.4 mm on the front panels and 4.3 mm on the back panels. Figure 3.52b shows the uplifts in the inner corners of the 2<sup>nd</sup> storey shear wall. The uplift values ranged from 15.2 mm to 19 mm at the +/-130% target displacements and increased to 18.3 mm to 25.9 mm during the next cycle when the structure encountered +/-160% target displacements. There was a slight decrease in force observed in the last cycle. The inner corners of the wall were constantly uplifted by the opposite side panel, and hence no compression was observed.

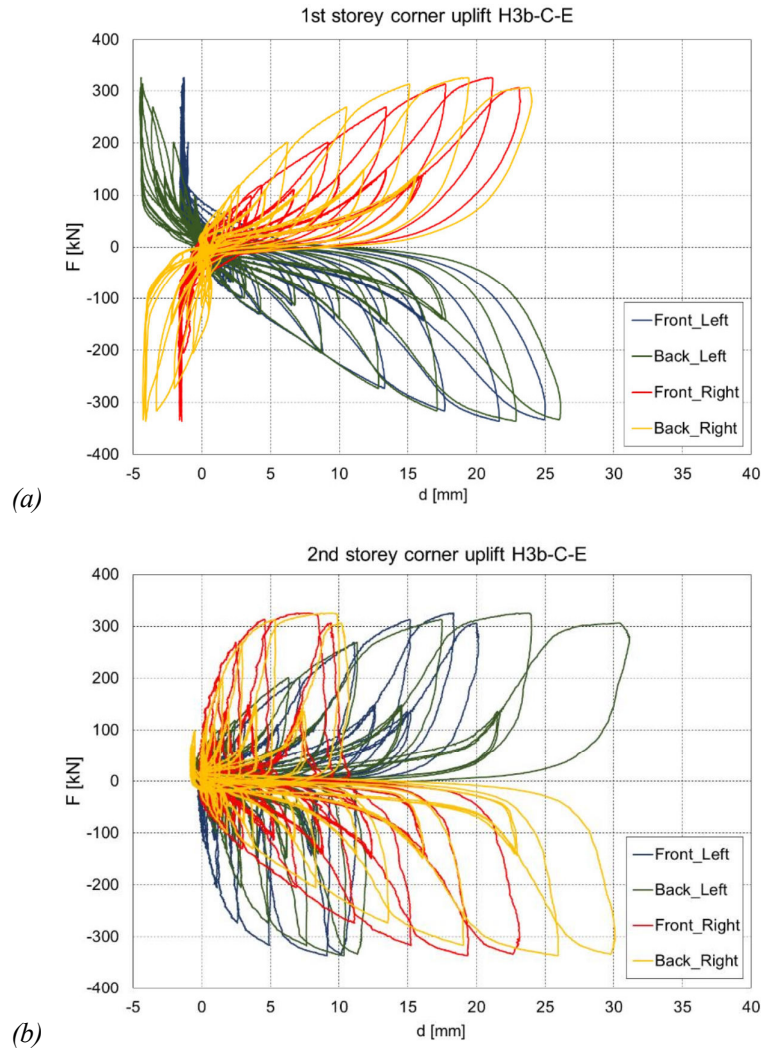


Figure 3.52. H3b inner corner uplifts at (a) 1<sup>st</sup> storey, (b) 2<sup>nd</sup> storey

### Panel sliding

The sliding at the base level (Figure 3.53a) was very small, with maximum values at the +130% target displacement of 2.6 mm and 3.7 mm for the front and back side panels, respectively. At the +130% target displacement the sliding at the 2<sup>nd</sup> level floor (Figure 3.53c) was 3 mm and 2.3 mm for the front and back side panels respectively, while in the +160% target displacement these values increased to 9.2 mm and 2.6 mm. At the -130% target displacement sliding was 1.7 and 0.8 mm for the front and back side panels respectively, while in the -160% target they were 1.2 mm and 0.7 mm.

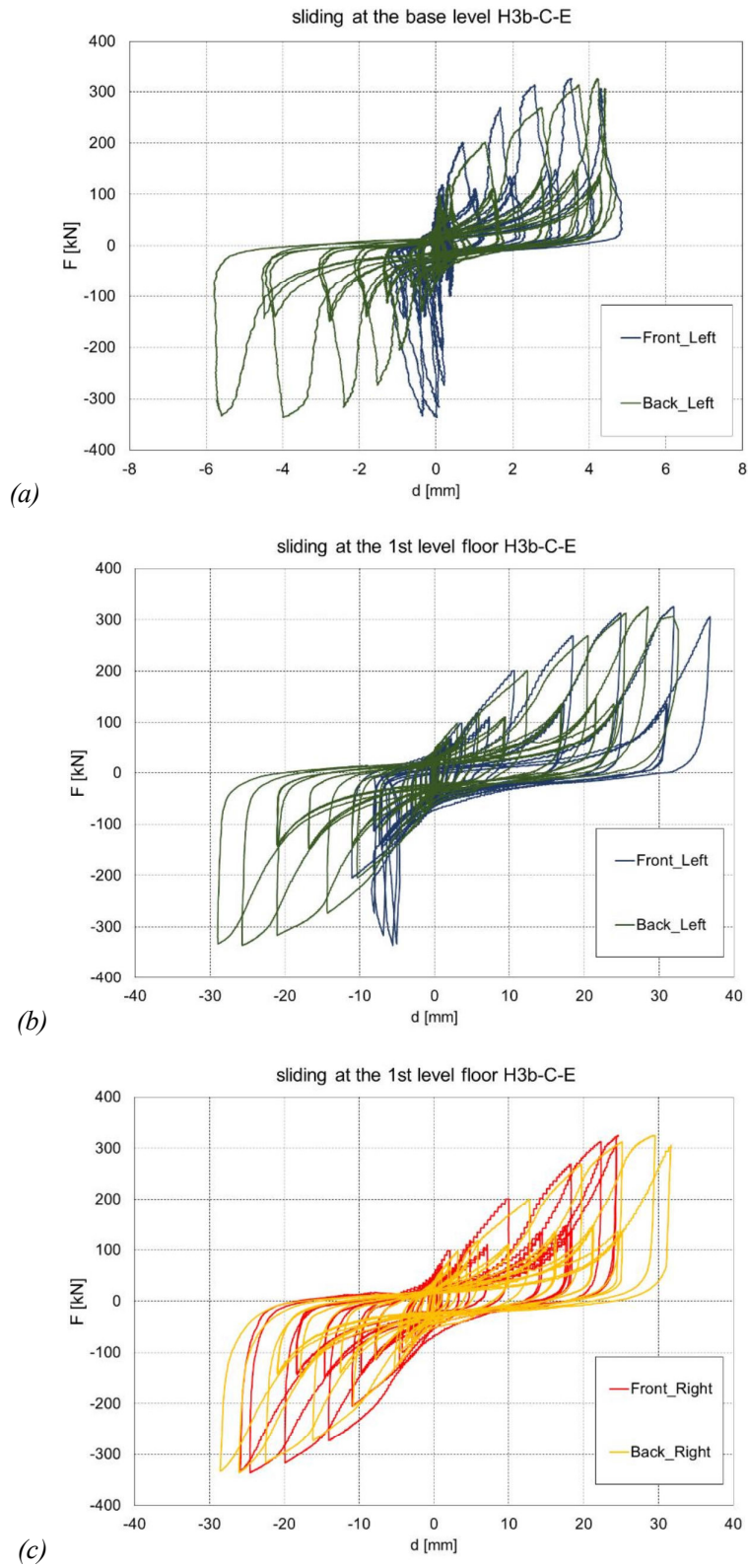


Figure 3.53. H3b panel sliding at: a) base level, b) 1<sup>st</sup> level floor left side, c) 1<sup>st</sup> level right side

At the +130% target displacement, sliding at the 1<sup>st</sup> level floor (Figure 3.54b) ranged from 22.3 mm to 25.6 mm, while at the -130% target displacement, it was between 6.8 mm and 22.5 mm. These values contributed approximately 10% of the total lateral displacement of the 2-storey shear wall. However, despite the significant contribution, only a minor reduction in strength was observed, and there was a slight increase in stiffness.

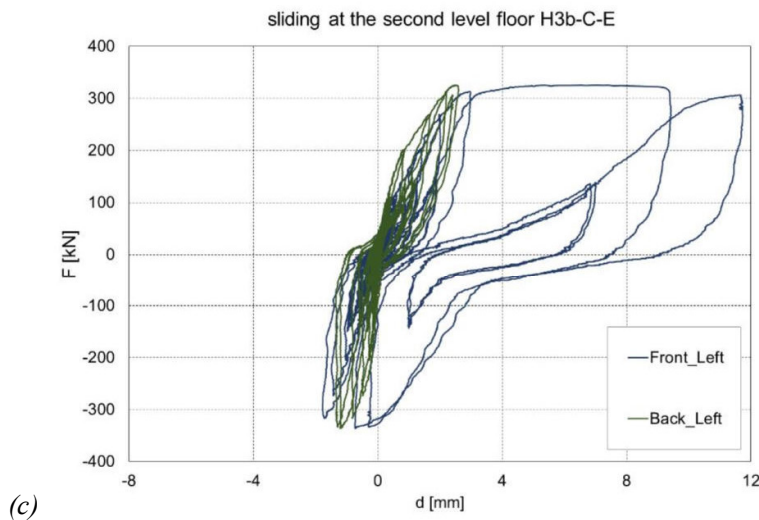


Figure 3.54. H3b panel sliding at 2<sup>nd</sup> level floor

### Panel-to-panel slip

The load-displacement curves of the 1<sup>st</sup> storey exhibited quasi-linear envelope patterns and remained so up to the +100% target displacement. At this displacement, the total load ( $F_{@+100\%}$ ) reached 267 kN. Panel slips at the +100% target displacement (Figure 3.55a) were approximately 25 mm, with negligible differences observed between the back and front panels or between the positive and negative cycles.

The panel slips in the 2<sup>nd</sup> storey shear wall (shown in Figure 3.55b) create a linear envelope up to the designated target displacement of +100% at this target displacement, the panel slipping measured approximately 9.5 mm. This slippage increased to 12.8 mm, when the target displacement of +130% was achieved with the same trends in back and

front panel and positive and negative cycles, also, no failures were observed in the spline connections, and there was no compression as the inner corners.

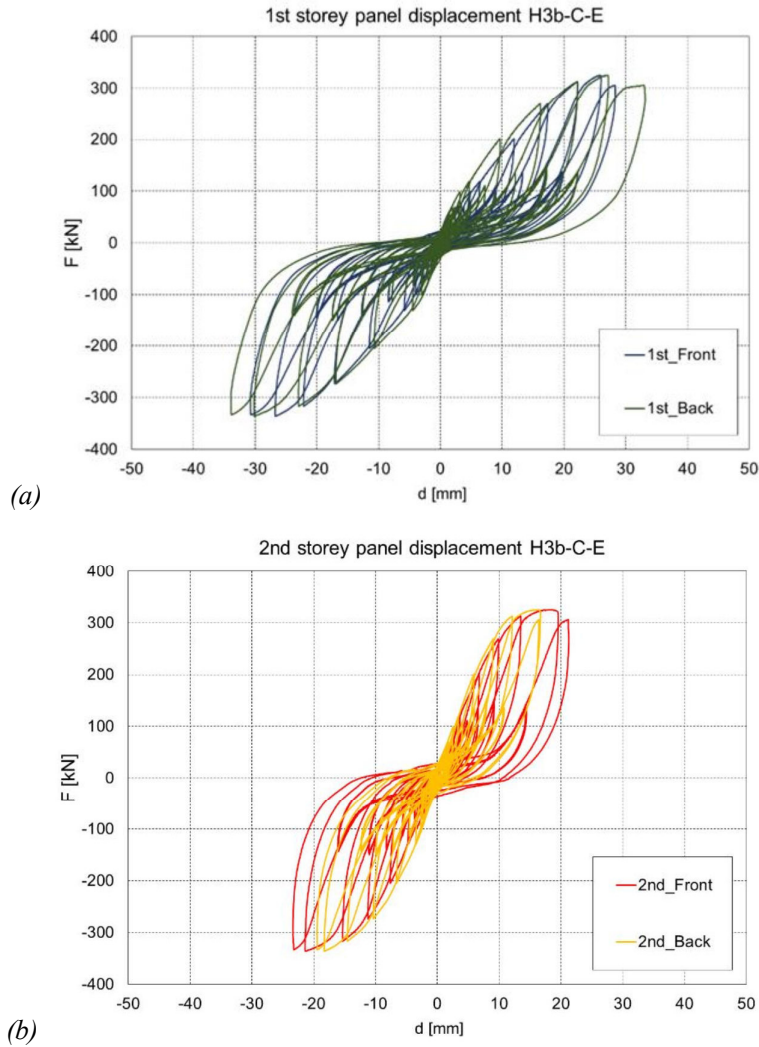


Figure 3.55. H3b panel displacements at: a) 1<sup>st</sup> storey, b) 2<sup>nd</sup> storey

### Panel distortion

Both 1<sup>st</sup> storey panels were distorted during their respective compression cycles with maximum values reaching 3.6 mm and 4 mm for the back left and front left panels, while the distortion during their tension cycles was only about 0.2 mm.

### 3.6.8 Results test #H4a

#### Horizontal storey displacements

The horizontal storey displacements are illustrated in Figure 3.56. As illustrated in Figure 3.56a, the envelope of the load-displacement curve was almost linear up to the 100% target displacement of 150 mm, with a maximum load of 257 kN. In the next cycle, where the top actuator moved to 195 mm, the total load increased slightly to 259 kN. However, during the last cycle, which involved a displacement of 240 mm (160% of the target displacement), some components of the load-resisting system failed, causing the total load  $F_{@+160\%}$  to decrease to 235 kN.

Both the positive and negative load-displacement curves had a similar shape, and the maximum negative force occurred at -130% of the target displacement,  $F_{@-130\%}$ , with a value of 282 kN. At this displacement, the 1<sup>st</sup> floor lateral displacements were 76 mm and -73 mm for the positive and negative directions, respectively. Meanwhile, the 2<sup>nd</sup> storey displacements were 119 mm and -122 mm, making them approximately 60% larger than those of the 1<sup>st</sup> floor (see Figure 3.56b).

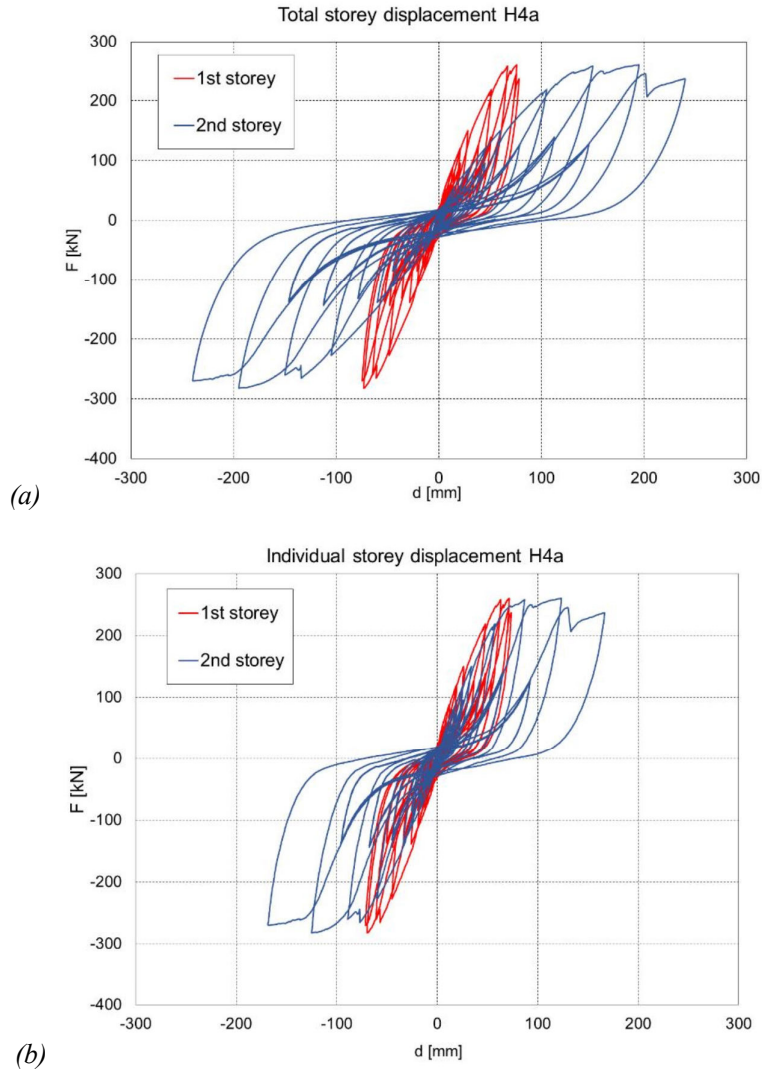


Figure 3.56. H4a (a) total storey displacements, (b) individual storey displacements

### Hold down and tension strap uplift

Figure 3.57 shows the vertical uplift experienced by the four HD and tension straps. The load-displacement curves for all HD were nearly linear up to the +130% target displacement, at which point the total load  $F_{@+130\%}$ , reached 259 kN. On the left side of the shear wall, the corresponding HD uplifts (Figure 3.57a) were 15.5 mm and 15 mm. At the -130% target displacement, the uplifts on the right side of the shear wall were 19.7

mm and 16 mm for the front and back HD, respectively. The negative HD uplifts indicate compression in the panel corners, with maximum compressions reaching 4.7 mm.

At the +130% target displacement, the tension strap uplifts on the left side of the shear wall measured 19.5 mm and 15 mm (Figure 3.57b). However, during the +160% target displacement, they significantly increased to 63 mm and 25.3 mm, indicating a sign of failure. On the right side of the shear wall, the tension strap uplifts were 20.5 mm and 29.5 mm, suggesting the onset of failure. In the subsequent displacement cycle, the uplifts exceeded 50 mm, further indicating the failure of the tension straps screws.

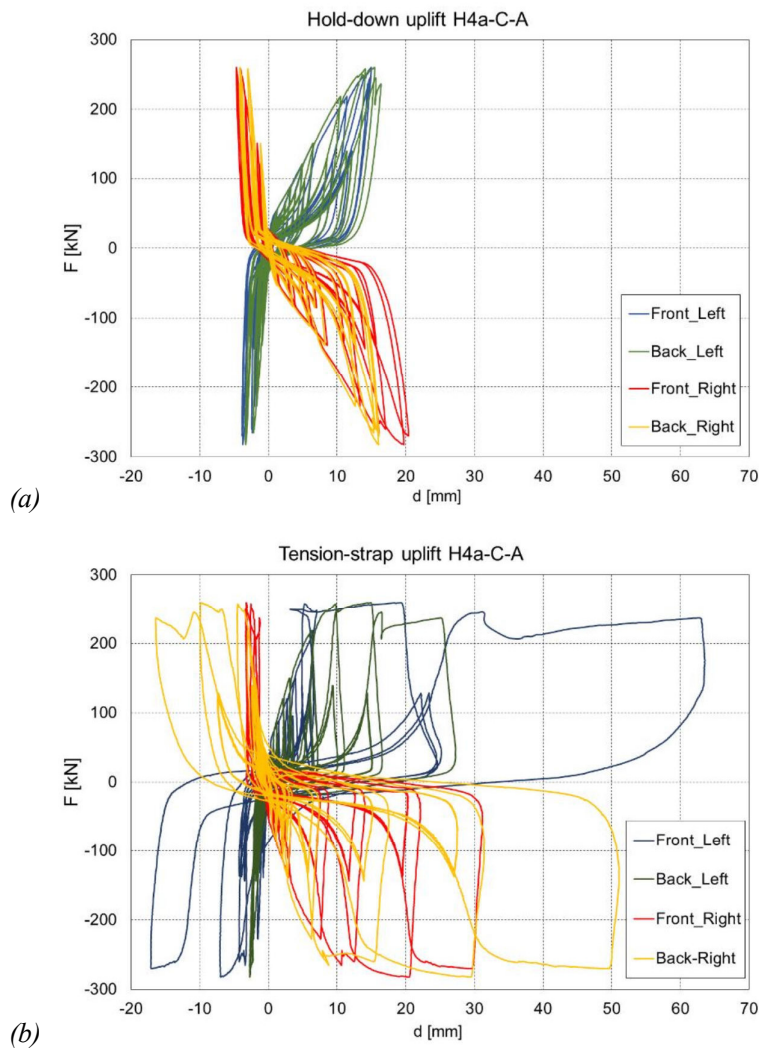


Figure 3.57. H4a uplifts at (a) the HDs, (b) tension straps

### First and second storey inner corner uplifts

The curves in Figure 3.58 illustrates the vertical uplift experienced in the four inner corners of the shear wall panels. The load-displacement curves showed quasi-linear behavior until reaching a displacement target of +70%, at which point the total load  $F_{@+70\%}$  reached 218 kN. In the 1<sup>st</sup> storey shear wall (Figure 3.58a), front and back right corners experienced uplifts of 10.8 and 8.8 mm. When the displacement target was set to -70%, uplifts on the right side of the shear wall varied from 10.2 mm to 10.8 mm, the differences between positive and negative target displacements were minimal.

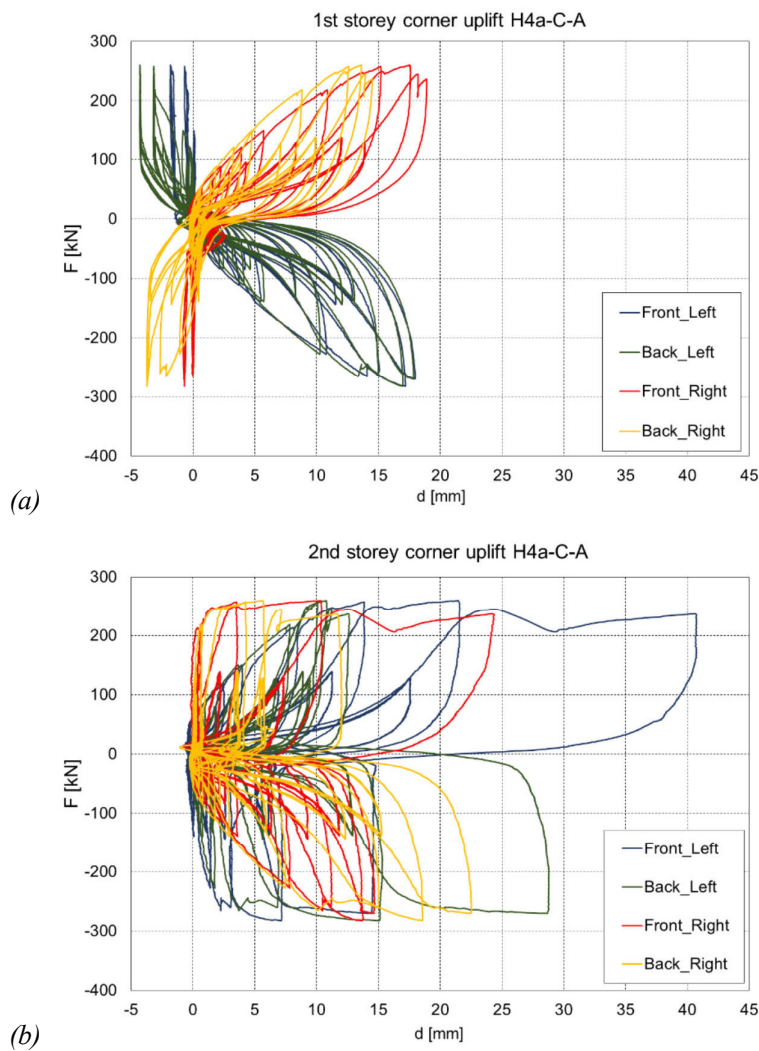


Figure 3.58. H4a inner corner uplifts at (a) 1<sup>st</sup> storey, (b) 2<sup>nd</sup> storey

Negative uplifts indicate compression in the panel corners, with the front panels experiencing uplifts close to 1 mm and the back panels ranging from 1.5 mm to 3.1 mm at +/-70% target displacement. In the 2<sup>nd</sup> storey shear wall (Figure 3.58b), uplifts in the inner corners ranged from 7.5 mm to 8.5 mm at the +/-70% target displacements. These values increased to a range of 24 mm to 41 mm at +/-160% target displacement when the structure exceeded its capacity. Compression was not observed as the inner corners.

### **Panel sliding**

At the base level (Figure 3.59a), the sliding was minimal, with maximum values of 1.5 mm and 2.6 mm for the front and back side panels, respectively, at the +130% target displacement. At the 2<sup>nd</sup> level floor (Figure 3.59c), the sliding values were 3.1 mm and 10.5 mm, and 2.2 mm and 3.3 mm at the +/-130% target displacement, respectively. These values increased to 13 mm and 4.6 mm, respectively, indicating failure in the back left SB. This failure is indicated by the increased sliding. However, it should be noted that the overall contributions of sliding at the base level and the 2<sup>nd</sup> level floor accounted for less than 6% of the total storey displacement.

At the 1<sup>st</sup> level floor (Figure 3.59b), the sliding reached values ranging from 16.6 mm to 18 mm at the +130% target displacement, and from 4.4 mm to 9.8 mm at the -130% target displacement. These sliding values contribute approximately 8% of the overall lateral displacement of the 2-storey shear wall.

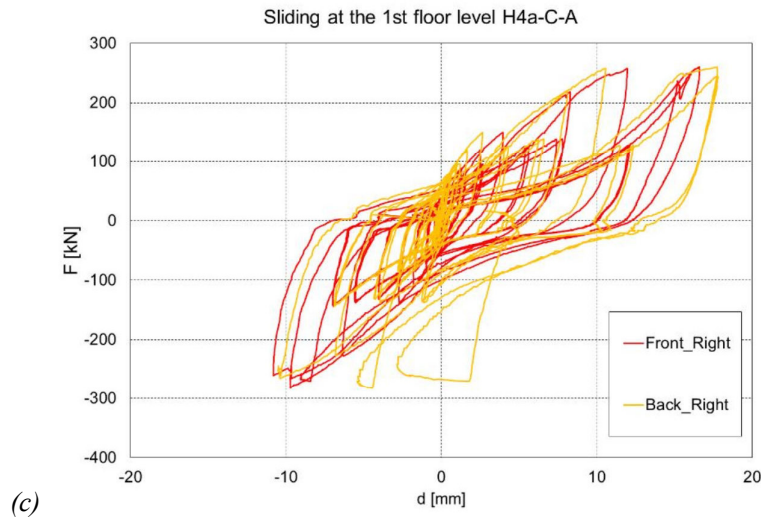
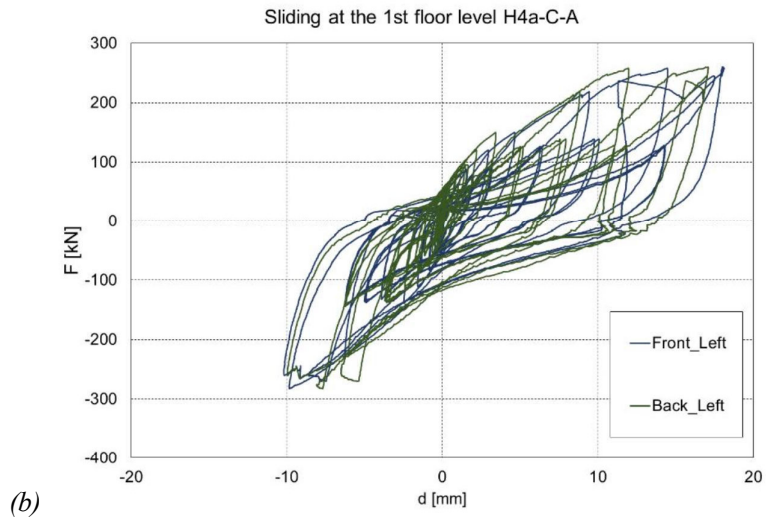
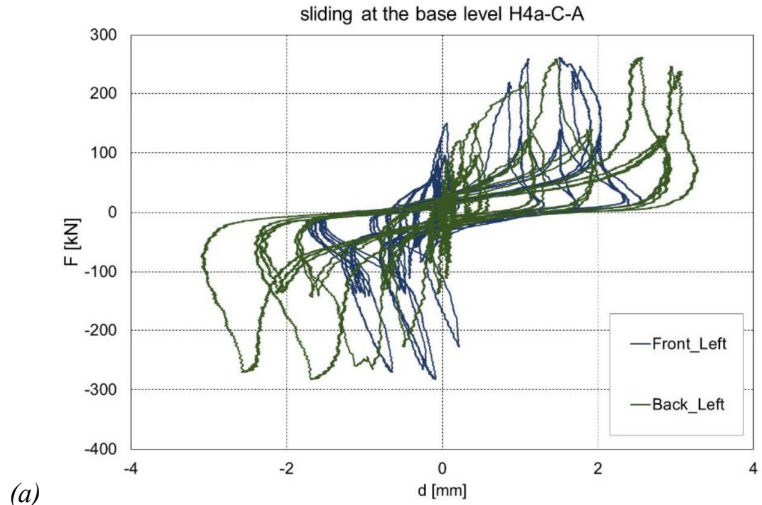


Figure 3.59. H4a panel sliding at a) base level, b) 1<sup>st</sup> level left, c) 1<sup>st</sup> level right

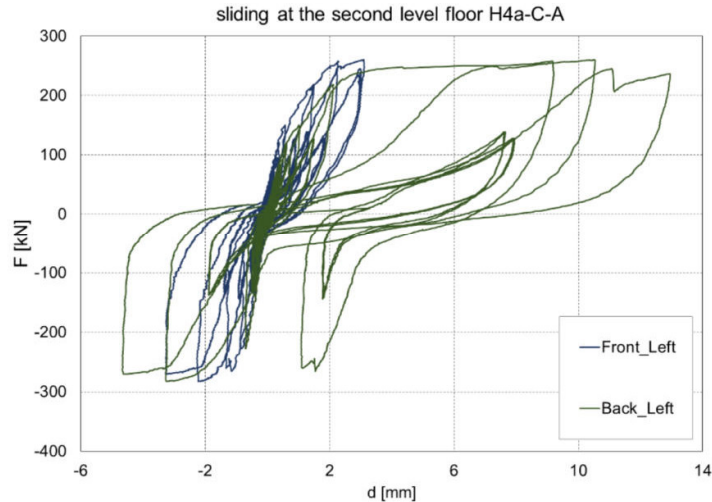


Figure 3.60. H4a panel sliding at 2<sup>nd</sup> level floor

### Panel-to-panel slip

Figure 3.61 presents the Panel-to-panel slips of coupled panel shear walls. The load-displacement curves for the first floor showed quasi-linear behavior up to a +130% target displacement, corresponding to a total load  $F_{@+130\%}$  of 259 kN. The panel slips, as shown in Figure 3.61a, were approximately 21 mm, with negligible differences observed between the back and front panels or between positive and negative cycles.

In the 2<sup>nd</sup> storey shear wall (Figure 3.61b), the panel slips exhibit a linear envelope up to a +70% target displacement, corresponding to a total load of approximately 218 kN. At the +70% target displacement, the slipping values were 6.1 mm (front panel) and 11 mm (back panel), while at the -70% target displacement, they were 7.2 mm (front panel) and 13.4 mm (back panel). During the subsequent cycles, when pushed to the 130% target displacement, the spline connection in the back panel failed, resulting in a slip of 39 mm.

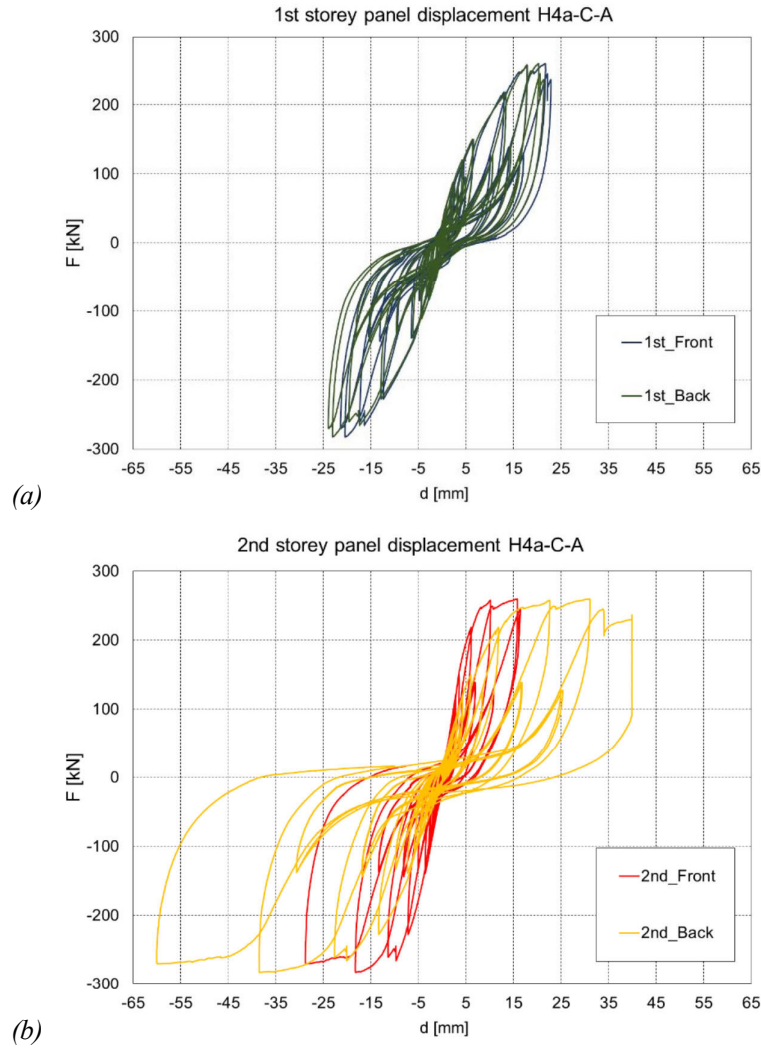


Figure 3.61. H4a panel displacements in test, a) 1<sup>st</sup> storey, b) 2<sup>nd</sup> storey

### Panel distortion

Figure 3.62 presents measurements of distortion in two 1<sup>st</sup> storey panels. These panels primarily experienced distortion during their compression cycles, with maximum values reaching 4.6 mm and 2.2 mm in front and back panels, respectively. In contrast, the distortion during their tension cycles was considerably lower, approximately 0.1 mm for the front panel and back panel.

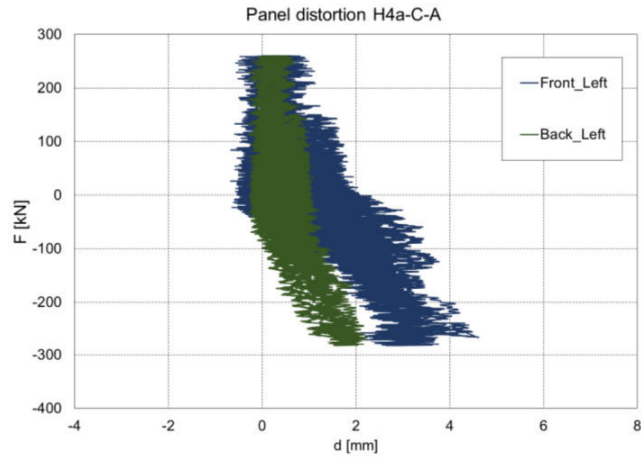


Figure 3.62. H4a panel distortion

### 3.6.9 Results test #H4b

#### Horizontal storey displacements

The horizontal storey displacements are illustrated in Figure 3.63. It must be noted that test #H4b was stopped at the 130% target displacement because the maximum actuator capacity was reached. The envelope of the load-displacement curve exhibited quasi-linear behavior up to 100% of the target displacement (equivalent to 150 mm) with a maximum load of 355 kN.

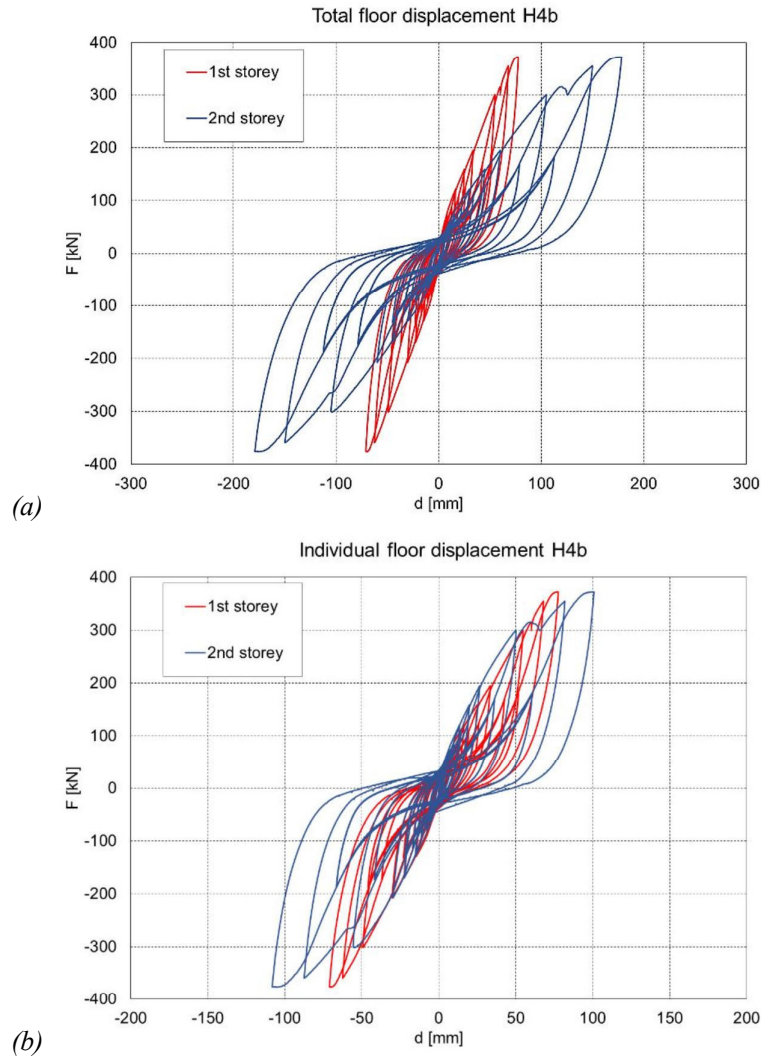


Figure 3.63. H4b (a) total storey displacements, (b) individual storey displacements

In the next cycle, the total load reached 373 kN at +130%, due to the actuator capacity limitation, preventing the structure from being pushed further. No signs of degradation in strength or stiffness were observed. The positive and negative envelopes were similar, with the maximum negative force occurring at -130% of the target displacement, reaching 376 kN. The lateral displacements of the 1<sup>st</sup> storey for the +/- 100% target displacements were 68 mm and -63 mm, respectively. The 2<sup>nd</sup> storey lateral displacements were approximately 30% larger, measuring 82 mm and -87 mm.

### **Hold down and tension strap uplift**

The vertical uplift experienced in the four HD and tension straps (two on the front shear and back shear walls each) are illustrated in Figure 3.64. The envelopes of the load-displacement curves were all quasi-linear up to the +100% target displacement when the total load  $F_{@+100\%}$  reached 355 kN. The corresponding HD uplifts (Figure 3.64a) on the left side of the shear wall were 10 mm and 12 mm. At the -100% target displacement, the uplifts on the right side of the shear walls were 12 mm and 12.1 mm. The maximum compressions at the +/-100% target displacements ranged from 1 mm to 3.4 mm.

At the +100% target displacement, the tension straps on the left side of the shear wall experienced uplifts of 7.6 mm and 9.3 mm (as shown in Figure 3.64b). On the right side, the uplifts for the tension straps were measured at 7.6 mm and 8.2 mm.

The negative uplifts of the tension straps indicate compression occurring in the corners of the panel. The maximum compressions observed on the left side at the +100% target displacement were 2 mm, while no compression was observed on the right side.

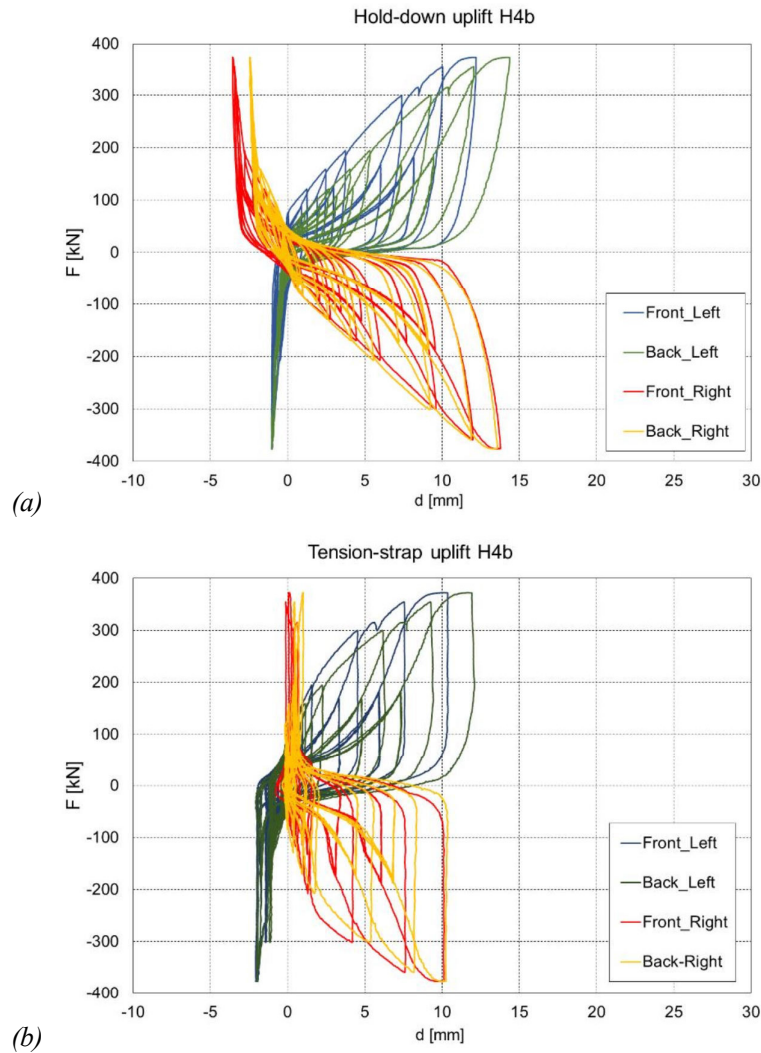


Figure 3.64. H4b uplifts at (a) the HDs, (b) tension straps

### First and second storey inner corner uplifts

Figure 3.65 illustrates the vertical uplift experienced in the four inner corners of the coupled shear walls. The load-displacement curves exhibited quasi-linear behavior up to the +100% target displacement, with a total load of 355 kN at  $F_{@+100\%}$ . In the 1<sup>st</sup> storey shear wall (Figure 3.65a), the corresponding right inner corner uplifts were measured 15.3 mm and 13 mm. At the -100% target displacement, the uplifts on the left side of the shear wall ranged from 13.7 mm to 14.6 mm. The differences between positive and negative target displacements were minimal. The negative uplifts corresponded to compression in

the panel corners, with the front left panel showing uplift close to zero and the other panels ranging between 2 mm and 4.1 mm.

In the 2<sup>nd</sup> storey shear wall (Figure 3.65b), the inner corner uplifts ranged from 6.1 mm to 9.8 mm at the +/-100% target displacements and increased to values between 10.1 mm and 13.6 mm during the subsequent cycle. No compression was observed as the inner corners were consistently slightly lifted by the opposite side panel during uplift.

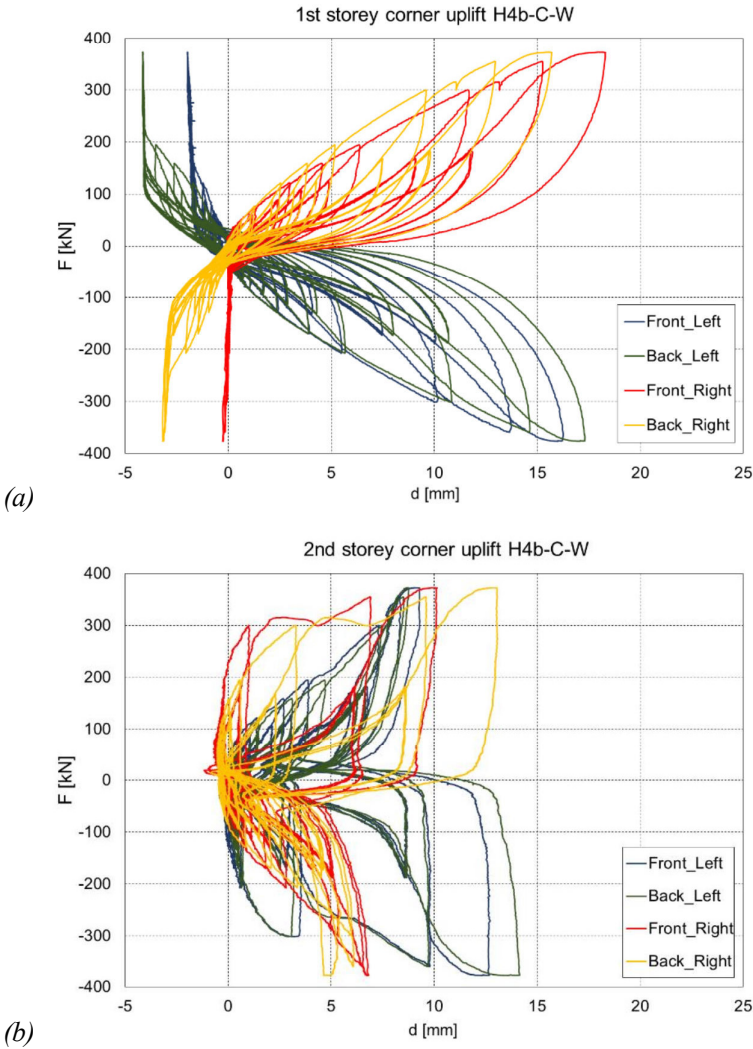


Figure 3.65. H4b inner corner uplifts at (a) 1<sup>st</sup> storey, (b) 2<sup>nd</sup> storey

### **Panel sliding**

The sliding values at each level (base level, 1<sup>st</sup> level floor, and 2<sup>nd</sup> level floor) are shown in Figure 3.66. Herein, all displacements are plotted against the total applied load. The base level sliding (Figure 3.66a) was minimal, with maximum values of 1.2 mm and 2.1 mm for the front and back side panels, respectively, at +130% target displacement. At the 2<sup>nd</sup> level floor (Figure 3.66c), the sliding was more significant, with values of 3.17mm to 17 mm at the +130% target displacement, and -2.6 mm and -20.8 mm at the -130% target displacement. Based on these findings, it can be concluded that the maximum sliding observed at the 2<sup>nd</sup> floor in this structure accounted for almost 10% of the storey displacement.

At the 1<sup>st</sup> level floor (Figure 3.66b), the sliding ranged from 14.8 mm to 20.5 mm at the +130% target displacement and from 11.8 mm to 17 mm at the -130% target displacement. These sliding values contribute approximately 10% to the overall lateral displacement of the 2-storey shear wall. No strength degradation was observed, and in fact, the stiffness appears to be increasing.

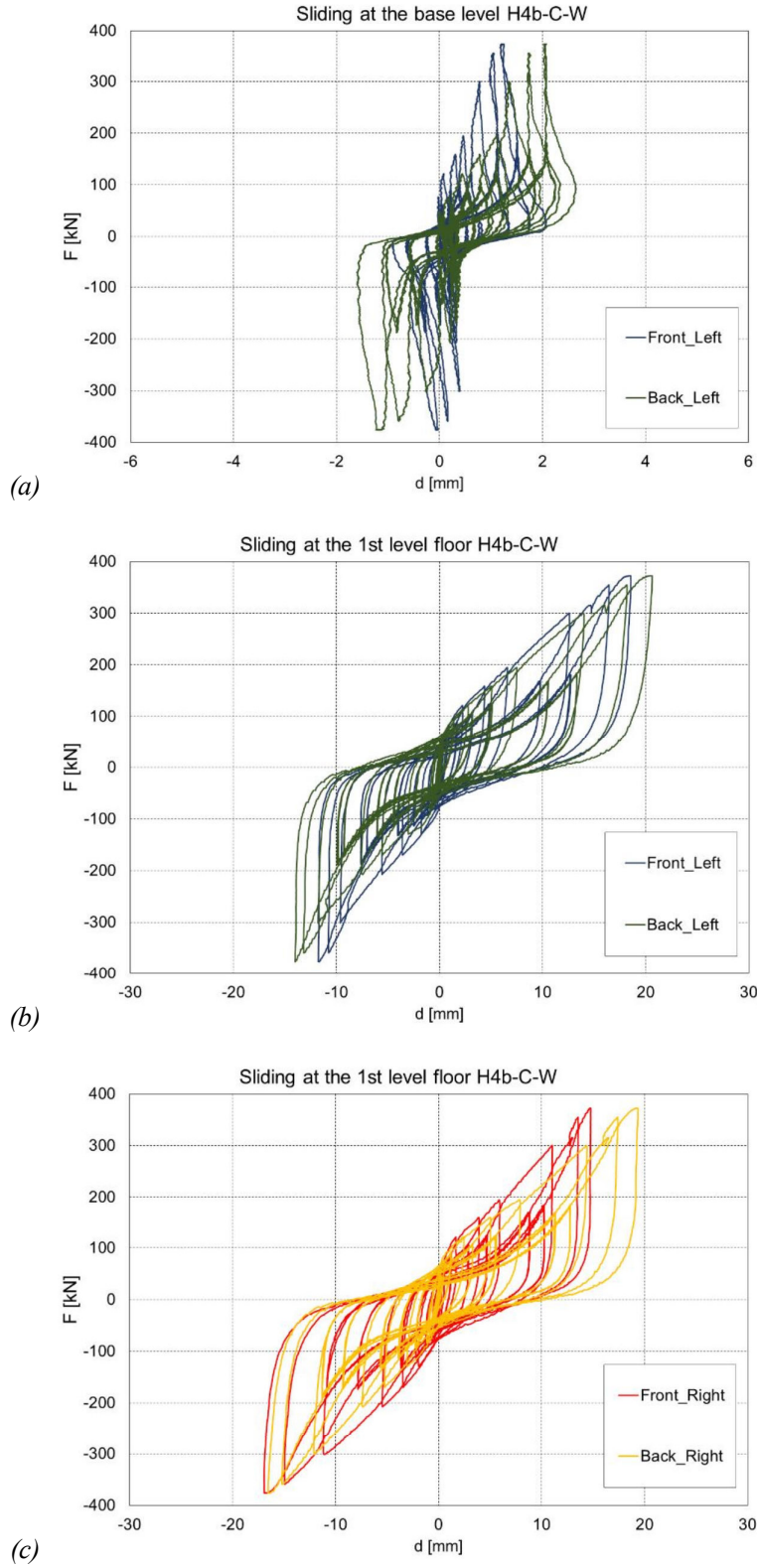


Figure 3.66. H4b panel sliding at a) base level, b) 1<sup>st</sup> level floor, c) 2<sup>nd</sup> level floor

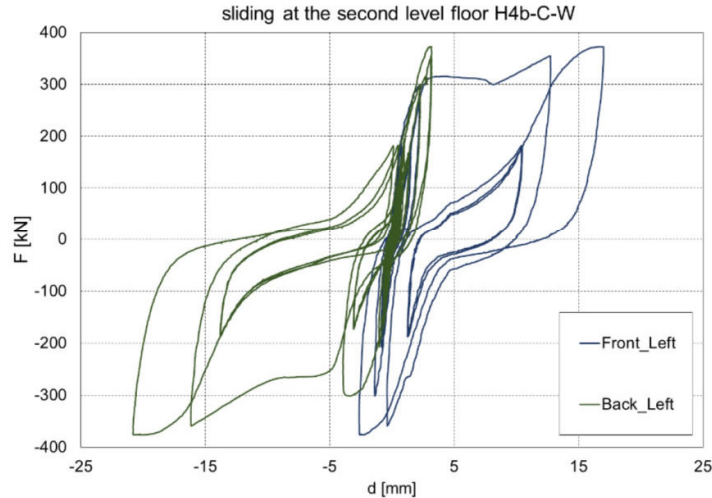


Figure 3.67. H4b panel sliding at 2<sup>nd</sup> level floor

### Panel-to-panel slip

The Panel-to-panel slips are shown in Figure 3.68. The load-displacement curves of the 1<sup>st</sup> storey exhibited quasi-linear behavior up to the +100% target displacement, with a total load  $F_{@+100\%}$  355 kN (Figure 3.68a). The corresponding panel slips were approximately 19.2 mm; they reached 22.3 mm in the following cycle, with negligible variations between the back and front panels or positive and negative cycles.

The panel slips in the 2<sup>nd</sup> storey shear wall (Figure 3.68b) exhibited a linear envelope until reaching the +/- 70% target displacement. At +70%, the slipping values were 9 mm (front) and 17.8 mm (back), while at -70% target displacement, they were 11.6 mm (front) and 20.5 mm (back). However, during the subsequent cycles when pushed to the -130% target displacement, the spline connection in the front panel failed.

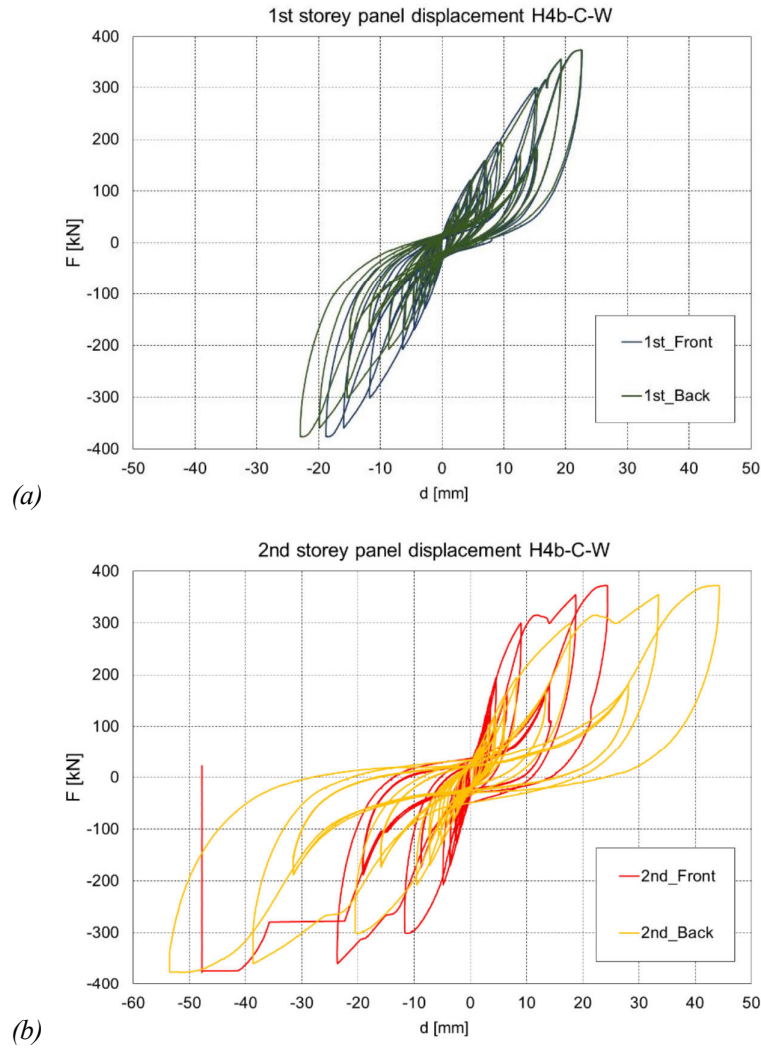


Figure 3.68. H4b panel displacements in test, a) 1<sup>st</sup> storey, b) 2<sup>nd</sup> storey

### Panel distortion

The two 1<sup>ST</sup> storey panels mainly experienced distortion during their tension cycles, with maximum values of 5-6 mm observed. In contrast, the distortion during their compression cycles was less than 1 mm.

### 3.7 Failure modes

One of the objectives of the experimental tests was to gain insights into the characteristics of CLT structures in terms of their overall performance and their failures. In neither the monotonic nor cyclic tests did the load decrease to 80% of the maximum resistance after reaching the peak force. There were no indications of global instabilities observed at the end of these tests. In most of the tests, the CLT panels remained undamaged, except for localized issues stemming from connection failures. The local failures were mainly caused by the shear failure of screws in the spline joints and tension straps.

Spline connections with screw fasteners within vertical shear walls permitted some slipping between the wall segments as they rocked as is shown in Figure 3.69.



*Figure 3.69. Relative displacement of the wall segments during CW rocking*

All coupled walls displayed rocking behavior, and as lateral displacement increased, there were instances of slight plastic deformations in the spline joint connections. The significant vertical displacement among these segments led to the spline screws yielding, marking the initial occurrence of yielding in the structures that was followed by some local crushing of spline or CLT panel eventually. This was the main source of energy dissipation in the CLT structures and confirming the successful achievement of the fundamental design goal for a flexible spline joint. Figure 3.70 displays the failure of the plywood spline joint (Figure 3.70a), the screws within it (Figure 3.70b), and the CLT panel located beneath the spline joint (Figure 3.70c). In structure #H4b, the presence of a perpendicular shear wall constrained the uplift forces in HD and tension straps. Consequently, the failure of spline screws is most prominent in this structure.

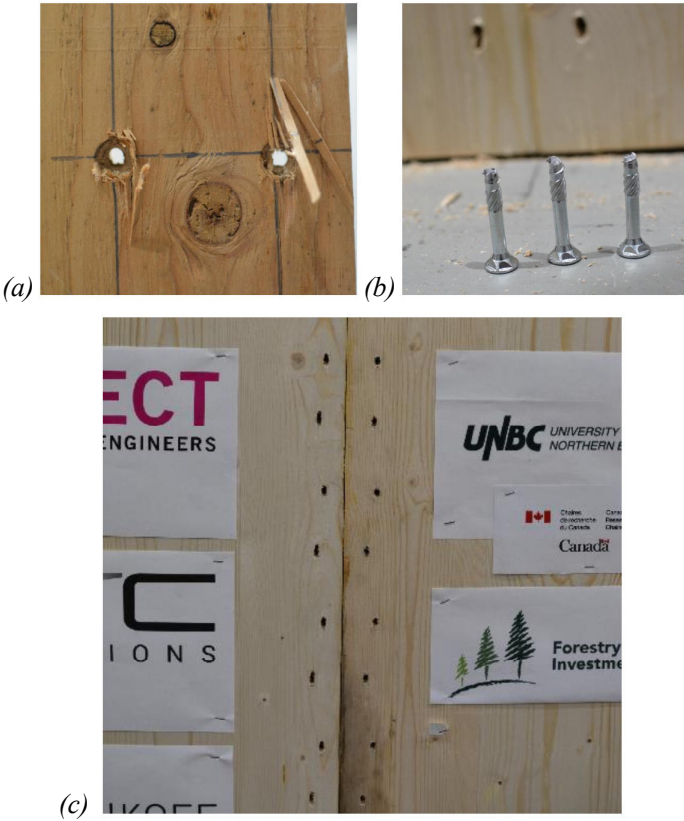
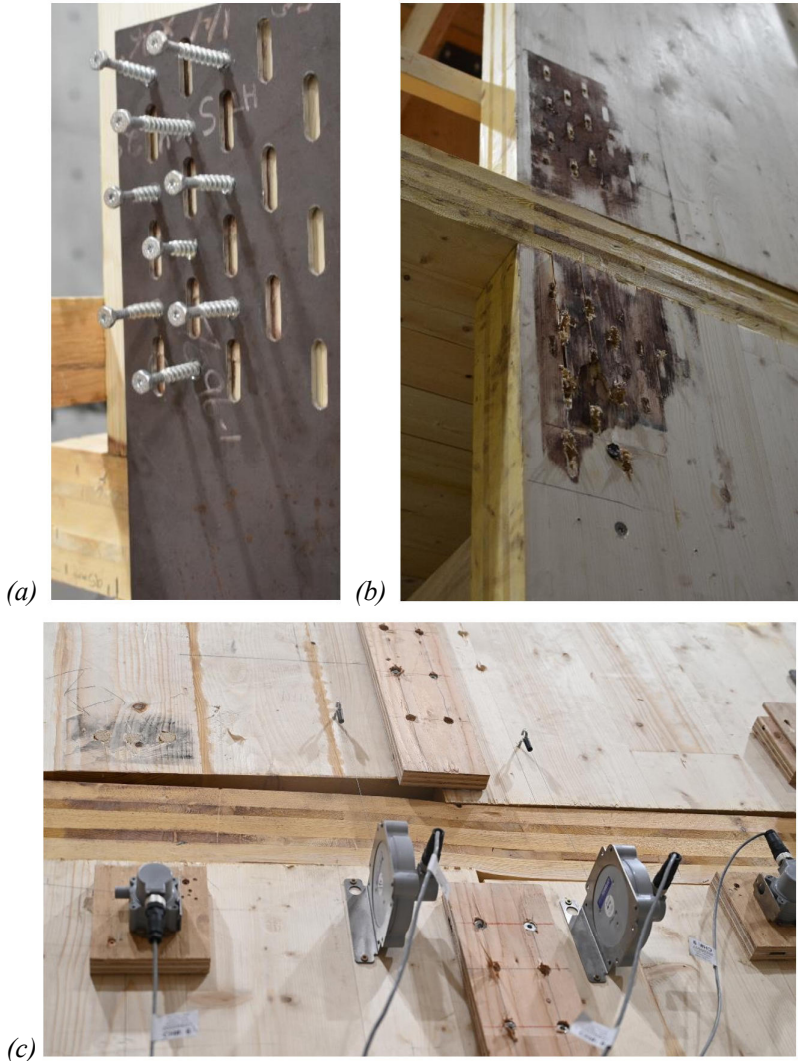


Figure 3.70. Spline joint after test: a) plywood, b) screws, c) CLT panel under spline

The rocking of the 2<sup>nd</sup> floor walls occurred due to the deformation of the screws holding the tension straps and consequently the penetration of the inner corners of the shear walls into the floor panels. Consequently, this rocking motion led to the failure of the tension strap screws and the CLT panel underneath it (see Figure 3.71) and the bending of the 1<sup>st</sup> floor panel that resulted in a slight rolling shear of minor layers of the 1<sup>st</sup> floor panel. The greater uplift in the tension strap of #H2a, caused by a 90° inclination angle, led to more embedment in the CLT panel under the tension strap compared to the other structures.



*Figure 3.71. Tension strap after test: a) screws, b) CLT panel under tension strap, c) floor panel bending*

The sliding of the 1<sup>st</sup> storey SB, led to some deformation in the bracket (Figure 3.72a and b) and failure of their STSs as illustrated in Figure 3.72, in addition, the embedment in the CLT panel under SB was observed. Since the highest values of sliding, due to replacing the bolts with STSs, happened in the structure #H3b the maximum embedment was witnessed in this structure, see Figure 3.72d.

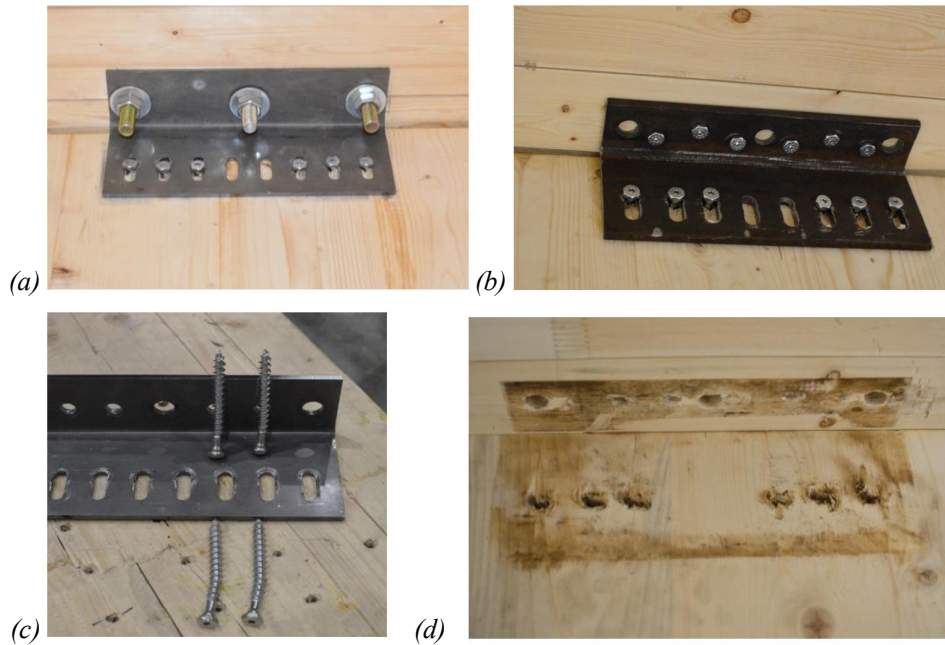


*Figure 3.72. SB after test: a, b) deformed SB, c) deformed screws, d) embedment in the CLT panel under SB*

The least favorable type of failure is the brittle failure of the CLT panel, and this has happened in the region of the tension strap connections in the structures #H3a and #H4 at the final stages of testing, particularly when subjected to the highest tension strap uplift. As illustrated in Figure 3.73a, a tensile crack running parallel to the wood grain in the panel's surface layer formed along the upper row of the tension strap screws, ultimately resulting in the delamination failure. And as demonstrated in Figure 3.73b, the shear wall of the structure #H4a underwent the plug shear of lamellas just behind the tension strap. A combination of rolling shear and delamination can be observed in this zone.

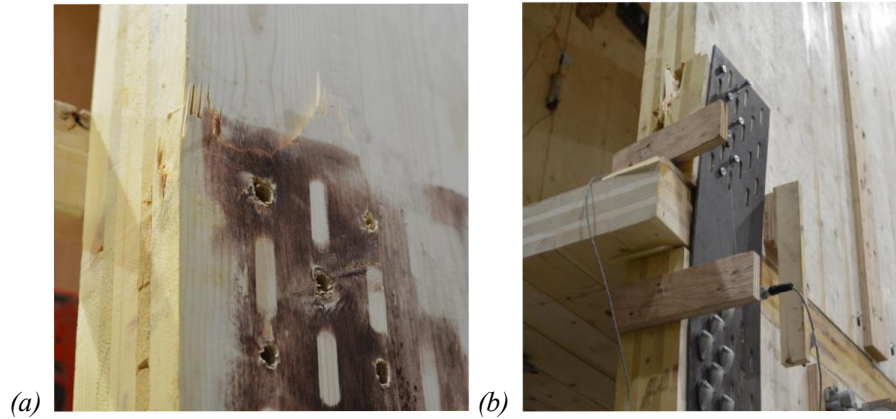


*Figure 3.73. Brittle local failure in the corner of CLT panel after test: a) H3a, b) H4a*

The 1<sup>st</sup> storey HDs remained intact because the wall uplift did not surpass the ultimate displacement capacity of the HDs. Only minor screw yielding was observed, while the HDs themselves were virtually undamaged. Since the structure #H1 lacked additional mass on the floors, the wall's rocking capacity was quite limited, and there was only minor failure in the 1<sup>st</sup> storey connections, see Figure 3.74. The base sliding in all structures was very small, and no signs of damage were evident in the base SB, thereby affirming the intended design objective of elastic shear brackets.



*Figure 3.74. HD after testing*

## 4 Analyses and discussions

### 4.1 Horizontal storey displacements at target displacements

The monotonic tests conducted on structure #H1, designated as #H1a and #H1b for pulling and pushing forces, respectively, are compared with the findings of the cyclic test performed on the corresponding structure labeled #H1c. In the Figure 4.1 the load-displacement curves for these three tests are presented. The 2<sup>nd</sup> storey displacement in the test #H1a is almost equal to the 1<sup>st</sup> storey displacement while, it is 3 times in the #H1b, and two times in the cyclic test #H1c at +100% target displacement.

The 1<sup>st</sup> and 2<sup>nd</sup> storey displacements for these three tests at different target displacements can be seen in Figure 4.2 and Figure 4.3. Regarding structure #H1b, the 1<sup>st</sup> storey displacement in the monotonic test is smaller by approximately 27% and 34% compared to the corresponding values in the cyclic test #H1c at +70% and +100% target displacement. In contrast, the 2<sup>nd</sup> storey displacement in structure #H1b is higher by around 10% and 13% compared to the corresponding values of structure #H1c. The distribution of lateral displacement across different stories depends on the stiffness of their connections. Consequently, it was expected that the displacement of the 2<sup>nd</sup> floor, during cyclic tests, will be greater because of the stiffness degradation in tension straps compared to the monotonic test. In contrast, the stiffness of HDs remained relatively stable without significant degradation throughout the test to emphasise the importance of tension strap stiffness in lateral displacements.

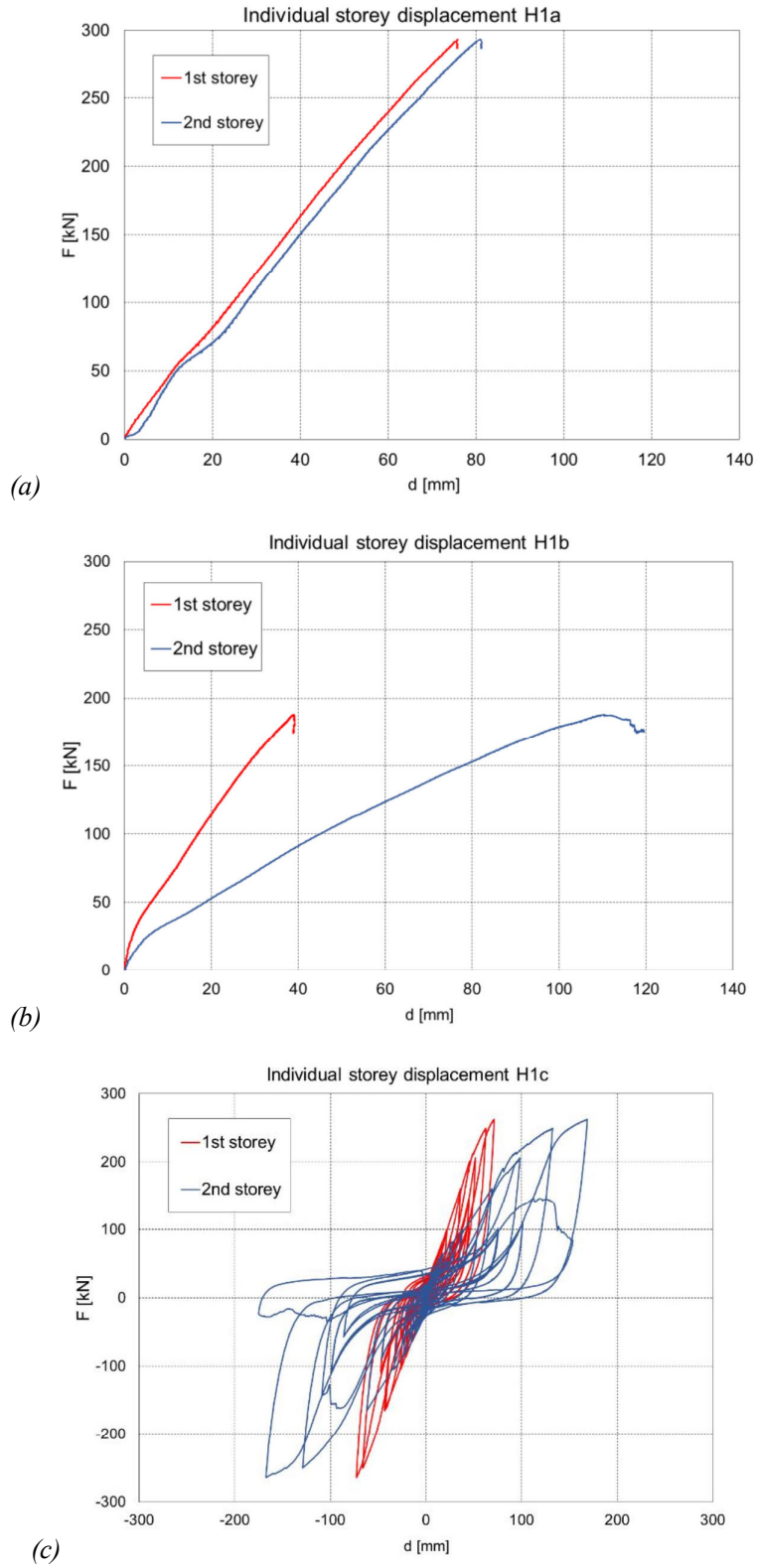
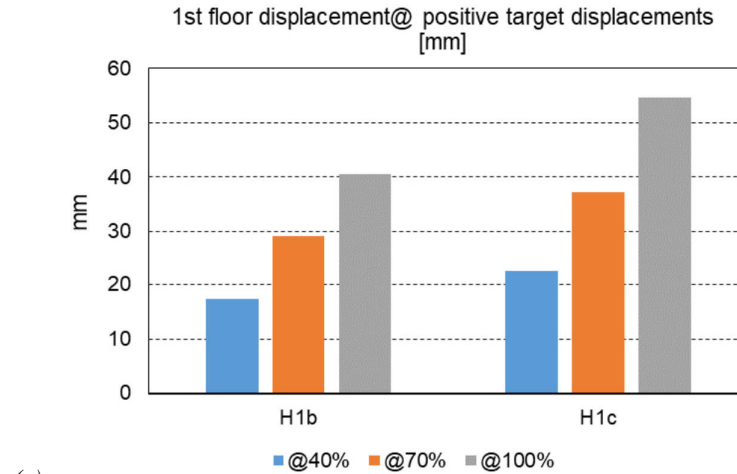
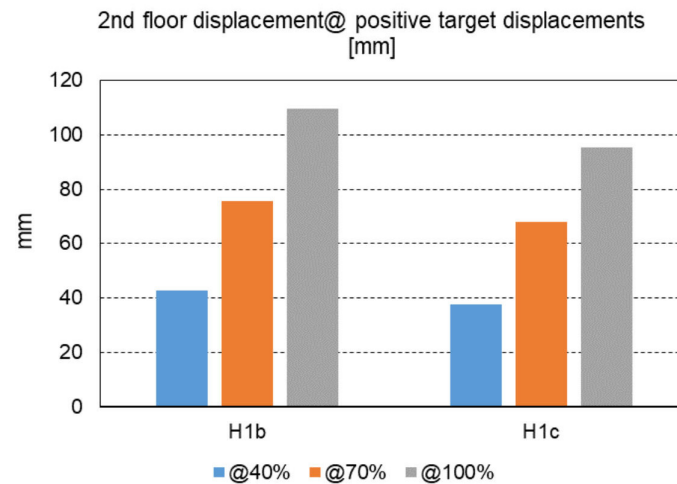


Figure 4.1. Individual floor displacements at the test: (a) H1a monotonic pulling, (b) H1b monotonic pushing, (c) H1c cyclic



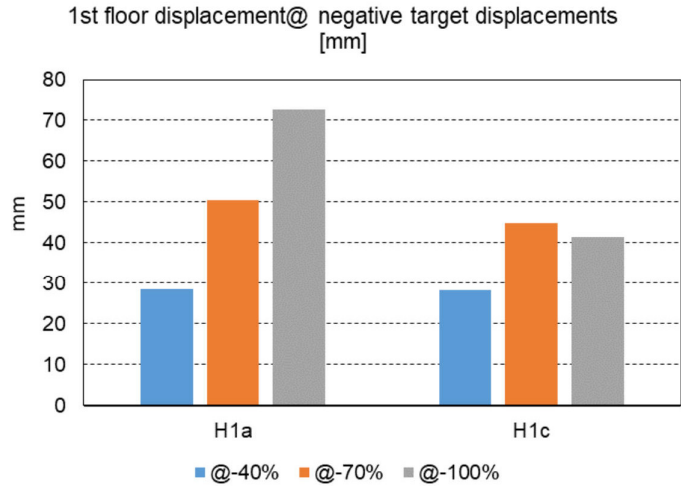
(a)



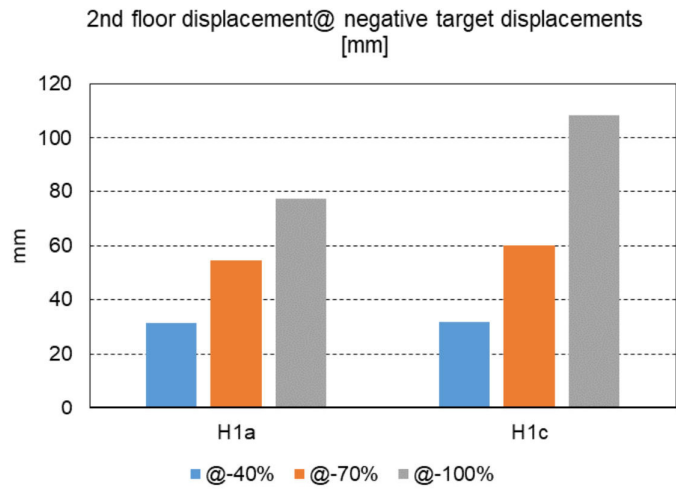
(b)

Figure 4.2. Lateral displacements for the tests conducted on structure #H1b and #H1c at positive cycles, (a) 1<sup>st</sup> floor, (b) 2<sup>nd</sup> floor [mm]

During test #H1a the load pattern differed from all other tests, as  $F_{total} = 2.1 F_{lead}$  indicating that  $F_2 = 1.1 F_{lead}$ , while  $F_2 = 0.5 F_{lead}$  in the cyclic test #H1c. The 1<sup>st</sup> storey displacement in the monotonic test is greater by approximately 10% and 40% compared to the corresponding values in the cyclic test #H1c at -70% and -100% target displacement due to different loading pattern used for this structure. Conversely, the 2<sup>nd</sup> storey displacement in structure #H1a is lower by around 11% and 40% compared to the corresponding values of cyclic test of #H1c.



(a)



(b)

Figure 4.3. Lateral displacements for the tests conducted on structure #Hb and #H1c at negative cycles, (a) 1<sup>st</sup> floor, (b) 2<sup>nd</sup> floor [mm]

The horizontal displacements for the 1<sup>st</sup> and 2<sup>nd</sup> floors of all structures under cyclic loads at +/- 100% and +/-130% target displacements are represented in Figure 4.4 to Figure 4.7. The lateral displacements are contingent upon the structure's stiffness distribution, i.e. the SB resisting sliding, HD and tension straps controlling uplifts.

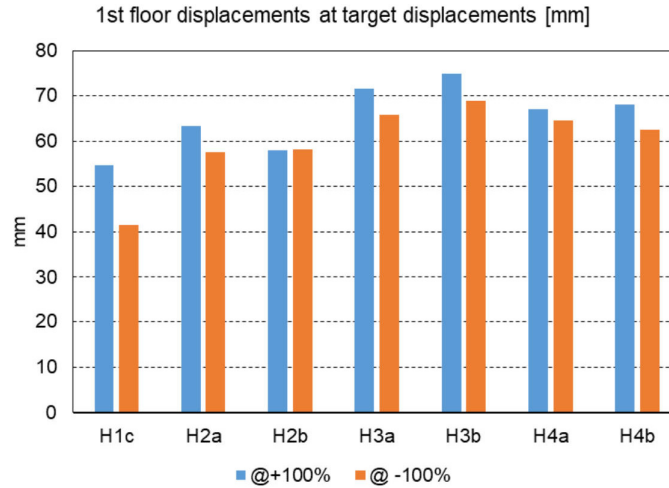


Figure 4.4. 1<sup>st</sup> storey displacements @ +/- 100% target displacement

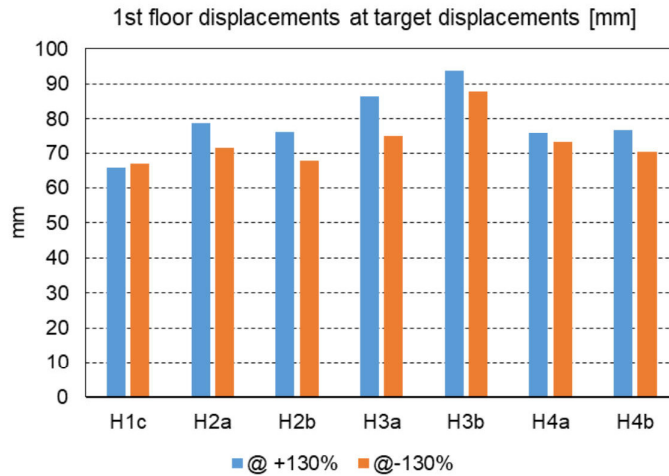


Figure 4.5. 1<sup>st</sup> storey displacements @ +/- 130% target displacement

It is noteworthy that among all structures, the details of HD, SB at the base level and the spline joints of both stories remained constant, therefore the differences in lateral displacement were due to the differences in tension straps and 1<sup>st</sup> floor SB, the extra masses on floors, and the acoustic layers.

Despite the same connections in the 1<sup>st</sup> storey, different lateral displacement values for the 1<sup>st</sup> storey are achieved. The largest 1<sup>st</sup> storey displacements were recorded for #H3b and #H3a that exhibited the minimum displacements on the 2<sup>nd</sup> floor (see Figure 4.6 and

Figure 4.7). The largest displacement on the 2<sup>nd</sup> floor was observed in #H1c, accompanied with the smallest 1<sup>st</sup> storey displacement. Notably, #H1c featured the fewest STSs on the tension strap, set at 90° in while #H3a and #H3b in angle were equipped with additional STSs on the tension strap, set at 45° at the bottom. The difference in tension strap stiffness on the stiffness distribution within the structures resulting in a maximum difference of 40% in lateral displacements on the 1<sup>st</sup> floor across all structures.

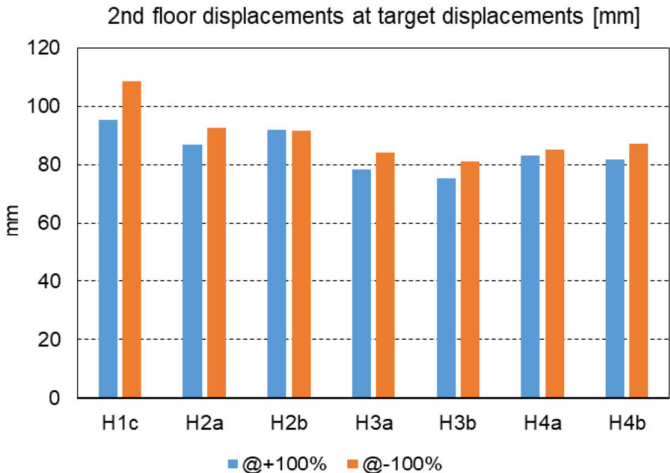


Figure 4.6. 2<sup>nd</sup> storey displacements @ +/- 100% target displacements

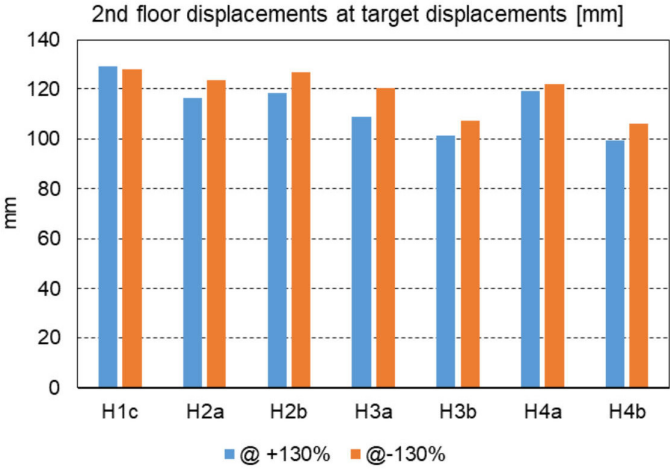


Figure 4.7. 2<sup>nd</sup> storey displacements @ +/- 130% target displacements

Structure #H2a, which included extra masses, displayed less variance in the lateral displacements of 78.8 mm and 116 mm in the 1<sup>st</sup> and 2<sup>nd</sup> stories compared to structure #H1c that exhibited 65.7 mm on the 1<sup>st</sup> floor and 129 mm on the 2<sup>nd</sup> floor. This suggests that strengthening the SB at the bottom of the 2<sup>nd</sup> storey shear wall and introducing dead load to the floors enhanced the overall performance. #H2a exhibited a 14% decrease in the difference between the ISD compared to #H1c.

Structures #H2a and #H2b exhibited displacements of approximately 77 mm and 117 mm on the 1<sup>st</sup> and 2<sup>nd</sup> floors, respectively, at 130% target displacement, indicating that the inclination angle of the tension strap screws did not have a significant effect on storey displacement, although this might be influenced by re-testing the structure. Structure #H2a underwent testing with 12 STSs featuring a 90° inclination angle on both sides of tension straps type 1. After the test, tension straps and their STSs, were replaced. Tension strap type 2 was installed, using 9 new STSs, each with a 45° inclination angle on both sides.

Although structures #H3a and #H3b utilized the same tension straps, the 1<sup>st</sup> storey displacement in #H3b measured 94 mm, surpassing #H3a's displacement of 86 mm. This difference stems from #H3b's substitution of bolts with STSs at the bottom of the 1<sup>st</sup> floor SB, leading to decreased SB stiffness. Consequently, #H3b experienced more displacement than #H3a on the 1<sup>st</sup> floor. Additionally, this alteration resulted in both stories sharing nearly equal horizontal displacement proportions in #H3b, contributing to a smaller 2<sup>nd</sup> storey displacement of 101 mm compared to #H3a's 109 mm.

Structures #H4a and #H4b exhibited nearly identical 1<sup>st</sup> storey displacements. These two structures shared the same connections as #H3b, but the presence of an acoustic interlayer in #H4a that acted like an elastic gap led to a reduction in friction between the shear walls and the floor panel, thereby facilitating the movement of the 2<sup>nd</sup> floor. The 2<sup>nd</sup> highest

displacement was observed in structure #H4a with the value of 119 mm at 130% target displacement. The inclusion of a perpendicular shear wall in #H4b prevented the structure from rocking leading to a lateral displacement of 99 mm, the smallest among all structures at 130% target displacement. Concerning the negative cycles, a consistent pattern like that observed in positive cycles is evident in Figure 4.4 to Figure 4.7. However, the negative values are slightly lower than their corresponding positive values due to the energy dissipation during the negative cycles, as the structure returns to its original neutral position.

### 4.2 Inter-storey drifts

The cumulative lateral displacement, combining the lateral displacements of the 1<sup>st</sup> and 2<sup>nd</sup> floors, is assessed at the roof level to determine whether the structure has achieved the desired target displacements. The percentage contributions of the 1<sup>st</sup> and 2<sup>nd</sup> floors to a +100% target displacement (150 mm) and +130% target displacement (195 mm) are depicted in Figure 4.8 and Figure 4.9.

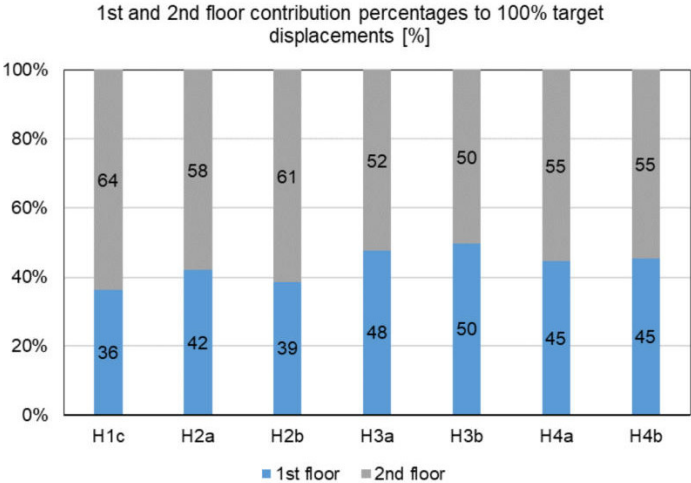


Figure 4.8. 1<sup>st</sup> and 2<sup>nd</sup> floor contribution percentages to +100% target displacement

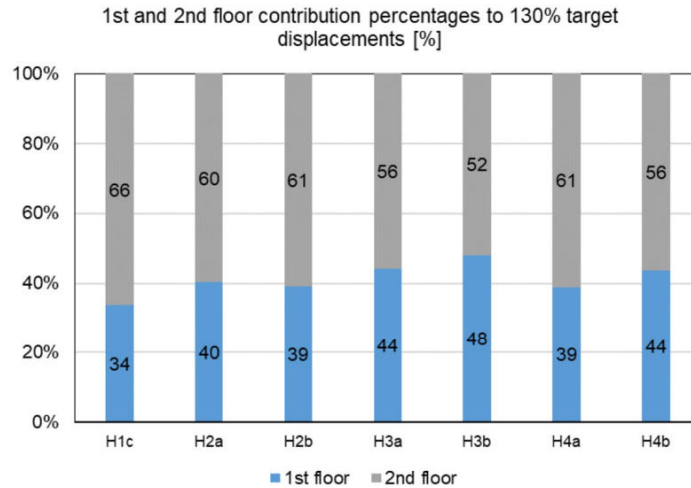


Figure 4.9. 1<sup>st</sup> and 2<sup>nd</sup> floor contribution percentages to +130% target displacement

The corresponding drift ratios in the 1<sup>st</sup> and 2<sup>nd</sup> stories at 100% and 130% target displacement are shown in Figure 4.10 and Figure 4.11, the displacement at the 3% and 4% drift are illustrated in the Figure 4.12. Across all structures, the 2<sup>nd</sup> floor contribution percentages were higher than those of the 1<sup>st</sup> floor. Furthermore, as the target displacement increased from +100% to +130%, the contribution percentage of the 2<sup>nd</sup> floor also increased. This observation could be linked to the failure of the 2<sup>nd</sup> floor STSs, leading to a decrease in the spline joint and tension straps' stiffness, consequently resulting in increased displacement. Consistent ISD indicate uniform stiffness across a structure's height, offering many benefits including reducing damages to both structural and non-structural elements, improving overall structural integrity, and facilitating uniform energy dissipation throughout the height of the buildings.

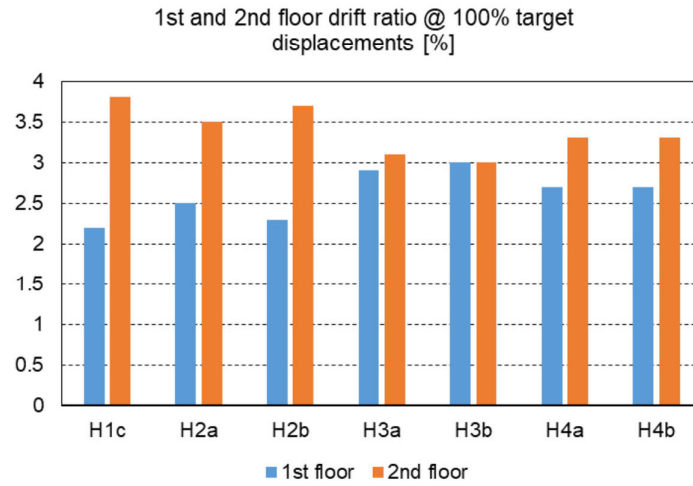


Figure 4.10. 1<sup>st</sup> and 2<sup>nd</sup> floor drift ratios @ +100% target displacement

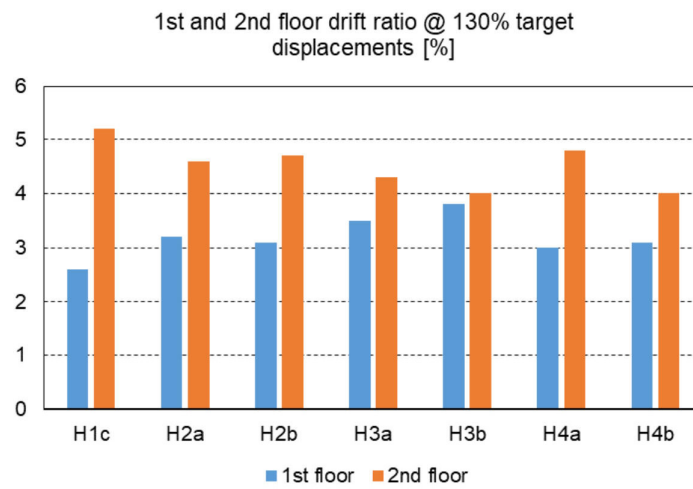
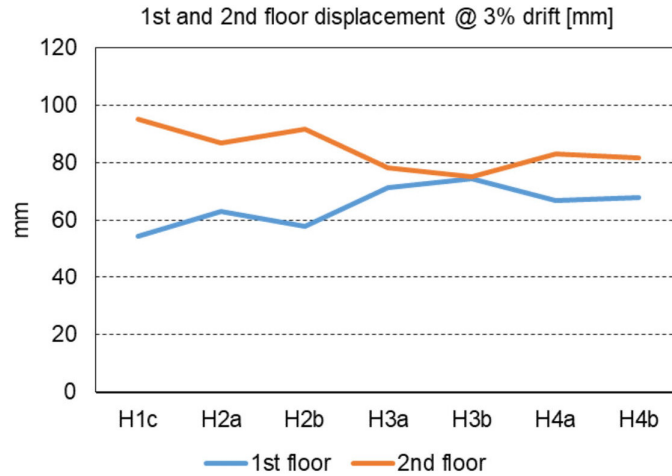
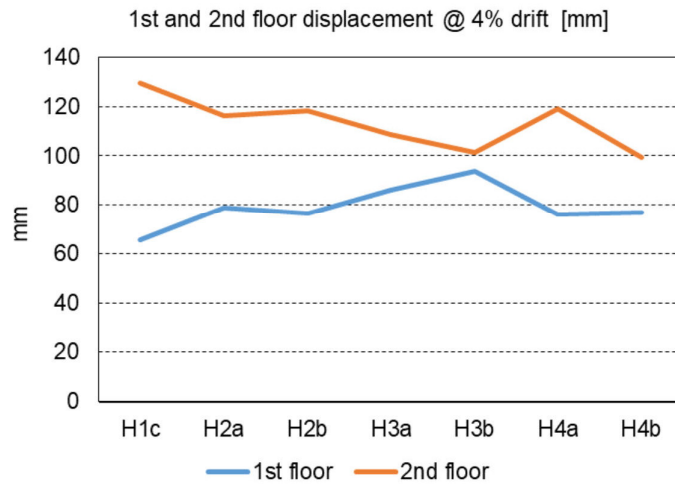


Figure 4.11. 1<sup>st</sup> and 2<sup>nd</sup> floor drift ratios @ +130% target displacement



(a)



(b)

Figure 4.12. 1<sup>st</sup> and 2<sup>nd</sup> storey displacements @ (a) 3% drift, (b) 4% drift

The consistency of HD across all structures highlights that the variation in drift between the 1<sup>st</sup> and 2<sup>nd</sup> floors predominantly stems from discrepancies in tension strap connections. Structures #H3a and #H3b were equipped with identical tension straps, exhibited nearly identical ISDs, but structure #H3b exhibited the most consistent ISD among all tested structures. In this configuration, the drift values were as follows:  $\Delta_{1st,100^+} = \Delta_{2nd,100^+} = 3\%$  and  $\Delta_{1st,100^-} = -2.8\%$ ,  $\Delta_{2nd,100^-} = -3.2\%$  for the 1<sup>st</sup> and 2<sup>nd</sup> stories at +/- 100% target. The 1<sup>st</sup> storey drift exhibited a 3% rise in the positive cycle and an 8% increase in the negative cycle at +/-100% target displacement compared to #H3a. These

increments were a result of decreased stiffness in the 1st floor SB in #H3b. This suggests that employing a tension strap featuring 9 STSs, angled at 45 and 90 degrees on the bottom and top, led to a more consistent drift across the structures compared to configurations where both sides had angles of either 45 or 90 degrees. Additionally, ensuring optimal structural performance heavily relies on selecting tension straps with sufficient stiffness. Structure #H4a shared the same tension strap but the acoustic layer had a detrimental effect and increased the 2<sup>nd</sup> floor drift. To assess the impact of acoustic interlayers on drifts, a comparison was made between structures #H3b and #H4a. The frictional coefficient is 0.25 when timber is in contact with timber, whereas it is 0.2 in the scenario of timber interacting with polyurethane. Concerning drifts, in the 2<sup>nd</sup> storey, the reduced friction between the shear walls and floor panels led to a 10% increase in  $\Delta_{2nd,100}$  and a 6% increase in  $\Delta_{2nd,100^-}$  in #H4a. Consequently, it can be concluded that the inclusion of the acoustic layer had a slight negative impact on maintaining a consistent stiffness distribution across the height of the structure and consequently on achieving a uniform drift. The highest discrepancy in ISD was observed in the structure #H1c with  $\Delta_{1st,100^+} = 2.2$ ,  $\Delta_{2nd,100^+} = 3.8\%$  and  $\Delta_{1st,100^-} = -1.7\%$ ,  $\Delta_{2nd,100^-} = -4.3\%$  for the 1<sup>st</sup> and 2<sup>nd</sup> stories at +/-100% target. This discrepancy between the drift on the 2<sup>nd</sup> floor, which was almost double that of the first floor, resulted from the application of less rigid tension straps in this structure.

### **4.3 Load-carrying Capacities at target displacements**

In the following section the effects of different parameters on the load-carrying resistances are discussed. The results of both monotonic and cyclic loading are shown in Figure 4.13 and Figure 4.14. The structure's load-carrying capacity under monotonic pulling force notably exceeds that under cyclic load, nearly doubling at 100% target

displacement. Conversely, under monotonic pushing force, the load-carrying capacity is marginally lower compared to the cyclic test, exhibiting an 8% increase in the cyclic test at 100% target displacement. Monotonic tests, conducted up to +/-100% target displacement, showcased a linear increase in load versus displacement. In contrast, the cyclic test extended until +/-160% target displacement. During this, there was a decrease in load-carrying capacity from -70% to -100% target displacement, followed by an increase in the subsequent cycle. Consequently, the cyclic load-carrying resistances were 10% and 21% lower than their corresponding values in the monotonic test at -40% and -70% target displacement, respectively.

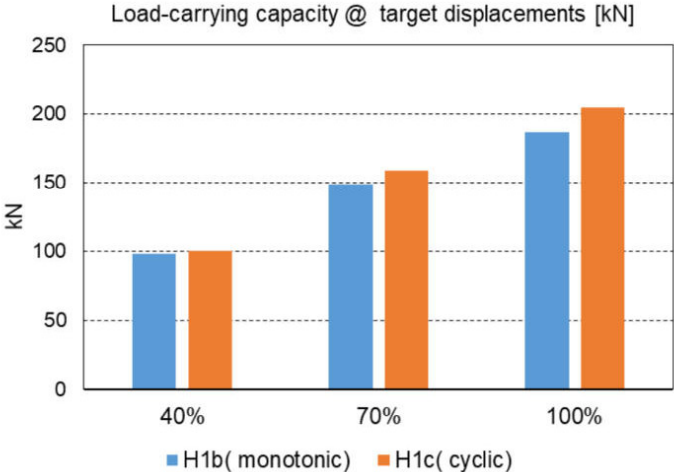
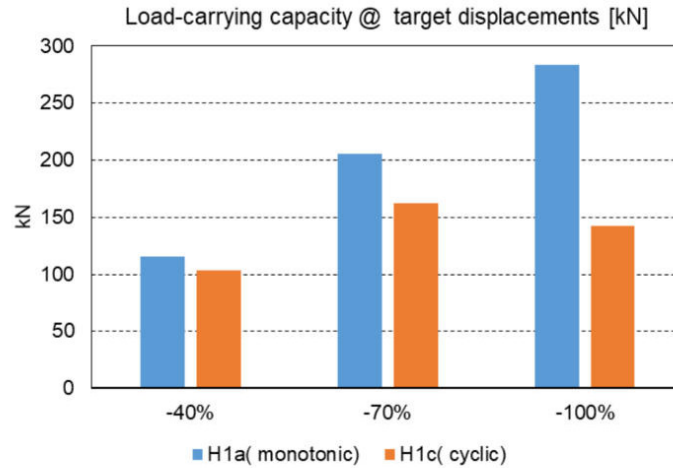


Figure 4.13. Load-carrying capacity @ 40%, 70% and 100% target displacements for the monotonic and cyclic tests conducted on the structure #H1



*Figure 4.14. Load-carrying capacity @ -40%, -70% and -100% target displacements for the monotonic and cyclic tests conducted on the structure #H1*

The load-carrying capacity for all structures under cyclic tests are illustrated in Figure 4.15 and Figure 4.16. The primary distinction between #H1c and #H2a lies in two key modifications: the enhancement of SB strength at the top of the 2<sup>nd</sup> storey shear wall and the addition of dead load to each floor in #H2a. These alterations had a positive impact on the structure's performance. Specifically, #H2a exhibited a 25% increase in capacity during positive cycles and a >15% increase during negative target displacements also showed a 28% increase in  $F_{max+}$  and a 17% increase in  $F_{max-}$  for #H2a.

The influence of the screw installation angle in the tension straps was investigated by comparing #H2a and #H2b. #H2a employed screws with a 90° inclination angle, while #H2b used screws with a 45° inclination angle. The load-carrying capacity of the structure with 90° inclination angles was found to be 14% higher than that of #H2b at +100% target displacement. Additionally, both  $F_{max+}$  and  $F_{max-}$  were 7% and 4% higher in #H2a, respectively, therefore, it is important to acknowledge that the inclination angle had only a minimal effect on the performance of the structures. However, this observation may be

influenced by the re-testing of structure #H2, where all STSs were installed at a 45° angle, potentially impacting the overall results.

The effect of replacing bolts with STSs in the connections between floors was evaluated in structures #H3a and #H3b. Structure #H3a exhibited the highest load-carrying capacity among the structures without perpendicular shear walls, with an  $F_{\max+}$  of 337 kN. This superior performance can be attributed to the highest strength of the SB on the 2<sup>nd</sup> floor of this structure. The top SB on the first level featured 3 Bolts + 8 STSs, while the bottom SB of the 2<sup>nd</sup> level had 3 Bolts + 6 STSs. In comparison to #H3b, #H3a had a load-carrying resistance that was 11% and 4% higher at +/-100% target displacement. Specifically, the  $F_{\max+}$  value in #H3a was 4% greater than that of #H3b.

The effect of adding acoustic layers was investigated through the comparison of #H4a and #H3b. Adding the acoustic layers resulted in reduction of load-carrying capacity by 4% and 5% in +/-100% target displacement and 25% and 19% at +/-130% target displacement. These layers decreased the stiffness between the shear walls and the floor and led to 25% reduction in  $F_{\max+}$  and 19% in  $F_{\max-}$ .

The influence of perpendicular shear walls was explored by analyzing and contrasting the findings from structures #H4b and #H3b. The addition of perpendicular shear walls led to an increase in stiffness and load-carrying capacity. Specifically, at +/-100% target displacement,  $F_{100+}$  increased from 267 kN to 355 kN, marking a 33% increase, while  $F_{100-}$  increased from -273 kN to -359 kN, representing a 32% increase. Additionally,  $F_{\max+}$  and  $F_{\max-}$  showed a 15% and 12% increase, respectively.

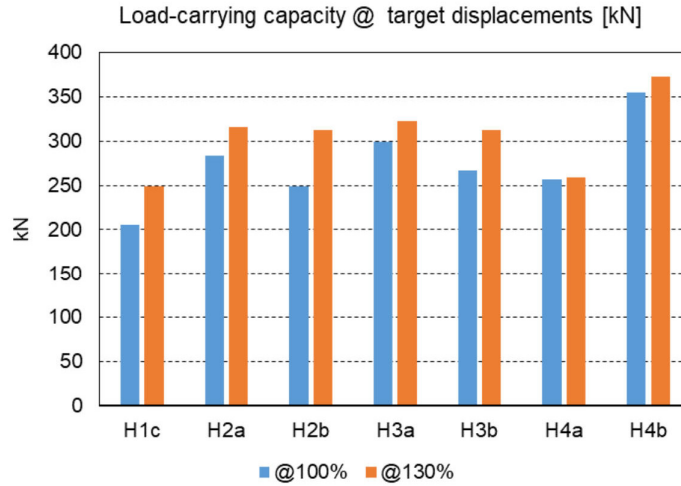


Figure 4.15. Load-carrying capacity @ +100% and +130% target displacement

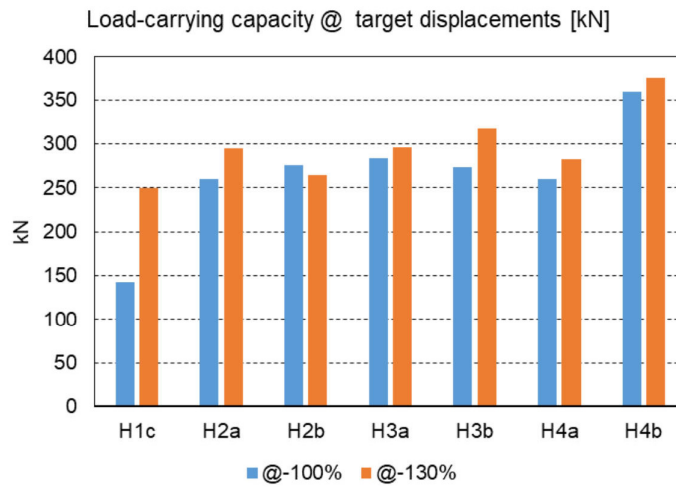


Figure 4.16. Load-carrying capacity @ -100% and -130% target displacement

#### 4.4 Shear wall uplifts at hold-downs & tension straps

The resemblance between the shapes of the load-uplift curves for HD and TS and the load-displacement curves of the entire structures suggests a close correlation. This similarity implies a direct influence of HD and TS behaviors on the overall seismic response of the structures. The response during positive and negative cycles mirrored

each other, and the load consistently rose in a linear manner until it almost reached a 70% target displacement.

In all nine tests, the details of the HD remained unchanged. However, different uplift values were observed across. The uplift measurements for the shear wall at the left and right-side HD at +/-100% and +/-130% target displacement is presented in Figure 4.17.

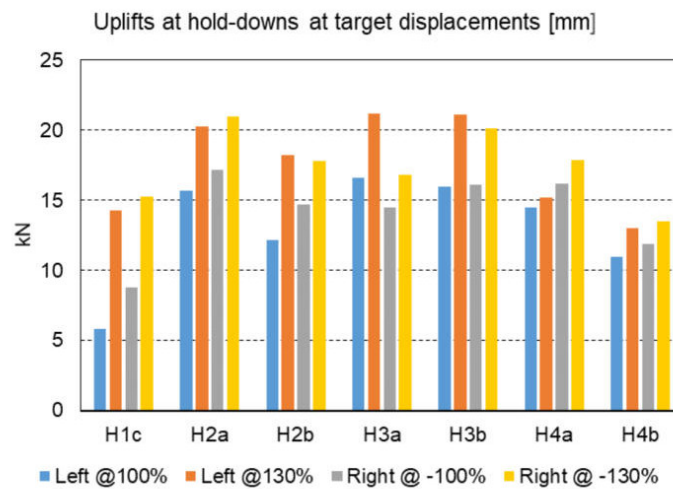


Figure 4.17. Uplifts at HDs at target displacements [mm]

In Figure 4.18, tension strap uplifts at +/-100% and +/-130% target displacement is shown. The uplift values in tension straps showed a discrepancy. It is important to note that the HD configuration remained consistent across all tests, and the observed variations in HD uplifts can be attributed to changes in tension strap stiffness. This means that concerning the stiffness of HD and tension straps, the total uplift gets distributed across the 1<sup>st</sup> and 2<sup>nd</sup> stories. Consequently, the uplift experienced in both stories directly linked to the stiffness of the tension straps and variations in stiffness result in distinct uplifts across the structures.

As can be seen in Figure 4.17, the lowest HD uplift, measuring 14.3 mm at 130% target displacement, was recorded in #H1c, which had the least stiff tension strap and the highest

tension strap uplift of 23.8 mm (see Figure 4.18). This was due to its configuration of having 8 STSs and an inclination angle of  $90^\circ$ , the most flexible tension strap.

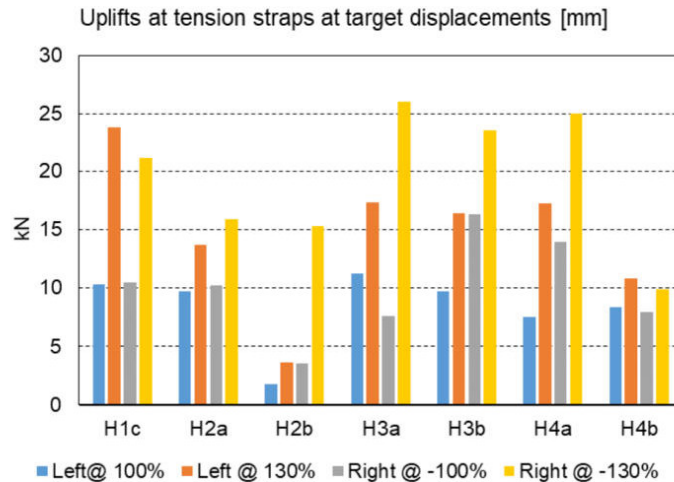


Figure 4.18. Uplifts at left-side tension straps at target displacements [mm]

The shear wall uplifts at left-side HD and tension straps at 100% and 130% target displacement are provided in Figure 4.19 and Figure 4.20. Comparing the results of the #H2a and #H2b, the structures #H2b exhibited the lower tension strap uplift till 130% target displacement. This structure featured 9 STSs on each side of the tension straps, with an inclination angle of  $90^\circ$  stiffness in these fact tension straps and, as a result, the less uplift of 3.6 mm at +130% target displacement. This observation aligns with the expectation since #H2a had a perpendicular inclination angle, which provides greater ductility compared to the  $45^\circ$  inclination angle in #H2b.

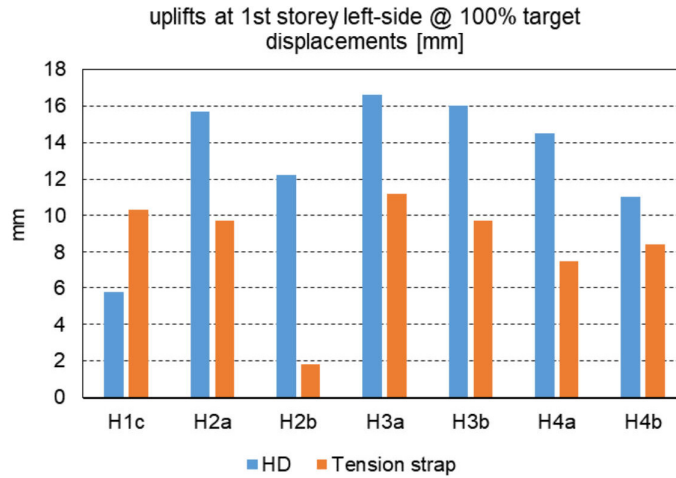


Figure 4.19. Uplifts at left-side HDs and tension straps @ 100% target displacement



Figure 4.20. Uplifts at left-side HDs and tension straps @ 130% target displacement

Similarly, in negative target displacements, the uplift values of #H2a in the right tension straps were higher than those in #H2b up to -130% target displacement that a failure happened in the tension strap of #H2b (see Figure 4.21 and Figure 4.22).

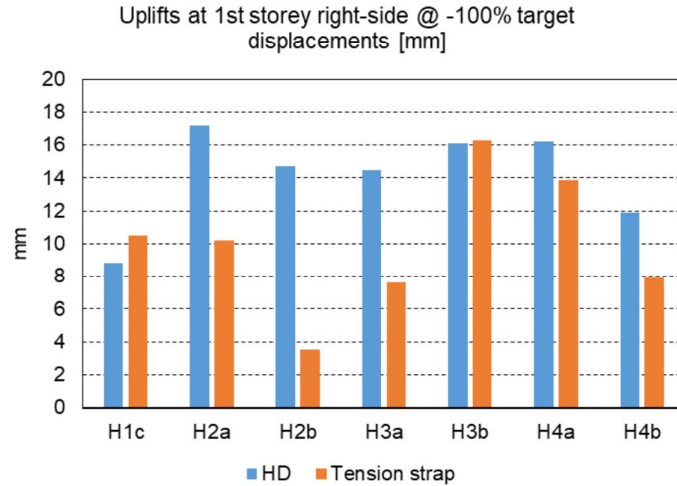


Figure 4.21. Uplifts at right-side HDs and tension straps @ -100% target displacement

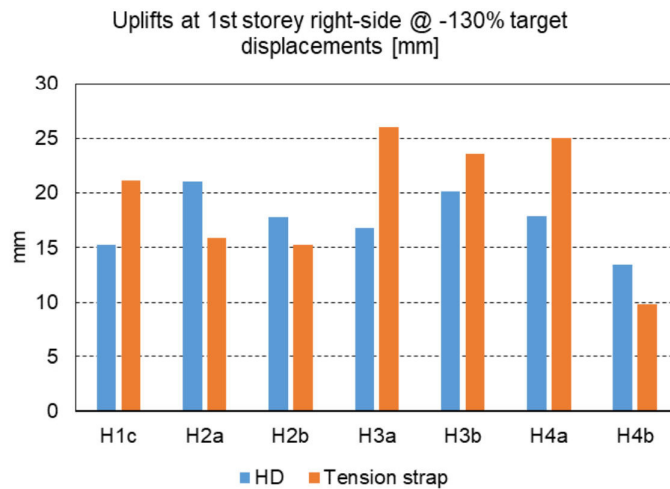


Figure 4.22. Uplifts at right-side HDs and tension straps @ -130% target displacement

Although #H2b showed the least tension strap uplift it did not exhibit the lowest 2<sup>nd</sup> storey displacement due to the high HDs' uplift that provided the 2<sup>nd</sup> floor. The small tension strap was compensated by the highest value of Panel-to-panel slip. Structures #H3a, #H3b, and #H4a shared the same configuration for their tension straps, all showing uplifts of around 17 mm at 130% target displacement, as depicted in Figure 4.18. These tension straps had inclination angles of 45 and 90 degrees at their

bottom and top ends. Reviewing Figure 4.8, it is evident that the most comparable contributions of the 1<sup>st</sup> and 2<sup>nd</sup> stories to the lateral displacement were observed in #H3a, #H3b, and #H4b, which all utilized this tension strap configuration. While structure #H4b shared the same tension strap details as the others, the presence of a perpendicular shear wall limited the tension strap uplift to 10.8 mm at +130% target displacement.

#### 4.5 Shear wall uplift at inner corners

A close correspondence between the right-side corner uplifts in the 1<sup>st</sup> storey and the left-side HD uplifts and left-side corner uplifts and right-side HD was observed. To provide a more detailed explanation, this correlation is further depicted in Figure 4.23 and Figure 4.24, where the structures #H2a and #H3a exhibited the highest right-side corner uplifts of 17.3 mm and 18.2 mm at 130% target displacement, and they correspondingly achieved the highest left-side HD uplifts among the structures, with values 20.3 mm and 21.2 mm, respectively, while the least values of HD and inner corner uplifts were observed in the structure #H1c.

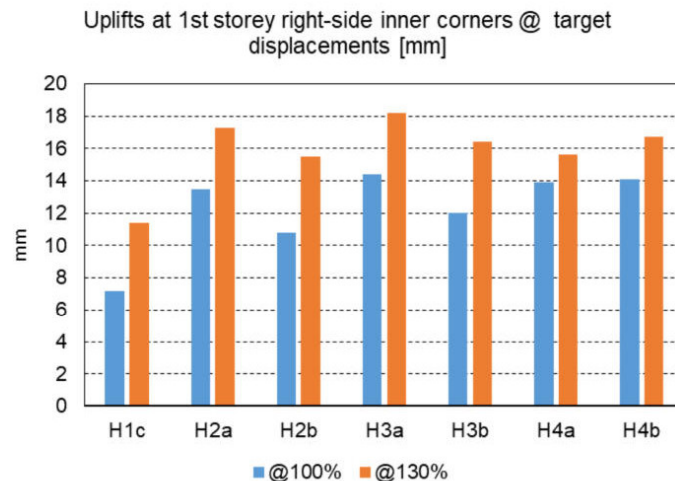
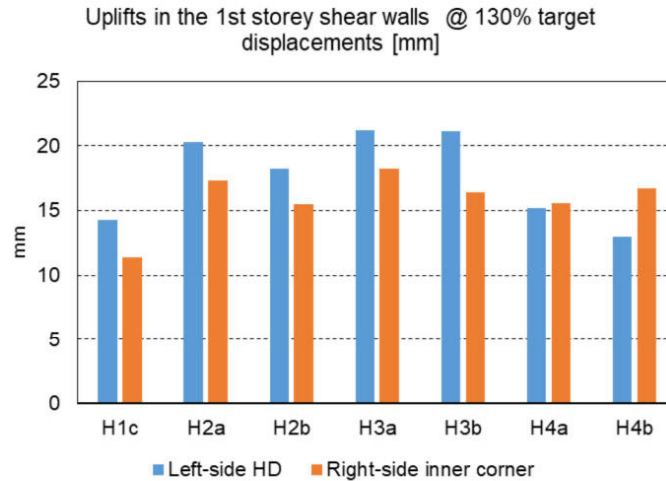


Figure 4.23. Uplift at 1<sup>st</sup> storey right-side inner corner @100% and 130% target displacement [mm]



*Figure 4.24. Uplift at left-side HD and right-side inner corner @ 130% target displacement*

One of the goals in designing a CLT shear wall is to achieve a CP behavior, aiming to dissipate energy in spline connections. This occurs when each panel individually rotates around its corner, allowing for relative displacement between panels. Figure 4.25 and Figure 4.26 show no uplift in the right-side corners in positive target displacements and no uplift in the left-side panel in negative target displacements.

The values ranged from almost 7 mm to 15 mm and from 12 mm to 18 mm at +/-100% and +/-130% target displacements respectively. There is a minimal difference between positive and negative cycles. The houses with higher load carrying capacity exhibited the higher inner corner uplifts due to more storey shear.

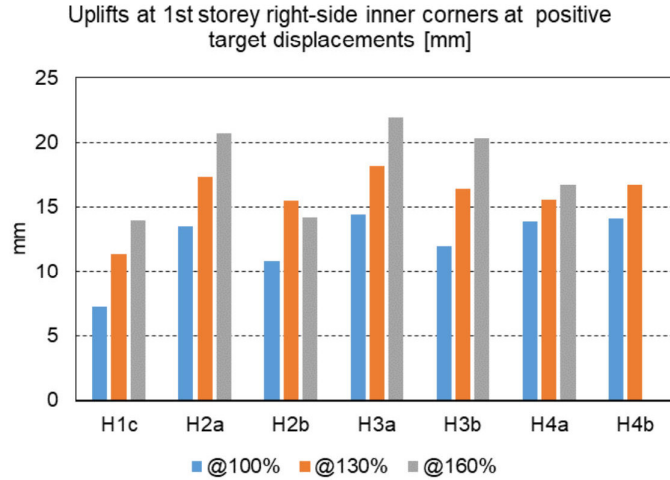


Figure 4.25. Uplift at 1<sup>st</sup> storey right-side inner corner at positive target displacements

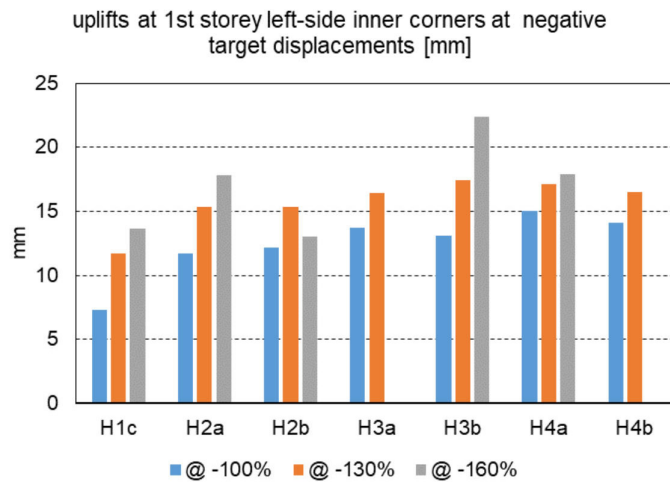


Figure 4.26. Uplift at 1<sup>st</sup> storey left-side inner corner at negative target displacements

These small negative values indicate that the compression zones at the rotation centers were small, providing support for the assumption that the panels rotate at their corners following CP behavior. This phenomenon is supported by the photos in Figure 4.27, showing that each panel had its own rotating center and was rocking individually. Notably, no compression was observed in the 2<sup>nd</sup> storey, as the inner corners were

consistently lifted slightly by the opposite side panel in an uplifting manner as shown in Figure 4.28.

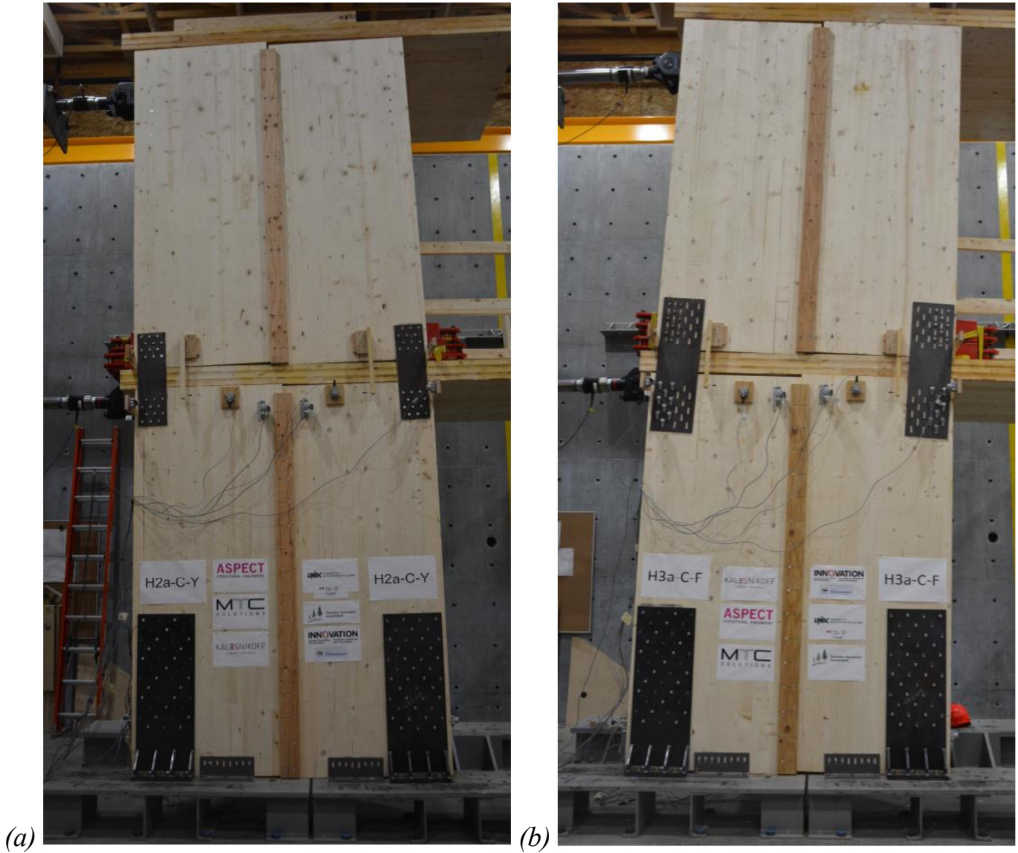


Figure 4.27. individual rotations of CP shear wall panels after test: (a) #H2a; (b) #H3a



Figure 4.28. Lifting the left corner upward due to the uplift in the right corner.

As detailed in Figure 4.29 and Figure 4.30, the inner corner uplifts in the 2<sup>nd</sup> storey ranged from 5 mm to 18 mm at the +/-130% target displacements. These values increased to a range of 9 mm to 23 mm during the subsequent cycle when the structure reached +/-160% target displacement. Therefore, it can be mentioned that there is no compression in the 2<sup>nd</sup> storey, also it was observed that the maximum values at +/-130 target displacement are related to the structures #H3a, #H3b and #H4a with the same stiffest tension straps.

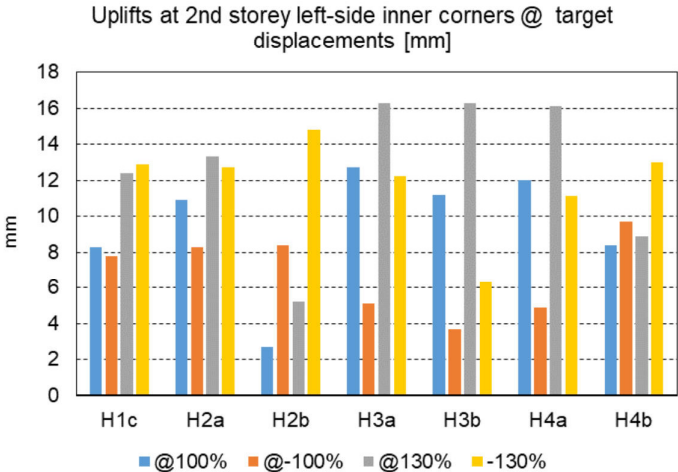


Figure 4.29. Uplift at 2<sup>nd</sup> storey left-side inner corners @ target displacements

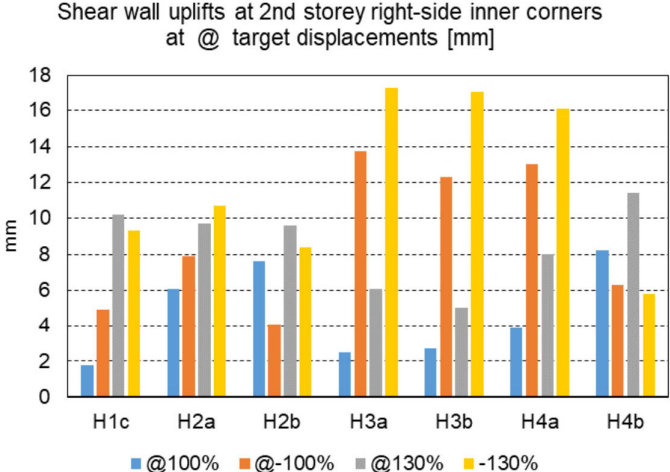
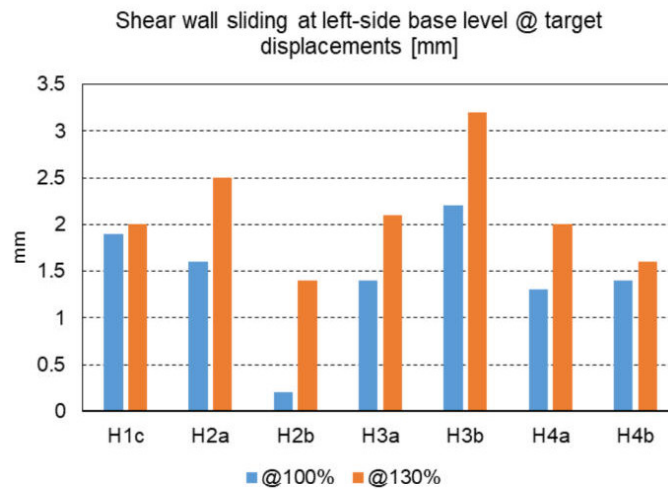


Figure 4.30. Uplift at 2nd storey right-side inner corners @ target displacements

## 4.6 The impact of SB on panel sliding

Sliding at the left side of the base level, monitored by sensors #12 and #28 (see Figure 3.15), is presented in Figure 4.31. Sliding at the left side of the 1<sup>st</sup> floor, recorded by sensors #6 and #22. Sliding at the right side of the 1<sup>st</sup> floor, captured by sensors #9 and #25, 1<sup>st</sup> floor sliding can be found in Figure 4.32 and Figure 4.33. Sliding at the 2<sup>nd</sup> floor, monitored by sensors #15 and #31, is illustrated in Figure 4.34.

A comparison of the results reveals variations in the base level sliding, despite having the same base SB details in all structures. Specifically, at the left side of the base level, the maximum sliding ranged from 0.2 mm to 2.2 mm at +100% target displacement and from 1.4 mm to 3.2 mm (refer to Figure 4.31) at +130% target displacement. These small values and this fact that no major damage was observed in the failure modes of base SB confirm the elastic behavior of SB, which aligns with one the design objective.



*Figure 4.31. Shear wall sliding at left-side base level at +100% & +130% target displacements*

As depicted in Figure 4.32 and Figure 4.33, the 1<sup>st</sup> floor sliding values ranged from 7 mm to 19 mm at 100% target displacement and from 9 mm to 25 mm at +130% target

displacement. The sliding measured on the 1<sup>st</sup> floor was significantly higher than values of the base level since due to the sensors installation they are determined as the total relative displacement between the shear walls of the 1<sup>st</sup> and 2<sup>nd</sup> stories, also values include the cumulative overturning effect of the 2<sup>nd</sup> storey.

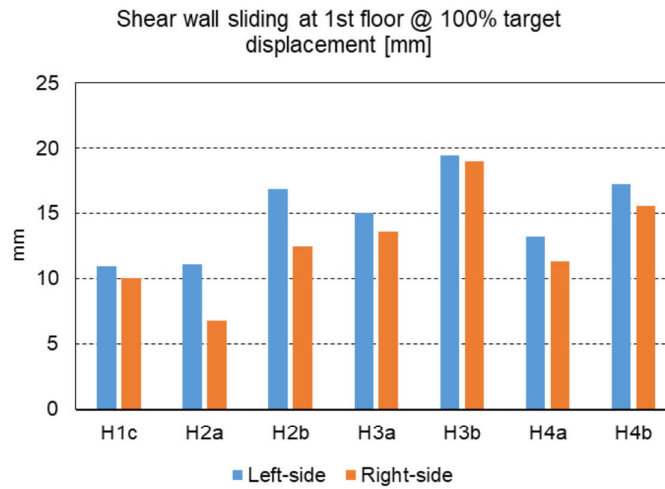


Figure 4.32. Shear wall sliding at 1<sup>st</sup> floor @ +100% target displacement

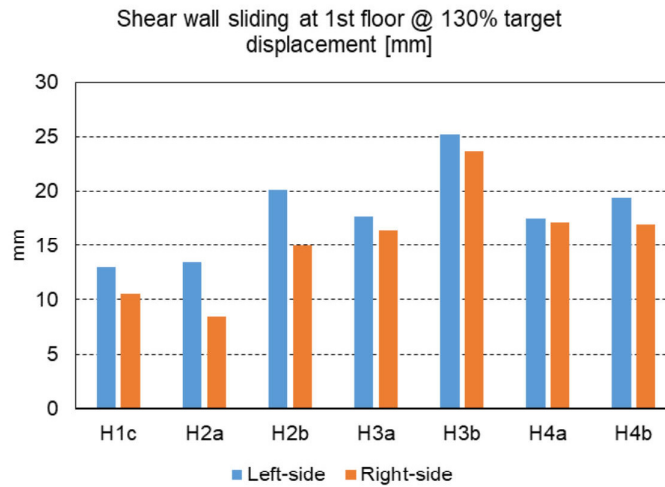


Figure 4.33. Shear wall sliding at 1<sup>st</sup> floor @ +130% target displacement

The left and right sides of the 1<sup>st</sup> floor recorded the highest values of 25.2 mm and 23.7 mm at 130% target displacement in #H3b, where 3 bolts of the SB were replaced

with 6 STSs on top and bottom, therefore, the SB were connected to the 1<sup>st</sup> floor with STSs instead of bolts. This suggests that the presence of STSs in the SB reduced stiffness, resulting in higher ductility and, consequently, more sliding.

The values of 2<sup>nd</sup> floor sliding are illustrated in Figure 4.34, and they are smaller compared to the base sliding for two main reasons. Firstly, this is due to the smaller shear forces experienced in the 2<sup>nd</sup> floor level compared to the base shear. Secondly, in all structures (except for structure #Hc1, which had 4 STSs while the others had 8 STSs on the 2<sup>nd</sup> floor) the configuration of the 2<sup>nd</sup> floor SB had more STSs and was slightly stiffer than the base SB. The highest value of 2<sup>nd</sup> floor sliding, equal to 9.9 mm at +130% target displacement, was noticed in #H4b. This can be attributed to the presence of a perpendicular shear wall which confined the uplift of the CLT shear walls therefore, despite applying similar tension straps in structures #H3a, #H3b, #H4a, and #H4b, the increase in lateral load in the first three structures resulted in an uplift of approximately 17 mm at 130% target displacement, whereas the fourth structure exhibited a lesser uplift of only 10.7 mm in tension straps. Consequently, the amplified load led to more sliding and the highest observed sliding of the 2<sup>nd</sup> floor specifically happened in structure #H4b.

As previously highlighted, the sliding values on the 1<sup>st</sup> floor are notably greater compared to those at the base and 2<sup>nd</sup> floor levels. Figure 4.35 and Figure 4.36 illustrate the impact of 1<sup>st</sup> floor, 2<sup>nd</sup> floor and base sliding on the overall drift. It is notable that with an increase in load from 100% to 130% target displacement, the contribution of sliding to drift decreases. This is because, initially, rocking was the primary cause of the drift. However, as the load increased, the uplift in tension straps also increased, leading to a greater share of contribution from rocking in the overall drift.

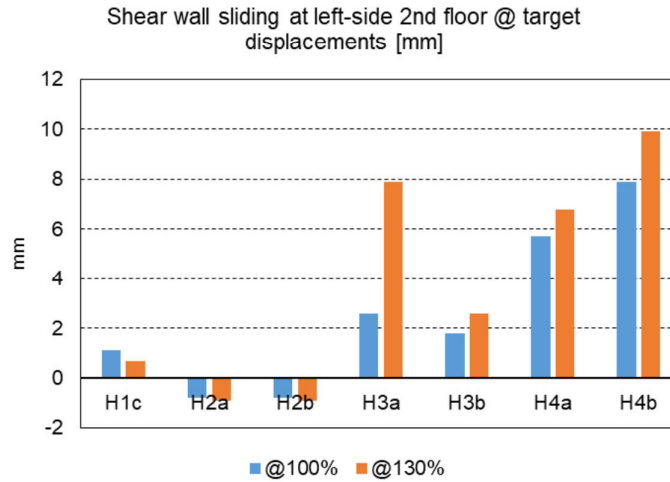


Figure 4.34. Shear wall sliding at left-side 2<sup>nd</sup> floor @ +100% & +130% target displacement

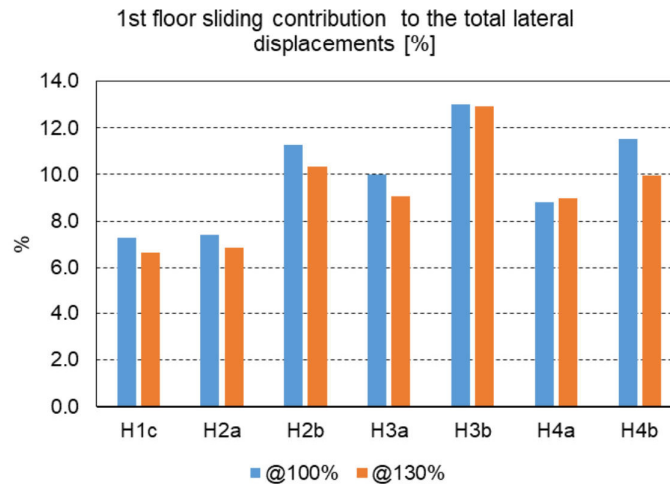


Figure 4.35. 1<sup>st</sup> floor contribution percentage to the total lateral displacement

Direct measurements were taken for the sliding at the base level and 2<sup>nd</sup> floor, gauged between the shear walls and either the base level or the 2<sup>nd</sup> level floor. However, upon reviewing the collected values, it became apparent that the combined contribution of these two sliding instances amounted to less than 5% of the total lateral displacement observed in the structures as shown in Figure 4.36.

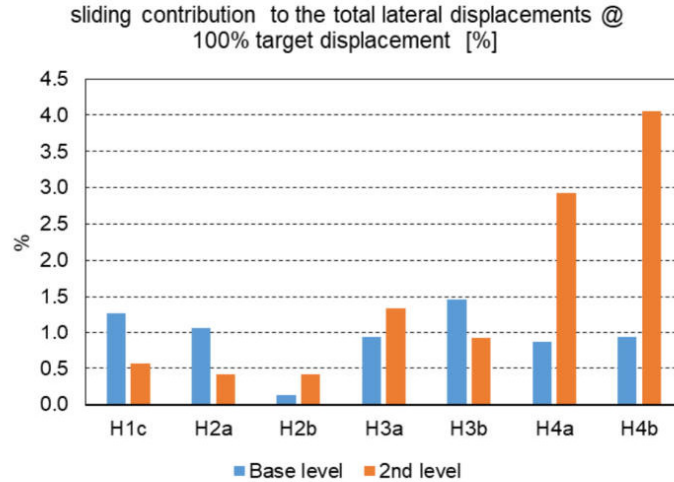


Figure 4.36. Base and 2<sup>nd</sup> level sliding contribution to the total lateral displacement [%]

#### 4.7 Panel-to-panel slip

The graphs in Figure 4.37 and Figure 4.38 present the Panel-to-panel slips for the 1<sup>st</sup> and 2<sup>nd</sup> stories at +/-100% and +/-130% target slips. All slips are positive during positive cycles, while no uplift occurs in the negative cycles. A notable observation is that the Panel-to-panel slips on the 1<sup>st</sup> floor were quite consistent across different structures, averaging around 15 mm at 100% and 20 mm at 130% target slips. Conversely, more significant variations were evident on the 2<sup>nd</sup> floor. This disparity in slips can be attributed to the specific characteristics of the tension straps, leading to varying degrees of rocking and panel-to-panel movement. Hence, variations in tension straps could impact the dissipation of energy on each storey, emphasizing that appropriately designed tension straps have the potential to ensure consistent energy dissipation across all levels. Notably, the maximum value of panel-to-panel slip on the 2<sup>nd</sup> storey was recorded in structure #H4b, measuring 33.7 mm at +130% target slip. The reason for this observation could be due to the presence of a perpendicular wall.

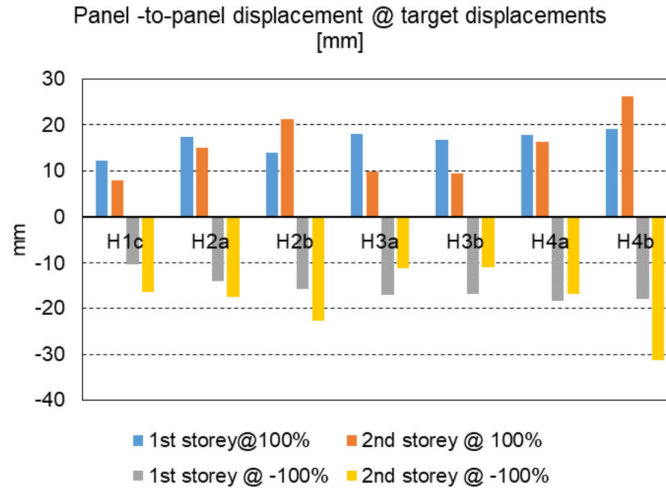


Figure 4.37. Panel-to-panel slip in the 1<sup>st</sup> and 2<sup>nd</sup> level @ +/-100% target displacements

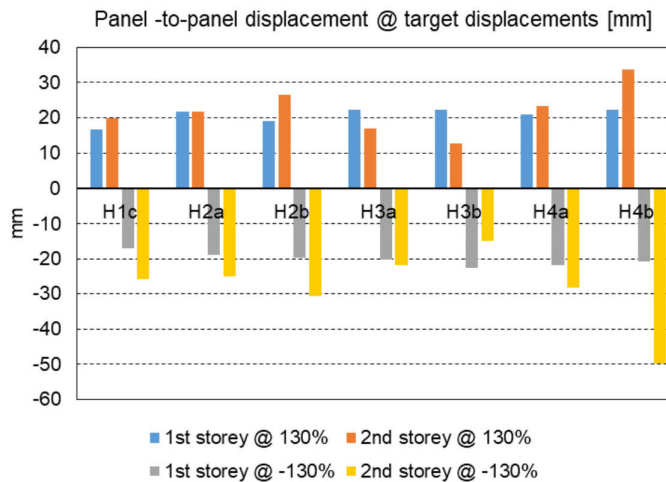


Figure 4.38. Panel-to-panel slip in the 1<sup>st</sup> and 2<sup>nd</sup> level @ +/-130% target displacements

As illustrated in the Figure 4.39, there are discrepancies between the panel-to-panel slips and the panel inner corner uplifts in the 2<sup>nd</sup> storey across all structures. The perpendicular shear walls restrict the movement or slip of the CLT shear walls on the 2<sup>nd</sup> storey. In scenarios where there is lateral movement or forces acting on the structure, the perpendicular shear wall may confine the CLT shear walls, limiting their ability to flex

or move freely. This confinement alters the way forces are distributed or resisted within the structure and hence a significant portion of the energy is dissipated in the spline joints in the 2<sup>nd</sup> storey, resulting in the highest value of panel-to-panel slip observed in the structure #H4b.

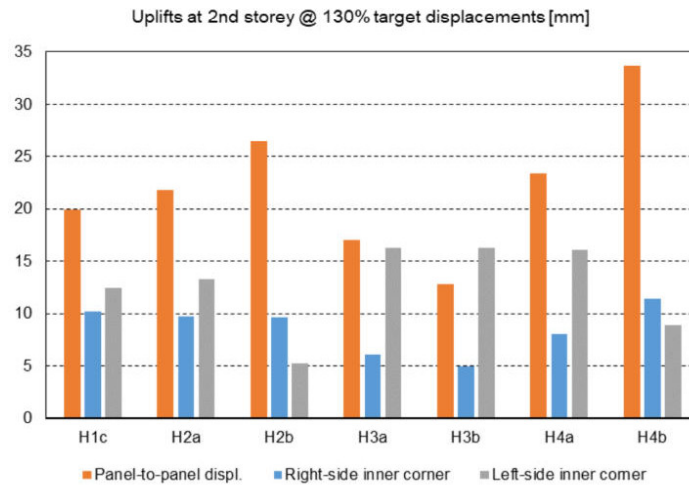


Figure 4.39. Panel-to-panel slips and inner corner uplifts of the 2<sup>nd</sup> floor @ 130% target displacement

#### 4.8 Panel distortion

The panel distortion of the front and back panels of the 1<sup>st</sup> storey for structures #H3a, #H3b, #H4a, and #H4b is detailed in Figure 4.40. The distortion values during positive target displacements, when CLT panels undergo compression, are lower than the values observed during negative target displacements when the panels are subjected to tension forces, and the maximum distortion was observed in #H4b, with values of 4.6 mm and 5.2 mm at -100% and -130% target displacements, respectively. This indicates that the presence of perpendicular walls results in increased structural stiffness, a higher load-carrying capacity and higher in-plane forces as a result, and greater panel distortion.

On the other hand, in the structures without perpendicular shear walls, the panel distortion values ranged from 0.1 mm to 2.9 mm at +/-100% target displacement and from 0.1 mm to 3 mm at +/-130% target displacement. When considering the 1<sup>st</sup> storey displacement, which was approximately 70 mm, the contribution of panel distortion to the lateral displacement is less than 5% at 130% target displacement. This further supports the assumption of rigid body behavior of CLT panels under lateral loads.

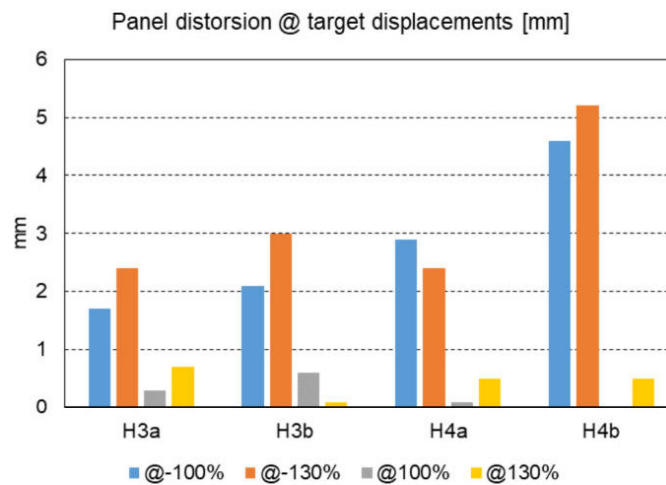


Figure 4.40. Panel distortion @ -100% and -130% target displacement [mm]

#### 4.9 Kinematic behavior of CLT shear walls

The overall horizontal displacement of CLT shear wall [39] can be divided into three major components: 1) Sliding, 2) Rocking (panel overturning), and 3) Panel distortion (combined effect of bending and shear deformation). Popovski et al. [39] examined the deformation components contributing to the lateral displacement of CLT shear wall structures and summarized that: **Rocking** component led to uplift deformations in HD and brackets as well as a global rotation of the structure; **Sliding** resulted in the horizontal displacement or slip of screws within the brackets; and **In-plane deformations**

encompassed shear and flexural in-plane deformations of CLT wall panels. The total storey lateral deformation is the sum of the four components.

4-1

represents storey deformation caused by the global rotation of the structure, or the deformation of a specific storey (i) in a building caused by the overall rotation of the entire structure. Global rotation refers to the rotation of the entire building as a single unit. while is the deformation resulted from rocking of the panels or the deformation of a specific storey (i) caused by the rocking motion of the individual panels in that storey. The deformation specifically captures the contribution of rocking motion to the overall deformation at a particular storey indicates the contribution of sliding and denotes the contribution of in-plane deformation of the wall panels. For the 1<sup>st</sup> storey, components and describe the same phenomena, necessitating consideration of only one component. These deformation components are presented in Figure 4.41.

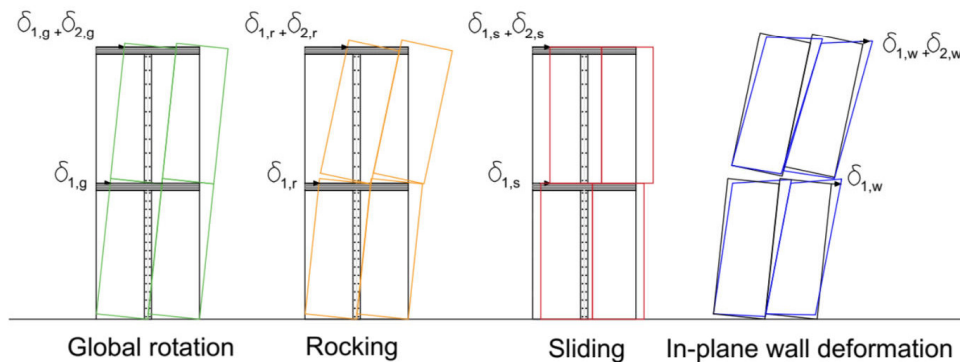


Figure 4.41. Lateral deformation components for a two-storey CLT building

The contribution percentage of rocking, sliding and panel distortion for all structures at 130% target displacement are calculated and presented in Table 4.1. There is an observed differences between the calculated total lateral displacement values and the measured total lateral displacement at 130% target displacement in the experimental tests. In this

study, the uplift values are derived from the average of HD and inner panel corners uplifts in the 1<sup>st</sup> storey, and the average of tension strap and inner panel corners uplift in the 2<sup>nd</sup> storey. These average uplift values were multiplied by the panel aspect ratio (2.5) to provide the horizontal displacement due to rocking. Similarly, the sliding values are averaged between the left and right panels. Finally, the slip between panels was measured parallel to the edge of the panels following the rotation of panel edges, exhibiting two components in both vertical and horizontal directions. the horizontal component of the panel-to-panel slip has been roughly estimated using its corresponding vertical component, which equals the corner panel uplift. As a result, the total calculated values slightly differ from the expected overall value of 195 mm at 130% target displacement. It is crucial to note that a portion of the 1<sup>st</sup> floor sliding results from the overall rotation of the 2<sup>nd</sup> storey. Therefore, the impact of rocking might be slightly higher than what is specifically outlined in these tables.

The main factor causing variation in the results of #H2a and #H2b is the uplift observed in the tension strap on the 2<sup>nd</sup> storey. Even though the structure #H2a shared the same shear brackets as #H2b and even had weaker shear brackets compared to #H3a, its sliding was less than these structures. It appears that the increased number of STSs in the tension strap of structure #H2a had an additional impact, reducing the sliding of the 1<sup>st</sup> floor, resulting in this structure showing the least sliding among all the structures.

The results for structures #H3a and #H3b are very close; the only viable difference is the average sliding of two structures as was predicted. The primary distinction between structures #H4a and #H4b emerges from the variance in the rocking behavior on the 2<sup>nd</sup> floor, which is notably restricted in #H4b compared to #H4a because of perpendicular shear wall. During the test #H4b, the maximum displacement applied was 178 mm instead of the intended 195 mm due to

reaching the maximum capacity of one actuator. Table 4.1 and Figure 4.42 show the percentage contributions of factors contributing to lateral displacement across all structures. The values indicate that almost 90% of the total deformation is attributed to uplift and that sliding contributes approximately 10%. Panel distortion of 5-ply CLT panels does not appear to have a significant share with less than 4% contribution.

The discrepancy in rocking percentages between structure #H2a and #H2b by 4% stems from the 90° inclination angle, generating greater uplifts in tension straps and consequently more rocking in #H2a. The sliding percentages between structures #H3a and #H3b differed by 2% due to the substitution of bolts with STSs, rendering the SB more flexible in #H3b. Structure #H4a exhibited 2% higher rocking than #H3b because of an acoustic layer reducing shear wall-floor friction, facilitating easier rocking. Notably, #H4b had the highest sliding percentages among all structures due to the perpendicular shear wall eliminating rocking potential. Consequently, increased lateral load led to heightened sliding, resulting in the maximum 2<sup>nd</sup> floor sliding values in this structure.

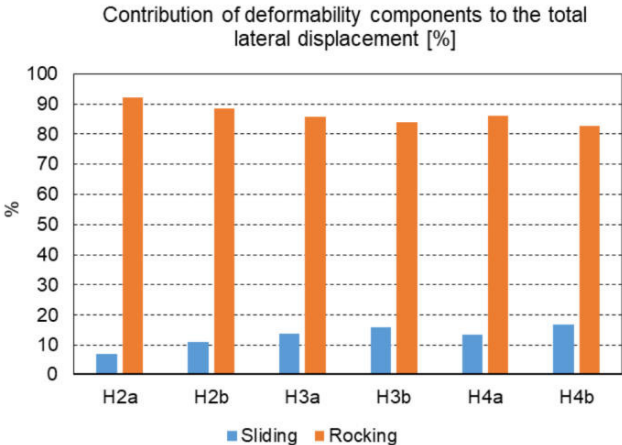


Figure 4.42. Comparison Sliding and rocking contribution percentages to the total lateral displacements in all structures

Table 4.1. Contribution percentage of components to the total lateral displacements

Deformation component [mm]	H2a	H2b	H3a	H3b	H4a	H4b
Base Sliding	1	1.2	2.1	3.2	2	1.6
1 <sup>st</sup> floor sliding (left)	7	10	18	25	18	19
1 <sup>st</sup> floor sliding (right)	10	15	16	24	17	17
average sliding	8.5	12.3	17	24	17.4	18.2
2 <sup>nd</sup> floor sliding	3.6	2.8	7.9	2.6	6.8	9.9
HD. uplift	21	18	21	21	15	13
1 <sup>st</sup> floor inner corner uplift	15	15	18	16	16	17
1 <sup>st</sup> floor average rocking	48	44	52	50	41	39
1 <sup>st</sup> floor Panel distortion	0.7	0.7	0.7	0.1	0.5	0.5
2 <sup>nd</sup> floor global rotation	48	44	52	50	41	39
tension strap uplift	15.9	15.7	17.3	16.4	17.2	10.8
2 <sup>nd</sup> floor inner corner uplift	12.7	14.8	9.7	9.6	16.1	5.8
2 <sup>nd</sup> floor average rocking	37.8	40.3	35.6	34.3	44	21.9
2 <sup>nd</sup> floor Panel distortion	0.6	0.6	0.6	0.4	0.5	0.5
1 <sup>st</sup> floor panel-to-panel slip	18.9	19.5	22.3	22.2	21	22.3
vertical component of slip	15.3	15.3	18.2	16.4	17.1	16.5
horizontal component of the slip	6.5	7.5	12.9	14.9	12.2	14.9
2 <sup>nd</sup> floor panel-to-panel slip	25.2	30.7	17	12.8	23.4	33.7
vertical component of the slip	10.7	8.4	6	5	8.2	13.1
horizontal component of the slip	20.7	28.4	16	11.8	22	31
total displacement (sum of the above components)	175	181	197	191	187	177
total sliding [%] =Σ sliding of the 1 <sup>st</sup> and 2 <sup>nd</sup> stories/total displacement	7.5	9	14	16	13	17
total rocking [%] = Σrocking of the 1 <sup>st</sup> and 2 <sup>nd</sup> stories/total displacement	91.8	90.3	86	84	86	83
total distortion [%] = Σdistortion of the 1 <sup>st</sup> and 2 <sup>nd</sup> stories/total displacement	0.7	0.7	0.7	0.3	0.6	0.6
total percentage [%]	100	100	100	100	100	100

#### 4.10 Comparison of 1<sup>st</sup> storey drifts to previous single-storey results

Single-storey shear walls made of 5-ply CLT panels with aspect ratios of 2:1 and 3:1 were experimentally tested at UNBC [37]. These panels were arranged in single-panel, coupled-panel, and triple panel setups. The STS connections were like the one used in current study. The performance of the shear wall was influenced by various parameters examined in the tests: aspect ratio, number of screws in the spline, and number of screws in the HDs. The values of the shear wall's load-carrying capacity ( $F_{max}$ ) and the corresponding panel displacement ( $d_{F_{max}}$ ) are compared with the findings of the present study in this section. Test labels beginning with "CP" are associated with UNBC tests, while those starting with "H" are linked to the current study.

The data in Table 4.2 indicates the maximum load-carrying resistance at the top level of the UNBC single-story shear walls ( $F_{max}$ ) [37] and the actuator lateral force on the 1<sup>st</sup> floor in the two-storey tests conducted in this study ( $F_{1st\ floor}$ ). In single-storey tests  $F_{1st\ floor}$  equals  $F_{max}$  and represents the total lateral force or base shear. In two-storey shear walls,  $F_{1st\ floor}$  equals half of the  $F_{max}$  and base shear equals the summation of the 1<sup>st</sup> and 2<sup>nd</sup> floor actuator loads.

The UNBC test results revealed a direct correlation between the load-carrying capacity  $F_{max}$  and the corresponding displacement,  $d_{F_{max}}$ , with the quantity of HD's STSs. In the single-story tests, HD had either 11 or 9 STSs, whereas in this study, the HD were equipped with 21 STSs and consequently, the total lateral force in two-storey shear walls was approximately three times that of the single-storey ones. The presence of an inverted triangular load distribution, with  $F_{max}$  at the top of the 2<sup>nd</sup> floor and  $F_{max}/2$  at the 1<sup>st</sup> floor, suggests that doubling the number of HD STSs led to a doubling of  $F_{max}$  at the top of the 2<sup>nd</sup> floor. According to the UNBC tests, there was not a significant impact on the behavior of the shear walls when the number of STSs in the spline joints increased from 16 to 19.

Table 4.2. Comparison between single-storey shear walls [37] and current study

Wall	#STS in HD	# STS in spline	Label	$F_{1st\ floor}$ [kN]	Base shear [kN]	$d_{Fmax}$ 1 <sup>st</sup> floor [mm]
Coupled 3 m x 1.5 m	11	19	CP7-2:1-11-19	142.4	142.4	75
	11	19	CP8-2:1-11-19	174.4	174.4	70
	9	16	CP9-2:1-9-16	149.6	149.6	70
	9	16	CP10-2:1-9-16	161.1	161.1	70
Coupled 3 m x 1 m	11	19	CP13-3:1-11-19	109.7	109.7	104.1
	11	19	CP14-3:1-11-19	102.8	102.8	80.1
	9	16	CP15-3:1-9-16	89.8	89.8	80
	9	16	CP16-3:1-9-16	93.6	93.6	104.1
Coupled 2.5 m x 1 m	21	16	H1c	132	395	74.8
	21	16	H2a	168	504	92.7
	21	16	H2b	157	470	66.8
	21	16	H3a	169	506	99.2
	21	16	H3b	163	488	109
	21	16	H4a	130	390	78.2
	21	16	H4b	187	560	76.8

This suggests that the performance of the spline joints remained nearly identical in both test series since both had 16 or 19 STSs. Consequently, the variation in lateral displacements can be attributed to the differences in the HD rather than changes in the spline joints. By comparing the lateral displacement of the 1<sup>st</sup> floor in single-storey and two-storey shear walls, the objective was to evaluate how tension straps and the presence of the second floor affect the 1<sup>st</sup> floor's lateral displacement. In single-storey shear walls, the displacements ranged from 70 mm to 104 mm. Notably, the 2:1 aspect ratio wall demonstrated higher capacity and lower lateral displacement (ranging from 70 mm to 75 mm) compared to the 3:1 aspect ratio wall, which showed displacements ranging from 80 mm to 104 mm. The two-storey shear wall, with an aspect ratio of 2.5:1, fell between these two ranges with the lateral displacement values of 66.8 mm to 109 mm.

Comparatively, when analyzing the 1<sup>st</sup> storey displacements between single-storey and two-storey shear walls, the range of displacement values is relatively similar, with slight

differences attributable to their aspect ratios and the number of STS used in their HD. The structure labeled #H1c, equipped with the most flexible tension straps among all the two-storey shear walls, displayed values closest to those of the single-storey shear walls. This finding indicates that the 2<sup>nd</sup> floor of #H1c did not demonstrate uniform displacement with the 1<sup>st</sup> floor. Instead, its behavior resembled that of the single-storey shear walls. On the other hand, the differences in tension strap stiffness contributed to the discrepancies in 1<sup>st</sup> storey displacements, essentially affecting the distribution of displacements across the structure's height and the stiffest tension straps could provide more displacement in 1<sup>st</sup> storey while the flexible ones led to more displacement in the 2<sup>nd</sup> storey.

## 5. Conclusions

### 5.1 Summary of findings

The main findings obtained from the analyses presented in this thesis are:

- 1- In all cyclic tests, the load-displacement curves were linear up to the 70% target displacement (105 mm). Beyond this point, the connections started to yield, reducing system stiffness. Load continued to increase, up to 130% or 160% of the target displacement, resulting in localized failures and reduced load capacity. In monotonic tests load increased linearly with displacement till almost 100% target displacement (150mm) where the tests stopped. Hence, the tested CLT structures met NBCC drift criteria without experiencing significant capacity reduction or failure.
- 2- Increasing the strength of the shear brackets at the bottom of the 2<sup>nd</sup> storey shear wall and adding dead load to each floor (#H1c vs #H2a) increased the load-carrying capacity of the shear walls by approximately 25%.
- 3- The impact of screw installation angle at the tension straps (#H2a vs #H2b) had only minimal impact on the load-carrying capacity and stiffness of the structures, although this has been influenced by re-testing the structure.
- 4- Substituting the bolts for STSs in shear connections between floors (#H3a vs #H3b) resulted in the most uniform ISD because of the higher stiffness of the bolts, and applying stronger SBs on the 2<sup>nd</sup> floor of the structure #H3a led to the highest load-carrying capacity.
- 5- The added acoustic layer (#H4a vs #H3b) had a small detrimental effect on performance and slightly decreased the load-carrying resistance.

- 6- Applying the perpendicular shear walls (#H4b vs #H3b) significantly increased load-carrying capacities of CLT structures with 15%.
- 7- Rocking was the primary factor contributing to the lateral horizontal displacement in all the structures, accounting for 80% to 95% of the total lateral displacement, and rocking was mainly governed by the stiffness of HDs and tension straps. The use of stiff enough tension straps which provide uniform stiffness across the height of the structure resulted in a consistent ISD between the two stories. Consequently, the details of tension straps play a crucial role in determining the overall displacement of structures.
- 8- The contribution of sliding to the total lateral deformations was less than 4% at the 2<sup>nd</sup> floor and less than 10% at the 1<sup>st</sup> floor. This suggests that the design objective of keeping the SB at an elastic limit was achieved. Additionally, it indicates that the SB configurations did not have a substantial impact. As a result, the utilization of STS for both legs of the SB can be deemed sufficient for preserving elastic behavior.
- 9- The contribution of panel distortion to the lateral displacement is estimated to be less than 4%. This finding further reinforces the hypothesis of rigid body behavior of CLT panel when subjected to lateral loads.

## **5.2 Outlook**

In this set of experimental tests, shear walls were re-tested, and reusing of CLT panels might have impacted the results when comparing different STS inclination angles in the tension straps. Furthermore, the shear walls were not tested to failure, preventing an accurate determination of their ductility. In future studies, it would be advisable to apply forces to the CLT structures that push them to their connection failure points for a more comprehensive assessment regarding their ductility and energy dissipation. Additionally,

it is worth noting that the placement of sensors on the first floor captured the overall relative displacement. To gain a more precise understanding of the pure sliding that occurred, it is recommended to collect data that accounts for the contribution of connections linking the shear wall at the 1st storey to the 1st floor, as well as those connecting the shear wall at the 2nd storey to the 1st floor. The outcomes of our study have practical applications in the design process, as they reveal disparities in the sliding behavior of the base SB and 1<sup>st</sup> floor level, along with variations in the performance of tension straps compared to HDs. These findings underscore the need for distinct considerations in the design of different structural elements at different levels. Conversely, these results can enhance our comprehension of the significance of tension strap design in achieving a uniform stiffness distribution throughout the height of structures.

In summary, the outcomes of this study not only inform the immediate design considerations for structures with different levels but also serve as a valuable resource for those involved in developing analytical design formulas and guidelines, especially in the context of taller buildings and the broader construction industry.

## References

- [1] NBCC (National Building Code of Canada), *Canadian Commission on Building and Fire Codes*. National Research Council of Canada, Ottawa, ON, 2020.
- [2] “WCR-2016-WEB.pdf.” Accessed: Apr. 06, 2023. <https://unhabitat.org/sites/default/files/download-manager-files/WCR-2016-WEB.pdf>
- [3] R. H. Falk and F. Handbok: wood as an Engineering Service, “*USDA Forest Service, Forest Products Laboratory, General Technical Report FPL-GTR-190, 2010: 509 p. 1 v.*”, vol. 190, 2010, doi: 10.2737/FPL-GTR-190.
- [4] Green Michael, “Tall Wood, ‘Tall Case’” Accessed: Jun. 14, 2023. [Online]. Available: <https://www.archdaily.com/220779/michael-green-presents-the-case-for-tall-wood-buildings>
- [5] C. D. Oliver, N. T. Nassar, B. R. Lippk Fuel, and Biodiversity Mitigation With Wood a *Journal of Sustainable Forestry*, ” *Forestry*, vol. 33, no. 3, pp. 248–275, Apr. 2014, doi: 10.1080/10549811.2013.839386.
- [6] U. Dangel, “Tall Wood Buildings: Design Michael Green *Technology Architecture & Design*,” vol. 2, no. 2, pp. 254–256, Jul. 2018, doi: 10.1080/24751448.2018.1497379.
- [7] “Sustainability and Life Cycle Analysis Wood Council - CWC. Accessed: Apr. 06, 2023. [Online]. Available: <https://cwc.ca/en/publications/ibs4-sustainability-and-life-cycle-analysis-for-residential-buildings/>
- [8] E. Karacabeyli and S. Gagnon, *Canadian CLT Handbook*, vol. 1. Vancouver, Canada: FPInnovations, 2019.



- [17] X. Zhang, “Seismic design of built-in timber joints of British Columbia, 2017. doi: 10.14288/1.0348302.
- [18] Z. Chen and Y.-H. Chui, “Resisting System Using Mass Timber Panel for High-Rise Buildings in Built Environment, vol. 3, Jul. 2017, doi: 10.3389/fbuil.2017.00040.
- [19] M. Shahnewaz, M. Popovskiy, and T. T-Laminated, “Resisting Timber Shear Walls for Platform-Type Connections *Journal of Structural Engineering*, vol. 145, no. 12, p. 04019149, Dec. 2019, doi: 10.1061/(ASCE)ST.1943-541X.0002413.
- [20] “Structural Design Guide | MTC Solutions. Accessed: Jun. 17, 2023. [Online]. Available: <https://mtcsolutions.com/resources/design-guides/structural-screws-connection-design-guide/>
- [21] A. Hossain, “EXPERIMENTAL STUDY OF SHEAR WALL CONNECTIONS WITH SELF-TAPPING-SCREWS FOR CROSS-LAMINATED-TIMBER PANELS”.
- [22] J. R. Brown, M. Li, T. Tanner, and D. Orthogonal joints in cross-laminated timber with self-tapping screws installed with mixed angles *Engineering Structures*, vol. 228, p. 111560, Feb. 2021, doi: 10.1016/j.engstruct.2020.111560.
- [23] A. Hossain, M. Popovskiy, and T. Tanner, “Experimental Study of Cross-Laminated Timber Connections Assembled with a Combination of Screws in Withdrawal and Screws in Shear *Engineering Structures*, vol. 168, pp. 1–11, Aug. 2018, doi: 10.1016/j.engstruct.2018.04.052.
- [24] C. Loss, A. Hossain, and T. Tanner, “Experimental Study of Cross-Laminated Timber Connections with Self-Tapping Screws *Engineering Structures*, vol. 173, p. 07004, Oct. 2018, doi: 10.1016/j.engstruct.2018.07.004.

- [25] L. Pozza, B. Ferracuti, M. Mariani, and CLT hold-down connections – Experimental Engineering Structures, vol. 160, pp. 95–110, Apr. 2018, doi: 10.1016/j.engstruct.2018.01.021.
- [26] Y. Shen, J. Schneider, S. Tesfamariam, behavior of bracket connections for cross-laminated timber (CLT): Assessment and comparison of experimental Journal of Building Engineering, vol. 39, p. 102197, Jul. 2021, doi: 10.1016/j.job.2021.102197.
- [27] ASTM, “Standard Test Methods for Cyclic Resistance of Walls for Buildings.” American Conshohocken, PA, 2011.
- [28] CEN, *EN12512 Timber Structures-Test Methods-Cyclic Testing of Joints Made with Mechanical Fasteners*. European Committee for Standardization (CEN), Brussels, Belgium, 2012.
- [29] D. Khai Tran and G. Y. variables of hold-down Design of angle bracket connections for lateral resistance enhancement of cross-laminated timber (CLT) walls considering the influence of wood species, load-grain angles, and floor conditions, *Structures*, vol. 48, pp. 1003–1017, Feb. 2023, doi: 10.1016/j.istruc.2023.01.020.
- [30] M. Popovski, J. Schneider, and M. Schwe cross-laminated Presented in Proceedings of the 11th World Conference on Timber Engineering, Riva del Garda, Italy, Jan. 2010.
- [31] M. Popovski and E. Karaca Laminated Timber Seismic Structures, ” presented at the World Conference Canada, Jan. 2012.
- [32] I. Gavric, M. Fragiaco, and T. Wall Cecco Systems: Experimental Tests Journal of Structural Analytical

*Engineering*, vol. 141, no. 11, p. 04015034, Nov. 2015, doi: 10.1061/(ASCE)ST.1943-541X.0001246.

[33] I. Gavrić, M. Fragiaco, M. Popovski, and S. Schneider, "Laminated Timber Panels under Cyclic Loads," 2013. doi: 10.1007/978-94-007-7811-5\_62.

[34] M. O. Amini, J. W. van de Lindt, D. Rammer, and S. Pei, "High-Aspect-Ratio Cross-Laminated Timber Shear Walls: Experimental and Numerical Investigation," *Journal of Architectural Engineering*, vol. 27, no. 3, p. 04021013, Sep. 2021, doi: 10.1061/(ASCE)AE.1943-5568.0000473.

[35] J. W. van de Lindt, M. O. Amini, D. Rammer, P. Line, S. Pei, and M. Popovski, "Seismic Performance of Laminated Timber Shear Wall Systems in the United States," *Journal of Structural Engineering*, vol. 146, no. 9, p. 04020172, Sep. 2020, doi: 10.1061/(ASCE)ST.1943-541X.0002718.

[36] M. O. Amini, J. W. van de Lindt, D. Rammer, S. Pei, P. Line, and M. Popovski, "Systematic experimental investigation to performance factors for cross-laminated timber structures," *Engineering Structures*, vol. 172, pp. 392–404, 2018, doi: 10.1016/j.engstruct.2018.06.021.

[37] Maj, M., Tannert, T., "UNBC Test Report,"

[38] A. Ceccotti, M. Follesa, M. P. Testa, and S. Aurilio, "Results on the Lateral Resistance of Cross-Laminated Wood Panels," *Proceedings of the 9th World Conference on Timber Engineering, Portland, Oregon, USA*, Jun. 2023.

[39] M. Popovski, I. Gavrić, and S. Schneider, "A-story CLT house subjected to lateral load," *Journal of Earthquake Engineering and Structural Dynamics*, vol. 41, no. 14, pp. 2111–2128, 2013, doi: 10.1002/eqe.2280.

- [40] J. W. van de Lindt *et al.*, “Experimental seismic behavior of a platform *Engineering Structures*,” vol. 183, pp. 408–422, Mar. 2019, doi: 10.1016/j.engstruct.2018.12.079.
- [41] American Society of Civil Engineers, Ed., *Minimum design loads for buildings and other structures*. in ASCE standard. Reston, Va: American Society of Civil Engineers: Structural Engineering Institute, 2010.
- [42] S. Momose, T. Nakagawa, T. Naitoh, H. Isoda, “Analytical Method to Reproduce Seismic Behavior of a Two-Story Cross-Laminated Timber Building at Large Displacement,” *Journal of Structural Engineering*, vol. 149, no. 6, p. 04023064, 2023, doi: 10.1061/JSENDH.STENG-11711.
- [43] Isoda Hiroshi *et al.*, “Experimental Behavior of L-Shaped and T-Shaped Cross-Laminated Timber to Evaluate the Effectiveness of Shear Walls,” *Journal of Structural Engineering*, vol. 149, no. 5, p. 04023036, May 2023, doi: 10.1061/JSENDH.STENG-11474.
- [44] I. Lukacs, A. Björn, “Strength and stiffness of cross-laminated timber (CLT) shear walls: State-of-the-art of an analytical approach,” *Engineering Structures*, vol. 178, pp. 136–147, Jan. 2019, doi: 10.1016/j.engstruct.2018.05.126.
- [45] M. Shahnewaz, T. Tanner, “Seismic Performance of Cross-Laminated Timber Shear Walls: Analytical and Experimental Results,” *ACI Structural Journal*, vol. 113, no. 2, p. 218, May 2019, doi: 10.29173/mocs96.
- [46] M. Shahnewaz, T. Tanner, M. Alam, “Seismic Design for Cross-Laminated Timber Buildings,” *Structures Congress 2017: business, professional practice, education, research, and disaster management—selected papers from the structures Congress 2017*, pp. 400–410, Apr. 2017, doi: 10.1061/9780784480427.034.
- [47] V. Nolet, D. Casagrande, and G. Pagnani, “Analytical Methodology to Predict the Elastic-Plastic Behavior of CLT Shear Walls: Multi-Phase Analytical Methodology to Predict the Elastic-Plastic Behavior of CLT Shear Walls,” *Journal of Structural Engineering*, vol. 149, no. 5, p. 04023036, May 2023, doi: 10.1061/JSENDH.STENG-11474.

*Engineering Structures*, vol. 179, pp. 640–654, Jan. 2019, doi: 10.1016/j.engstruct.2018.11.017.

[48] D. Casagrande, G. Doudak, L. Mauro, and A. Polastri, Establishing the Elastic Behavior of Multipanel CLT Shear Walls Subjected to Lateral Loads, *Journal of Structural Engineering*, vol. 144, no. 2, p. 04017193, Feb. 2018, doi: 10.1061/(ASCE)ST.1943-541X.0001948.

[49] ANSI/APA PRG 320. (2017), *Standard for Performance-Rated Cross-Laminated Timber*. American National Standard, APA, Tacoma, WA, 2017.

[50] CSA, *CSA O86-14 Engineering Design in Wood*. Canadian Standard Association, Mississauga, Canada., 2014.

[51] CSA, *CSA O86-16 supplement Engineering Design in Wood*. Canadian Standard Association, Mississauga, Canada., 2016.

[52] CSA, *CSA O86-19 Engineering Design in Wood*. Canadian Standard Association, Mississauga, Canada., 2019.

[53] NDS. (2015), *National Design Specification for Wood Construction*. Washington, DC. American Wood Council, 2015.

[54] IBC, *International Building Code (IBC)*. International Code Council, Falls Church, VA, USA., 2015.

[55] IBC, *International Building Code (IBC)*. International Code Council, Falls Church, VA, USA., 2021.

[56] American Society of Civil Engineers, *Minimum Design Loads for Buildings and Other Structures*, 7th ed. Reston, VA: American Society of Civil Engineers, 2022. doi: 10.1061/9780784412916.

[57] EN 1995 (2004) Design of structures of timber for earthquake resistance, Part 1: General rules, seismic actions and rule Standardization. Brussels, Belgium.

- [58] M. Follesa *et al.*, “ A p r o p o s a l f o r a n e w B a c k g r o u n d E u r o c o d e I N T E R 2 0 1 5 M e e t i n g , 2 0 1 5 .
- [59] M. Follesa *et al.*, “ T h e n e w p r o v i s i o n s f o r t h e s e i s m E u r o p e a n E n g i n e e r i n g S t r u c t u r e s , ” v o l . 1 6 8 , p p . 7 3 6 – 7 4 7 , A u g . 2 0 1 8 , d o i : 1 0 . 1 0 1 6 / j . e n g s t r u c t . 2 0 1 8 . 0 4 . 0 9 0 .
- [60] D. Casagrande, G. D o u d a k , a n d M . M a s r o - b a s e d “ A p r o p o s a l f o r t h e d e s i g n o f m u l t i - s t o r e y C L T b u i l d i n g s , ” p r e s e n t e d a t t h e I n t e r n a t i o n a l E n g i n e e r i n g R e s e a r c h , I N T E R P a p e r 1 5 - 1 . 5 8 , A u g . 2 0 2 1 .
- [61] R o t h o b l a a s , “ S o u n d p r o o f i n g S o l u t i o n s . A R C H I T E C T U R E ” <https://www.rothoblaas.com/catalogues-rothoblaas>
- [62] “ A S T M E 2 1 2 6 | S t a n d a r d T e s t M e t h o d s f o r C y c l i c ( R e v e r s e d ) L o a d T e s t f o r S h e a r R e s i s t a n c e o f V e r t i c a l E l e m e n t s o f t h e L a t e r a l F o r c e R e s i s t i n g S y s t e m s f o r B u i l d i n g s | D o c u m e n t C e n t e r , I n c . ” A c c e s s e d : J u n . 1 9 , <https://www.document-center.com/standards/show/ASTM-E2126>

# Appendix 1: Failure modes after testing

## A.1.1. Structure #1

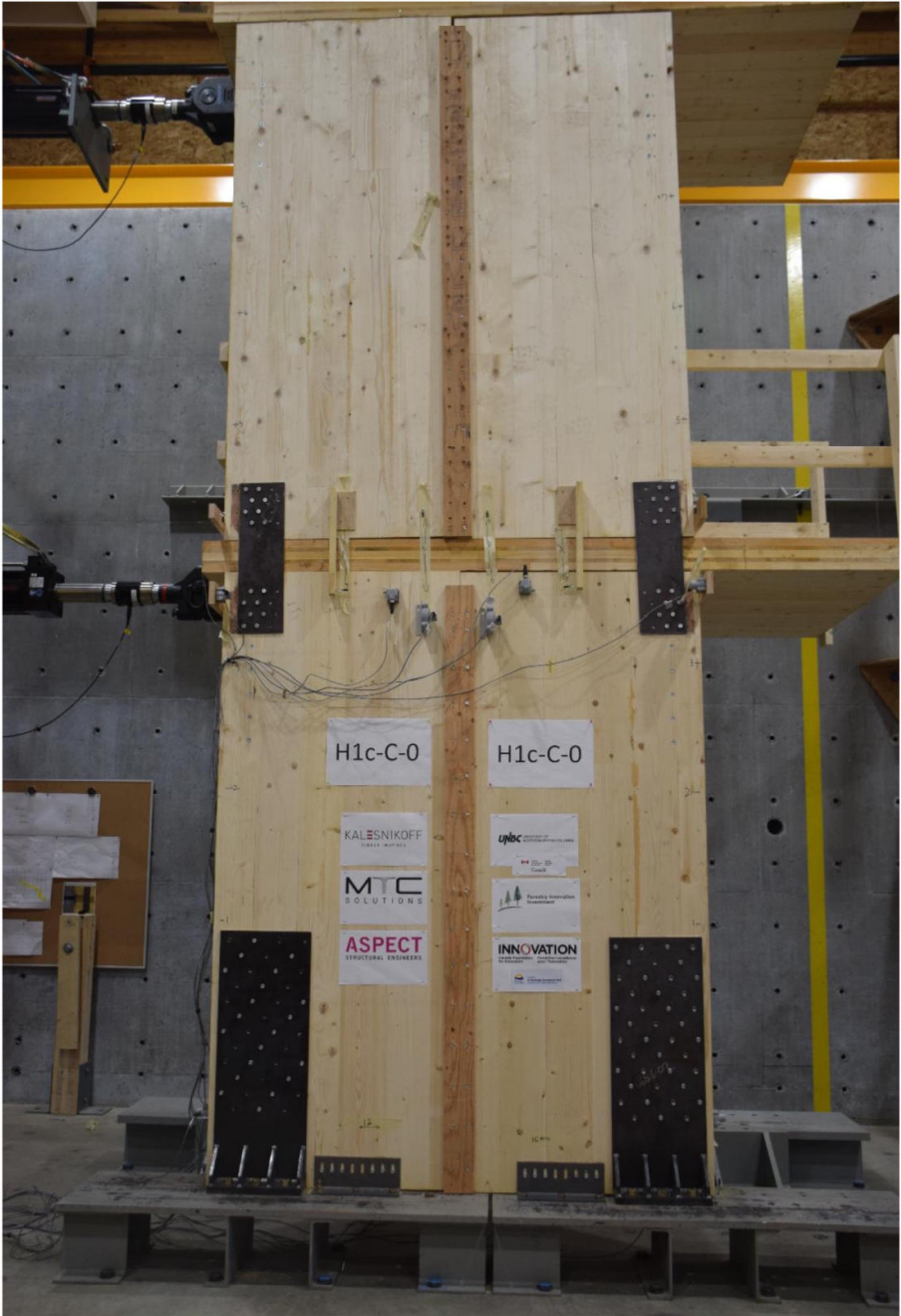
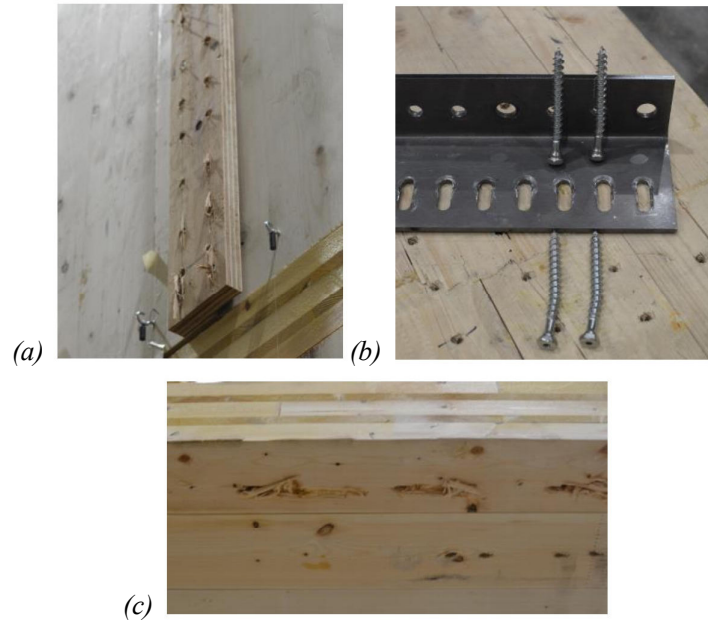


Figure A.1. H1c deformed shape of structure after test



*Figure A.2. H1c elements after test: a) spline LVL, b) SB screws, c) CLT panel under spline joint*



*Figure A.3. H1d deformed shape of structure after test*

### A.1.2. Structure #2



*Figure A.4. H2a deformed shape of structure after test*



*Figure A.5. H2b deformed shape of structure after test*



(a)



(b)



(c)

Figure A.6. H2b deformed elements after test: a) SB b) CLT panel under tension strap, c) CLT panel under spline joint

### A.1.3. Structure #3



*Figure A.7. H3a deformed shape of structure after test*



*Figure A.8. H3a elements after test: a) spline plywood, b) spline joints screws, c) tension strap screws, d) failure of CLT panel under tension strap, e) embedment in the CLT panel under SB, f) deformed HD screws*



*Figure A.9. H3b deformed shape of structure after test*



(a)



(b)

*Figure A.10. H3b deformed elements after test: a) crushed LVL spline and shear failure of spline screws b) floor panel bending*

#### A.1.4. Structure #4



*Figure A.11. H4a deformed shape of structure after test*



(a)



(b)

*Figure A.12. H4a deformed elements after test: a) brittle local failure in the corner of CLT panel b) SB deformation*



*Figure A.13. H4b deformed shape of structure after test*

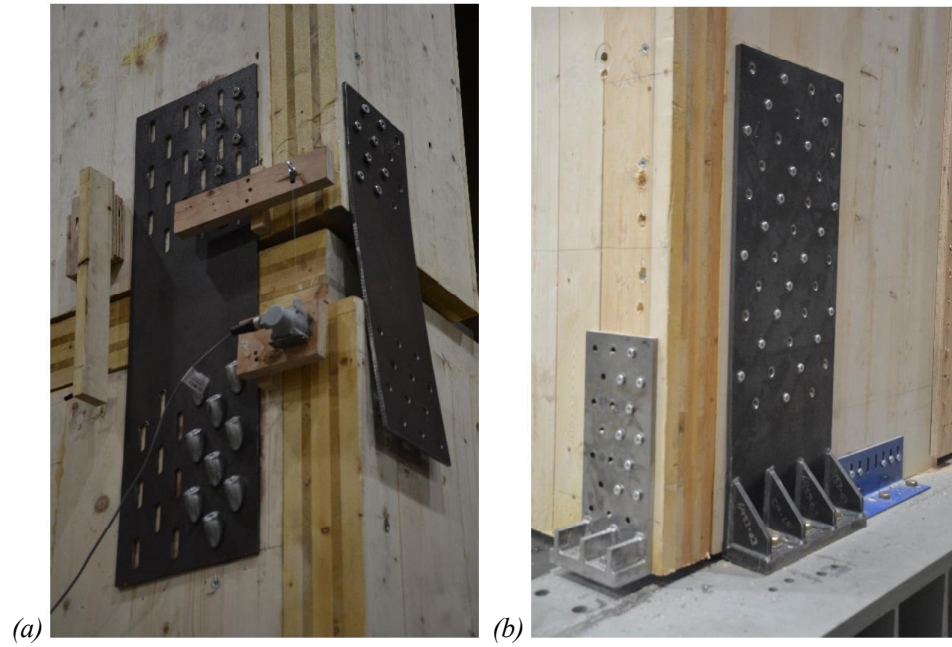


*Figure A.14. H4b deformed elements after test: a) rocking and sliding of the CLT panel in the 2<sup>nd</sup> storey b) rocking of the first storey*

## Appendix 2. Detailed results

### A.2.1. Load-carrying resistance at target displacement

Table A.1. Load-carrying resistances at target displacements [kN]

Target	H1c	H2a	H2b	H3a	H3b	H4a	H4b1)	H4c2)
40%	100	164	121	163	119	150	195	
-40%	-104	-139	-132	-171	-130	-139	-205	
70%	159	236	172	244	201	218	300	
-70%	-163	-212	-205	-254	-205	-227	-300	
100%	205	283	249	299	267	257	355	198
-100%	-143	-260	-276	-284	-273	-260	-359	-219
130%	249	316	313	323	313	259	373	288
-130%	-250	-295	-264	-296	-317	-282	-376	-308
160%	261	336	130	336	321	235		290
-160%	-262	-309	-142		-336	-268		-312
Fmax+	263	336	313	337	325	260	373	291
Fmax-	-264	-309	-297	-297	-336	-282	-376	-312

Note 1) Test #H4b was stopped at the 130% target displacement because the maximum capacity of one actuator was reached.

Note 2) Test #H4c was started at the 100% target displacement after the hold-downs of the perpendicular walls in test H4b were removed.

## A.2.2. Storey displacements at target displacements

*Table A.2. First storey displacements at target displacements [mm]*

Target	H1c	H2a	H2b	H3a	H3b	H4a	H4b	H4c
40%	22.6	28.2	28.1	30.3	30.3	28.3	33.5	
-40%	-28.2	-26.0	-25.5	-30.0	-26.9	-28.5	-30.3	
70%	37.2	47.6	40.0	52.9	52.2	51.1	54.8	
-70%	-44.8	-43.2	-41.6	-51.3	-49.3	-48.6	-49.4	
100%	54.6	63.2	57.9	71.6	74.7	66.9	68.0	61.9
-100%	-41.5	-57.5	-58.1	-65.8	-68.9	-64.6	-62.5	-59.0
130%	65.7	78.8	76.4	86.3	93.8	76.0	76.8	75.6
-130%	-66.9	-71.4	-67.9	-74.8	-87.8	-73.3	-70.4	-72.6
160%	74.8	92.7	66.8	99.2	109.2	78.2		81.7
-160%	-73.2	-80.9	-55.1	0.0	-105.6	-74.7		-77.5

*Table A.3. Second storey displacements at target displacements [mm]*

Target	H1c	H2a	H2b	H3a	H3b	H4a	H4b	H4c
40%	37.4	31.8	31.9	29.8	29.8	31.7	26.6	
-40%	-31.8	-34.0	-34.4	-30.1	-33.2	-31.6	-29.7	
70%	67.7	57.5	64.9	52.1	52.9	53.9	50.3	
-70%	-60.1	-61.8	-63.3	-53.7	-55.8	-56.4	-55.6	
100%	95.3	86.8	91.9	78.4	75.3	83.1	81.9	88.1
-100%	-108.5	-92.6	-91.8	-84.2	-81.1	-85.4	-87.4	-91.1
130%	129.4	116.2	118.4	108.7	101.2	119.0	99.2	119.3
-130%	-128.1	-123.6	-126.9	-120.2	-107.2	-121.8	-106.1	-122.5
160%	165.1	147.3	173.2	140.9	130.9	161.8		158.4
-160%	-166.7	-159.2	-184.6		-134.5	-165.3		-162.6

Table A.4. First floor drift ratios at target displacements [%]

Target	H1c	H2a	H2b	H3a	H3b	H4a	H4b
40%	0.9	1.1	1.1	1.2	1.2	1.1	1.3
-40%	-1.1	-1.0	-1.0	-1.2	-1.1	-1.1	-1.2
70%	1.5	1.9	1.6	2.1	2.1	2.0	2.2
-70%	-1.8	-1.7	-1.7	-2.1	-2.0	-1.9	-2.0
100%	2.2	2.5	2.3	2.9	3.0	2.7	2.7
-100%	-1.7	-2.3	-2.3	-2.6	-2.8	-2.6	-2.5
130%	2.6	3.2	3.1	3.5	3.8	3.0	3.1
-130%	-2.7	-2.9	-2.7	-3.0	-3.5	-2.9	-2.8
160%	3.0	3.7	2.7	4.0	4.4	3.1	
-160%	-2.9	-3.2	-2.2	0.0	-4.2	-3.0	

Table A.5. Second floor drift ratios at target displacements [%]

Target	H1c	H2a	H2b	H3a	H3b	H4a	H4b	H4c
40%	1.5	1.3	1.3	1.2	1.2	1.3	1.1	
-40%	-1.3	-1.4	-1.4	-1.2	-1.3	-1.3	-1.2	
70%	2.7	2.3	2.6	2.1	2.1	2.2	2.0	
-70%	-2.4	-2.5	-2.5	-2.1	-2.2	-2.3	-2.2	
100%	3.8	3.5	3.7	3.1	3.0	3.3	3.3	3.5
-100%	-4.3	-3.7	-3.7	-3.4	-3.2	-3.4	-3.5	-3.6
130%	5.2	4.6	4.7	4.3	4.0	4.8	4.0	4.8
-130%	-5.1	-4.9	-5.1	-4.8	-4.3	-4.9	-4.2	-4.9
160%	6.6	5.9	6.9	5.6	5.2	6.5		6.3
-160%	-6.7	-6.4	-7.4	0.0	-5.4	-6.6		-6.5

### A.2.3. Shear wall uplifts at hold-downs and tension straps

Table A.6. Shear wall uplifts at left-side hold-downs [mm]

Target	H1c	H2a	H2b	H3a	H3b	H4a	H4b	H4c
40%	5.1	7.0	4.5	6.4	6.3	6.5	4.5	
-40%	-2.4	-2.1	-1.3	-0.9	-1.2	-1.4	-0.6	
70%	8.9	11.5	7.3	11.5	11.4	10.9	8.3	
-70%	-2.8	-2.6	-1.8	-1.4	-1.7	-1.9	-0.9	
100%	5.8	15.7	12.2	16.6	16.0	14.5	11.0	9.9
-100%	-1.2	-3.0	-2.2	-1.8	-2.4	-2.3	-1.0	-3.2
130%	14.3	20.3	18.2	21.2	21.1	15.2	13.0	12.6
-130%	-4.4	-3.4	-2.5	-2.1	-2.8	-3.6	-1.0	-3.3
160%	8.8	24.9	17.5	25.5	25.0	15.4		14.1
-160%	-2.4	-3.7	-2.2		-3.3	-3.6		-3.3

Table A.7. Shear wall uplifts at right-side hold-downs [mm]

Target	H1c	H2a	H2b	H3a	H3b	H4a	H4b	H4c
40%	-3.4	-1.7	-1.5	-1.7	-4.3	-1.4	-2.4	
-40%	5.5	8.2	5.5	6.6	6.6	8.4	5.8	
70%	-5.2	-2.5	-2.0	-2.5	-5.7	-3.0	-2.8	
-70%	9.7	13.3	9.7	11.3	11.8	13.0	9.4	
100%	-7.8	-3.2	-2.9	-3.3	-6.7	-3.5	-2.9	-3.5
-100%	8.8	17.2	14.7	14.5	16.1	16.2	11.9	11.7
130%	-6.4	-3.9	-3.6	-3.9	-7.3	-4.4	-3.0	-3.6
-130%	15.3	21.0	17.8	16.8	20.1	17.9	13.5	14.4
160%	-6.7	-4.6	-2.9	-4.5	-7.8	-4.4		-3.7
-160%	17.2	23.9	15.0		24.0	18.2		15.7

Table A.8. Shear wall uplifts at left-side tension straps [mm]

Target	H1c	H2a	H2b	H3a	H3b	H4a	H4b	H4c
40%	2.4	2.5	0.1	2.8	2.5	3.5	1.9	
-40%	-0.9	-1.2	-0.9	-1.6	-2.2	-1.2	-1.2	
70%	6.7	6	0.7	6.4	5.8	6.4	5.3	
-70%	-1.3	-2.4	-1.4	-1.8	-2.5	-1.8	-1.3	
100%	10.3	9.7	1.8	11.2	9.7	7.5	8.4	10.7
-100%	-3.1	-3.1	-1.5	-2.4	-3.1	-3.3	-2	-2.3
130%	23.8	13.7	3.6	17.3	16.4	17.2	10.8	16.8
-130%	-4.3	-3.5	-1.8	-3.5	-3	-4.9	-2	-2.4
160%	33.6	17.8	4.7	24.1	26	44.2		30
-160%	-5.4	-3.9	-3.2		-2.9	-9.9		

Table A.9. Shear wall uplifts at right-side tension straps [mm]

Target	H1c	H2a	H2b	H3a	H3b	H4a	H4b	H4c
40%	-1.9	-0.6	-1.7	-1.8	-1.8	-1.9	0.3	
-40%	2.3	2.8	0.0	3.1	5.7	2.9	1.5	
70%	-3.6	-1.4	-2.4	-2.4	-2.4	-2.5	0.4	
-70%	5.5	6.2	1.1	6.9	10.1	6.9	4.8	
100%	-3.1	-2.1	-3.1	-3.2	-2.5	-3.5	0.2	-0.8
-100%	10.5	10.2	3.5	-7.6	16.3	13.9	7.9	8.9
130%	-6.0	-2.7	-3.4	-6.4	-2.8	-6.6	0.6	-0.9
-130%	21.1	15.9	15.7	-26.1	23.6	25.0	9.9	15.5
160%	-7.1	-3.1	-4.2	-11.5	-3.5	-8.9		-0.8
-160%	30.5	22.2	47.4		32.3	39.7		26.6

#### A.2.4. Shear wall uplifts at inner corners

Table A.10. Shear wall uplifts at 1<sup>st</sup> storey left-side inner corners [mm]

Target	H1c	H2a	H2b	H3a	H3b	H4a	H4b	H4c
40%	-1.0	-0.2	-0.7	-0.7	-1.2	-0.4	-2.6	
-40%	3.2	4.1	4.2	4.8	4.2	5.6	5.6	
70%	-1.7	-0.7	-0.8	-1.3	-1.5	-1.8	-3.0	
-70%	7.0	8.1	7.9	9.5	8.7	10.5	10.5	
100%	-3.3	-1.0	-0.8	-1.3	-2.6	-1.9	-3.0	-4.1
-100%	7.3	11.7	12.2	13.7	13.1	15.0	14.1	12.4
130%	-2.9	-0.9	-0.5	-1.2	-2.9	-3.1	-3.1	-4.1
-130%	11.7	15.3	15.3	16.4	17.4	17.1	16.5	16.0
160%	-2.9	-0.7	-0.3	-1.0	-2.9	-3.1		-4.0
-160%	13.6	17.8	13.0		22.3	17.9		17.8

Table A.11. Shear wall uplifts at 1<sup>st</sup> storey right-side inner corners [mm]

Target	H1c	H2a	H2b	H3a	H3b	H4a	H4b	H4c
40%	2.4	5.3	4.2	5.4	3.5	5.2	5.8	
-40%	-0.5	0.4	-0.8	-0.5	-0.2	0.2	-1.0	
70%	4.8	9.7	6.7	10.0	7.7	9.8	10.6	
-70%	-1.2	0.3	-1.2	-1.0	-1.0	-0.5	-1.5	
100%	7.2	13.5	10.8	14.4	12.0	13.9	14.1	11.8
-100%	-1.7	0.0	-1.2	-1.1	-1.8	-1.4	-1.6	-3.8
130%	11.4	17.3	15.5	18.2	16.4	15.6	16.7	15.1
-130%	-2.9	-0.3	-1.1	-1.1	-2.4	-2.2	-1.7	-3.8
160%	14.0	20.7	14.2	21.9	20.3	16.7		17.4
-160%	-3.1	-0.6	-1.2		-2.8	-2.2		-3.9

Table A.12. Shear wall uplifts at 2<sup>nd</sup> storey left-side inner corners [mm]

Target	H1c	H2a	H2b	H3a	H3b	H4a	H4b	H4c
40%	0.9	3.8	0.5	4.2	2.8	3.8	4.3	
-40%	0.2	1.4	2.7	0.4	1.1	0.4	0.6	
70%	3.8	8.0	1.2	8.8	6.7	8.2	7.4	
-70%	1.1	4.0	5.7	1.4	2.0	1.6	3.3	
100%	8.3	10.9	2.7	12.7	11.2	12.0	8.4	4.7
-100%	7.8	8.3	8.4	5.1	3.7	4.9	9.7	10.2
130%	12.4	13.3	5.2	16.3	16.3	16.1	8.9	5.9
-130%	12.9	12.7	14.8	12.2	6.3	11.1	13.0	15.7
160%	15.5	14.9	4.9	19.9	21.2	26.7		7.5
-160%	21.3	20.3	38.7		9.7	21.6		27.2

Table A.13. Shear wall uplifts at 2<sup>nd</sup> storey right-side inner corners [mm]

Target	H1c	H2a	H2b	H3a	H3b	H4a	H4b	H4c
40%	-1.1	0.8	1.8	-0.1	0.3	0.3	0.2	
-40%	2.0	2.5	0.8	3.9	3.3	3.3	3.1	
70%	-0.6	2.7	5.6	0.8	1.3	0.6	2.2	
-70%	5.0	5.4	2.1	8.2	7.6	7.7	5.7	
100%	1.8	6.1	7.6	2.5	2.7	3.9	8.2	11.2
-100%	4.9	7.9	4.1	13.7	12.3	13.0	6.3	4.7
130%	10.2	9.7	9.6	6.1	5.0	8.0	11.4	16.9
-130%	9.3	10.7	8.4	17.3	17.1	16.1	5.8	6.4
160%	16.6	14.4	30.0	10.8	9.2	18.0		28.0
-160%	10.5	11.0	12.9		22.6	18.5		6.0

### A.2.5. Shear wall sliding

Table A.14. Shear wall sliding left-side base level [mm]

Target	H1c	H2a	H2b	H3a	H3b	H4a	H4b	H4c
40%	0.3	0.2	-0.4	0.3	0.3	0.2	0.8	
-40%	-0.6	-0.4	-0.2	-0.2	-0.1	-0.3	0.3	
70%	0.9	0.8	-0.3	0.8	1.0	1.0	1.1	
-70%	-0.8	-0.5	-0.3	-0.3	-0.4	-0.1	0.1	
100%	1.9	1.6	0.2	1.4	2.2	1.3	1.4	2.2
-100%	-1.0	-0.8	-0.7	-0.8	-0.7	-0.7	-0.3	-1.0
130%	2.0	2.5	1.4	2.1	3.2	2.0	1.6	2.0
-130%	-1.5	-1.0	-1.2	-1.5	-1.2	-0.9	-0.6	-1.2
160%	2.4	3.5	2.7	2.8	3.9	2.4		2.3
-160%	-1.9	-1.3	-1.8		-2.0	-1.6		-1.6

Table A.15. Shear wall sliding left-side 1<sup>st</sup> floor [mm]

Target	H1c	H2a	H2b	H3a	H3b	H4a	H4b	H4c
40%	6.7	3.9	9.0	5.3	5.7	4.0	7.0	
-40%	-7.8	-2.3	-3.4	-5.3	-4.6	-2.9	-6.6	
70%	9.8	8.1	12.7	10.4	11.5	9.1	13.3	
-70%	-11.7	-3.6	-6.3	-11.1	-10.7	-6.2	-10.7	
100%	10.9	11.1	16.9	15.0	19.5	13.2	17.3	15.6
-100%	-11.2	-5.1	-8.7	-14.4	-11.2	-10.1	-12.0	-8.6
130%	13.0	13.4	20.2	17.7	25.2	17.5	19.4	17.5
-130%	-13.6	-7.0	-10.0	-15.2	-13.9	-8.8	-12.9	-10.5
160%	13.1	15.1	19.7	18.9	30.2	13.5		15.2
-160%	-13.2	-7.4	-1.7		-15.6	-6.4		-8.6

Table A.16. Shear wall sliding right-side 1<sup>st</sup> floor [mm]

Target	H1c	H2a	H2b	H3a	H3b	H4a	H4b	H4c
40%	7.5	2.9	7.2	4.3	5.3	3.3	6.9	
-40%	-8.5	-2.9	-5.3	-6.4	-5.0	-3.3	-6.5	
70%	10.2	5.4	8.8	9.0	11.3	8.2	12.7	
-70%	-12.5	-5.3	-9.4	-12.5	-10.9	-6.6	-11.6	
100%	10.0	6.8	12.4	13.6	19.0	11.3	15.5	14.6
-100%	-13.3	-8.0	-12.7	-15.6	-15.1	-10.6	-15.1	-10.8
130%	10.5	8.5	15.0	16.4	23.7	17.2	17.0	16.8
-130%	-14.8	-9.9	-14.6	-16.2	-21.2	-7.1	-16.6	-12.5
160%	10.4	9.9	9.9	17.3	27.0	16.5		16.2
-160%	-14.0	-10.1	-2.0		-25.3	-3.3		-9.6

Table A.17. Shear wall sliding 2<sup>nd</sup> floor [mm]

Target	H1c	H2a	H2b	H3a	H3b	H4a	H4b	H4c
40%	0.3	-0.4	-0.4	0.5	0.5	0.8	0.9	
-40%	-0.5	-0.8	-0.6	-0.3	-0.4	-0.4	-0.9	
70%	0.4	-0.7	-0.5	1.4	1.1	1.8	2.2	
-70%	-1.1	-1.7	-1.0	-0.5	-0.7	-0.8	-2.6	
100%	1.1	-0.8	-0.8	2.6	1.8	5.7	7.9	9.4
-100%	-1.4	-2.6	-1.9	-0.9	-1.0	-0.1	-8.3	-7.6
130%	0.7	-0.9	-0.9	7.9	2.6	6.8	9.9	11.4
-130%	-2.7	-3.6	-2.8	-0.6	-1.3	-2.7	-11.4	-9.8
160%	1.3	-0.9	-0.5	15.0	5.9	8.0		13.3
-160%	-3.3	-4.6	-3.2		-1.0	-4.0		-12.5

## A.2.6 Panel-to-panel slip

*Table A.18. Panel-to-panel slip on 1<sup>st</sup> storey [mm]*

Target	H1c	H2a	H2b	H3a	H3b	H4a	H4b	H4c
40%	4.2	6.8	5.8	7.0	5.5	6.5	9.3	
-40%	-4.5	-4.7	-6.0	-6.2	-5.2	-6.3	-7.5	
70%	7.9	12.5	9.0	12.9	10.8	13.2	15.3	
-70%	-9.5	-9.6	-10.8	-12.2	-11.1	-12.6	-13.6	
100%	12.3	17.3	13.9	18.1	16.8	17.8	19.2	17.6
-100%	-10.3	-14.1	-15.9	-17.1	-17.0	-18.5	-17.9	-18.2
130%	16.8	21.7	19.2	22.3	22.2	21.0	22.3	21.5
-130%	-16.8	-18.9	-19.5	-20.2	-22.5	-21.8	-20.7	-22.3
160%	19.7	25.5	17.2	26.3	26.6	22.1		24.0
-160%	-19.0	-22.0	-16.6		-28.5	-22.7		-24.4

*Table A.19. Panel-to-panel slip on 2<sup>nd</sup> storey [mm]*

Target	H1c	H2a	H2b	H3a	H3b	H4a	H4b	H4c
40%	3.1	4.6	7.9	3.1	3.5	4.8	6.4	
-40%	-3.3	-4.5	-8.9	-3.3	-4.1	-5.4	-7.2	
70%	5.1	8.7	15.3	6.0	6.4	9.0	13.4	
-70%	-6.5	-10.1	-16.2	-6.1	-7.1	-10.3	-16.0	
100%	7.9	15.1	21.2	9.9	9.5	16.4	26.1	21.5
-100%	-16.5	-17.6	-22.7	-11.1	-10.8	-17.0	-31.2	-22.3
130%	19.9	21.8	26.5	17.0	12.8	23.4	33.7	28.6
-130%	-25.9	-25.2	-30.7	-21.7	-14.9	-28.4	-49.8	-29.9
160%	27.8	29.9	50.9	23.0	18.1	28.0		28.6
-160%	-38.1	-37.6	17.3		-19.9	-44.4		-43.3

**A.2.7 Panel distortion**

*Table A.20. Panel distortion [mm]*

Target	H1c	H2a	H2b	H3a	H3b	H4a	H4b	H4c
40%				0.0	0.2	0.8	0.2	
-40%				0.4	0.5	1.8	2.5	
70%				0.6	0.4	0.2	-0.4	
-70%				1.1	1.3	2.2	3.2	
100%				0.3	0.6	0.1	0.0	
-100%				1.7	2.1	2.9	4.6	1.7
130%				0.7	0.1	0.5	0.5	-0.5
-130%				2.4	3.0	2.4	5.2	2.7
160%				0.6	0.1	0.0		-0.8
-160%				0.0	3.4	2.5		3.3